

Offshore pumped hydropower storage
Technical feasibility study on a large energy storage facility
on the Dogger Bank

L.H. de Vilder

Master thesis

 **Witteveen**  **Bos**

 **TU Delft**

Offshore Pumped Hydropower Storage

Technical feasibility study on a large energy storage facility on the Dogger Bank

By

Lucas de Vilder

To obtain the degree of

Master of Science

In Hydraulic Engineering

Specialization in Hydraulic Structures and Flood Risk

Faculty of Civil Engineering and Geosciences
Delft University of Technology
The Netherlands

16th October 2017

Graduation committee

Chairman
Supervisor
Supervisor
Supervisor
Company supervisor

Prof. Dr. Ir. S.N. Jonkman
Prof. Ir. A.Q.C. van der Horst
Ir. J.D. Bricker
Ir. W.F. Molenaar
Ir. E.J. van Druten



Preface

This report presents my graduation work to conclude my Master Hydraulic Engineering and specialisation Hydraulic Structures and Flood Risk at the Delft University of Technology. The topic of this research is to develop a better understanding of how an offshore pumped hydropower storage facility scales with its storage and power capacity by using existing construction technologies. The research has been conducted in cooperation with the engineering and consulting agency Witteveen+Bos.

First of all, I would like to express my gratitude towards the members of my graduation committee. I would like to thank Bas Jonkman for your extensive feedback after every single meeting and Jeremy Bricker for always being available whenever I needed some guidance. Thanks to Wilfred Molenaar for always expressing your concerns and safeguarding the principles of hydraulic engineering. Aad van der Horst, thank you for joining the committee and enthusiasm to deal with the challenges of execution.

A special thanks to Emiel van Druten, your fascination for civil engineering and supervision on the graduation process has truly been inspiring. To all the colleagues of Witteveen+Bos, thank you for the opportunity to work alongside you and your willingness to assist every time I needed your expertise. Thanks to the other graduates for the enjoyable time and good atmosphere in the office.

Finally, I would like to thank my family, friends, flatmates and girlfriend for your support during my entire study.

Lucas de Vilder
Delft, October 2017

Summary

To combat global warming a transition towards renewable energy sources (RES) is essential. Although RES have much lower life-cycle emissions, they do not offer a continuous and fully predictable output like their fossil-fuelled counterparts. Energy storage is paramount in order to include the growing share of these intermittent sources into the grid and provide a reliable supply of energy.

In 2016 a long term vision which involves the creation of an artificial island on the Dogger Bank in the North Sea was presented. The island would act as the central spill in an interconnected future economy fuelled by RES. Currently there are no competitive energy storage technologies under consideration that could contribute to this 'energy hub'.

In Europe pumped hydropower storage (PHS) represents over 90% of the grid-connected storage capacity and continues to be identified as the most cost-efficient energy storage technology available today and in the future. Unfortunately, conventional PHS is restricted to mountainous areas and the remaining potential (2291GWh) does not suffice to future demand (estimated at 3596GWh).

The plans of developing a large wind farm via the construction of an island made it an attractive base to test the contribution and feasibility of a substitute to conventional PHS: inverse offshore pumped hydropower storage (IOPHS). It relies on the same principles as conventional PHS, only the process is inverted. When the wind farm generates a surplus of energy, the excess power is used to drive hydraulic turbines which pump the water out of the artificially created lake into the surrounding sea. Then when there is a higher demand for energy than the wind farm generates at that time, the sea water is allowed to flow back into the interior lake driving the same turbines.

Although the idea of inverse offshore pumped hydropower storage has been around for years, it has never been constructed. The objective of this research is to identify the possible design alternatives and determine how the costs of an offshore pumped hydropower storage facility scale with the power and storage capacity, using existing construction technologies.

The construction of the storage plant consists of four main elements: the dam, dredging works, turbines and the turbine housing. For the dam and dredging process that collectively are responsible for the creation of the storage capacity, it was found that when thick clay layers are present the costs are dominated by:

1. Maximum practically achievable reservoir depth
2. Armouring of the dam to cope with the wave conditions
3. Combination of inner slope stability and uplift of the inner toe
4. Dredging equipment and the operational waves during the excavation of the stiff clay
5. Sealing of the underlying sand layer

The costs of the power capacity depend on the turbines and the housing that are governed by:

1. Construction method of the turbine housing and connecting penstock and tailrace
2. Type and size of turbines
3. Maintenance costs of the electrical and mechanical parts
4. Preventive measures against cavitation from the turbine runners

When all costs are combined (except for planning and design costs) the expenditure scales as estimated in Table 1. The dedicated equipment is required to enable an efficient dredging process in the offshore conditions.

Element	Capital costs (m€)	Operational and maintenance costs (m€/yr)
Dedicated equipment	310	-
Storage reservoir (E=GWh)	$10^3 \times 0.7209 \times E^{0.389}$	$10 \times 0.7209 \times E^{0.389}$
Power generation (P=GW)	$10^3 \times 0.8746 \times P^{0.9118}$	$40 \times 0.8746 \times P^{0.9118}$

Table 1: Total costs of an offshore pumped hydropower storage plant in the North Sea with a maximum head difference of 40 metres. The operational cost of the dredging equipment is included in the storage capacity

It should be noted that the results are certainly not limited to a single location on the Dogger Bank, rather they are universally applicable. The stated design choices and relative costs components may act as guidance from which the given formulae and factors could easily be transposed to any other site. By doing so it can quickly be assessed if an inverse PHS system is possible and whether it provides a profitable business case.

The computed costs were obtained in a deterministic way. After a selection of future scenarios and uncertainties were taken into account, the levelised cost of storage (LCOS) was estimated. For a 25GWh storage capacity and 2.65GW of installed power the LCOS may vary from 68.2€/MWh to 19.0€/MWh of which 40€/MWh is found the most realistic.

In the worst case scenario the offshore pumped hydropower variant would remarkably be just as competitive as a conventional PHS plant. More importantly the studied alternative is a factor 3 to 18 times less expensive than batteries or power to gas (both are currently under consideration to incorporate the large shares of wind energy from the North Sea).

The considered reservoir is expected to have a Net Present Value of 610 million euros and a payback period of 23 years, which in favourable conditions could become 2.9 billion euros. Consequently it was not only found that constructing an inverse offshore pumped hydropower storage facility in the middle of the North Sea that can cope with the discussed failure mechanisms is possible. In addition the operation would be highly profitable.

This research presents a viable offshore pumped hydropower storage facility that is undoubtedly worthwhile, without relying on potential revenues or investments from other functions. Thereby it may offer a valuable link in the transition towards a green economy and within the development of large scale offshore wind energy in the North Sea.

The idea of Luc Lievense about artificially creating an energy storage reservoir has been laying on the shelf for nearly four decades. At the time wind energy did not develop as quickly as initially expected and the project lost interest. Nowadays offshore wind is being installed and planned on an unprecedented scale, making the business case for energy storage more lucrative than it has ever been before. Therefore the time to initiate the realisation of inverse pumped hydropower storage is now.

Content

Preface.....	IV
Summary.....	V
1. Introduction.....	12
1.1 Climate action	12
1.2 Integrating renewable energy into the grid.....	14
1.3 Long term plan: ‘Energy hub in the North Sea’	16
1.3.1 Contribution of energy storage to the ‘energy hub’	17
1.4 Problem definition	19
1.5 Reading guide.....	20
2. Analysis on energy storage.....	21
2.1 Energy storage outlook	21
2.1.1 Global	21
2.1.2 European Union	22
2.1.3 The Netherlands.....	23
2.1.4 Overview	23
2.2 Future demand for energy storage.....	24
2.2.1 Future energy demand.....	24
2.2.2 Future renewable energy market share	25
2.2.3 Required energy storage capacity	26
2.2.4 Types of energy storage services	27
2.3 Energy storage technologies.....	28
2.3.1 Pumped hydropower storage	28
2.3.2 Compressed air energy storage	31
2.3.3 Batteries.....	33
2.3.4 Vehicle to grid	35
2.3.5 Power to gas	36
2.3.6 Comparison of energy storage technologies.....	38
2.3.7 Concluding remarks on energy storage technologies	41
2.4 Potentially realisable pumped hydro storage.....	42
2.5 Future demand versus potentially realisable energy storage	44
2.5.1 Need for alternative energy storage technologies.....	44
2.6 Overview of energy storage islands.....	45

3. Technical design approach	46
3.1 Boundary conditions	47
3.2 Functional requirements	47
3.3 Failure tree	47
3.4 Principal scaling of reservoir dimensions	50
3.5 Volume balance	53
4. Dam design	54
4.1 Sea defence	55
4.2 Inner slope	59
4.2.1 Protection against waves	59
4.2.3 Phreatic line	63
4.3 Water retaining measures	64
4.3.1 Slurry bentonite wall	64
4.3.2 Sheet piles	65
4.3.3 Jet-grouting	65
4.3.4 Replacement of sand layer	66
4.3.5 Choice of measure	66
4.4 Failure mechanisms	68
4.4.1 Macro stability	70
4.4.2 Micro stability	74
4.4.3 Piping	75
4.4.4 Seepage	76
4.4.5 Bursting of the clay layer	78
4.4.6 Overtopping	79
4.5 Final design and concluding remarks	80
5. Dredging works	84
5.1 Selection of dredger	84
5.2 Dredging operation	85
5.3 Specifications and costs	89
5.4 Environmental measures	94
6. Power generation	95
6.1 Selection of turbine	95
6.2 Runner diameter	97
6.3 Cavitation prevention	100

6.4 Pump-turbine characteristics.....	100
7. Housing of turbines	102
7.1 Construction method	103
7.1.1 In-situ: pneumatic caisson.....	104
7.1.2 In-situ: open caisson	105
7.1.3 Prefab: modular box caissons.....	106
7.1.4 Hybrid: prefab bottom caisson + in-situ superstructure.....	108
7.1.5 Choice of method	109
7.2 Main dimensions and volumes.....	110
8. Costs & benefits.....	112
8.1 Dam costs.....	112
8.1.1 Water retaining costs.....	113
8.2 Dredging costs.....	114
8.3 Pump-turbine costs.....	115
8.4 Housing of turbine costs.....	117
8.5 Operational and maintenance costs.....	118
8.6 Total costs.....	119
8.7 Levelised cost of storage	121
8.7.1 Comparison with other energy storage technologies	123
8.8 Benefits.....	124
8.8.1 Hypothetical revenues and payback period.....	125
8.8.2 Contribution of energy storage to the 'Energy hub' in the North Sea	127
9. Discussion.....	128
9.1 Storage capacity	128
9.2 Power capacity.....	130
9.3 Levelised cost of storage	131
9.4 Comparison with previous literature	132
9.5 Remarkable findings.....	133
10. Conclusion	135
10.1 Dam design.....	137
10.2 Dredging process	137
10.3 Power generation	138
10.4 Housing of turbines.....	139
10.5 Scaling of an offshore pumped hydropower storage facility.....	140

11. Recommendations.....	141
Bibliography	143
List of figures	149
List of tables	157
Appendices.....	160
Appendix A: Options to help integrating intermittent renewables	161
Appendix B: Alternative pumped hydropower storage systems.....	162
B.1 Plan Lievense	162
B.2 Energy Island	164
B.3 Slufter	167
B.4 Taiwan Integrated Energy and Service Island	169
B.5 Underground pumped hydro storage	172
B.6 Stored Energy in Sea.....	174
Appendix C: Scalars of energy storage islands	176
Appendix D: Dogger Bank conditions	178
Appendix E: Risks associated to inverse offshore pumped hydro storage	182
Appendix F: Influence of toe material on slope stability	183
Appendix G: Seepage and bursting mechanism for a closed aquifer.....	185
G.1 Seepage	185
G.2 Bursting.....	187
Appendix H: Construction method of the dam	191
Appendix I: Location of the powerhouse and penstock design.....	193
Appendix J: Connecting box caissons with Gina gaskets	197

1. Introduction

Firstly an outline on the challenges of the future energy supply will be given, explaining climate change as a driver for switching to renewables, which bring their own challenges. Furthermore, the alternatives for energy storage will be discussed as interconnectivity, flexible demand and generation or the curtailment that would follow when these flexibility options are not sufficiently implemented. Lastly a long term vision is presented, that involves the creation of an artificial island in the middle of the North Sea. The island would act as the central spill in an interconnected future economy that is fuelled by renewable energy sources (RES). For that future situation it will ultimately lead to the question how energy storage can contribute to this multifunctional concept.

1.1 Climate action

The world energy consumption started rising ever since the (coal-fired) industrial revolution. Subsequently when World War II was over, other finite energy sources like oil and gas grew exponentially (see Figure 1). The emissions originating from usage of these fossil fuels are considered one of the drivers of today's climate change. It has been concluded with 95% certainty that: "The human influence on the climate system is clear and is evident from the increasing greenhouse gas concentrations in the atmosphere" (Intergovernmental Panel on Climate Change, 2013).

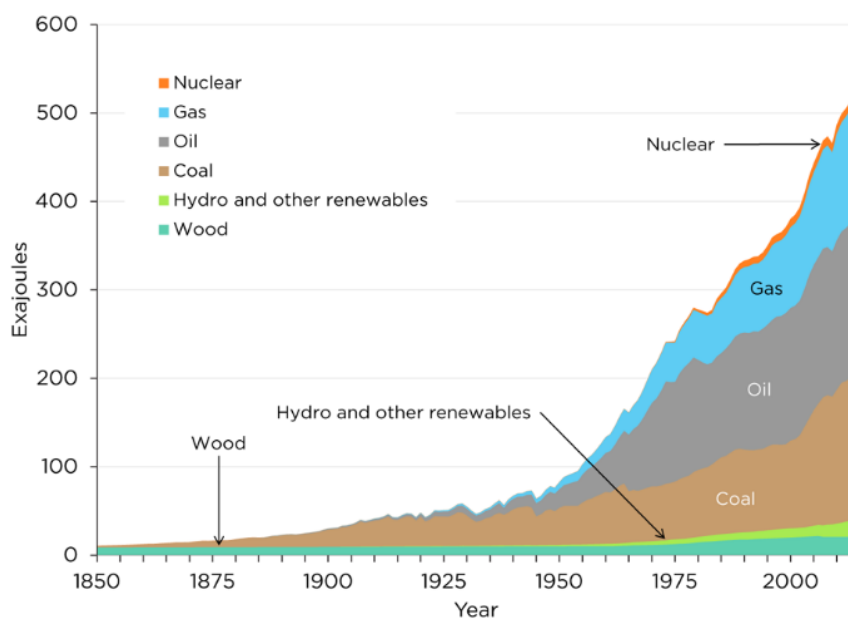


Figure 1: World primary energy consumption per fuel type from 1850 to 2014, based on data from BP, Statistical Review of World Energy (source: Heinberg & Fridley,

Climate change is perceived as undesirable and something that requires action, which results in international partnerships, treaties and agreements like 'Kyoto' and 'Paris'. The main goal of these pacts is to avoid "dangerous anthropogenic interference with the climate system" (Rio Earth Summit, 1992) and mitigate the pressure on the climate by reducing the energy consumption and the emission of

harmful gases. Due to the increasing global population (UN 2015 projections), it is unlikely that the amount of energy we use collectively is going to fall (in this century). Consequently it is of utmost importance to generate power without the corresponding release of damaging gases and move from a fossil fuel-based economy to a sustainable system. To initiate momentum towards a 'decarbonised' economy goals have been set, like the European Union 2020 targets as shown in Figure 2.

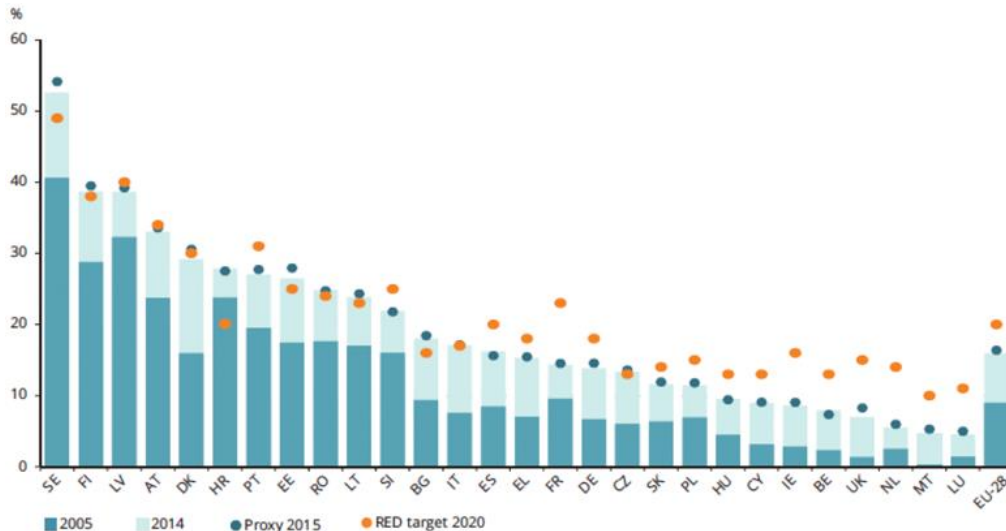


Figure 2: European Union 2020 objectives for renewable energy source (RES) shares in the energy mix (source: European Commission, 2016)

As can be seen above, The Netherlands ranks worst after Malta and Luxembourg in achieving their renewable energy targets from all 28 Member States! Alarmingly the Netherlands only managed to go from a 5.8% RES share in 2015 to a 5.9% RES share in 2016, which is still far away from their 14% objective (Timmer & Van Zuijlen, 2017).

However, change is on the way and even the Netherlands started investing and moving towards an environmentally sustainable energy supply. As of 2023 a total of 4.45 GW offshore wind power is planned to be operational and an interconnector capacity of 9.1 GW to nearby nations. In combination with investments in other RES and infrastructure this should lead to a 16 % renewable energy share in 2023 (Ministerie van Economische Zaken, 2016).

This trend towards a decarbonised economy is happening on a global scale, as can be seen in Figure 3. Especially wind and solar power are in the lift, being accountable for 90% of global investments in RES in 2015. Due to these developments in RES like onshore wind, hydropower and biomass are now all competitive or cheaper than for example gas, coal or oil-fired power plants (IRENA, 2017).

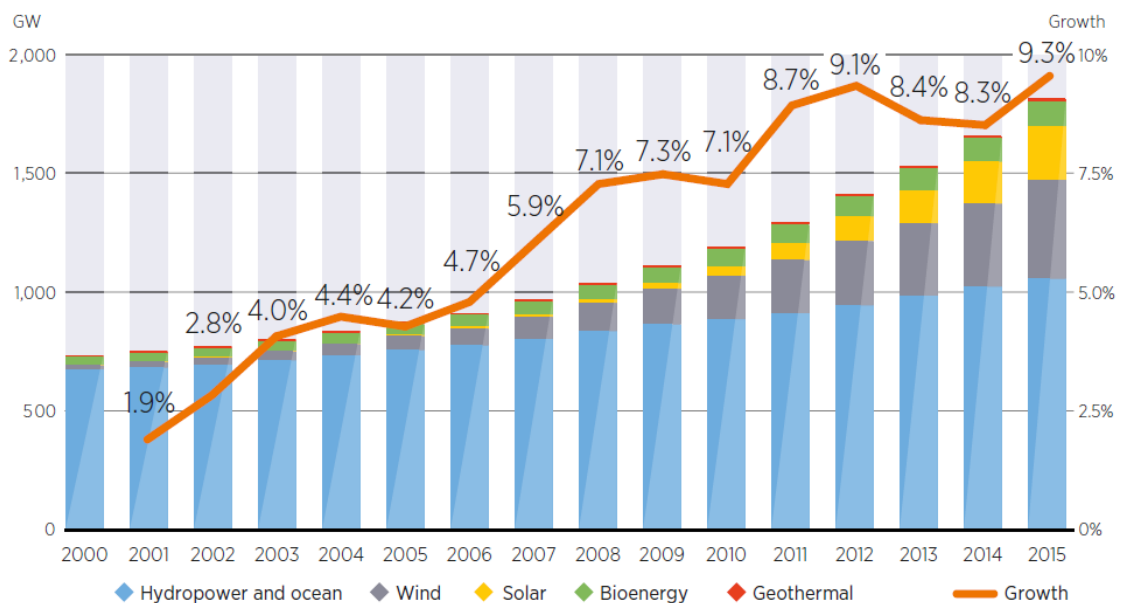


Figure 3: The renewable power capacity worldwide and its growth rate over the last years (source: Irena, 2017)

1.2 Integrating renewable energy into the grid

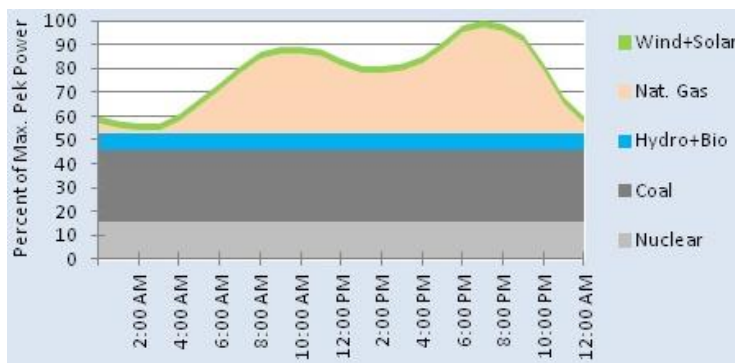


Figure 4: Typical power curve in the United States (source: Miller, 2013)

Traditionally the daily gap between the base-load supply and demand is made undone by ramping-up and – down a gas peak power plant as in Figure 4. Besides the fact that conventionally generated flexible power is expensive and inefficient, it emits large shares of greenhouse gases (GHG). In order to achieve future climate targets not only the

base-load, but also the flexible power supply needs to be generated by renewables.

Renewable energy sources (RES) like wind and solar are becoming more dominant in the energy power mix (WEC, 2016c). Although these RES have much lower life-cycle emissions, 14 g/kWh of CO₂ equivalents for wind energy compared to 1001 g/kWh for coal (IPCC, 2011). The intermittency of wind and sun poses a real challenge for integrating them into the power system (WEC, 2016b). How the wind and solar energy supply may fluctuate during a week is depicted in Figure 5.

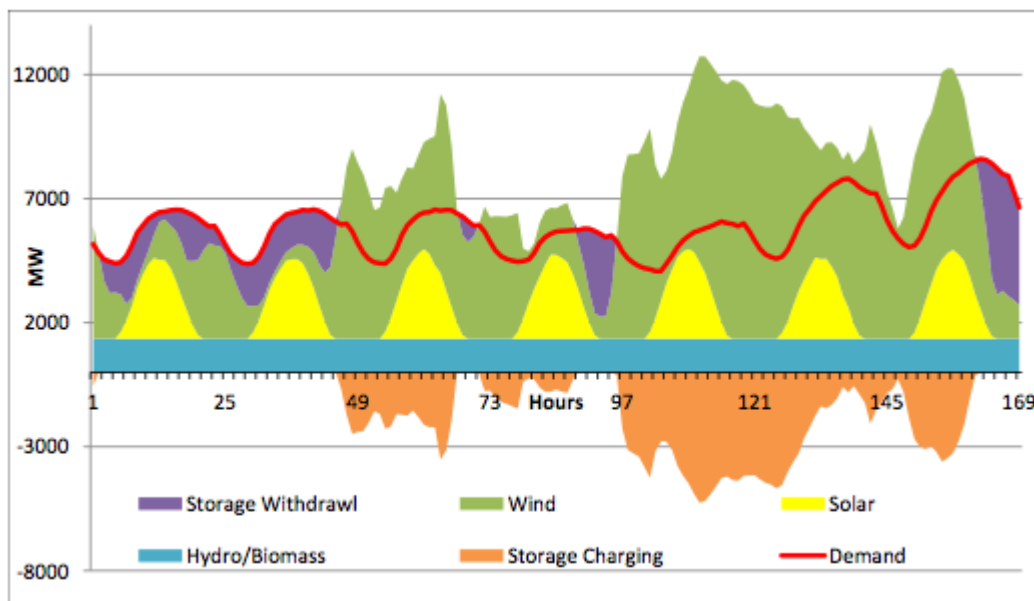


Figure 5: The hourly supply and demand of energy for Minnesota, USA, in a hypothetical 100% RES scenario during a week (Wed – Tue) in July, 2007. Note how energy storage and withdrawal levels the difference between the intermittent supply and the energy demand (source: Makhijani et al., 2012)

Even though Figure 5 illustrates the challenge of integrating wind and solar power it also shows the possibility of operating a reliable energy system powered by RES. Wind and solar power complement each other rather well, with the wind blowing mostly during the night and in winter, and the sun shining during the day and peaking in summer. However, problems arise when the wind does not blow and the sun does not shine. For these days and moments that the RES supply cannot match the exact energy demand, alternatives are required in order to guarantee energy security (see Figure 7).



Figure 7: Flexibility options that can help absolving the differences in electric energy supply and demand (source: Posthumus & Van der Vegte, 2017)

The main possibilities to deal with the challenges posed by variable renewable energy sources are:

- Flexible power: Generate power exactly according to the demand
- Demand side management: Adjust the energy demand to the supply
- Energy storage: Store energy when supply exceeds demand and release when required
- Interconnectors: Connect regions/countries with different energy demands and supplies
- Do nothing: Do not fully commit to RES and accept irreversible climate change

Note that the various alternatives do not exclude each other. On the contrary, the first four opportunities will all be necessary to transfer to a decarbonised economy. The options above are further explained in Appendix A: Options to help integrating intermittent renewables. If these flexibility options are not sufficiently implemented the grid will not be able to cope with the intermittency from the RES, with the consequence that for example wind turbines will be shut down and energy will be 'lost' accordingly. This curtailment of RES can be monetized by multiplying the amount of energy 'that could have been generated' times the price at which the electrical energy 'could have been sold'. The loss of revenue (due to curtailment of RES) is already a very serious issue, as can be seen in Figure 6. The European Commission projects for 2050 that annually 20 billion euros

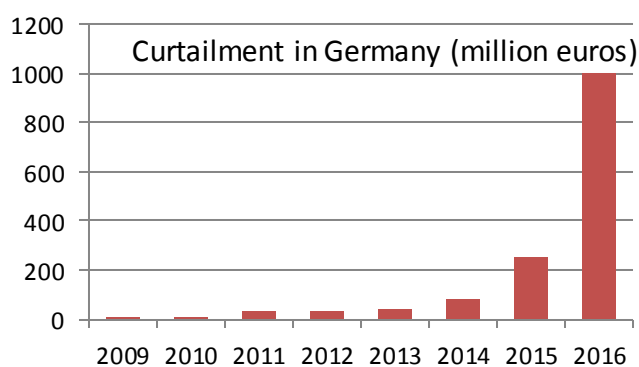


Figure 6: The loss of revenue according to network operators in Germany (Timmer & Van Zuijlen, 2017), mostly due to insufficient energy storage and grid capacity between the (enlarged) wind power generation in the north and the energy demand in the south (source: Dickson, 2017)

might be lost due to curtailment when extensive Pan-European grid investments are not placed in coherence with the growing RES share (e-Highway2050, 2013).

From the various ways that can help incorporating large shares of RES into the grid, it is chosen to focus on possibilities regarding energy storage. Energy storage offers the most promising addition to the challenging project explained in the next section.

1.3 Long term plan: 'Energy hub in the North Sea'

Over the next decades it is expected that all possible near-shore wind capacity will be installed, which is more beneficial compared to far-shore from a constructability and connection to the grid perspective. Once far-shore wind power becomes necessary (>2035), shallow waters with good wind conditions will be the area of choice (Van der Hage, 2017).

The Dogger Bank comprises of over 17,600 square kilometres of shallow water (13 to 40m deep) throughout the British, Dutch, German and Danish waters of the North Sea. TenneT recently launched their plans to develop an immense wind farm (>30 GW) on this very same area and connect it to all the North Sea countries (see Figure 8). To enable the construction of a profitable wind farm this far offshore an island needs to be build. Such an island brings several advantages like:

- HVDC-converter stations no longer require offshore platforms, but can be built on land
- Interconnector cables can be laid from and to the island, instead of running separately between all the countries, saving more than half the distance
- By adding a port to the island the logistics of constructing, operating and maintaining the wind farm are massively simplified



Figure 8: The hypothetical location on the Dogger Bank of the energy hub with its interconnector cables indicated with the dashed lines (top) and an impression of the envisioned island by TenneT (bottom). The figure was modified from Van der Hage (2017) and Börger et al. (2014)

The **Witteveen + Bos** engineering consultancy is planning to develop a better understanding of the challenges and opportunities regarding the "Energy hub". It plans to do so by guiding a number of students enlightening different aspects of the project simultaneously such as:

- Feasibility study of the hub and spoke concept in the North Sea: Developing a site selection model to determine the optimal location (Gerrits, 2017)
- Nature enhancing opportunities for coastal defences: Opportunity study for the Dogger Bank (Frölke, 2017)
- Offshore pumped hydropower storage: A technical feasibility study on a large energy storage facility on the Dogger Bank (topic of this thesis)
- A study of the economic benefits of the island, interconnector cables and energy storage (expected in 2018)

The resulting reports are meant to have as little 'overlap' as possible. Therefore it might seem like important subjects like environmental impact, site selection and potential benefits are not

sufficiently addressed in this report. However, as can be deduced from the previously stated parallel projects, those topics are thoroughly investigated in the other studies. Additionally has to be mentioned that, unless otherwise stated, all the work presented in this report originates from the author itself.

1.3.1 Contribution of energy storage to the ‘energy hub’

Within the plans of creating a central spill in the North Sea, to develop large-scale wind power, it is thought that energy storage could be a valuable asset within the whole project. When the artificial island, interconnector cables and wind turbines are in place, all ingredients an energy storage facility could wish for are present:

- The interconnector cables between the North Sea countries allow for buying and selling of energy to many different markets.
- By being right next to the wind power source, the storage facility can stock wind energy directly at times of abundance and provide energy once required, when otherwise the energy would be lost (avoided curtailment and security of supply).
- The ability of storing energy locally for later moments also results in deferral of disproportional grid investments, since they do not need to cope with the maximum wind power capacity. To put it into perspective: by avoiding 300 kilometres of a 700 MW interconnector cable, 600 million euros are saved.
- With all the wind power generation and electrical infrastructure to transform alternating current (AC) to direct current (DC), there will be a large demand for frequency control services, which energy storage might fulfil.
- The presence of a port on the ‘energy hub’ enables an easy way of transporting equipment and materials that are necessary for the construction and operation of the storage facility.

Pumped hydropower storage (PHS) is the oldest and most well-established storage technology (see Figure 9). PHS consists out of two connected waterbodies, one upper- and one lower reservoir. In times of energy abundance (or low prices) water is pumped from the lower to the upper reservoir where the energy is ‘stored’. Then when there is a shortage of energy, the water is released from the upper reservoir, driving the turbines, and flows back into the lower reservoir. Unfortunately the appropriate geographic conditions for PHS are scarce and the remaining sites will not suffice to future demand (explained in chapter 2).

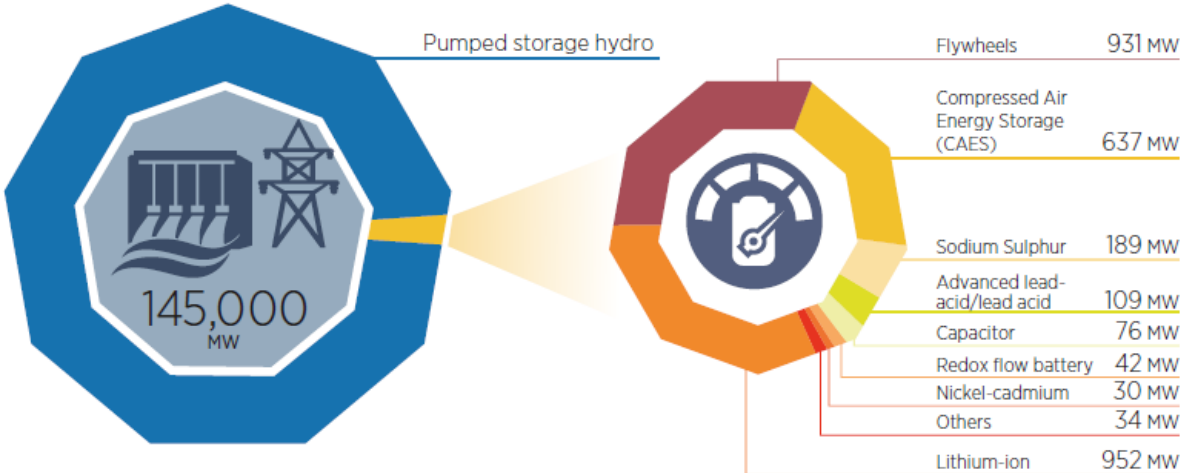


Figure 9: The existing storage technologies and their global share in energy storage (source: IRENA, 2017)

The lack of mountains in the Netherlands did not stop Luc Lievense in trying to use the efficient pumped hydro technology so he conceived a way to 'artificially' create the required hydraulic head difference that enables power generation. Lievense launched his idea in 1979 in a response to the prior oil boycott from the Middle-East and resistance against nuclear energy. The energy storage system would reduce the dependency on foreign policies and help integrating renewable energy into the grid. By erecting a circular dam a higher inner reservoir would be created of which the water level could be adjusted to either store or withdraw energy.

At the time there was a lot of resistance due to the risk of a flood when the dam would break. Additionally, wind energy did not develop as quickly as was first expected, reducing the need for large investments in energy storage.

The idea of constructing a circular dam to obtain a PHS plant came back in 2007, with the study of KEMA and the Lievense consultancy agency (De Boer et al., 2007). It relies on the same ideas as conventional PHS, only the process is now inverted (see Figure 10). When the wind farm generates a surplus of energy, the excess power is used to drive hydraulic turbines which pump the water out of the artificially created lake into the surrounding sea. Then when there is a higher demand for energy than the wind farm generates at that time, the sea water is allowed to flow back into the interior lake driving (the same) turbines.



Figure 10: An artist impression of an inverse offshore pumped hydropower storage plant (source: De Boer et al., 2007)

By lowering the water level in the reservoir instead of raising it, there is no longer a potential flood hazard related to the storage system. The main requirement to enable this inverse process is a thick clay layer in order to create an impermeable 'tub'.

The occurrence of large stiff clay layers on the Dogger Bank in combination with the local power generation, the need for energy storage and the required dredged material to construct the 'energy hub', make it a fruitful base to test the feasibility of an offshore pumped hydropower storage facility.

1.4 Problem definition

Although the idea of “inverse pumped hydro storage” has been around for years, it has never been executed. Therefore many uncertainties and challenges still cloud the feasibility of such a project. In the handful of studies that have been performed certain design choices remained rather unclear, like the head difference between reservoirs, storage and power capacity, water retaining measures and the dam design. This particular thesis will try to identify the possible design alternatives and answer the question: **“How do the costs of an offshore pumped hydropower storage facility on the Dogger Bank scale with the power and storage capacity, using existing construction technologies?”**

The main research question will be answered step-by-step with dividing it into the following sub-questions:

1. What are the construction method alternatives, considering the Dogger Bank geology and bathymetry, for the dam to cope with seepage, piping, overtopping and stability issues and what is the maximum head difference achievable?
2. What is the preferred dredging strategy to obtain the required depth following from question 1.?
3. What is the ideal turbine setup to deliver the necessary power with the given head difference?
4. What is the most cost effective construction method for the housing of the turbines, in-situ, prefab or a hybrid alternative?
5. What are the benefits of energy storage, for both storage and power services?

1.5 Reading guide

To answer the main research question many topics need to be touched upon and investigated. This is done via the following structure:

The available large-scale energy storage technologies and which can best be adopted to contribute to the North Sea 'energy hub'	Ch. 2
The technical design approach, including the principal scaling factors, volume balance and boundary conditions	Ch. 3
The dam design and necessary water retaining measures. Here the maximum achievable head difference between the reservoirs is determined. This serves as input for the dredging and turbine part	Ch. 4
The dredging works. Combined with the dam design it forms the scalar for the costs of storage capacity	Ch. 5
The choice and size of (pump) turbines	Ch. 6
The construction method and position of the turbine housing and connecting penstock and tailrace. This together with the turbines results in the scalar for the costs of power capacity	Ch. 7
The scaling of the costs and of the individual parts and the complete storage system (these form the results of the performed study). Additionally, the levelised cost of storage is determined and the potential revenues and payback period. Once the costs and benefits are known, the impact an energy storage system can have on the 'energy hub' can be estimated	Ch. 8
Discussion of the obtained results. The reliability of the obtained results and comparison with findings from previous studies.	Ch. 9
The best alternative to consider	Ch. 10
Necessary further research to be able to implement a sound energy storage facility in the North Sea	Ch. 11

2. Analysis on energy storage

This chapter gives an overview of developments and technologies to store energy. At the end of this chapter it should be clear what the best alternative to investigate is for the Netherlands to cope with energy security and the difference between energy demand and supply. The answer is obtained via a set of sub-questions:

- What are the views and trends regarding energy storage on a global, European and national level?	§2.1
- What is the future demand for energy storage and which are the types of storage services?	§2.2
- What are the large scale energy storage alternatives and how do these compare?	§2.3
- How do the future demand and potentially realisable energy storage match?	§2.5
- What is the best alternative to consider?	§2.6

2.1 Energy storage outlook

In this section there is elaborated on the prospect of energy storage from different angles narrowed down from a global level to the European Union to the view of the Netherlands.

2.1.1 Global

The International Renewable Energy Agency (IRENA) expects electricity storage to become a vital part of power systems with high renewable shares (IRENA, 2012). With the fast growing renewable energy market, the global investment in grid-connected storage is estimated to rise from USD 1.5 billion in 2010 to around USD 35 billion in 2020. Where today's grid stability in networks with a high share of renewable energy is safeguarded by an elaborate interconnection system, which allows more than e.g. 20% of wind energy, this might become insufficient when the renewable energy share grows in all regions (IRENA, 2012). The International Energy Agency (IEA) states in their World Energy Outlook 2016 that energy storage becomes essential after the share of wind and solar output surpasses one-quarter of the power mix. In case no investments are made curtailment of wind and solar energy in times of abundance, could idle the equivalent of up to 30% of the investment in the wind farms and solar parks (IEA, 2016).

Simulations taking into account a high renewable energy share indicate that in Western Europe a storage capacity of about 90 GW would be required by 2050, with 30% of wind power generation. Globally storage need to be provided for the usage of wind power between 190 GW and 300 GW (IRENA, 2012).

Pumped hydro power is the only large scale option which is regarded as commercially viable at present. Other storage technologies, such as hydrogen- or large scale battery storage, need further development to become competitive (IRENA, 2012).

2.1.2 European Union

The European Energy Directive (EED) regards energy storage as an essential element to facilitate the transition towards a sustainable electricity network (European Commission, 2012). Many values of electricity storage are identified such as: allowing a large share of renewable sources in the energy mix, letting base-load plants (nuclear, coal) run at higher efficiency by storing their output at times of low demand, avoiding the curtailment of wind and solar power, increased flexibility and reliability on the grid (Ugarte et al., 2015a). The benefits of storage and their position in the energy chain (generation, transmission, distribution and end-use) is explained for large scale and distributed storage in Figure 11.

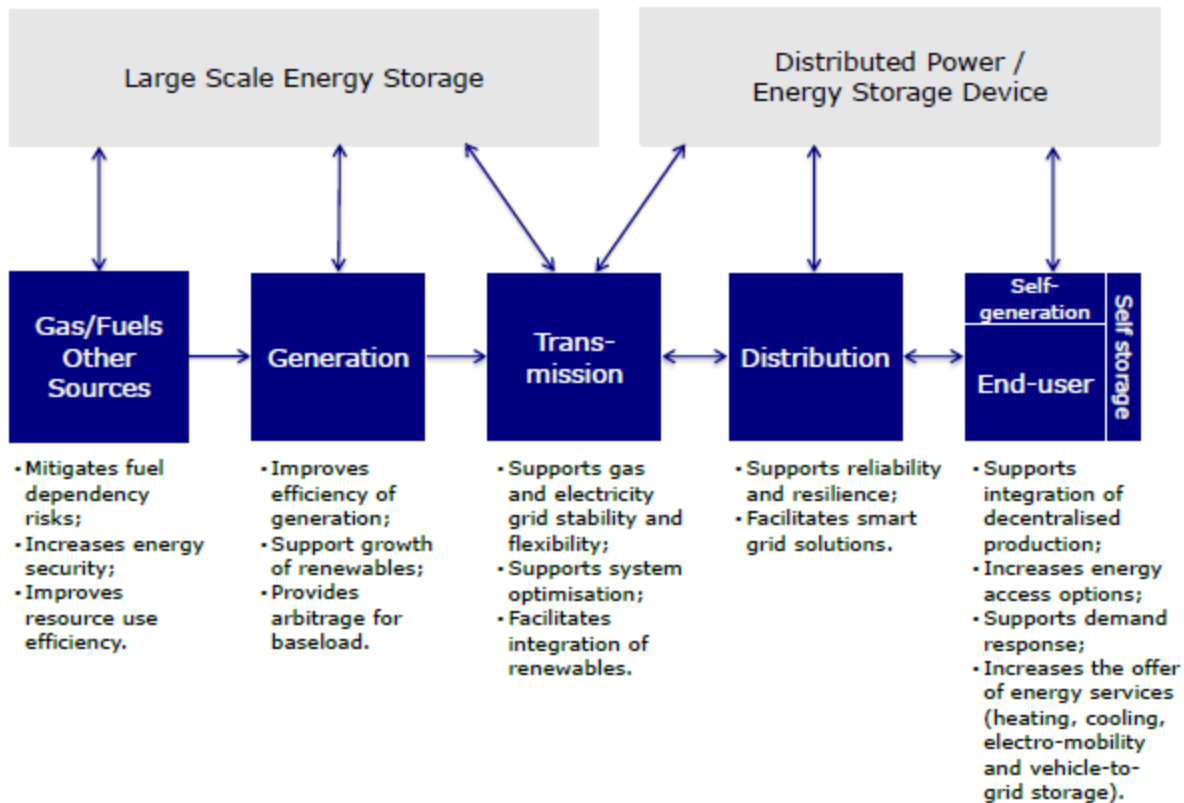


Figure 11: Value of storage in the whole energy chain (source: Ugarte et al., 2015a)

Currently regulations and policies are unclear about who is permitted to own and operate storage facilities, which does not encourage investment in energy storage (Ugarte et al., 2015b). Furthermore electricity stored temporarily is taxed twice, since the storage facility is also considered as a 'consumer'. New legislation and policy should avoid these double grid fees and taxes and allow for ownership and management of storage (Clerens, 2016).

The European Union desires a common approach for all Member States to develop and implement competitive storage solutions in an integrated network. A level playing field needs to be created for all technologies (sustainable and fossil-fuel based) and ideas have to be developed to make renewable energy producers contribute to a balanced system (Ugarte et al., 2015b).

Large pumped hydro power is cost competitive and already holds a major role in the flexibility of energy systems. In the short term no other storage methods can compete. However, in the longer term some alternatives might enhance their business cases and join the market (Ugarte et al., 2015a).

2.1.3 The Netherlands

Electricity storage systems are recognised as an important potential source of flexibility, which can be used for all alternating services: trade and supply, balancing and efficient use of the grid. Research by Frontier Economics (Ministerie van Economische Zaken, 2016) shows that the energy security of the Dutch network is guaranteed, without large scale energy storage applications, up to 2035. To enable the energy transition towards a sustainable system, the Netherlands focuses on further integration and strengthening of the international grid. Between now and 2021 the interconnection capacity is extended from 5.9 GW to 9.1 GW, with cables like the Cobra to Denmark and others to Germany (Ministerie van Economische Zaken, 2016).

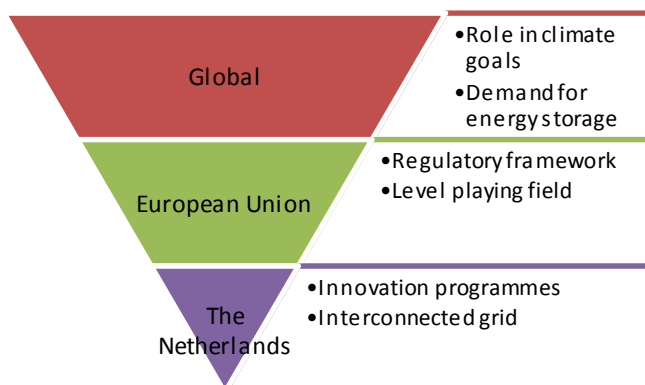
As mentioned in the European view, the double taxation on energy storage will be reviewed. At present, both the supplier of electricity storage as the end-user are taxed, where natural gas is deliberately exempt from double taxation.

There is an opportunity to combine the installation of offshore wind farms with other assets like energy storage to reduce the costs for the society of the energy transition (Ministerie van Economische Zaken, 2016). Further technological development of energy storage and distribution is sought through the stimulation of innovation, which is required for up-scaling the renewable energy production. It is recommended by the Energy Storage Roadmap NL 2030 to focus on solutions which offer multiple functions like wholesale, balancing and reserve capacity (which characteristics will be explained in 2.2.4)(DNV GL, 2015).

With no suitable locations for pumped hydro power, there is no competitive technology available for long term storage. There are innovation programmes that contribute to the flexibility of the electricity system such as the development of smart-grids, heat storage and power-to-gas (Ministerie van Economische Zaken, 2016).

2.1.4 Overview

The value and importance of energy storage is acknowledged on all levels. On a global scale the general demand and benefits are worked out, regardless the local policies. Energy storage is mainly seen as a facilitator of a high renewable energy share in the power mix, which is required to achieve climate goals like limiting the global warming to 2 °C. The European Union strives for creating a level playing field between storage technologies, fossil-fuel based options and nations as well as having a common regulatory framework among all Member States that enable the development and public and private investments in energy storage. The focus within the Netherlands is on innovation of promising technologies, since there is no competitive solution for the long-term yet. Pumped hydro



power, which is regarded as the most viable option globally and within the EU, is not feasible in the Netherlands due to geographic restrictions. For now the Dutch grid is sufficiently resilient without storage and there is chosen to strengthen the international electricity network. Figure 12 depicts the focus on energy storage per level.

Figure 12: Focus on energy storage per level

2.2 Future demand for energy storage

The prospective need for energy storage is computed through three steps. The time horizon is set on 2050 and the scope is set on North- and West-Europe, since this area is well (inter) connected and fits within the area of influence of the project. Firstly the future energy demand is worked out, when secondly the share of energy from renewable sources in this future scenario is determined. Once the amount of renewable energy that will be generated is known, the corresponding need for energy storage to facilitate the integration of fluctuating sources is defined. Afterwards the various services that energy storage can provide are introduced.

2.2.1 Future energy demand

The Energy Roadmap 2050 from the EEA stresses the need for a significant reduction in energy consumption. The decarbonisation of the economy will be obliged by more stringent requirements for energy utilities, new buildings and the renovation and upgrading of existing buildings. Economic growth and energy consumption needs to be decoupled and all Member States need to take adequate measures in all economic sectors (European Commission, 2012). These combined efforts should lead to a reduction in energy demand of 41 % by 2050 compared to the usage in 2005-06, which was 1831 million toe¹ (European Commission. Directorate-General for Energy, 2016). Even though the total energy consumption will decrease, the peaks in demand during the day will most likely increase for the use of electric charging of vehicles or heat pumps. This growth in peak power demand is another argument for incorporating storage systems in the energy chain.

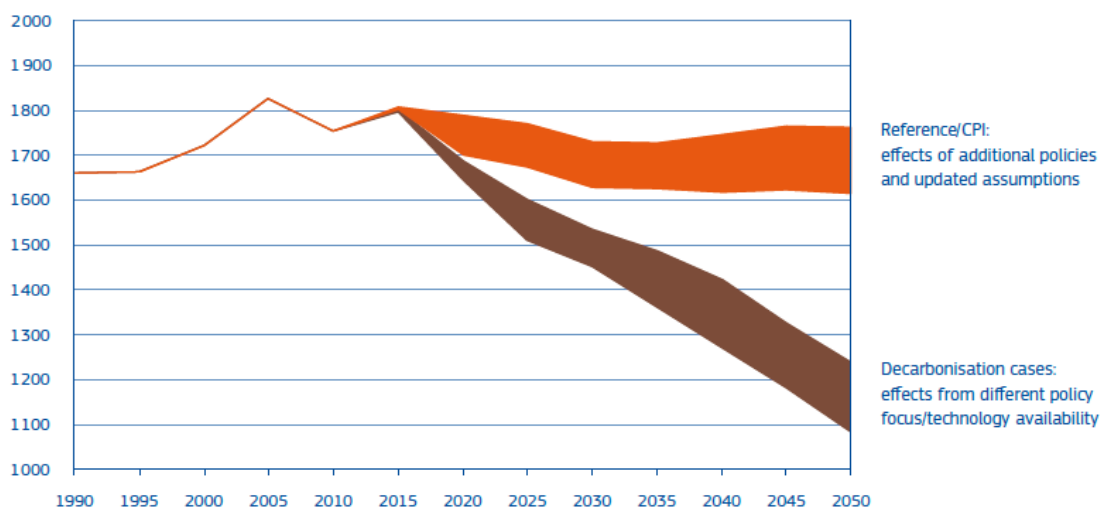


Figure 13: Decrease in gross annual energy consumption in million toe (source: European Commission, 2012)

¹ Tonne of oil equivalent (toe) is an energy unit, which is used to describe large amounts of energy. One toe is equal to the energy that is released by burning one tonne of crude oil, defined as 11.63MWh.

2.2.2 Future renewable energy market share

In all EU decarbonisation scenarios the strongly supported renewable sources rise drastically, attaining shares between 40 % and 60 % of primary energy consumption (European Commission, 2012). The expected fuel shares in the EU are shown in Figure 14, in which RES represents renewable energy sources.

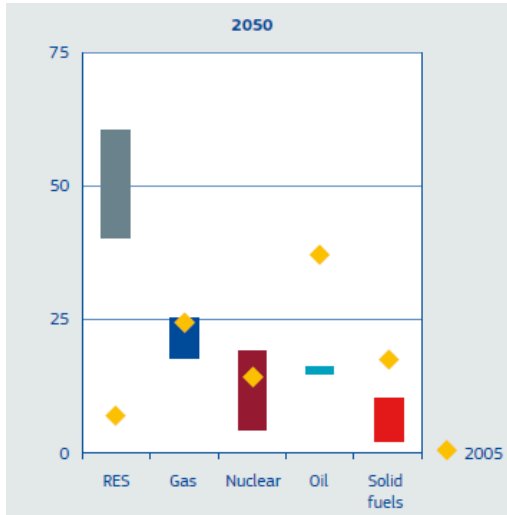


Figure 14: Range of fuel shares in primary energy consumption (%) (source: European Commission, 2012)

The International Energy Agency worked out the scenario where the regulations to limit global warming to 2 °C is enforced, which should mostly be achieved by switching to renewable energy sources. In this scenario, depicted in Figure 15, the European Union is estimated to consume 44 % of its energy usage from renewables (IEA, 2014).

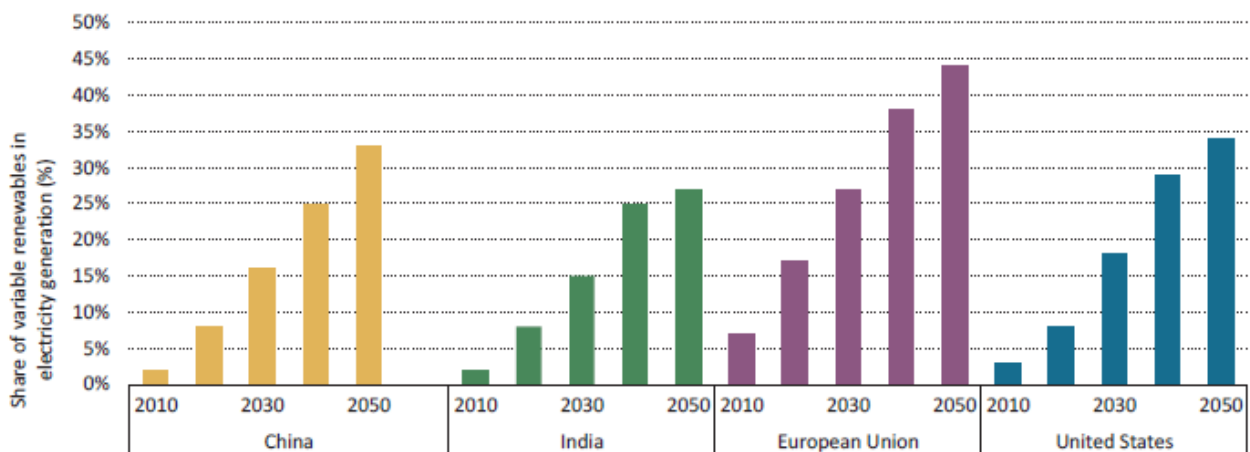


Figure 15: Share of variable renewable energy generated (source: IEA, 2014)

2.2.3 Required energy storage capacity

There is no definite answer to the amount of energy storage that is required to integrate a significant amount of variable renewable energy into the system. The necessary storage is highly dependent on other aspects within the energy chain like the size of the system, the quality of the grid, regulation on the demand side, the other generation technologies and interconnectivity with neighbouring systems. This vast number of factors of influence results in a wide range from 20 % to 60 % of expected need for energy storage per renewable energy share according to comprehensible studies by Fraunhofer, BET and IRENA (Ugarte et al., 2015a). These estimates are in line with the experience gained from a pilot project that combined a wind farm with sodium-sulfur batteries in Minnesota, USA. The project found that for each MW of wind generated, 0.2 MW to 0.4 MW of storage would be required (Himelic & Novacheck, 2011).

Combining the reduced energy demand with 41 % by 2050, a renewable energy share between 40 % to 60 %, and the need for energy storage ranging from 20 % to 60 %, leads to a required storage power output of 115 GW as lower boundary and 516 GW as upper boundary for the EU-28. Considering storage facilities need to be charged before they can generate, the installed capacity needs to increase to allow for the charging time. Assuming e.g. a capacity factor/generation ratio of 0.45, the required storage power varies from 255 GW to 1148 GW.

Within the scope for North- and West-Europe, including Switzerland and Norway, where the largest energy demand originates (European Commission. Directorate-General for Energy, 2016), the respective need for storage ranges from 221 GW to 996 GW. Observing the future well interconnected grid and ambitions for very high usage of renewable energy sources; a scenario with 60 % of RES and 20 % of required storage per share of RES is found most probable, resulting in a required capacity of **3584 GWh** and an output of **332 GW** by 2050. To put it into perspective: globally the installed energy storage withheld 143 GW in 2015 (IRENA, 2015).

2.2.4 Types of energy storage services

In order to assess the value and make a distinction between various storage technologies, first the different types of functionalities are introduced. The applications depend on the required time of discharge and the amount of power. The terminology among sources may vary, but a common distinction between services is: long-term storage, short-term storage and distributed battery (self) storage (IEA, 2014).

2.2.4.1 Long-term storage

This service is mostly provided by bulk-storage technologies, which can provide power for a long period of time (hours to days or for seasonal purposes). It is used to decouple the moment of generation and consumption of electric energy (Rahman, 2012). A typical application is arbitrage, where low-priced energy is bought and stored during periods of low demand and sold again during peak hours when prices are high.

2.2.4.2 Short-term storage

These applications operate for a period of seconds to minutes to assure the continuity of power by frequency regulation, voltage support and to enable switching between energy sources, while safeguarding the supply (Rahman, 2012), (IEA, 2014).

2.2.4.3 Distributed battery (self) storage

Batteries have a widespread application field; they can be deployed in both distributed and centralised systems, mobile or fixed and either connected to the grid or 'behind the meter' for self-consumption (IEA, 2014). The latter is done by end users with for example combining solar panels and storage. Although this 'self-optimisation' of energy usage is not necessarily the most efficient (when considering the total system) this distributed storage share is likely to grow, driven by the desire of the consumer to be self-reliant (DNV GL, 2015). When connected to the grid the battery storage could, besides the integration of renewables, serve as frequency regulation and add flexibility on the 'demand-side' for energy (IEA, 2014).

A more comprehensive explanation of the applications is given in the Technology Roadmap Energy Storage (2014) by the International Energy Agency. Figure 16 illustrates the services storage can provide.

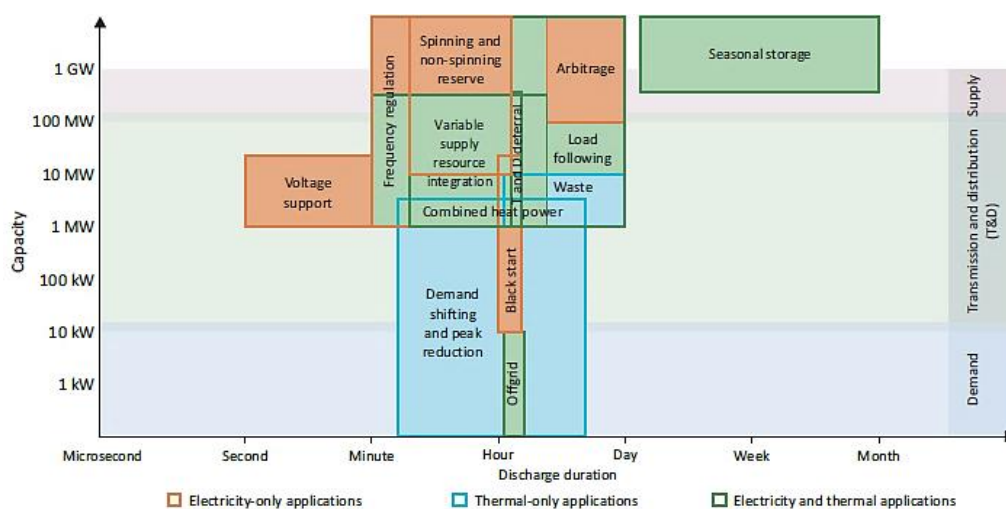


Figure 16: Energy storage applications categorised by their power output, time of discharge and their location in the energy chain (source: IEA, 2014)

2.3 Energy storage technologies

In this section options are reviewed that have the potential of storing large amounts of energy and who can help integrating large shares of renewable energy into the grid.

2.3.1 Pumped hydropower storage

Pumped hydropower storage (PHS) consists out of two connected waterbodies, one upper- and one lower reservoir. In times of energy abundance (or low prices) water is pumped from the lower to the upper reservoir where the energy is 'stored'. Then when there is a shortage of energy, the water is released from the upper reservoir, driving the turbines, and flows back into the lower reservoir.

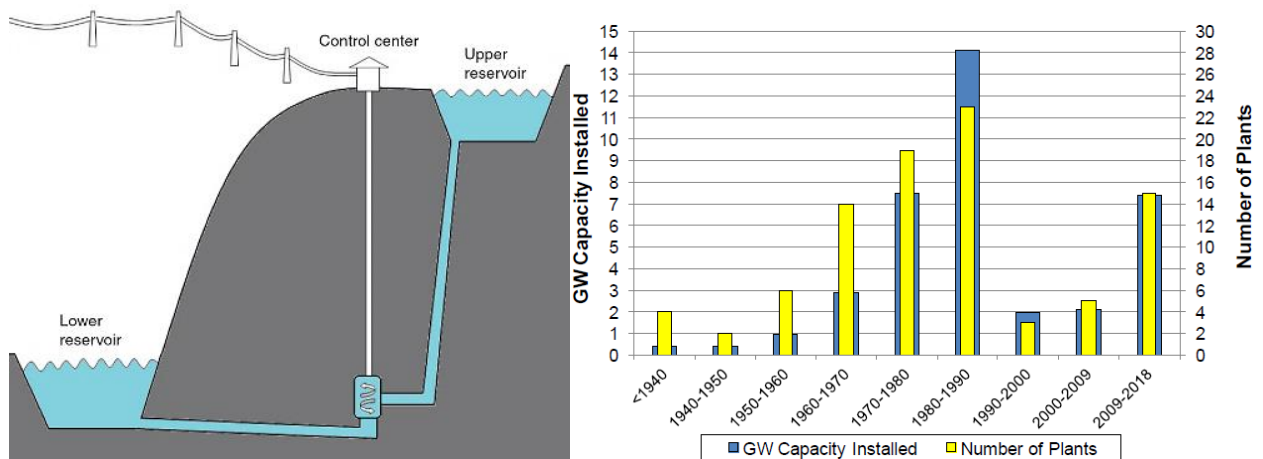


Figure 17: Schematisation of a PHS system (left) and the development of PHS in the EU (right) (source: Letcher, 2016 and Pérez-Díaz et al., 2014)

Europe has around 230 PHS facilities that have a combined capacity of 41 GW. Most of these storage systems were built in the 1970s and 80s out of energy security concerns and alongside the development of nuclear power plants (to provide peak power on top of the baseload power from the nuclear plants and black starts). Nowadays PHS is making a revival with the growing share of intermittent renewable energy and their responsive need for storage, see Figure 17.



Figure 18: Pumped hydro storage facility Hohenwarte 2, Germany (source: Deutsche Energie-Agentur)

2.3.1.1 Technique

Energy is stored by effectively raising the potential energy of the water by pumping it to a higher level. The relation between head and energy is as follows:

$$E_p = mgh = \rho Vgh = \rho A' \delta hgh$$

- E_p = potential energy (J)
- m = mass (kg)
- g = gravitational acceleration (m/s^2)
- h = head, difference in water level between upper- and lower reservoir (m)
- ρ = density of water (kg/m^3)
- V = volume of water (m^3)
- A' = effective surface area, equal to the surface area for a rectangular reservoir (m^2)
- δh = 'thickness' of water layer of upper reservoir (m)

The power then that can be generated is dependent on the discharge rate and the efficiency of converting the potential energy in electrical energy:

$$P = \rho g Q h \eta$$

$$P = \frac{E_p}{t}$$

- P = power (W)
- Q = discharge of water (m^3/s)
- η = efficiency (-)
- t = time (s)

From the equations above it can be deduced that the power and storage capacity mostly rely on the difference in head, reservoir size and possible discharge. Naturally these are very location dependent parameters, resulting in a large range of storage plant layouts. The typical characteristics of a pumped storage plant are given in Table 2.

Characteristic	Range
Head	5 – 1200 m
Storage capacity	100 MWh – 5 TWh
Installed power	20 – 3000 MW (10 – 500 MW per turbine)
Roundtrip efficiency	75 – 85 %
Response time	45 s (from full pumping to full generation mode)
Levelised cost of energy storage (WEC, 2016a)	0.06 – 0.13 €/kWh

Table 2: PHS characteristics



Figure 19: The Okinawa Yanbaru seawater PHS plant in Japan (source: Fujihara et al., 1998)

2.3.1.2 Seawater pumped hydro storage

Although there has been experience with hydropower since 1890, there has only been one plant using seawater. The Okinawa Yanbaru station in Japan (Figure 19) was a 30 MW pilot project that commissioned in 1999 and ran successfully till it was taken out of operation in 2016. The plant was closed, since there was a lack of growth of population and therefore there was not as much demand for storage. Nevertheless it is considered as a successful trial for using the ocean as a lower reservoir. The power plant continued operation during the passage of a typhoon, where stable generation and pumped storage were maintained. The water level fluctuated by

approximately 50 cm, which resulted in an output variation of 1 – 2 %. To cope with the corrosive environment additional measures were required. The penstock was made of fire retardant polymers and the runners from stainless steel. Where conventional steel had to be used, there was cathodic protection or anti-corrosion coatings (Fujihara et al., 1998). There were no issues with marine growth or environmental impacts (Waterpowermagazine, 2000).

2.3.1.3 Technological development

With the revival of PHS to integrate renewable energy sources and large installed capacity, there is still ongoing technological improvement of this mature technology. The electro-mechanical part is enhanced with improved generators, gearboxes and variable-speed turbines. From the operational perspective, management schemes are improved, which increase plant efficiency and result in higher revenues. One of the results of the developments in the electro-mechanical part is the reduced response time, now a Francis turbine can switch from full load pumping mode to full load turbine mode within 45 seconds and in 60 seconds the other way (Pérez-Díaz et al., 2014).

Additionally it is worth elaborating on the variable-speed technology, which enables PHS facilities to regulate the frequency in both generation and pumping mode and run at higher efficiency in both modes at partial load as well. This technology is already widely applied and besides adding stability to the grid, it can increase the roundtrip efficiency by as much as 5 % for a 250 MW turbine (Rudelle, 2016).

2.3.2 Compressed air energy storage

With Compressed Air Energy Storage (CAES) air is pumped into a depleted salt dome or gas reservoir where it is stored under pressure using a surplus of electricity. When energy is needed, the compressed air is heated and expanded in an expansion turbine driving a generator for the production of power. In case waste heat is captivated and used for heating the air via a recuperator (Figure 20), the efficiency increases from approximately 42 % to 55 %. The efficiency level can be raised further by also using the waste head generated by the compressor up to 70 %, which is referred to as the adiabatic method (Energy Storage Association, 2017). There are only two existing CAES plants, one in Huntorf, Germany, and one in McIntosh, USA. Both rely on the diabatic method, where only heat from the expansion turbines is recuperated. For heating the air prior to the electricity generation natural gas is used, making it not a completely CO₂ free facility. However, the emissions are cut by 2/3 compared to conventional gas fired turbines (Energy Storage Association, 2017).

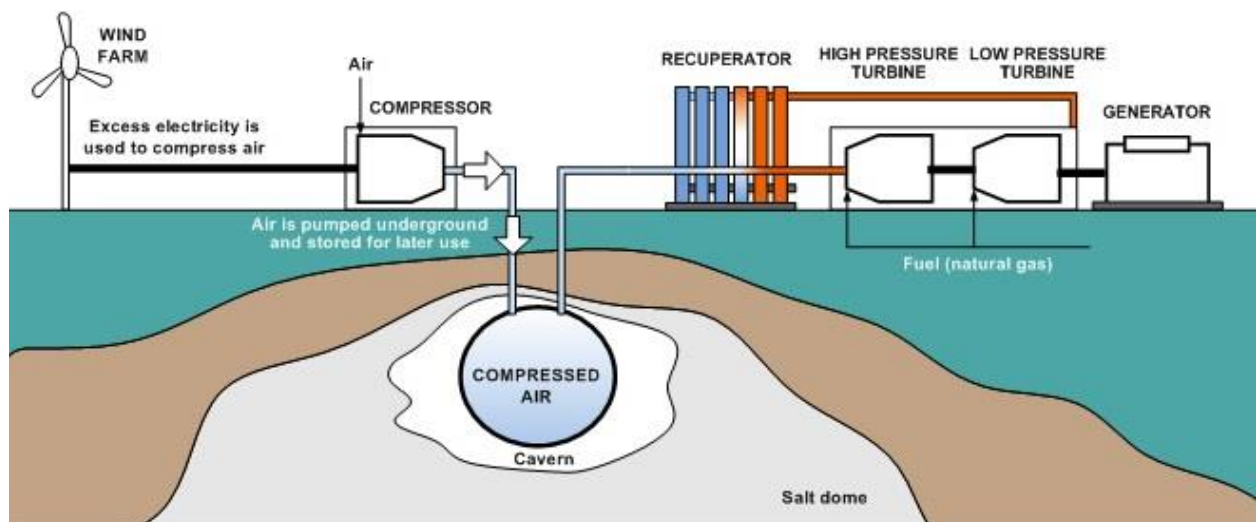


Figure 20: Schematization of a CAES system (source: San Martín et al., 2011)

2.3.2.1 Technique

When air is compressed, its temperature will rise correspondingly.

$$T_2 = T_1 \left(\frac{P_2}{P_1} \right)^{\frac{K-1}{K}}$$

- T_1, T_2 = temperature before and after compression
- P_1, P_2 = Absolute pressure before and after compression
- K = polytropic index of the irreversible compression

After compression the generated heat can be either retained by the stored air itself or extracted and stored in another medium. Later the same heat could be returned to the air before its being expanded in the turbines (adiabatic method).

The electrical performance of a CAES system can be estimated by the electricity that can be generated per storage volume.

$$\frac{E_g}{V_s} \quad ; \quad E_g = \eta \int_0^t m_T W_{CV,TOT} dt$$

- E_g = energy generated
- V_s = volume of storage reservoir
- η = efficiency
- t = time required to empty the storage reservoir
- m_T = air mass flow rate
- $W_{CV,TOT}$ = total mechanical work, per unit mass

Based on the above equations it can be deduced that the performance of CAES depends largely on what is being done with the ‘waste’ heat and to what level the air can be compressed. Some typical numbers belonging to a CAES system are shown in Table 3.

Characteristic	Range
Storage capacity	1.5 – 3.0 GWh
Installed power	100 – 500 MW
Roundtrip efficiency	40 – 55 % (60 – 70 % planned)
Response time	5 - 15 min
Levelised cost of energy storage (WEC, 2016a)	0.08 – 0.15 €/kWh

Table 3: CAES characteristics

2.3.2.2 Technological development

Although there are only two existing CAES plants, many are planned and expected to start operation around 2020. Where the Huntorf and McIntosh (Figure 21) facilities have efficiencies of 42 and 55 % respectively, future stations will be equipped with improved waste heat systems leading to efficiency levels up to 70 %. The reaction time of several minutes is similar to conventional gas fired turbines (Energy Storage Association, 2017).



Figure 21: The McIntosh CAES plant in Alabama, USA
(source: <https://www.wired.com/2010/03/compressed-air-plants/>)

2.3.3 Batteries

Batteries are a form of electrochemical energy storage and can basically be divided into two subgroups: flow- and classic batteries. Where with classic compositions ions migrate from the cathode through the electrolyte towards the anode during charging, flow batteries only consist out of two separated electrolyte liquids which act as the cathode and anode themselves. The tanks that contain the electrolytes can easily be scaled up, allowing for large-scale applications. However, the energy density of flow batteries is much lower than for classic batteries, restricting its use to large-scale non-mobile applications (EASE, 2017).

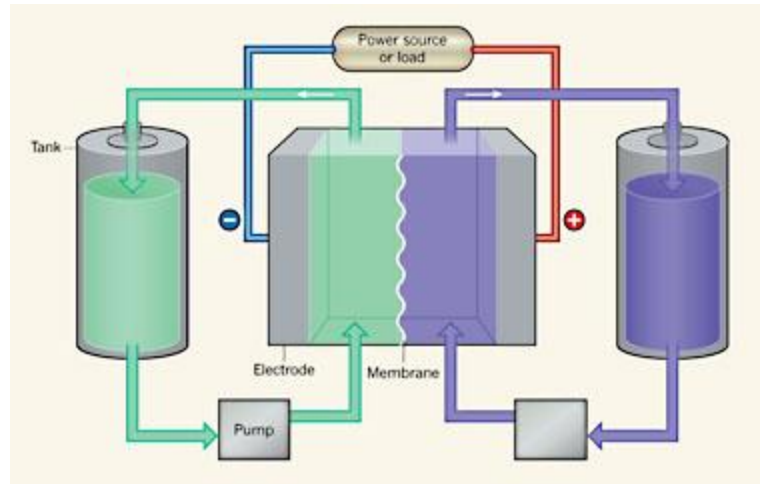
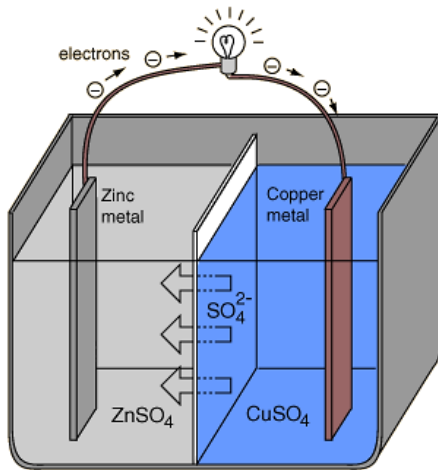


Figure 22: Schematization of a classic battery (left) and a flow battery (right) (source: <http://hyperphysics.phy-astr.gsu.edu/hbase/Chemical/electrochem.html>)

2.3.3.1 Technique

The relation between power, current and resistance, as found by James Prescott Joule, is given as:

$$I = \frac{E}{R} \quad ; \quad P = I^2 R = \frac{E^2}{R}$$

- I = current (A)
- E = voltage (V)
- R = resistance (Ω)
- P = power (W)

The energy capacity depends on the time that a battery can deliver power. Consequently the performance of electrochemical storage relies namely on the difference in charge between the electrodes, the ease they 'lose' their electrons to the electrolytes, the ability of the electrolytes and membrane to transfer the charge and the size of the whole system. Generalised figures for battery storage projects are shown in Table 4.

Characteristic	Range
Storage capacity	0 – 10 MWh
Installed power	0 – 50 MW
Roundtrip efficiency	65 – 92 %
Response time	milliseconds
Levelised cost of energy storage (WEC, 2016a)	0.11 – 0.70 €/kWh

Table 4: Characteristics for classic and flow batteries combined

In 2008 a wind-to-battery project was launched in Minnesota, USA. A 1 MW and 7.2 MWh sodium-sulfur battery was added to a 10 MW wind farm (see Figure 23). The overall efficiency of the system, including auxiliary energy requirements, varied between 67.6 % to 78.9 %, depending on the mode of operation. From all the services, the energy storage system provided, frequency regulation was the most aggressive on the batteries. The University of Minnesota found that the optimal ratio of storage to wind for the single goal of shifting wind generation is 0.2 – 0.4 MW per MW of installed wind power, under the restriction that the storage should generate power for 6 peak load hours per day (Himelic & Novacheck, 2011).



Figure 23: The sodium-sulfur battery connected to the wind farm (source: Himelic & Novacheck, 2011)

2.3.3.2 Technological development

There is general consensus that electrochemical storage is most likely to experience the largest development. The automotive, energy and other mass markets are all poised to reduce battery costs and improve their applicability (EASE, 2017). With smarter production methods, increased energy density and lifetime, other (cheaper) materials and recycling processes, the costs of for example Li-Ion are expected to drop by 30 to 50 % by 2025 (Energy Storage Update, 2015).

2.3.4 Vehicle to grid

Vehicle to grid (V2G) is basically one of the applications of distributed battery storage. Various services are subscribed to integrating electric vehicles (EVs) with the grid, from large-scale renewable energy integration and peak shaving to balancing and ancillary services. There are many pros and cons related to the implementation of V2G.

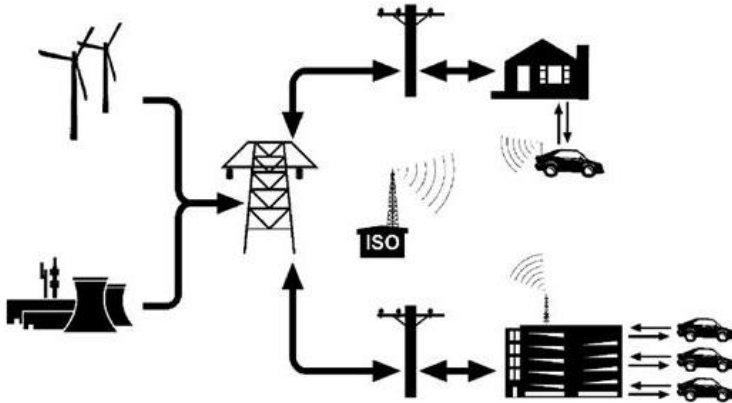


Figure 24: V2G schematisation within a smart-grid (source: <http://www.seminarreports.in/2013/05/vehicle-to-grid.html>)

Considering the amount of automotive vehicles the potential storage capacity is enormous. With the batteries reacting instantaneously, high-value regulation services can be provided. Furthermore, the EVs can act as spinning reserves (payments are received for solely having power available and additional payments for when power is actually dispatched).

Research suggests that vehicles will most likely not play a role in the wholesale market, since centralised stations can generate power more economically. However, V2G systems show compelling results for the ancillary market, where money may be lost per kWh sold, the capacity payments for being available should more than make up for it (Kempton & Tomić, 2005). Consequently electric vehicles can reduce the required capacity for back-up power from conventional plants and therefore defer additional investments in redundancy and capacity of the electric infrastructure.

On the contrary there are arguments against the V2G philosophy. JB Straubel, Chief Technical Officer of Tesla inc., states that feeding power back into the grid would have too much of a negative impact on the battery life. The battery pack in EVs is not designed to need as many cycles to charge/discharge as stationary batteries are. Delivering power back into the grid will thus be uneconomical due to the deterioration of the batteries. Considering the battery lifetime, 'dynamic loading' is seen as a potential asset for the grid. Under dynamic loading it is understood that, although the EVs may be plugged in for a long period of time, the batteries are only charged when electric energy is abundant and so they reduce the peaks and alleviate the pressure on the grid.

Ultimately it is expected that electric vehicles will only allow dynamic charging and not feeding back into the grid in the near and middle term future. Therefore V2G is more of a 'demand response' measure than it is actual energy storage.

Evolution of EVs, batteries and V2G integration will take some time. Furthermore, electric vehicles disrupt three big industries: automotive, utility and oil. Conversely the arguments for electric commuting regarding emissions and the future electric power generation are compelling. Nissan already deployed a trial of V2G in the United Kingdom in 2016, where one hundred EVs can be connected to a domestic battery pack for power exchange. For now it is yet to be determined what the actual possibilities are regarding vehicle-to-grid technology.

2.3.5 Power to gas

With power to gas (P2G) often there is referred to the process of converting electric energy into hydrogen via electrolysis. The hydrogen can then be stored in a pressure vessel until energy is requested and the hydrogen is turned back into power and fed into the grid. Additionally, the hydrogen can be combined with carbon dioxide to form methane, synthetic natural gas (SNG), which can be directly injected into the existing gas network (only 0.1 % of hydrogen itself is allowed to be mixed with natural gas to be incorporated in the gas system). The processes and potential applications P2G offers are depicted in Figure 25.

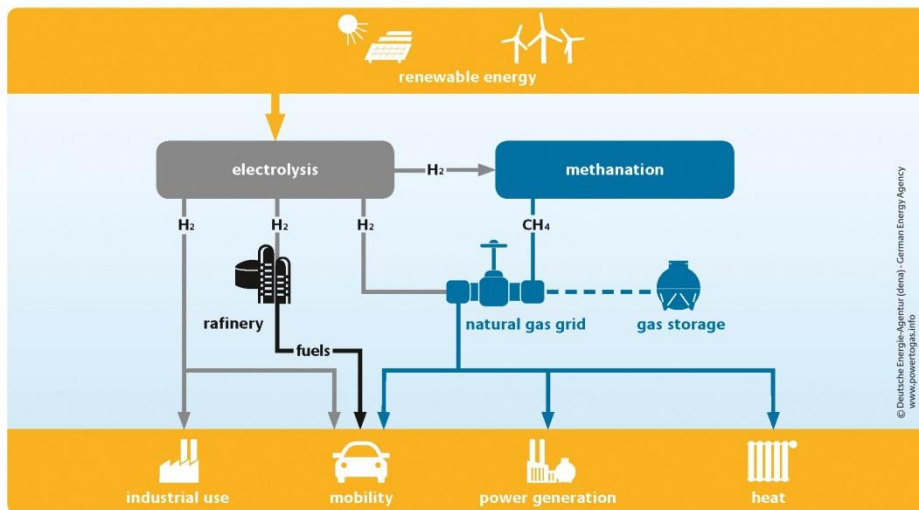


Figure 25: Power to gas technology and possible applications (source: Deutsche Energie-Agentur)

Unlike battery storage, gas can be stored for virtually unlimited time without slowly draining its energy content. This specific feature makes gas storage highly suitable for long-term and seasonal storage. Currently there are circa 40 relatively small projects operating in Europe with many more in the pipeline (European Power to Gas Platform, 2017).

2.3.5.1 Technique

Hydrogen is produced from water through an electrolysis reaction. Water is first split into protons, oxygen and electrons at the anode. The protons flow through a membrane towards the cathode, where the electrons travel through an external circuit. Thirdly the hydrogen and electrons recombine at the cathode and hydrogen is produced. This process of generating hydrogen from power has an efficiency of roughly 75 %, which can be improved to 86 % when the waste heat is recouped (Deutsche Energie-Agentur, 2017). However, this only represents the conversion from power to hydrogen. When electric power is transferred into hydrogen, which is then turned into methane, little power remains for consumption, as can be seen in Figure 26.

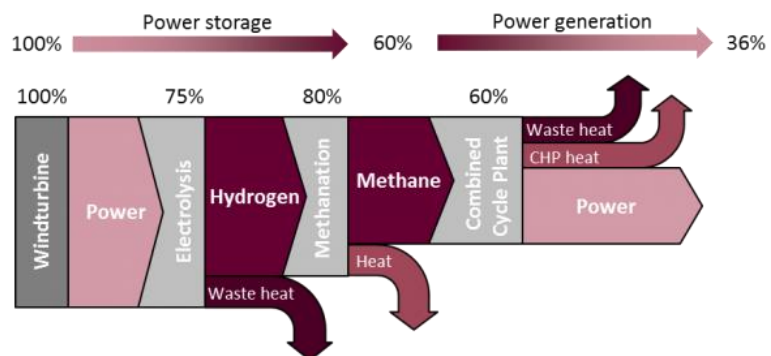


Figure 26: Power to gas to power schematization (source: <http://energy.sia-partners.com/enabling-integration-renewables-europes-energy-system>)

In Table 5 the general figures of a P2G system are shown. With the existing gas infrastructure already in place, the storage capacity is extremely large. Combined with the ability of maintaining its energy when stored, it is highly suitable for long-term storage.

Characteristic	Range
Storage capacity	10 MWh – 10 TWh
Installed power	1 MW – 2 GW
Roundtrip efficiency (power-gas-power)	35 – 46 % (For methane and hydrogen resp.)
Response time	10 min
Levelised cost of energy storage (WEC, 2016a)	0.31 – 0.70 €/kWh

Table 5: Characteristics of a power to gas energy storage system

On the island of Utsira, Norway, the first full-scale wind power and hydrogen plant combination started operation in 2004 (Figure 27). The project aimed to demonstrate how safe, efficient and continuous energy could be supplied to remote areas from renewable energy sources. Even though the system operated successfully, several challenges were encountered. The wind energy utilisation was only 20 %, reflecting the need for more efficient components and processes. Ultimately it was concluded that a similar system should be competitive with conventional remote-site power supplies in about five to ten years (IPHE, 2011).

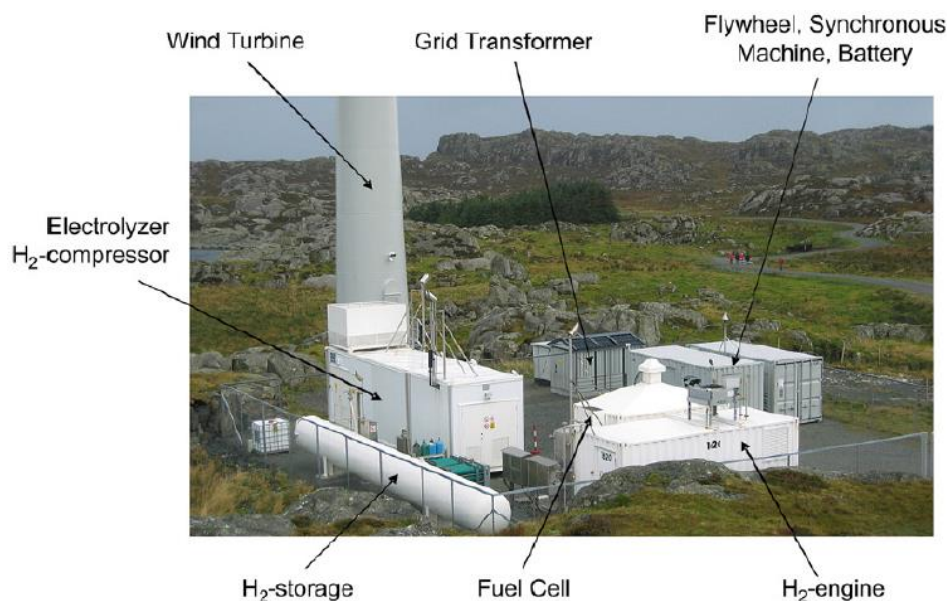


Figure 27: The wind power and hydrogen plant in Utsira, Norway (source: IPHE, 2011)

2.3.5.2 Technological development

As for the batteries and vehicle to grid technology there are various drivers for P2G development, from a utility, mobility and industry perspective. For now there is no viable business case for hydrogen or SNG. Besides improving efficiencies of the electrolyser and methanation steps, increasing the hydrogen admixture in the natural gas network, research and demonstration of employing underground caverns for storage is on the way (EASE, 2017).

2.3.6 Comparison of energy storage technologies

Based on the characteristics of the reviewed technologies in Table 6 it can be deduced that although they are all relatively large-scale storage solutions, they are still bound to different applications (see Figure 16). Note that vehicle to grid is not included in the table, since the storage and power capacity fully relies on the number of electric vehicles and the local grid infrastructure. The efficiency and response time of V2G will be similar to other batteries and the levelised cost of storage (LCOS) higher.

Characteristic	PHS	CAES	Batteries	P2G
Storage capacity (GWh)	0.1 – 5,000	1.5 – 3.0	0 – 0.01	0.01 – 10,000
Installed power (MW)	20 – 3000	100 – 500	0 – 50	1 – 2000
Roundtrip efficiency (%)	75 – 85	40 – 55	65 – 92	35 – 46
Response time (min)	<1	5 - 15	<<1	10
Levelised cost of energy storage (€/kWh)	0.06 – 0.13	0.08 – 0.15	0.11 – 0.70	0.31 – 0.70

Table 6: Generalised characteristics of energy storage technologies

The limited scalability of battery systems make them comparatively unsuitable for balancing the output of large wind farms. From the remaining three technologies, PHS, CAES and P2G, pumped hydro distinguishes itself with its higher efficiency and shorter response time. A higher roundtrip efficiency results in larger quantities of energy that can be bought and sold and therefore a higher utility rate and corresponding revenues. A significantly shorter response time opens up other energy value markets like frequency regulation from which earnings can be generated on top of the long-term services.

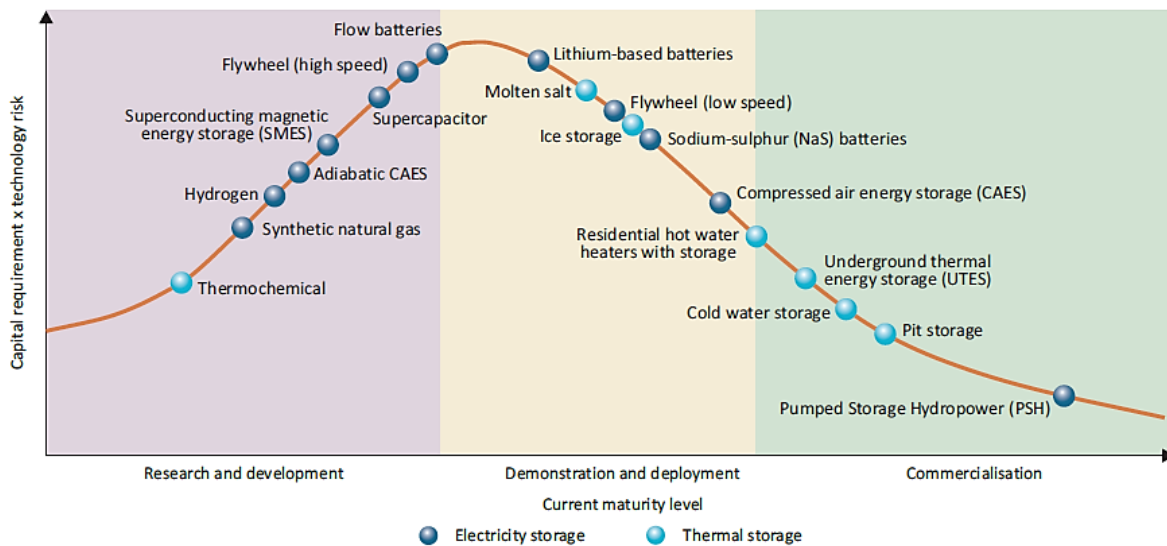


Figure 28: Maturity level of energy storage technologies (source: IEA, 2014)

As is depicted in Figure 28, PHS is the most well-established energy storage provider with over 100 years of experience and technological development. Consequently pumped hydro projects carry the least amount of risk and uncertainty.

In terms of environmental impact the reviewed options differ in their 'footprint'. PHS can have a notable effect in the local area, because it is the least energy dense storage alternative and therefore requires a large area. Furthermore, a dam can impede fish-migratory routes and sediment transport in case a valley is 'closed' to create the required difference in hydraulic head. Current CAES and

(synthetic) power to gas methods are not emission-free by themselves and the production of batteries can necessitate disputable mining activities. Overall it is hard to tell which technology is the most environmentally sensitive, since for most cases it will be location dependant. If future adiabatic CAES can discard the need for natural gas in the process, it will most likely become the most environmentally sound solution.

2.3.6.1 Levelised cost of energy storage

It can be difficult to assess what the actual costs of various storage methods are, as they have other investment and operation costs, efficiencies, utility rates and lifetime. To enable comparison between storage technologies the LCOS is used. Although this term suggests that all factors of influence on costs are covered, not all LCOS-analyses contain the same inputs. Thus one has to be cautious when using LCOS from different sources. In this analysis the values and approach of the World Energy Council (WEC) from 2016 are used.

$$LCOS = \frac{I_0 + \sum_{t=1}^n \frac{A_t}{(1+i)^t}}{\sum_{t=1}^n \frac{M_{el}}{(1+i)^t}}$$

- LCOS = Levelised Cost Of energy Storage (€/MWh)
- I_0 = Investment costs (CAPEX) (€)
- A_t = Annual total costs in year t (OPEX) (€)
- M_{el} = Produced electricity in each year (MWh)
- n = Technical lifetime (years)
- t = Year of technical lifetime (1,2,...,n)
- i = Interest rate (WACC) (%)

According to this formula, the average cost per ‘produced’ / stored kWh are as shown in Figure 29.

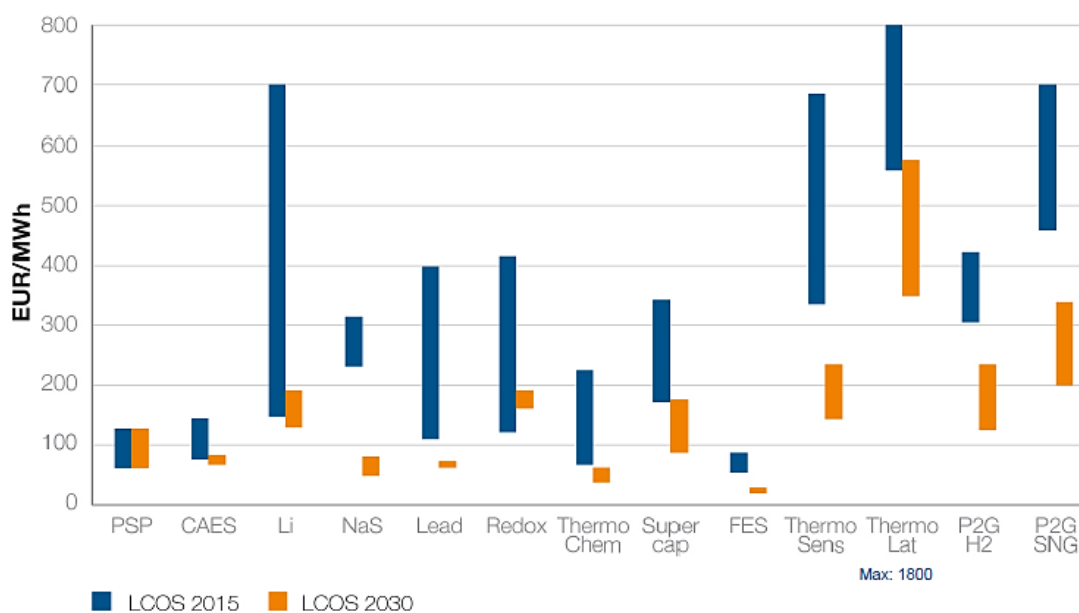


Figure 29: Range of levelised cost of storage for various technologies (source: WEC, 2016a)

All storage technologies are expected to have a massive drop in LCOS, except for PHS (which reflects its level of maturity). Based on this figure it appears that pumped hydro power will no longer be the single most-economic technology by the year of 2030. However, when the energy storage facility is combined with a wind farm, the expected LCOS tells a different story; see Figure 30.

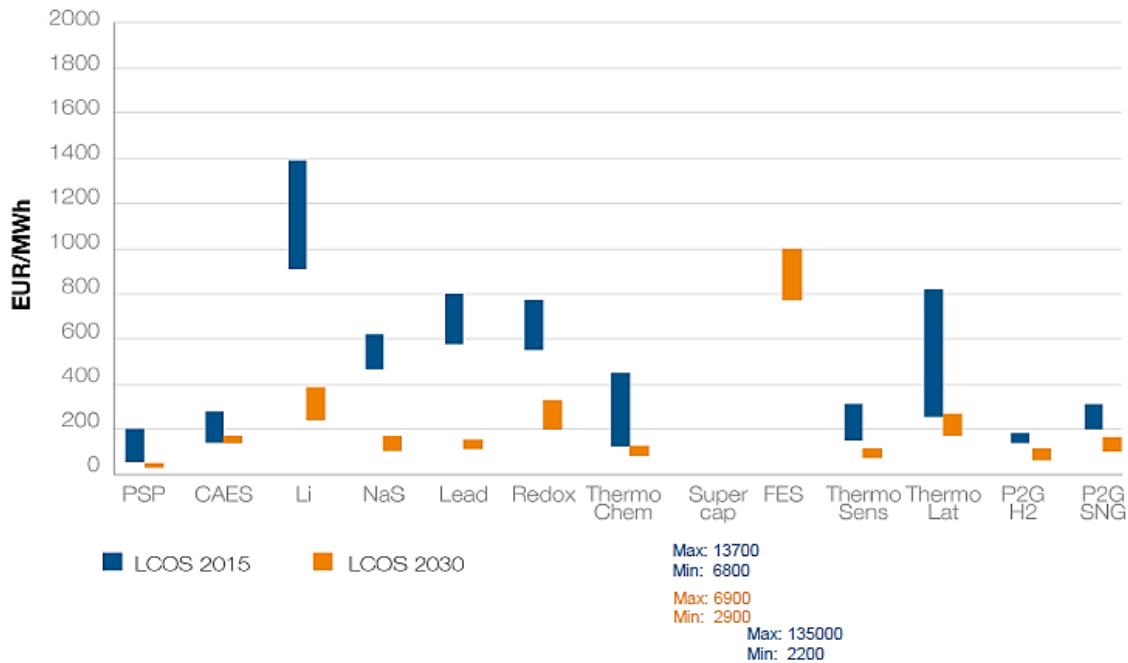


Figure 30: Levelised cost of storage for various technologies in combination with a wind farm (source: WEC, 2016a)

The reason that batteries are much less suitable to store wind energy is because they are very sensitive to the number of discharge cycles and require a (suboptimal) higher storage capacity over power ratio. It is important to note that this specific LCOS analysis is for wind conditions where it is necessary to store energy for a 24 hour period and no short-term applications, as described in 2.2.4.2, are included in the revenue stream.

In a study by the Energy research Centre of the Netherlands (ECN) the market value of large scale electricity storage options for the Netherlands was investigated (De Joode et al., 2014). From the reviewed PHS, CAES and P2G, the pumped hydro alternative proved to be most beneficial. Due to its higher efficiency PHS could not only benefit from storing a surplus of wind energy, but also from the day-ahead market (arbitrage).

2.3.7 Concluding remarks on energy storage technologies

In Europe pumped hydro storage represents circa 90 % of the grid-connected storage capacity and continues to be identified as being the most cost-efficient large-scale energy storage technology available today (Pérez-Díaz et al., 2014) and in the future (WEC, 2016a).

CAES is a good alternative, but also restricted to suitable sites. For heating the air prior to the electricity generation natural gas is used, making it not a completely CO₂ free facility (emissions are cut by 2/3 compared to gas turbines). New CAES facilities that are being developed hope to raise the roundtrip efficiency from a mere 55 % to 70 % by taking additional heat recovery measures. In case future demonstration projects manage to exclude the usage of natural gas altogether, this technology can become a valuable link in a sustainable energy chain.

Battery costs are expected to fall in the near future (WEC, 2016a). The sodium-sulfur flow battery looks especially suitable for stationary 'large-scale' applications, where the lithium-ion battery seems most appropriate for mobile applications (considering its energy density compared to a lead-acid battery). Nevertheless it is unlikely that batteries will provide long-term and bulk energy storage services, due to its physical constraints.

As is explained in 2.3.4 Vehicle to grid, it is expected that electric vehicles will only allow dynamic charging and not feeding back into the grid in the near and middle term future. Therefore V2G is more of a 'demand response' measure than it is actual energy storage. Yet it is a technology prone to extensive research, considering the large interest of the automotive industry. Consequently current beliefs might turn out different in the future.

Hydrogen storage and usage is inevitably related to safety issues, especially for the transportation sector. Converting power to gas to power is simply too uneconomical on a day-to-day basis. Using existing gas infrastructure is one of the main advantages of P2G and for synthetic natural gas especially. However, the carbon that is added to hydrogen for making SNG will eventually be emitted anyway; counteracting the initial gains from carbon capture from e.g. coal fired power plants. Therefore this type of P2G is not sufficiently sustainable to meet climate change goals.

Considering investments to be made in new infrastructure it is likely that a single energy carrier will dominate the market in the future. Whether this will become gas or electric power is yet to be seen. In terms of efficiency it is preferable to have an economy (power generation, industrial-, transportation- and domestic use) running on a single type of energy, to minimise energy conversions and their corresponding losses. Where power to gas has a slight advantage with its infrastructure already in place, an all-electric system has the upper hand with higher efficiencies, safety in mobile applications and sustainability. Along this line of reasoning it is favourable to have an energy storage system with electric power as its output too.

Based on the literature reviewed, data obtained and future developments taken into account, it is concluded that pumped hydro is the best storage alternative to incorporate large shares from renewable energy sources into the energy market.

2.4 Potentially realisable pumped hydro storage

In the previous section it was concluded that PHS offers the most-economic solution to deal with inevitable future energy security and reliability issues. In this paragraph there is checked whether there is enough potential left yet to develop, to suffice to future need.

A study by the eStorage-group into the potential locations for new PHS plants in North-Western Europe (see Figure 31) was identified as the most-reliable and transparent source (eStorage, 2015). Firstly a Geographic Information System (GIS) model, based upon the findings by an earlier model (Gimeno-Gutiérrez & Lacal-Aránategui, 2013) from the Joint Research Centre (JRC), was used to point out a theoretical potential of new PHS locations. The results from the GIS-model were presented to a group of (local) experts, who reduced the theoretical potential to a more realistic ‘realisable potential’.

The GIS-model is limited to existing water bodies (excluding the sea), so no upper- or lower reservoir would need to be constructed. Closing a valley in order to create a head difference was also precluded as an option, due to the possible environmental impact. The other criteria used to identify two suitable water bodies are presented in Table 7.

Criterion	Value
Energy storage capacity	> 1 GWh
Distance between water bodies (length penstock)	< 10 km
Head difference	> 80 m
Average slope (limit friction losses)	> 5%

Table 7: Selection criteria used by the GIS-model to recognise potential PHS sites

Moreover projects that would overlap with restricted zones were cancelled out. Under restricted zones are understood: World or National protected areas, infrastructure, industrial and residential areas. Secondly, the identified water bodies were passed onto expert groups of each country, who used local legislation, expertise and demands to narrow down the potential further. The results of the GIS-model and expert selection are given in Table 8.

Assessment	Number of sites	Identified potential (GWh)
GIS-model	714	6924
Expert groups	117	2291

Table 8: Results obtained by the eStorage study

Note the large reduction in water body pairs and potential by the expert-groups. The large difference can be subscribed to varying interest of each nation compared to the criteria used in the GIS-model. For example, Norway (which possesses 54 % of the realisable potential) is not interested in reservoirs that are only bit larger than one GW. The distribution of realisable potential over the included nations can be seen in Figure 31.

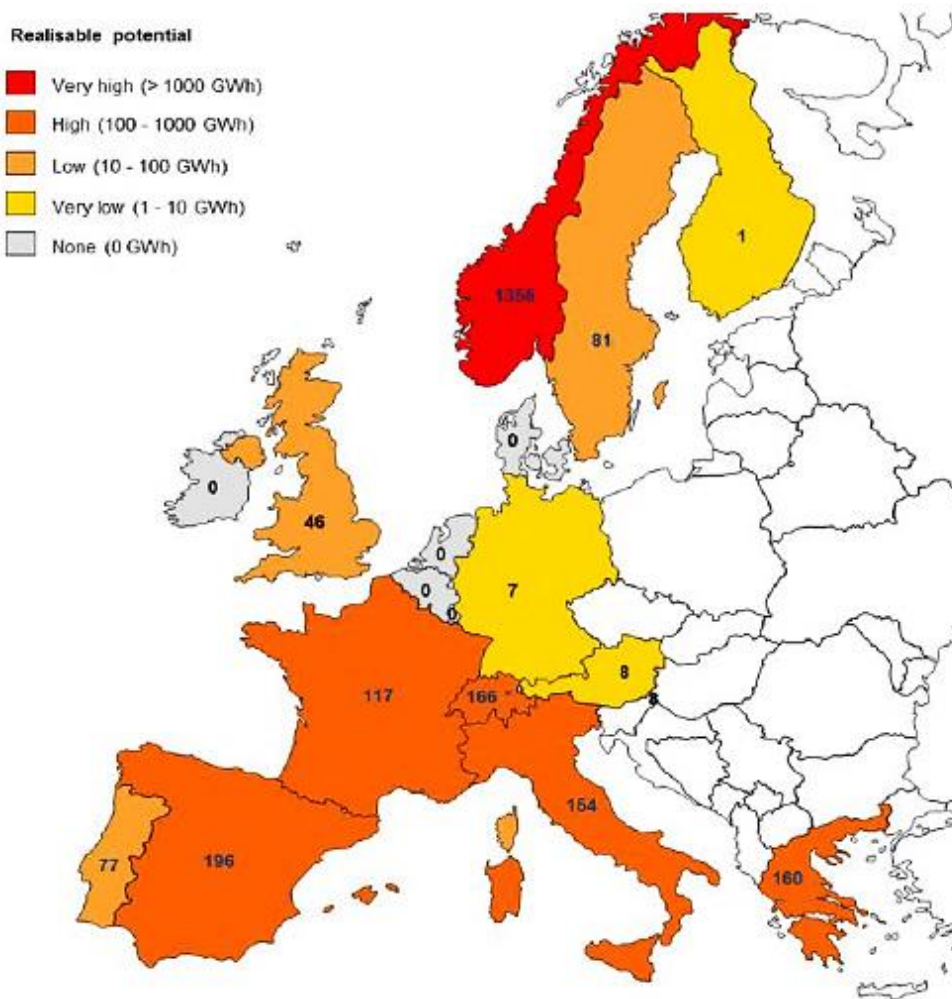


Figure 31: Realisable potential per country (source: eStorage, 2015)

Over half of the PHS potential in the considered area lies in Norway, with the Alps and Pyrenees containing 13 % and 5 % respectively. This illustrates the large dependence of PHS on the geologic conditions.

2.5 Future demand versus potentially realisable energy storage

Today PHS is the only competitive and commercially viable large scale energy storage technology. Therefore it is assumed that saying the remaining PHS left to develop is equal to the potentially realisable energy storage capacity is a just first estimation.

The future demand for energy storage (as worked out in 2.2.3) was determined for North- and West-Europe through the following steps:

1. Energy demand in 2050: 59 % of the usage in 2005-06
2. Renewable energy share: 40 - 60 % of energy demand
3. Required energy storage: 20 – 60 % of renewable energy share

From these ranges, a scenario with 60 % of renewable energy and 20 % required storage per renewable share was chosen, for this particular region. Those assumptions led to a future storage demand of **3584 GWh** for North-Western Europe (including Norway and Switzerland) by the year of 2050.²

In the previous section the remaining potential for PHS was identified. For the same region a realisable potential of **2291 GWh** exists. Although this already fulfils a large part of the required future storage capacity, it is not nearly enough. Furthermore it is unlikely that all the identified sites will be realised, due to potential political and local opposition and the fact that the available locations for new PHS do not coincide with the source of energy storage demand.

2.5.1 Need for alternative energy storage technologies

Since the 'first' option, conventional pumped hydro storage, does not suffice to the energy storage demand, it is worth to look into the second-best alternative. The main drawback of conventional PHS is the limited occurrence of two suitable existing water bodies (see Figure 31). Other than that, it is the preferred storage method in combination with a wind farm (Figure 30). Therefore there is chosen to look into alternative energy storage options, which rely on the same principles and technology as the proven PHS. Between the alternatives there is sought for innovative solutions that pump water from one reservoir to the other just the same, using identical equipment, but are not restricted to the same geologic conditions. Appendix B contains six of these ideas that could complement the conventional PHS in order to enable a secure energy supply.

² Energy usage of North- and West-Europe in 2005-06 was 18477 TWh/yr. With the mentioned percentages this results in a required energy storage capacity of: $0,59 \cdot 0,6 \cdot 0,2 \cdot 18477 = 1308$ TWh/yr. This is equal to 3584 GWh per day.

2.6 Overview of energy storage islands

From the case studies on 'energy islands' the gathered data on costs components and their corresponding storage or power capacity are presented here (see Appendix B for the case studies). Even though only five different designs were reviewed, for different locations and plans originating from 1985 to 2014, the costs estimates can still give insight in the dominant cost components.

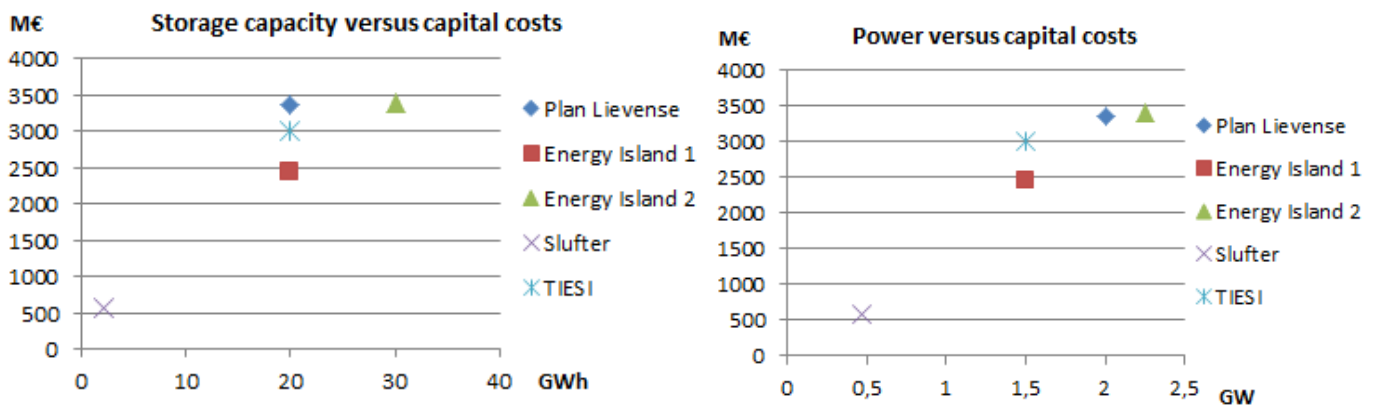


Figure 32: Relation between storage capacity and costs (left) and between power and costs (right)

From the graphs above it becomes clear that it is hard to get an idea of the impact of a larger reservoir or higher installed power, since both factors are incorporated in the two graphs. Therefore a cost breakdown into the following five groups is made:

- Dredging and dam construction → scales with the reservoir dimensions/capacity
- Housing of turbines (all civil works to facilitate the operation of the turbines, including in-outlet system) → scales with the required power output
- Pump-turbines (containing all the mechanical and electrical parts related to the turbines) → scales with the required power output
- HV cable + grid connection → scales with the required power output and distance
- Other

Although the scaling components are certainly not linear (the dredging works for example will be relatively more economic for large quantities) they provide a very accessible way of getting a first estimation of the total capital costs ($\pm 17\%$).

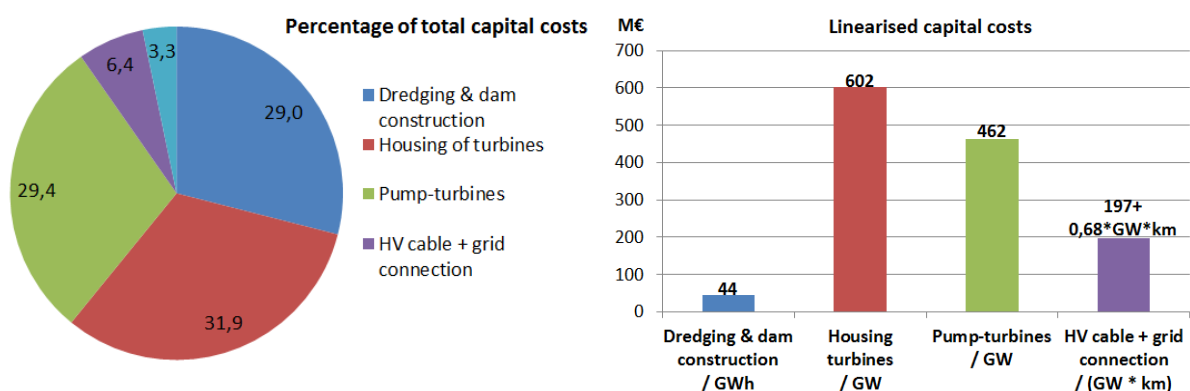


Figure 33: Costs breakdown (left) and linearized 'scaling' components (right) further explained in Appendix B

The costs breakdown clearly shows that there are four main topics to look into for the technical design: the dredging and dam construction (separate subjects), the pump-turbines and their housing. The obtained scalars (elaborated in Appendix D) can be used to compare acquired costs estimates with previous research.

3. Technical design approach

From the literature study it was deduced that an offshore pumped hydropower facility consists out of four main elements: the dam, dredging works, turbines and the turbine housing. The dam and dredging process are collectively responsible for the creation of the storage capacity. The pump-turbines and its housing create the power capacity. The two tracks of 'storage' and 'power' are almost completely uninfluenced by each other. Only the head difference that can be retained by the dam serves as input for the choice of turbine and the structure of the housing (see Figure 34). Note that the dam design and dredging method do have a profound mutual impact on each other, just like the turbines and its housing.

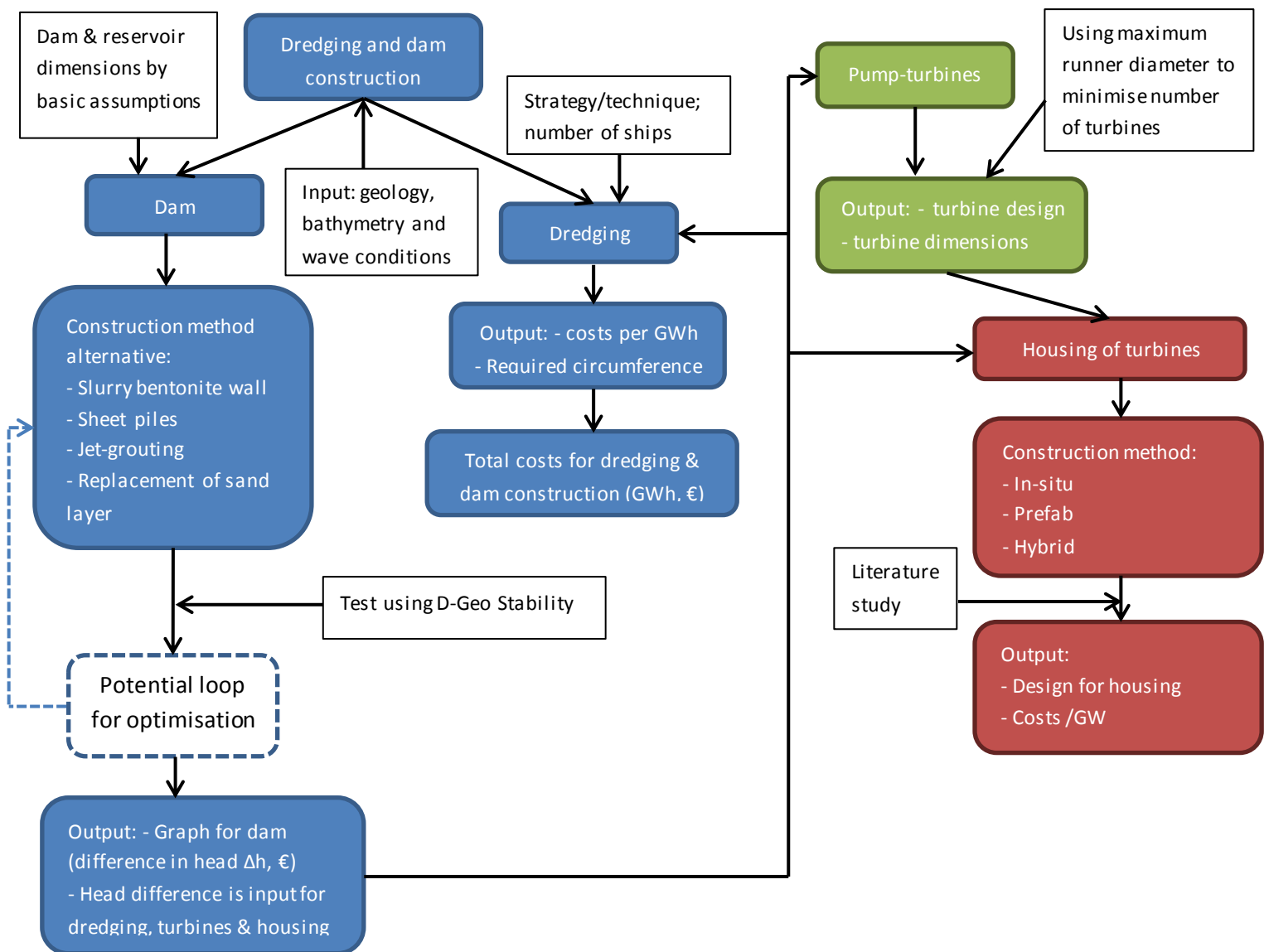


Figure 34: The stepwise design approach of the inverse offshore pumped hydropower facility

The geological conditions, bathymetry, wind and wave conditions are stated in Appendix D: Dogger Bank conditions. Combined they lead to the boundary conditions presented in the next section. For a more profound site description there is referred to either Frölke (2017) or EMU Ltd et al. (2011).

3.1 Boundary conditions

- Significant wave height with a return period of 300 years: 8m and 9s period
- Water depth of 20m
- Wind speeds up to 30m/s for a storm duration of 6 hours
- Highest Astronomical Tide (HAT) of +1.19m and Lowest Astronomical Tide (LAT) of -1.04m
- Storm surge level of 1.40m
- Sea level rise of 3mm/year, which leads to 0.3m at the end of the functional lifetime
- The following simplified soil conditions:

(m)	Soil type and depth ³	Unit weight, γ_d (kN/m ³)	Internal angle of friction, ϕ'_d	Cohesion, c'_d (kN/m ²)	Permeability seepage (m/d)
0	Clay	20	21.24	11.54	0.01
-23	Sand	20	27.96	0	1.0
-30	Clay	20	21.24	11.54	0.01
-65	Sand	20	27.96	0	1.0
-200	Impermeable layer	-	-	-	0

Table 9: Soil stratification and characteristics per layer according to NEN 9997

3.2 Functional requirements

- *Energy function.* The offshore pumped hydropower plant has to be able to store and release electrical energy.
- *Retaining function.* The dam has to remain on its location, retain water safely and prevent large quantities of water flowing from the surrounding North Sea into the storage lake. The same requirement counts for the bottom of the reservoir.
- *Bearing function.* The dam needs to support a road over which heavy equipment can drive to either transport goods related to the powerhouse or for maintenance works on the dam itself.
- *Transmitting function.* The pumped hydropower plant has to be connected to the European grid.

3.3 Failure tree

To get an insight in what may prevent the energy storage facility from fulfilling its functions a failure tree has been made. The failure tree could act as guidance in a future stadium when a more detailed or probabilistic design is demanded. The failure modes of the dam are presented in a failure tree by itself, because of the numerous possibilities. A short note on the risks associated to an inverse offshore pumped storage facility is included in Appendix E: Risks associated to inverse offshore pumped hydro storage.

³ Relative to the seabed level, which is assumed to lay 20m below MSL.

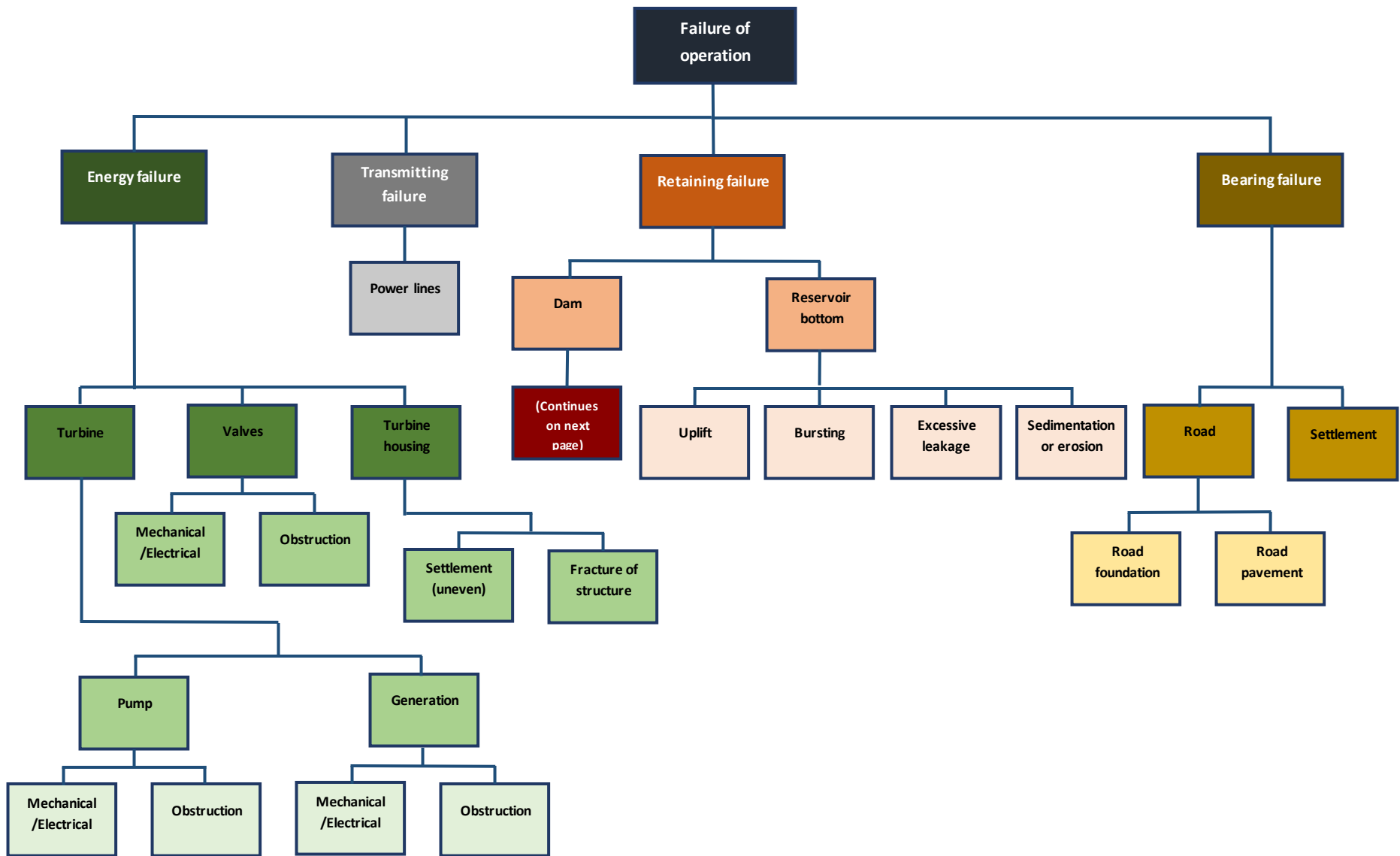


Figure 35: Failure tree of operation based on the functional requirements

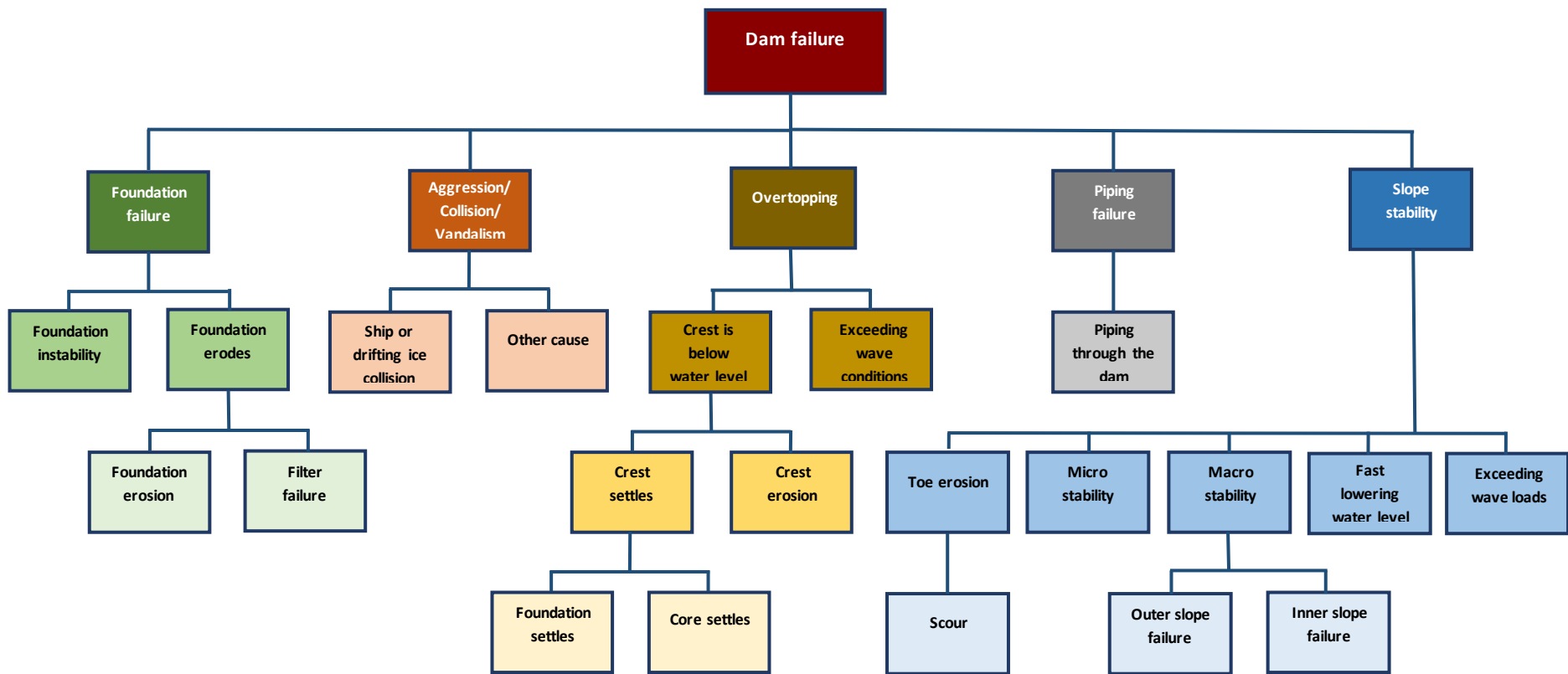


Figure 36: Failure tree of the dam

3.4 Principal scaling of reservoir dimensions

In this section it is shown how an energy storage reservoir scales by adjusting its main parameters: the surface area and/or the reservoir depth. Note that the assumed dimensions differ from the measures as used in the design for the sea defence for the most extreme conditions. On average the crest height for example will be lower than is required for the stretches that have to endure those maximum loads. The average conditions are more relevant when defining the material balance. For the energy storage capacity and the dam dimensions the following considerations are made:

- W_c The crest width is set at 16m (wide enough for two wire cranes to pass each other)
- h_c The crest height is 10m above sea level (limited overtopping for a wide range of different outer slopes)
- d_b The water depth of the sea is 20m
- α_1 The outer slope is 1:5
- α_2 The inner slope is 1:4 (Does not have to sustain serious wave attack or run-up)
- $\frac{H_{max}}{H_{min}}$ The ratio between the maximum and minimum head is 1.25 (typical for a Francis turbine)
- The roundtrip efficiency is 80% (De Boer et al., 2007 and Rijkswaterstaat et al., 1985)
- The reservoir is made circular, since this is the most beneficial shape in terms of circumference and storage volume
- The reservoir is dug out either to a depth of -40m or -60m (depending on the scenario) relative to the mean sea level

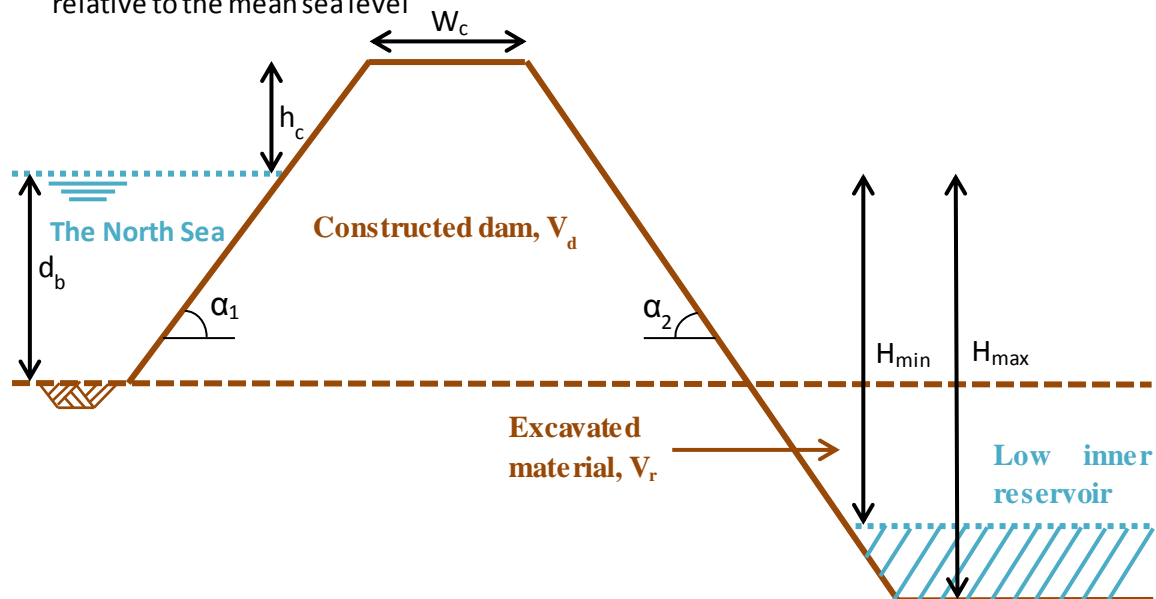


Figure 37: Reservoir design with the parameters that are necessary as input. The numbers used for the parameters are given in Table 10. The maximum and minimum head depend on till what depth the reservoir is excavated.

With the assumptions made above there is looked at how the storage reservoir scales when you increase either the surface area or the depth of the reservoir and the influence on the volume balance.

In scenario 1 (S1) the reservoir is made in such a way that there is an even volume balance, so all the material for the dam construction (V_d) originates from the inner reservoir (V_r) and there is no redundant material ($V_d = V_r$).

Scenario 2 (S2) is also based on an even material balance. However the ‘Energy Hub Island’ (with all the port and electric facilities required to operate the offshore wind farm on the Dogger Bank) will also be constructed with the dredged material from the reservoir. The volume of the complete energy island (V_i) is 190.000.000 m³. Thus the balance for scenario 2 withholds: $V_d + V_i = V_r$

Scenario 3, 4 and 5 (S3, S4, S5) also have a maximum hydraulic head difference of 40 metres, like scenario 1 and 2. They are built to such a scale that their storage capacities are 10GWh, 20 GWh and 30 GWh respectively.

Scenario 6, 7 and 8 (S6, S7, S8) have an increased hydraulic head. In those scenarios the reservoir is brought to a depth of 60 metres. The desired storage capacities similarly range from 10GWh, 20GWh to 30GWh for S6, S7 and S8 respectively.

The input parameters, as explained above and shown in Figure 37, are depicted in Table 10.

Parameters input	Symbol	Unit	Value scenario 1,2,3,4,5	Value scenario 6,7,8
Maximum head difference	H_{max}	m	40	60
Width crest	W_c	m	16	16
Freeboard	h_c	m	10	10
Water depth	h_b	m	20	20
Outer slope angle	α_1	rad	1/5	1/5
Inner slope angle	α_2	rad	1/4	1/4
Roundtrip efficiency	η	%	80	80

Table 10: Parametric values used for the dam dimensions and storage capacity computations

The storage capacity is mainly a function of the fluctuating water volume and the head difference, as can be deduced from the formula:

$$\text{Storage capacity: } E = mgh = V_w \rho g \bar{H} \quad ; \quad V_w = (H_{max} - H_{min}) \frac{1}{4} \pi D_w^2$$

$$E = \frac{1}{4} \pi D_w^2 \rho g \frac{(H_{max}^2 - H_{min}^2)}{2}$$

$$\text{Circumference: } L_D = \pi D$$

- E = Storage capacity (J)
- m = Mass of water (kg)
- g = Gravitational acceleration (m/s²)
- h = Height (difference) (m)
- V_w = Fluctuating water volume (m³)
- ρ = Density of water (=1025) (kg/m³)
- H_{max} = Maximum head difference (m)
- H_{min} = Minimum head difference (m)
- D_w = Average diameter of water surface (m)
- L_D = Total length of dam (m)
- D = Centre-to-centre diameter of the dam (m)

Since with an increasing diameter the storage capacity grows quadratic, whereas the dam construction works enlarge linearly, it shows that the larger the diameter becomes the more favourable the construction works are. The optimum reservoir size will thus be limited by the revenues that can be generated with the energy storage facility, since the larger the reservoir

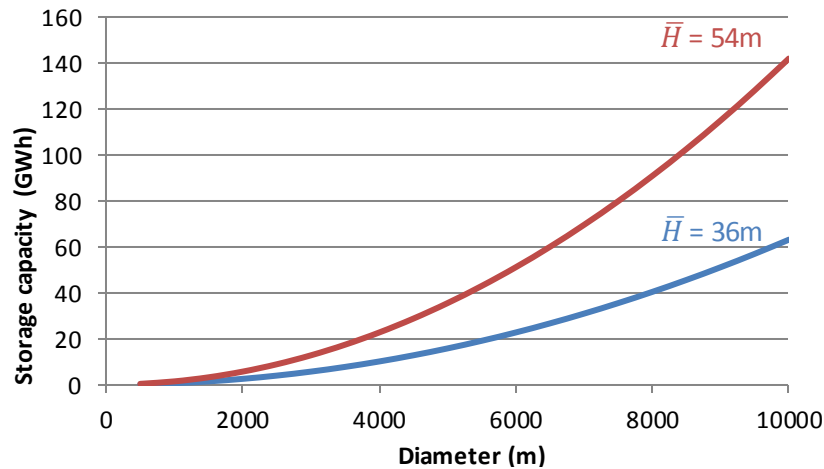


Figure 38: The relation between the storage capacity, average head difference and reservoir diameter

becomes the lower the relative utility rate will be. An extremely large reservoir on an average day might only be used for 10%, where a small one could be utilised fully. Therefore the favourable large reservoir (from a constructability perspective) has to be balanced with the specific utility rate (a larger reservoir generates relatively lower revenues). Figure 38 gives a visual impression of the storage capacity resulting from a certain head and diameter.

The values, as shown in Table 10, were used to compute the necessary reservoir dimensions and the material balance. The results are given in Table 11.

Parameters output	Symbol	Unit	Scenario 1	Scenario 2	Scenario 3	Scenario 4	Scenario 5	Scenario 6	Scenario 7	Scenario 8
Maximum head	H_{\max}	m	40	40	40	40	40	60	60	60
Minimum head	H_{\min}	m	32	32	32	32	32	48	48	48
Diameter C-C	D	m	1,478	4,324	4,355	6,003	7,267	3,170	4,268	5,111
Storage capacity	E	GWh	0.77	9.84	10.00	20.00	30.00	10.00	20.00	30.00
Material left for other purposes	V_{red}	$10^6 \cdot \text{m}^3$	0	190 (=V _i)	193	421	654	195	408	623

Table 11: Dimensions and storage capacities for the various scenarios

Table 11 gives a good impression of the scale of the various storage reservoirs. Furthermore, excavating till a larger depth decreases the required surface area and circumference significantly. For example scenario 7 only has 70% of the diameter of scenario 4 and just half the surface area, whereas the storage capacities are the same.

Another striking element of creating such a storage reservoir is the amount of material that needs to be displaced, ranging between 250 and 750 million cubes! Consequently the creation of a storage facility and 'energy hub island' would be mutually beneficial, since the island could easily be constructed from the dredged material obtained from the storage reservoir. Naturally the spare material could also be used to add other functions to the storage plant or sold for other purposes.

3.5 Volume balance

One of the conditions for a feasible project is an even volume balance. If not, either material has to be sourced somewhere else and be shipped to the site or redundant material has to be shipped and deposited at another site. Both methods would make the project excessively expensive. There are 3 main choices that can be made to end up with an even volume balance:

1. The reservoir is made in deep(er) water, so that the dam requires relatively a lot of material and only a little bit of dredging is necessary to obtain the desired head difference.
2. The reservoir is made in intermediate water, this way the dams still need a lot of material. However, to attain the preferred head difference between the North Sea and the inner reservoir, enough dredged material becomes available to construct the “Energy Island”.
3. The energy storage facility is constructed in relatively shallow water on the Dogger Bank. Since the exact geology throughout the Dogger Bank is still unknown, making the design suitable for the average depth will mark it the most widely applicable for this project. Furthermore, the costs of the dam itself (which are solely a great expense) stay limited. Additionally, the redundant material from the dredging can be put to different use: either by adding other ‘land-demanding’ functions that can generate extra revenue to the island or by selling the material for someplace else.

The three main alternatives for obtaining a level volume balance are shown in Figure 39 and quantified in Table 12.

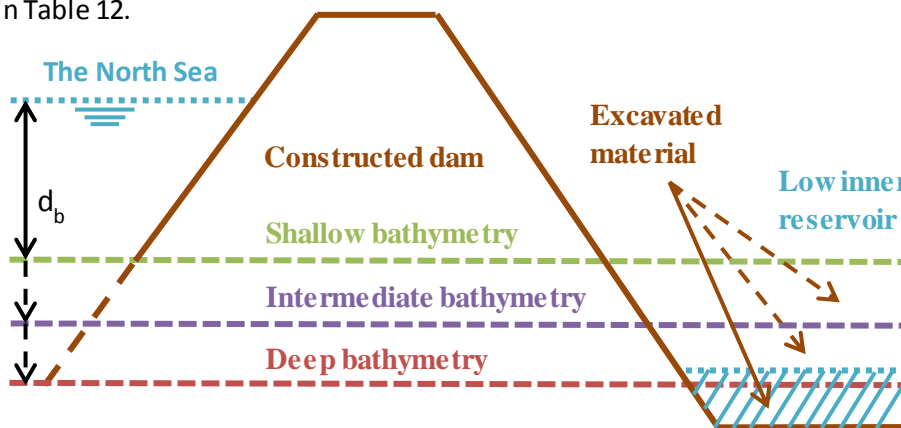


Figure 39: The volume balance depends on the relation between the initial water depth, the required dam size and the volume that needs to be excavated from the inner reservoir to attain the desired head difference

Volume balance scenario	Water depth (m)	Thickness of layer to be dredged from reservoir (m)	Total dam volume (10 ⁶ m ³)	Redundant material (10 ⁶ m ³)
A. Deep water	33.8	6.2	153.4	0
B. Intermediate water	27.6	12.4	119.8	190 (= “Energy Island”)
C. Shallow water + additional functions	20.0	20.0	84.4	420 (= “Energy Island” + other functions)

Table 12: The characteristics of the three volume balance scenarios. Note that the numbers relate to a storage reservoir with a maximum head difference of 40m and 20GWh storage capacity (Scenario 4). The dam and dredging volumes are indicative and may change slightly according to the choice of slopes and crest width.

From the presented scenarios the shallow water alternative (20m depth) is chosen, since the (unexploitable) dam costs stay limited and it allows for many extra functions that can contribute to the overall project.

4. Dam design

The dam design can be split up in three main parts: the sea defence on the outer slope, the inner slope and the works necessary in order to create an impervious storage reservoir. For all three aspects alternatives have been looked at. Once a preliminary design is made it can be verified on the applicable failure mechanisms. This loop of designing and verification eventually leads to a 'final' design. The designing process is materialised in Figure 40.

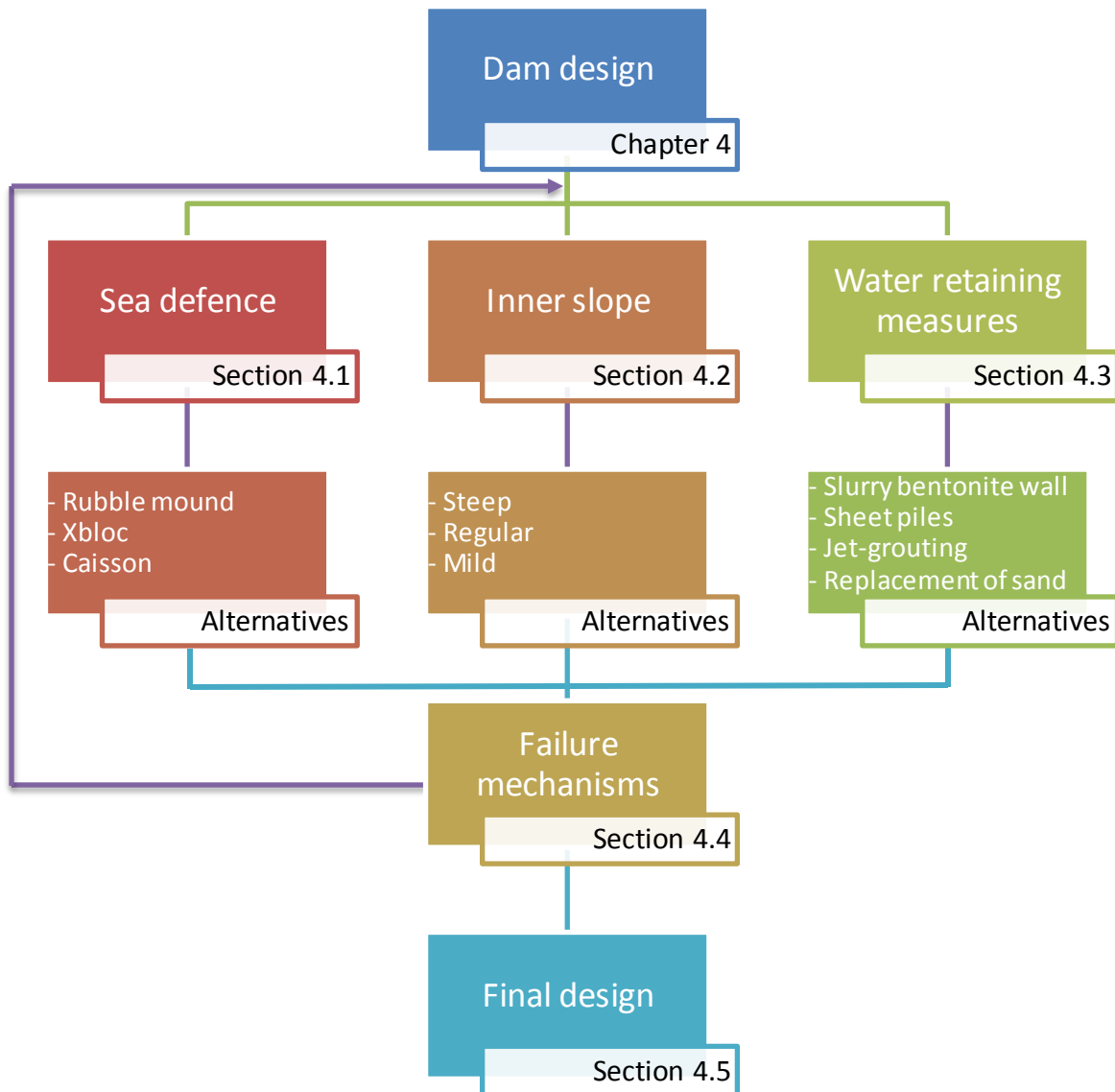


Figure 40: Design process of the dam

For the protection against the waves it quickly became clear that a conventional single layer concrete armour would be the best option. A soft protection would require high maintenance costs in conditions with 8m waves. A rubble mound breakwater is not feasible either, due to the extreme wave conditions. Generally a protection of natural rock is limited to a significant wave height of 3.5 metres. In terms of load resistance an alternative could be a caisson structure. Since the dam will have to be constructed in the middle of the North Sea, the logistics of a caisson periphery will be challenging. Furthermore it would be precarious to create a fully water retaining circumference of 20 kilometres. Eventually an Xbloc armour unit was chosen based on its limited amount of concrete.

4.1 Sea defence

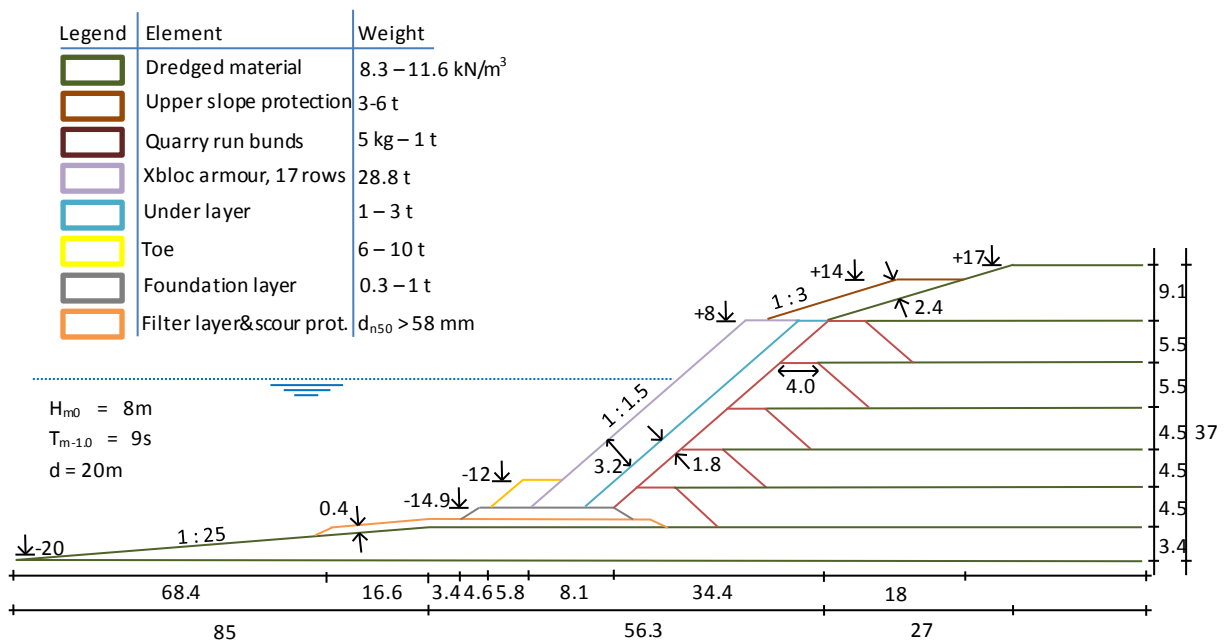


Figure 41: Cross section of outer dam protection. All measures are in metres. This is a preliminary design, a few adjustments where necessary to meet the macro stability criterion as explained in §4.4.1 Macro stability.

The philosophy behind the design is to have an armour layer as light as possible and requiring the minimum of concrete elements. This is done under the assumption that the concrete armour units form the most expensive element in the design. For the remaining (rock) layers, the same approach of using the minimum ‘weight-class’ is adopted. Matching gradings are used to optimally profit from the production of the quarry (Verhagen et al., 2012). A governing depth of 20 metres is used. The significant wave height and period at the toe have been obtained via an extreme value analysis, resulting in 8m and 9s respectively, with a return period of ~300 years (Frölke, 2017).

Here the design will be explained, going from left to right and from the bottom to the top. Firstly a gradual inclining **foreshore** is created to reduce the depth at the toe. A lower depth at the toe results in a lighter design of the toe itself, see the equation used for dimensioning the toe (Van der Meer, 2012). Furthermore, the reduced depth of the toe leads to smaller maximum wave heights, so a milder maximum load on the armour layer can be taken into account (Delta Marine Consultants, 2014). The slope of 1:25 of the foreshore is limited, since a steeper gradient could lead to unfavourable wave impact on the armour layer (Delta Marine Consultants, 2014).

To be able to construct the steep slope that is necessary for the interlocking of the armour units, **quarry run bunds** are made. These minimally 4m wide bunds fulfil two functions: retaining the dredged material and increase the permeability of the shore protection, which again allows for lighter armouring (Delta Marine Consultants, 2014). The bottom three bunds can be constructed with Side Stone Dumping Vessels (SSDS), whereas the top two will be built with land-based equipment. The bunds are made of sufficiently large quarry run, so no extremely fine material, since it does not add to the volume, but does contribute to the transportation costs (Verhagen et al., 2012).

The core of **dredged material** will be constructed stepwise. Once the quarry run bunds are created on the outer- and inner-slope, the space in between is backfilled by dredging vessels. Without the retention by the bunds, the dredged material would take on its natural slope equal to about half its angle of internal friction, resulting in an inclination of 1:7.

The 20m long **scour protection** should prevent instability of the toe caused by erosion in front of the structure. For determining the required stone size, $d_{n50} > 58\text{mm}$, the Shields formula is used:

$$d_{n50} = \frac{\bar{u}_c^2}{\Psi_c \Delta C^2} \quad ; \quad \bar{u}_c = \omega a_b = \omega \frac{1}{2} H \frac{1}{\sinh(kh)} \quad ; \quad C = 18 \log \left(\frac{12R}{k_r} \right)$$

- d_{n50} = Median nominal diameter of rock
- \bar{u}_c = Velocity caused by orbital motion of waves
- Ψ_c = Shields parameter
- Δ = Relative (rock) density
- C = Chézy coefficient
- ω = Orbital frequency
- a_b = Wave amplitude at bottom
- H = Wave height
- k = Wave number
- h = Water depth
- R = Hydraulic radius (\approx water depth)
- k_r = Roughness of bottom

First the maximum current velocity, caused by the waves, is computed when afterwards the stone diameter is worked out (allowing occasional movement, $\Psi = 0.03$). The length is as such that in case a scour hole in front of the protection reaches its equilibrium depth, the foundation layer of the toe remains untouched (in case the slope would reach the conservative angle of 1:10). The maximum scour depth, 1.35m, is determined through the Sumer & Fredsøe (2005) iterative equations:

$$S = H \frac{0.3 - 1.77 \exp\left(-\frac{\alpha}{15}\right)}{\sinh\left(\frac{2\pi h}{L}\right)^{1.35}}$$

- S = Maximum scour depth
- α = Slope angle of protection
- L = Wave length

Since the scour protection only needs to consist out of a relatively 'light' layer, it will be made out of the same material as the filter layer to reduce the complexity of the construction works. Possibly the

scour protection could be placed as a falling apron, since it is easier and quicker to install.

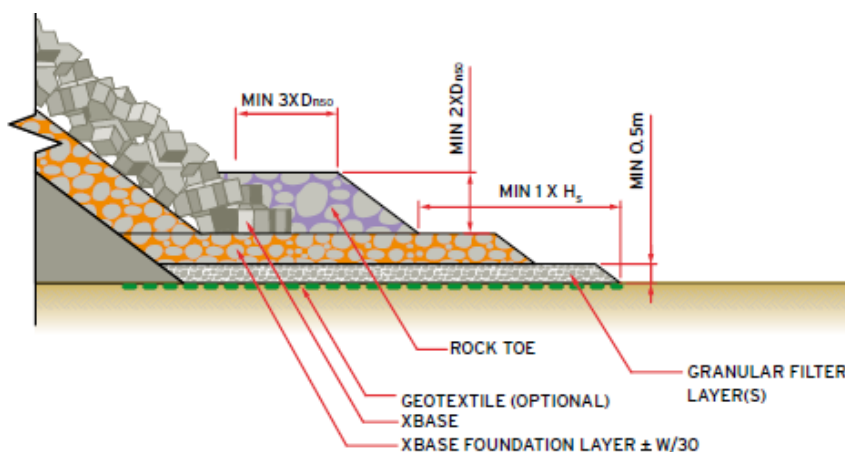


Figure 42: Layout of a toe on a sandy seabed (source: Delta Marine Consultants, 2014)

The **filter layer** has not been designed yet at this stage. This layer has to prevent particles flowing out from the dredged material underneath. The filter extends 'one significant wave height' in front of the toe, as recommended (Delta Marine Consultants, 2014).

The **foundation layer**, on top of the filter layer, serves as a stable base for the rock toe on top. It is 1.3m thick, consists out of 0.3 – 1t rock ($M_{50,found} = M_{50,toe} / 15$) and extends four (1 extra to ensure a stable toe and thereby stable armour layer) median nominal diameters (2.6m) in front of the rock toe.

To prevent the armour from sliding down the slope a **toe** is placed. For the determination of the stone size the Van der Meer (1995) design formula was used:

$$\frac{H_s}{\Delta d_{n50}} = \left(2 + 6.2 \left(\frac{h_t}{h} \right)^{2.7} \right) N_{od}^{0.15}$$

- H_s = Significant wave height
- Δ = Relative (rock) density
- d_{n50} = Median nominal diameter of rock
- h_t = Water depth above toe
- h = Water depth in front of toe
- N_{od} = Damage value (0.5, start of damage, is used)

Based on this formula a grading of 6 – 10t suffices for the toe, with the dimensions as suggested in Figure 42, except for the one extra 'rock diameter' width for additional safety.

The concrete armour units cannot be placed directly on the quarry run. The 'pores' between the armour elements are so large that material from underneath would be washed out. Therefore an additional layer is necessary: the **under layer**. Usually these have a rock mass which is around a tenth of the weight of the concrete units. The grading and thickness (1.8m) are as suggested by the Xbloc calculator tool (Delte Marine Consultants, n.d.).

The **Xbloc armour** layer is computed with the same tool as for the under layer. The Hudson formula gives an approximation to control the output of the Xbloc calculation tool:

$$M = \frac{\rho_s H_s^3}{K_D \Delta^3 \cot(\alpha)}$$

- M = Required unit weight
- K_D = Stability parameter (=16 for Xblocs; decreases for milder slopes)
- α = slope on which the armour units are placed

According to this formula the Xblocs need a minimum weight of 25.7t. However, besides the wave height and water depth, the needed unit mass is also determined by:

- Frequent occurrence of the near design wave height (causes rocking of the units)
- The seabed slope (breaking of the waves)
- The crest height (the top units on a low crested structure do not benefit from interlocking as much as the bottom units)

- The core permeability (a permeable structure allows for some transmission of the wave energy, instead of reflecting back on the armour)
- The slope (a steeper slope increases the interlocking between the armour units, which leads to enhanced stability⁴)

For the chosen wave height and the design high water level of +1.5m the tool advises to use 28.8t heavy elements, which are 3.3m high. First an Xbase unit (see Figure 42) is placed on top of the foundation layer when afterwards the armour can be constructed, using land-based wire cranes, from the bottom up. For the whole armour layer 17 rows of randomly placed Xblocs are required.

The Xbloc armour continues till 'one significant wave height' above still water level. The remaining dam does not need to continue with, a difficult to realise, 1:1.5 slope, since the rock on the **upper slope protection** does not rely on interlocking. A three-to-six tonne grading is chosen for the double layer, 2.4m high, to complete the protection of the dam. The protection runs until +14m, slightly above the limit that recommends armouring till 0.5 times the run-up that would be present on a smooth slope (Van der Meer, 2002)⁵.

The **crest level** was initially set at +16m, which would allow an overtopping discharge of 10 litres per second per metre according the Van der Meer (2002) formula:

$$R_c = \frac{\ln\left(\frac{q}{0.2\sqrt{gH_{m0}^3}}\right) H_{m0}^3 \gamma_f \gamma_\beta}{-2.3}$$

- R_c = Free crest height above still water line
- q = Overtopping discharge (in this case 10l/s/m)
- g = gravitational acceleration
- H_{m0} = Significant wave height at the toe
- γ_f = Roughness reduction factor (weighted average for Xblocs and upper protection)
- γ_β = Angle of incidence reduction factor (=1 for waves approaching perpendicular to the structure)

One metre is finally added to the crest height for safety reasons and to counter future settlement of the dam body (Bezuyen, 2012).

The presented preliminary design is entirely feasible and there is a lot of experience in constructing such a structure. The many different layers and gradings do make it logistically challenging. The relatively large usage of dredged material for the core and the proven concept of the Xblocs causes that this conventional design remains to be preferred and used for later cost computations.

⁴ The opposite is true for non-interlocking concrete armour units or rock. These elements rely on gravity only and the armour does not act as a whole as it does for interlocking units. Therefore the stability diminishes with an increasing slope for rock or concrete (antifer) cubes.

⁵ In order to take the maximum allowable influence (reduction) factors into account for the effect of roughness on the slope, certain restrictions apply. First one has to compute the hypothetical run-up if the slope(s) would be perfectly smooth (in this case 26.5m). Secondly one is allowed to use the roughness 'reduction' factor in case the 'roughness creating elements' are placed $0.25 * \text{Run-up}_{\text{smooth}}$ below the water line (=6.6m) and $0.5 * \text{Run-up}_{\text{smooth}}$ above the water line (=13.3m). Therefore there is chosen to apply the slope protection till +14m (The theoretical background of this method is rather unclear, however in practise this methodology is widely accepted and applied, see Van der Meer (2002)).

4.2 Inner slope

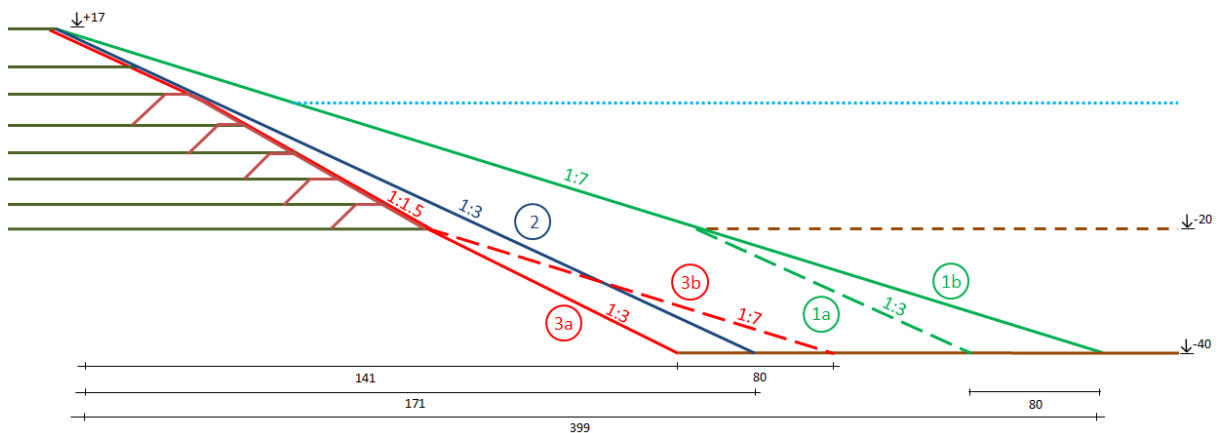


Figure 43: The inner side of the dam with the various slopes that are considered during the design phase

Several choices for the slope of the inner side of the dam can be made. One can either focus on making it as steep as possible to obtain a minimum diameter and thereby limited circumference to be protected. Another option is to use the least amount of imported material like rock to reduce the costs. However, the dredged material is not able to sustain a steep angle. Therefore this choice will result in a wider dam and corresponding larger diameter in order to store the same amount of energy. Those possible choices are reflected in the following scenarios that belong to Figure 43:

- 1. Requires the least amount of work. The dredged material is deposited and allowed to take on its natural angle of repose, which is roughly 1:7. For 1a it is assumed that the clay layer underneath is stable under a steeper slope, since it remains untouched. 1b continues with the mild slope till the bottom of the reservoir.
- 2. An intermediate alternative with a slope of 1:3. Possibly measures will have to be taken to construct such a slope from the dredged material.
- 3. The alternative aimed to need the minimum diameter in order to have a certain amount of storage capacity. Quarry bunds will be required to construct the steep slope, like is done for the outer protection works. In case the dam necessitates a 'toe' in order to guarantee stability against sliding, a scenario like 3b might be the outcome.

Which alternative is best will be determined during the stability check of the inner slope in 4.3. 4.1

4.2.1 Protection against waves

Although the inner reservoir is free from swell waves, local wind induced waves will be present. The severe wind conditions on the North Sea partially transfer their energy to the water surface, which translates to the creation of waves. In Figure 44 the occurring wind speeds are depicted.

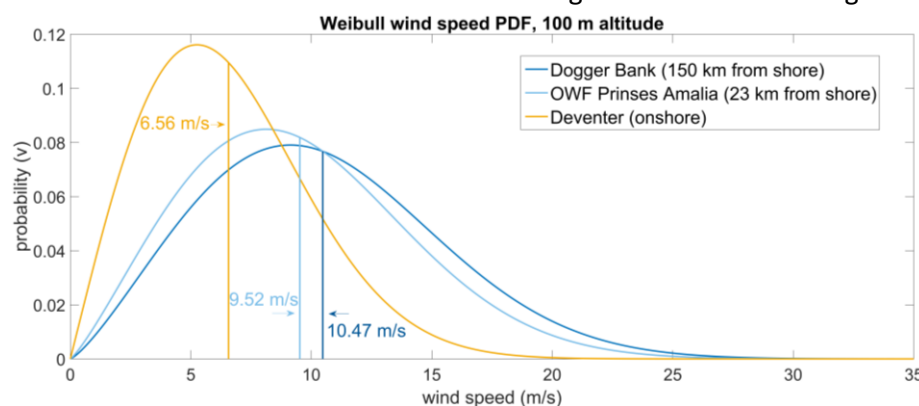


Figure 44: Probability density function of the wind speed at the Dogger Bank and near- and onshore for reference (source: Gerrits, 2017)

To compute the resulting wave height for a certain wind speed, first the velocity at 10m height needs to be determined:

$$u = u_{ref} \frac{\ln\left(\frac{z}{z_0}\right)}{\ln\left(\frac{z_{ref}}{z_0}\right)}$$

- u = Desired wind speed (10m)
- u_{ref} = Reference wind speed (100m)
- z = Altitude of desired wind speed (10m)
- z_0 = 'Roughness' factor (0.0002 for water (European wind atlas))
- z_{ref} = Reference height where wind speed is known (100m)

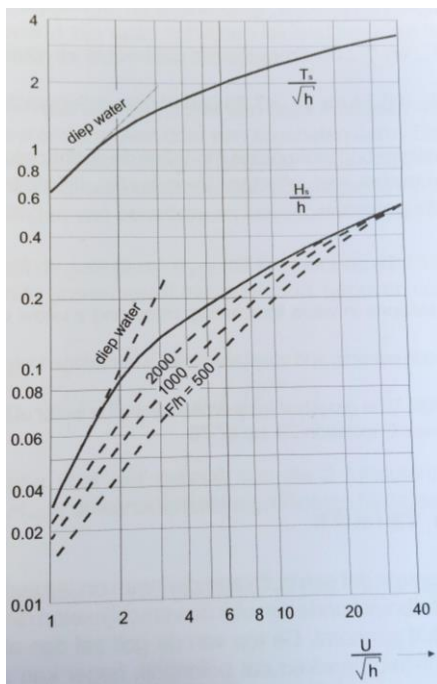


Figure 45: Nomogram valid for shallow and intermediate waters (source: Bezuyen et al., 2012)

The maximum wind speed at the Dogger Bank of 30m/s results in a velocity of 25m/s at an altitude of 10 metres. The maximum waves will be created when the depth is at its largest, for now we assume that to be 8 metres and the largest fetch (7000m). Using the graph as in Figure 45, the wind speeds can cause a significant wave height up to 1.5m. According to the Hudson formula, as used earlier for the outer protection works in §4.3.1, the rock armour for the slope protection needs to weigh more than 327kg. For the stability number K_D in the Hudson formula a value of 2.0 was used, as is recommended for breaking waves (CIRIA, 2007). However the Van der Meer formula seems to be more accurate, since it does consider the wave period, storm duration, core permeability and damage value, where Hudson does not. For 'plunging' waves (valid for a breaker parameter of 0.5 – 3) the Van der Meer formula states the following:

$$d_{n50} = \frac{H_s}{\Delta 6.2 P^{0.18} \left(\frac{S}{\sqrt{N}}\right)^{0.2} \xi^{-0.5}}$$

- d_{n50} = Median nominal diameter of rock
- H_s = Significant wave height
- Δ = Relative density
- P = Permeability parameter (=0.1 for armour + filter on clay or sand)
- S = Damage level parameter (=5 some damage)
- N = Number of waves (\approx duration of storm / wave period)
- ξ = Breaker parameter

For a six hour storm duration and on a slope of 1:3.75 (adjusted scenario 1a) the necessary weight of the rock becomes 297kg. Consequently a grading of 300 – 1000kg will be used for the **slope protection** at 'high water level'. Since the wave height decreases for shallower water, the protection can evenly be executed lighter towards the bottom. Six metres from the bottom a grading of 60 – 300kg will form the armour, which reaches till the bottom.

The rock armour cannot be placed directly on top of the clay. First a **geotextile** is placed and secondly an **under layer**. The under layer consists out of a standard 40 – 200kg grading and will be two nominal diameters wide. The under layer is rather heavy, relative to the rock armour, but is still the lightest (CIRIA et al., 2007) to meet the criterion of having one-fifteenth of the rock armour weight (Van den Bos, 2017a). Due to this substantial under layer the geotextile will have to be evenly robust.

The slope protection needs to extend till somewhat higher than the water level when the reservoir is full. This is to deal with the run-up and prevent erosion just above the water line. The **run-up** is determined with the Van der Meer formula for wave run-up on dikes:

$$Ru_{2\%} = H_{m0} 1.75 \gamma_b \gamma_f \gamma_\beta \xi_0$$

- $Ru_{2\%}$ = 2% wave run-up level above water line
- H_{m0} = Significant wave height at the toe (in this case H_s was used)
- γ_b = Berm reduction factor (no berm so equal to 1)
- γ_f = Roughness reduction factor (=0.55 for double layer of armour rock)
- γ_β = Incident wave angle reduction factor (=1 for perpendicular wave attack)
- ξ = Breaker parameter

The resulting run-up reaches till 2.3m above the water line. Therefore the slope protection extends to this very same level.

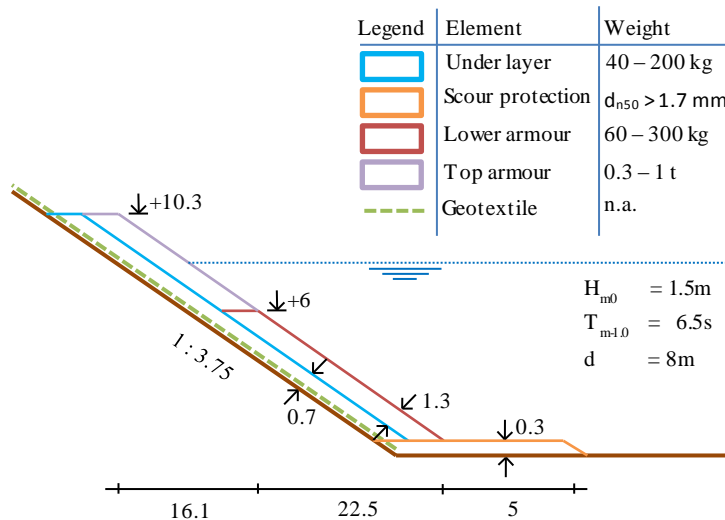
Since the water body in the inner reservoir is enclosed by the surrounding dike, wind **set-up** may also play a role. The principle of set-up is that the water level increases at one side to create a gradient. The force resulting from this gradient balances with the force of the wind on the water surface. The gradient and set-up of the water is computed through:

$$i = c \frac{u^2}{gh} \quad ; \quad S_{up} = iR$$

- i = Gradient
- c = Friction coefficient (=3.75*10⁻⁶)
- u = Wind speed (=24.7 m/s)
- g = Gravitational acceleration
- h = Water depth (=8m)
- S_{up} = Set-up
- R = Radius (1400 – 3500m)

For the various reservoir capacities the set-up ranges from 4cm to 10cm. The effect of wind set-up is therefore neglected in the further design process.

Ultimately a minimum **scour protection** should be added on the inner side of the dam. With the changing water levels and corresponding waves, the maximum required scour protection should consist out of a d_{n50} larger than 1.7mm. Therefore a 5m long thin layer of gravelly sand will be placed to prevent scour. The layer will have a minimum thickness, which is most economical from a construction versus material cost point of view (in the order of 0.3m).



All layers and dimensions are schematised in Figure 46. The water level is depicted as if the reservoir would be full.

Figure 46: Inner slope protection. All measures are in metres and relative to the reservoir bottom.

Slope protection during construction

The construction time of an offshore hydropower storage facility, as considered in this report, is likely to last for more than 5 years. During this period the inner side of the dam remains exposed to (refracted and diffracted) waves from the North Sea until the circular dam is completed. Hence, some sort of measure needs to be taken to protect the inner slope around sea water level for during the construction stage. There are four options:

1. Do nothing (accept erosion and counter by additional dredging).
2. Protect inner slope against wave attack with a reasonable return period corresponding to the construction time of the dam.
3. Temporarily protect slope and use material for another part later on.
4. Use a kind of mattress for protection around sea water level for the construction period and 'slide' the mattress down when the dam is finished, so the mattress can serve as protection around the inner water level fluctuations during its operational life.

A cost-benefit analysis, including potential risks, is recommended to choose the most appropriate solution. Due to the limited time of a Master thesis, this is left for future studies.

4.2.3 Phreatic line

It is very important to know exactly the height of the phreatic line and where it ‘crosses’ the slope of the dam. Whether soil is above or underneath the water table can make a large difference in its unit weight and shear resistance. The shape is approximated with the method of Dupuit, using b for the width of the dam as indicated in Figure 47. As one can see, the water ‘flows’ out of the dam far before it has reached the bottom of the inner reservoir. Consequently the discharge through the dam is not restrained by the full width, but only by part of the dam (indicated with b').

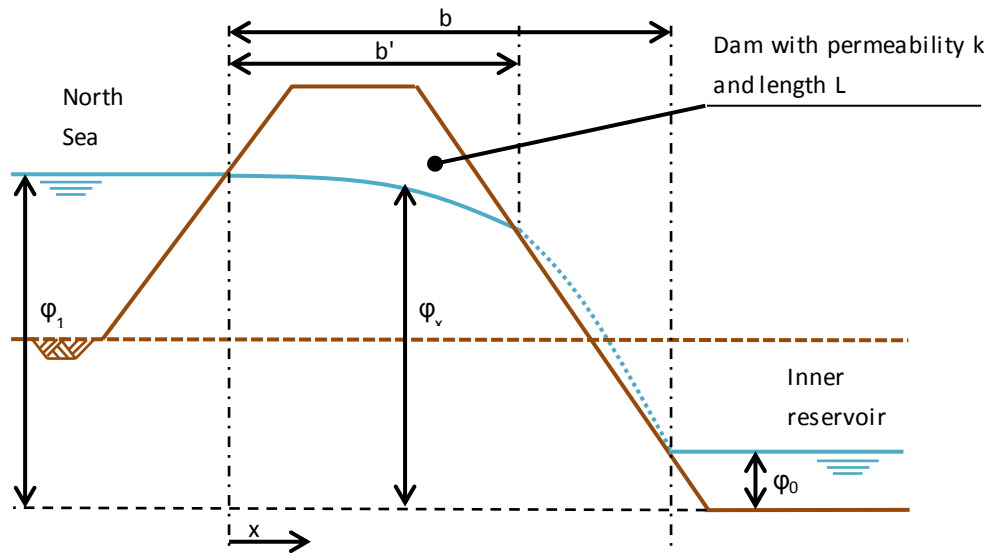


Figure 47: Phreatic line through the dam according to the Dupuit method. Note that no infiltration from precipitation is taken into account. Due to the hard surface on the crest and the nature of the material used for the dam, infiltration is neglected.

$$\varphi_x = \sqrt{\varphi_1^2 - (\varphi_1^2 - \varphi_0^2) \frac{x}{b}}$$

$$Q_d = \frac{kL(\varphi_1^2 - \varphi_0^2)}{2b'}$$

- φ_x = Head for a certain distance x ($\varphi = \varphi_1$ for $x = 0$ and $\varphi = \varphi_0$ for $x = b$) (m)
- x = Distance from ‘impermeable’ part of the dam at the North Sea side (m)
- b = Length from start of ‘impermeable’ part till inner reservoir (m)
- Q_d = Total discharge through the dam (m^3/d)
- k = Permeability of dam material ($=0.01\text{m}/\text{d}$) (m/d)
- L = Length of circumference (m)
- b' = Length from start of ‘impermeable’ part till the point where water flows out (m)

The total discharge through the dam ranges from $350\text{m}^3/\text{d}$ till $1400\text{m}^3/\text{d}$, depending on the reservoir size and depth. For the alternatives with a 40m maximum head difference this is 60 litres of water per day per metre of dam. Although this might seem like a significant amount, it barely leads to a head loss of $0.05\text{mm}/\text{d}$, as will be further discussed in section 4.3.4.4 Seepage.

Consequently it is not necessary to take any measures to reduce the seepage through the (day!) dam. The properties of the dredged material that is used for the dam construction offer sufficient resistance against water leaking through.

4.3 Water retaining measures

The whole concept of pumped hydropower storage relies on a certain water level difference between two reservoirs. In order to sustain such a water level difference, it is vital that water is prevented (or at least limited to a negligible level) from flowing from one reservoir to the other. Fortunately the subsoil consists mostly out of clay (see §4.1.4 Geology), which will keep the water out. Unluckily there is also a sand layer present from -23m till -30m below the seabed that could easily convey a continuous water flow from out- to inside. In order to create a feasible project the water transport through the sand layer has to be stopped. There are various measures and materials available that could fulfil this task, the ones that are considered are shown in Figure 48 and explained below.

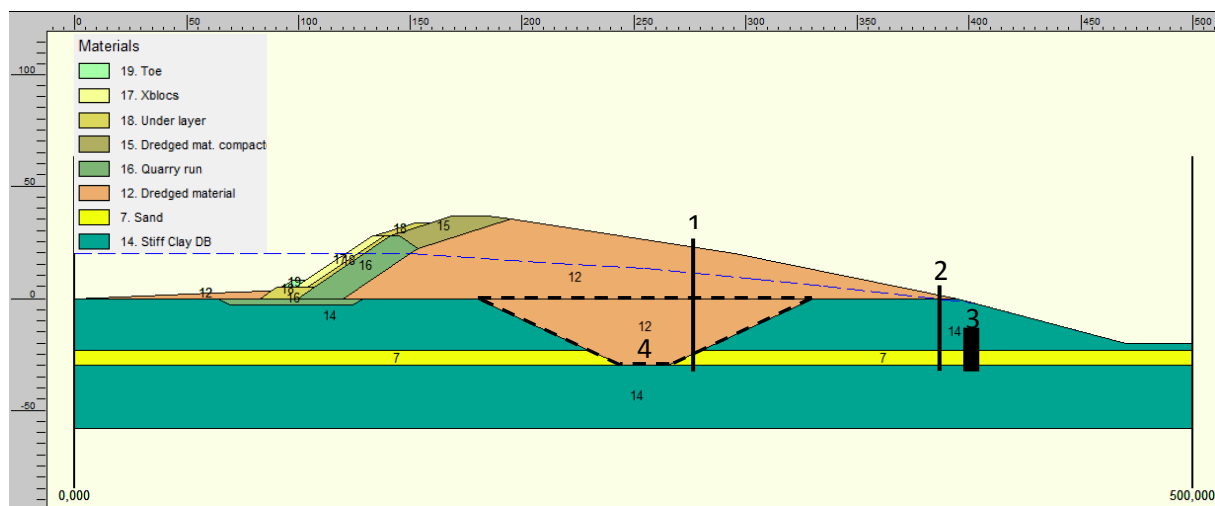


Figure 48: Possible measures that can be taken to 'close' the sand layer: 1) Slurry bentonite wall. 2) Sheet piles 3) Jet grouting. 4) Replacement of sand layer.

4.3.1 Slurry bentonite wall

Diaphragm walls are commonly used to keep earth and water from flowing into building pits, tunnels or other excavations. The sole difference between a diaphragm wall and a slurry bentonite (SB) wall is that a SB wall only serves as an impregnable wall, so without structural function. Where the dug trench is eventually filled-up with concrete (and possibly reinforcements) for a diaphragm wall, the trench for a SB wall is not filled with concrete. Instead the material that is excavated can be used again in the slurry wall, once it is mixed with a bentonite mud to obtain the preferred permeability assets. Such a SB wall has the advantage that no concrete is required, which will drastically lower the costs.

Generally the maximum length that can be achieved is 60m, whereas the width could vary between 0.8m and 1.5m. Although a SB wall is meant to prevent water flowing through, it is never 100% impregnable. A safe permeability of $5 \cdot 10^{-10}$ m/s can be assumed (Boscardin et al., 2006). One of the advantages of this technology is that it can be executed simultaneously with the remaining dam construction. To ensure a high operation rate, the retention structure should be installed on the inner side of the dam 3m above mean sea level. Preferably the SB wall reaches till 1m below the sand layer. Therefore the slurry bentonite wall should be at least 54m long (=1+30+20+3m). A width of 1.0m is chosen on the basis of constructability, cost-effectiveness and reliability. A SB wall basically consists out of a long series of ± 3 m wide panels. Between each panel there is a transition, which forms the Achilles' heel. Hence, for a circumference of 20km there will be more than 6000 transitions. To construct such a continuous wall, one could call a challenge.

4.3.2 Sheet piles

Sheet piles are probably the most common (temporary) retaining structure. The experience with the technology, the prefabricated material and the interlocking transitions make sheet piles a reliable method. Although they are about half the price of a SB wall, there are a few prevailing disadvantages. Most of all, the length of sheet piles is maximally 31m (where 54m is required in order to be installed from land like the SB wall). Therefore either the sheet piles would have to be installed, from water-based equipment 20m below mean sea level or from within a temporary drained building pit. The first will be extremely difficult from a construction point of view. The second will be just as hard and over proportionally expensive. Ultimately this option is disregarded then due to the limitation in sheet pile length.

4.3.3 Jet-grouting

In a way jet-grouting is similar to creating a slurry bentonite wall, since both techniques involve replacing the permeable sand with an impermeable mixture of mostly bentonite and earth. The process of jet-grouting is depicted in Figure 49. An advantage of jet-grouting is that the construction method is relatively quick and straightforward. Besides, no impermeable 'columns' have to be created till the surface level, but only in and around the water conveying sand layer. The columns can be up to 3m wide and to 'ensure' the impermeability of the consecutive row of columns, one or more rows can be installed adjunctively. This leads to a set of 'overlapping' columns, which combined should retain the water from flowing into the inner reservoir.

Unfortunately no knowledge on depth restrictions could be found. Therefore it is unknown whether this technique can be employed from the dam or additional waterborne equipment would be necessary. Lastly some failures of jet-grouted walls have been documented (The metro tunnel in The Hague for example). The unknown achievable depth together with an unconvincing history leads to the fact that this option is set aside for now. After further research and a comprehensive reliability study, jet-grouting might return as a potential candidate.

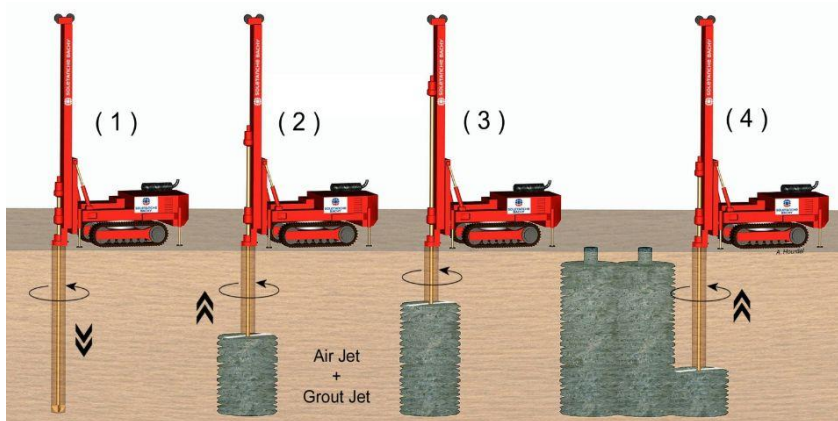


Figure 49: The construction sequence of a jet-grouted wall (source: <http://udc.com.vn/en>)

4.3.4 Replacement of sand layer

The previous three methods all try to stop the water flowing through the sand layer by placing some sorts of obstruction. The concept of 'replacement of the sand layer' just takes the whole conveying substrate out and replaces it with clay from which the permeability properties are verified. Consequently there are no transitions and the later soil characteristics are fully controlled.

So far it has been assumed that the geology on the Dogger Bank has a homogeneous lithology (as depicted in Figure 132). This almost certainly will not be the case and thus it is likely that the depth (and thickness) of the sand layer will vary over space. Because this is the only technique, which is best executed from water and it starts directly on the seabed, it is the best alternative to deal with the changing soil conditions.

Opposed to the former technologies, this one does not involve installing any material, which is alien to the site. The clay that replaces the sand can be dredged from the 'inner-reservoir-to-be', where the dredged sand can be used for other purposes within the project. In the preliminary computations 10% has been added to necessary volumes to allow for settlements and creep. The trench that has to be dug to reach the sand layer is minimally 5 metres wide and has slopes of 1:1.5 in clay and 1:2 in the sand layer, which have been verified on their slope stability (Figure 50). In total 1925m³/m will have to be moved in order to replace the sand layer.

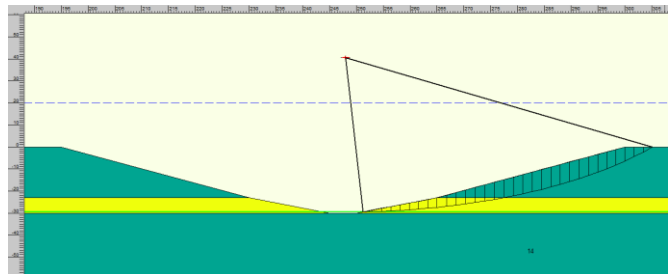


Figure 50: Slope stability of the trench to replace the sand layer. The critical sliding mechanism through the stiff clay and the sand has a safety factor of 1.08

4.3.5 Choice of measure

From the four alternatives discussed only two remain: the slurry bentonite wall and the replacement of the sand layer. Both are competitive options making it hard to pick the most suitable. In terms of construction time they are similar, since both can be executed during the dam construction itself. From a reliability perspective the dredging variant holds the upper hand, due to the absence of transitions. The environmental impact of the two has not been studied, but is not expected to point out a preferred option. The dredging process is likely to cause more emissions during the construction phase, where the SB wall is a complicated asset once the lifetime of the storage facility has been fulfilled. Ultimately it is up to the costs to make a selection.

From Figure 51 it can be concluded that replacing the sand layer with clay is always more cost-effective. Furthermore the lithology might change over depth, which makes the dredging alternative the chosen measure, because it offers much more flexibility. For the Dogger Bank location the replacement costs are 11,825€/m, whereas the SB wall costs 17,500€/m. Looking at Figure 51 it are the mobilisation costs, which determined the preferred solution. Since the slurry bentonite wall first has to excavate 23m before it only reaches the seabed, the 'mobilisation' costs of this technology are far higher. The costs of the dredging rise rapidly due to the fact that not only the dredging itself becomes more expensive but also the volume of the trench grows fast at increasing depths. The dredging costs (5.8€/m³ for an average depth of 30m) are based on the use of a grab dredger in combination with a split hopper barge as are specified in chapter 5. Dredging works.

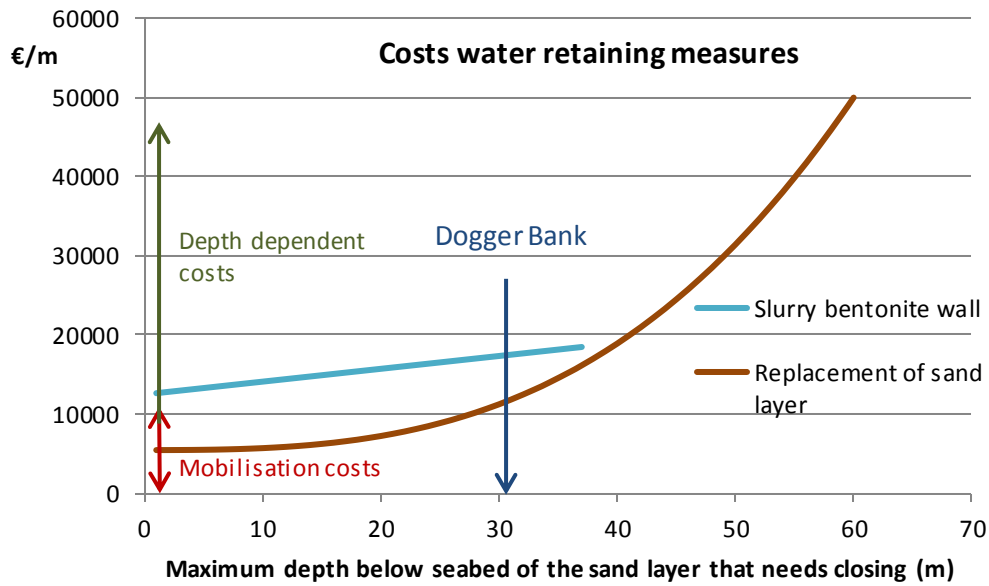


Figure 51: The costs of the retaining measures as they progress over depth. The mean sea level is 20m above the bed level. The slurry bentonite wall is assumed to be installed from 3m above the sea level and have a maximum length of 60m. Therefore the maximum reachable depth of the SB wall is 37m.

The discharges through the retaining measures are computed according to the Darcy formula:

$$Q_{rm} = \frac{k}{w_{rm}} H_{max} t_s$$

- Q_{rm} = Discharge through retaining measure (m³/s)
- k = Permeability retaining measure ($5 \cdot 10^{-10}$ for SB and 10^{-8} for sorted clay)(m/s)
- w_{rm} = Width retaining measure (1m for SB and 5m for replaced sand) (m)
- H_{max} = Maximum head difference (40m) (m)
- t_s = Thickness sand layer (7m) (m)

The parameters mentioned above result in a leakage of 12.1 l/d/m for the slurry bentonite wall and 48.4 l/d/m through the placed clay. Compared to a fluctuating water volume of the inner reservoir of roughly 200 billion litres, the losses through the retaining measure can be neglected.

4.4 Failure mechanisms

There are many ways nature can ‘force’ a dam to fail. Figure 52 shows several examples of the most common failure modes for dikes. The mechanisms for a dike and the dam that is being considered are very similar. Therefore these modes are chosen to investigate primarily. Furthermore the erosion of the inner slope, due to wind-induced waves on the inner reservoir, is reviewed in 4.3.2.1 and the ‘breaking-up’ of the clay layer underneath the reservoir is discussed as well. Other modes like settlement (partially dealt with for the outer protection), collision by ships or drifting ice remain for future studies.

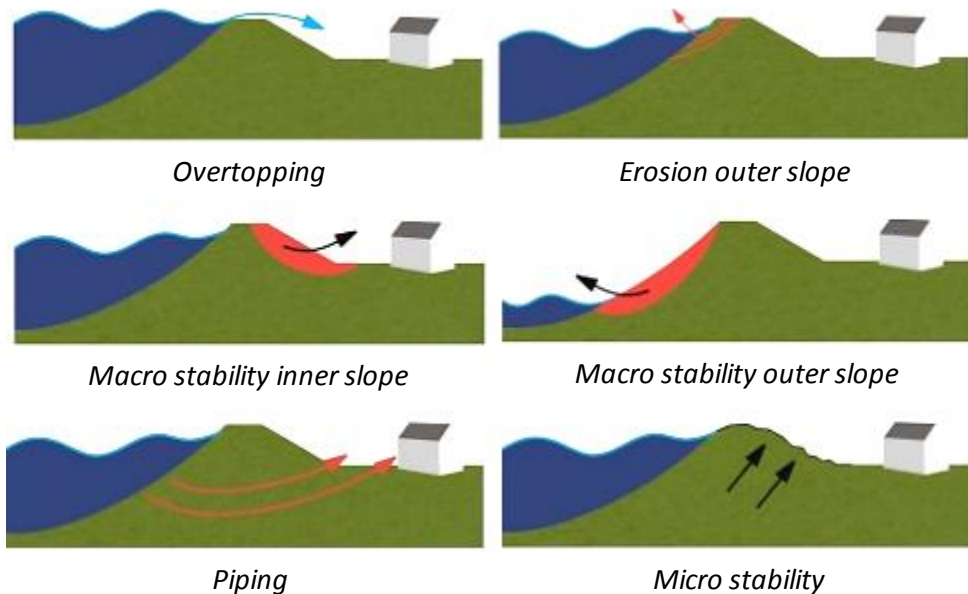


Figure 52: Most occurring failure mechanisms for dikes (source: Peeters, 2012)

Not all events happen under the same critical conditions. For example, the outer slope is more unstable during low water, whereas overtopping is more likely during high water levels. Additionally, some mechanisms are triggered easier when the construction has not been completed yet, like when certain parts remain exposed to wave action, which would later be protected. Consequently, all failure modes need to be verified for their own governing conditions. These circumstances are shown in Table 13 (note that the erosion of the outer slope is already dealt with in the design of the sea defence in 4.3.1).

Failure mechanism	Method	Water level North Sea		Water level inner reservoir		Governing phase	
		Low	High	Empty	Full	Construction	Operational
Macro stability outer slope	Bishop, Uplift-Van (D-Geo)	✓			✓	✓	
Macro stability inner slope	Bishop, Uplift-Van (D-Geo)		✓	✓		✓	
Micro stability	Guidelines		✓	✓		✓	✓
Piping	Bligh (+Griffith)		✓	✓			✓
Seepage	Deputit & Darcy		✓	✓			✓
Bursting	Archimedes		✓	✓			✓
Overtopping	Van der Meer		✓	✓		✓	✓

Table 13: Governing situations per failure mechanism. The high and low water levels on the North Sea are respectively $\pm 1.5\text{m}$ from still water level (Kvale et al., 2006). A full inner reservoir corresponds to H_{min} level of Table 11

To ensure an acceptable standard of safety, factors are applied to the characteristics of the soil. The NEN 9997 code is used, with the safety factors as given in Table 14. Risk category 1 is chosen, since the risk of failure only affects economic values and no loss of life(s).

Soil parameter	Symbol	Safety factor risk category 1
Angle of internal friction ⁶	$\gamma_{\varphi'}$	1.2
Effective cohesion	$\gamma_{c'}$	1.3
Undrained shear strength	γ_{c_u}	1.5
Compressive strength	γ_{q_u}	1.5
Unit weight	γ_Y	1.0

Table 14: Safety factors of soil parameters for overall stability by NEN9997

When applied to the characteristic values (as suggested by NEN 9997) of the various soil types, the properties become as stated in Table 15. These are the numbers which have been used during the computations and the verification of the failure mechanisms.

	Toe	Xbloccs	Under layer	Quarry run	Dredged material ⁷	Sand	Stiff clay DB
Dry unit weight (kN/m ³)	23	24	23	23	17	18	19
Submerged unit weight (kN/m ³)	26.5	24	26.5	26.5	18	20	20
Cohesion (kN/m ²)	0	0	0	0	10.4	0	11.54
Friction angle (°)	49.96	n.a.	49.96	39.81	19.04	27.96	21.24

Table 15: Material properties (design values) of the elements which are used

⁶ This factor is applied to $\tan(\varphi')$

⁷ The dredged material consists out of stiff clay from the Dogger Bank. By dredging the clay mechanically the soil properties are minimally affected. In contrast to hydraulic dredging the clay does not need to be cut into fine pieces or mixed with water for transportation. Therefore the dredged material characteristics are 'only' reduced by 10% compared to the original clay parameters.

4.4.1 Macro stability

The slopes of the dam are limited by its resistance against sliding downwards. The slip surface can lay relatively close to the slope his surface, but could also lay much deeper, which would result in the quite spectacular failure mode of a complete slope collapsing. In the failure mechanism ‘macro stability’ the most critical sliding plane(s) is searched for. Consecutively the slopes are adjusted in order to end up with a safe and most cost-effective (slimmest) design.

Theory

Determining the maximum achievable slope can be difficult when the soils are both cohesive and frictional. Especially when the slope consists out of multiple soil layers, inclinations and a non-horizontal water table. Due to the complexity there are many different calculation methods, all with their own assumptions and shortcomings. One of the more widely used methods is the one

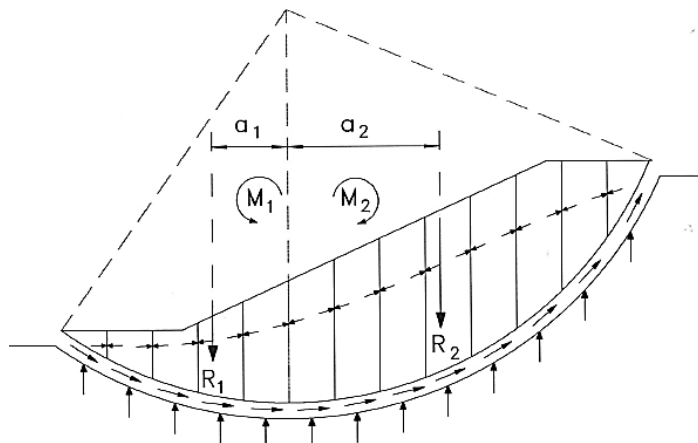


Figure 53: Schematisation of a slope stability analysis. The slices are in vertical force equilibrium. The resulting moments (M_1+M_2) and shear force along the circular failure plain are in moment equilibrium (source: Bezuyen et al., 2012).

developed by Bishop (see Figure 53). The slope is divided into slices who (depending on their position) either contribute to the overturning moment (M_2) or the resisting moment (M_1). Combined they form the driving moment (M_2+M_1) that has to be outbalanced by the shear force along the sliding plane times its arm (the radius).

The shear stress results from the vertical equilibrium and is a function of the effective soil stress and cohesion:

$$\tau = c_d + \sigma' \tan(\varphi'_d)$$

$$\sigma' = \sigma - p$$

- τ = Shear stress (N/m²)
- c_d = Cohesion, design value (N/m²)
- φ'_d = Angle of internal friction, design value (rad)
- σ' = Effective soil stress (N/m²)
- σ = Total stress (N/m²)
- p = Water pressure (N/m²)

Note the influence water pressure has on the shear resistance and thereby overall stability. A large water pressure results in a small effective soil stress and shear resistance. Furthermore, if an impermeable layer is situated on top of a permeable subsoil with a higher than hydrostatic water pressure, the water tries to uplift the impermeable layer, like in Figure 54.

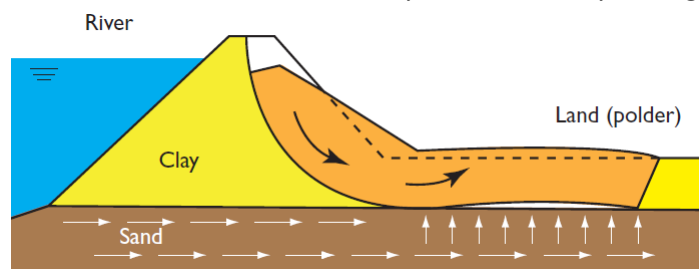


Figure 54: The uplift mechanism that is caused by a water overpressure under the clay layer (source: Van 't Hoff & Van der Kolff, 2012)

As the water pressure tries to lift-up the overlaying clay layer, the clay itself (that kind of starts floating as a whole on the water) loses most of its internal soil strength and thereby its resistance to sliding (only the cohesion between particles remains). This mechanism can lead to large parts of soil sliding horizontally, instead of along a circular plain. Therefore the Uplift-Van method has been devised, which is not restricted to circular failure modes. Especially for the inner slope of a dike or dam the Uplift-Van method can be governing.

The D-Geo stability software has been used to perform safety checks against sliding (Bishop and Uplift-Van). Even though safety factors were applied to the input parameters, a safety factor of at least 1.1 was strived for to allow for construction tolerances. A uniform top load of 100kN/m^2 is added to the crest, so heavy equipment and machinery is able to be transported over the dam during its operational life.

Outer slope

The lowest low water level (-1.0m) is the governing situation for the outer slope stability. A lower water level results in a smaller overburden on top of the 'toe', which leads to less contra weight against the sliding down of the upper part of the slope. The computations were made for a situation where the maximum scour hole has developed in front of the toe. The largest driving moment occurs when the dam has been fully constructed and a large load is passing over the dam. These conditions lead to the most critical sliding plane as shown in Figure 55.

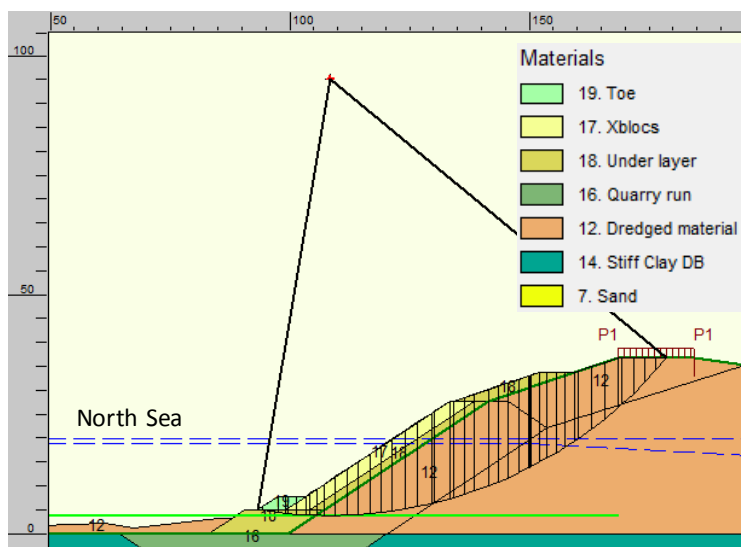


Figure 55: Critical sliding plane for the outer slope. Under uniform top load of 100kN/m^2 and a maximally developed scour hole in front of the toe

a foundation layer of quarry run. This is to guarantee sufficient shear resistance. Additionally, the foundation layer of the toe starts right from the seabed to restrict future settlement of the toe .

The governing mechanism (Bishop) from Figure 55 has a safety factor of 1.17. Under these extreme conditions this is found acceptable.

The initial design had to be adjusted slightly. At first it was the idea to raise the whole bed level 3.4m and from there on start to construct the dam. However, the sliding mechanism is very sensitive to the material that is used at the toe of the dam and its subsoil (see Table 16 and Appendix B). Since the stability of the toe is so crucial there is chosen to first dig a 3m deep trench and place

Soil parameters	Quarry run	Stiff clay DB	Dredged material	Muck
Dry unit weight (kN/m^3)	23	19	17	11
Submerged unit weight (kN/m^3)	26.5	20	18	11
Cohesion (kN/m^2)	0	11.54	10.4	0
Friction angle ($^\circ$)	39.81	21.24	19.04	0
Safety factor	1.18	1.11	1.09	0.78

Table 16: The influence of the material from the toe/dam foundation layer on the slope stability

Inner slope

For the inner slope the stability is most alarming when the water level in the North Sea is at its highest. Assuming that the highest astronomical spring tide, sea level rise and storm surge occur simultaneously, the water level difference between reservoirs becomes 42.9m (=1.2 + 0.3 + 1.4 + 40). The inner slope stability is tested, by supposing that this extreme water level difference is permanent and the phreatic level through the dam has fully adjusted its course. With an estimated permeability of core material of 0.1m/d this is a very conservative assumption, because neither the tide nor the storm surge will endure long enough to make the phreatic line fully attuned.

The circumstances mentioned above bring the prevailing slope failure to the one displayed in Figure 56, with a safety factor of 1.11 according to the Uplift-Van method.

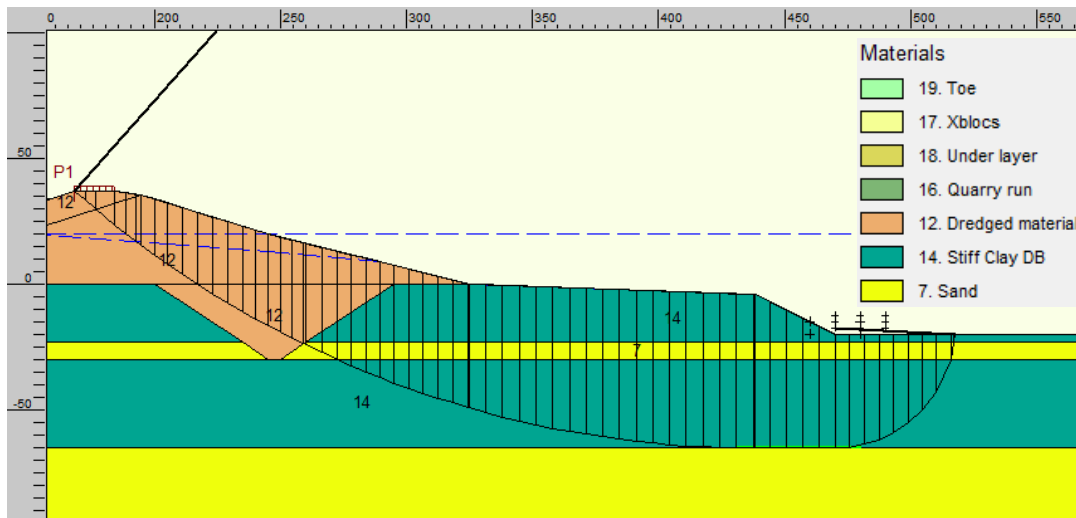


Figure 56: The critical sliding mechanism for the inner slope. The continuous phreatic line at +20m (=MSL) is the water pressure in the bottom sand layer, which tries to uplift the thick clay layer. Without the large inner berm the slope would only have a safety factor of close to 1.0

Due to the uplift mechanism as explained before in Figure 54, the large inner berm had to be added to the dam design. The water pressure (caused by the head difference between the North Sea and inner reservoir) acting upon the thick clay layer reduces its effective soil stress to almost nothing. Therefore the shear resistance is nearly only determined by the clay cohesion. Consequently the large berm had to be added to generate a higher effective soil stress (σ') and resulting shear resistance ($\tau = c' + \sigma' \tan(\varphi')$), as depicted in Figure 57.

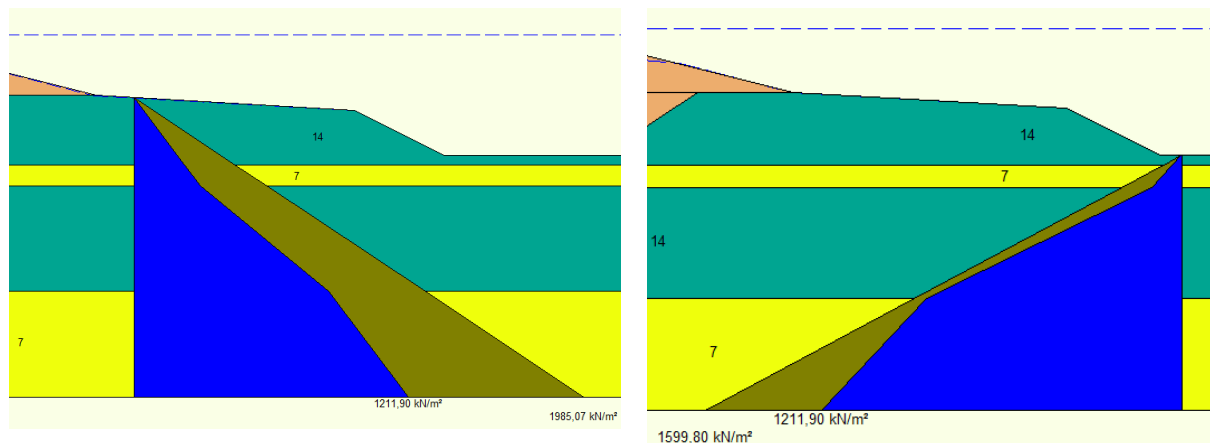


Figure 57: The influence of the inner berm on the shear resistance. When there is no surcharge on the reservoir bottom there is almost no effective soil stress, the difference between the green and blue pressures (right). Hence the inner berm is added to create sufficient shear stress in the thick clay layer to prevent sliding failure (left).

In the unrealistic, but extreme event of when the phreatic line in the dam would remain at MSL and all the water from the inner reservoir would have been pumped-out, the safety factor would be 1.0. Although this is solely a fictional situation, since the water level in the dam will always somewhat adjust to the water level in the inner reservoir, it does indicate that at least the first time when the water level is lowered to its operational level, this has to be done gently. By gradually lowering the water level to operational levels, the phreatic line within the dam will drop equally.

From the various slopes that were discussed in §4.2 Inner slope, none of them made it to the eventual design. It showed that the ‘mild’ slope scenario was too conservative, while the steeper alternatives were simply impossible or required vast amounts of quarry material. Furthermore the inner slope now consists out of four gradients:

- 1:3.6 from the crest till the sea water level (+17 to 0)
- 1:4 for the middle part that continues till the original seabed level (0 to -20)
- 1:28.3 for the inner berm to avoid standing water (-20 to -24)
- 1:2 from the berm till the reservoir bottom (-24 to -40)

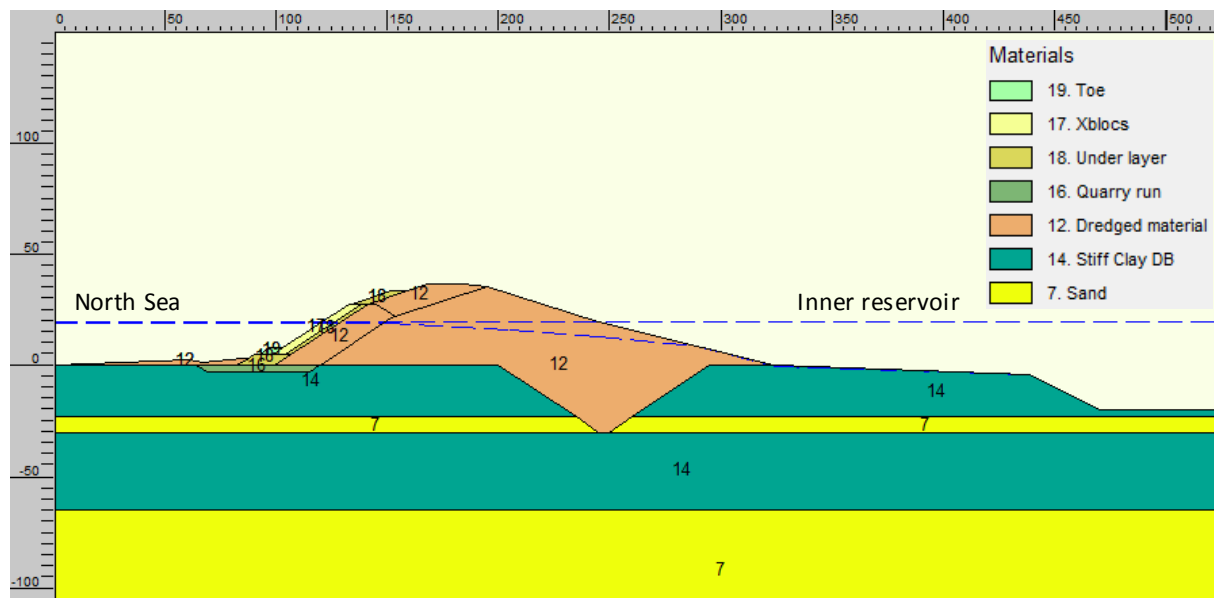


Figure 58: The dam design that is checked safe from a macro stability perspective. Note that the inner berm solely consists out of material that remains untouched (it has not been dredged and deposited there like the rest of the dam). The continuous phreatic line at +20m (=MSL) is the water pressure in the bottom sand layer, which tries to uplift the thick clay layer. The other phreatic line reflects the water table for the other layers.

The inner slope as a whole is responsible for a footprint of 286 metres! This enormous length brings up questions like whether it would be more economical to use a crown wall or even a caisson to reduce the dam dimensions. Additionally it has to be noted that for the design all the material was 100% consolidated. The effect of the level of (over) consolidation and drainage operations may influence the design of Figure 58. These considerations are further described in the recommendations chapter.

4.4.2 Micro stability

The loss of stability of very thin layers on the surface of the slope, due to water flowing through the dam is categorised under the failure mechanism “Micro stability”. The danger from micro stability related issues comes from inside the dam body, mostly triggered by a high phreatic line throughout the dam. This high water table could then initiate the washing out of material from the core of the dam (Ministerie van Verkeer en Waterstaat, 2007). Furthermore an instable surface layer can be created or when the core is covered by an impermeable day layer, a potential head difference between the core and clay could drive the protective clay layer away. The mechanisms for micro stability failure are depicted in Figure 59.

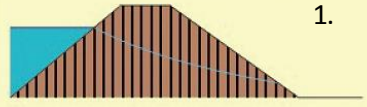
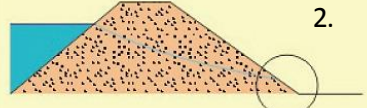
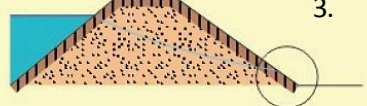
type dijk	micro-instabiliteit
kleidijk	 <p>1. geen probleem</p>
zanddijk	 <p>2. uitspoelen</p>
zanddijk met kleiafdekking	 <p>3. afdrukken/afschuiven</p>

Figure 59: The type of micro-instability depends on the type of dike: a homogeneous clay dike poses no threat (1), a sand dike is susceptible to the washing out of material (2), a sand core with clay cover can cause excessive pressure on the (impermeable) clay layer and ‘push’ it off (3). (source: Ministerie van Verkeer en Waterstaat, 2007)

However, rapid drawdown of water in the inner reservoir due to pumping might have an effect on the overall stability other than is taken into account for the macro stability computations. When the phreatic level inside the dam is still high from the moment the reservoir was full, the additional force could initiate the washing out of material, due to the increased potential head difference. Although this effect should not cause problems for this type of dam (Ministerie van Verkeer en Waterstaat, 2007), it is something that needs to be verified in a future stage.

Based on these figures and the fact that the dam will be constructed out of clay, it can be concluded that no micro stability issues are to be expected. This is stated once again in the guidelines for safety checks on primary water defences, which says: “A dike can be assumed ‘safe’ for micro stability when one of the following conditions is met:

- The inner toe has a well-functioning drainage system
- The core consists out of impermeable material (till at least above the water table)
- The dike is sandy and has an inner slope of less than 1:5 and no clay cover”

Considering the dam which is proposed for the ‘final’ design consists fully out of clay, this failure mechanism does not require adjustments to the design.

4.4.3 Piping

To prevent piping, the self-accelerating outflow of sediment through the dam (see Figure 60), the length along which the water may flow has to be sufficiently long to resist the water flow. The wider a dam will be the lower are the flow velocities and thus the risk of piping. The minimum required leakage length is determined through the formula of Bligh:

$$L \geq H_{max} C_B$$

- L = Leakage length (m)
- H_{max} = Maximum head difference (+high water level) (m)
- C_B = 'Seepage' coefficient (=3 for weak clay, according to Griffith) (-)

For a maximum head difference of 42.9m (= 40m + Highest Astronomical Tide + Sea Level Rise + Storm Surge), the part of the dam where the water flows through needs to be at least 129m wide. The preferred alternative for the inner slope has a leakage length of 158m. Knowing that the required leakage length is actually much shorter than the 129m (due to the conservative choice for the weak clay seepage coefficient), it can be concluded that piping will not form a hazard for the dam safety.

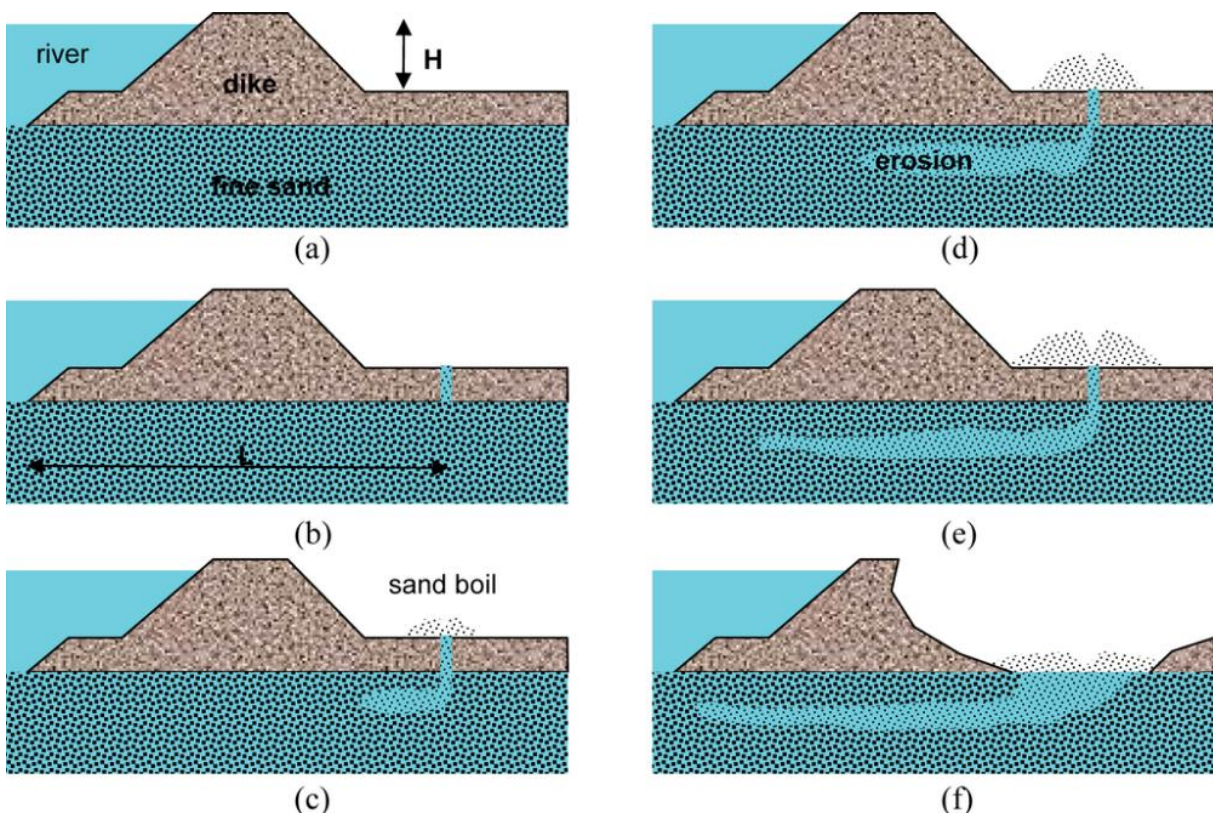


Figure 60: The development of piping for a river dike: Water level rises (a) ; Seepage initiates (b) ; Sand boil appears (c) ; Backward erosion (d-e) ; Failure (f) (source: Imre et al., 2015)

4.4.4 Seepage

Seepage by itself does not pose a threat to the overall stability, other than the issues dealt with in the micro stability section (§4.3.3.2) and it does not turn into piping. The sole disadvantage is a direct loss of revenue, since the water that flows into the reservoir needs to be pumped out again. It is therefore vital for the ‘efficiency’ of the system that the seepage stays limited. However one has to keep in mind that it is impossible to prevent water flowing in completely and there will always be some seepage. In order to quantify the amount of water reaching the inner reservoir it is best to make a distinction between seepage through the dam itself (see §4.3.2.2 and Figure 47 for more context about seepage through the dam) and through the layers underneath the storage reservoir.

The water flow through the dam can be estimated with the Dupuit formula, which is based on the head difference, the permeability of the soil and the flow length. The maximum seepage and head loss, when the reservoir is empty becomes:

$$Q_d = \frac{kH_{max}^2}{2L} \quad ; \quad H_{loss} = \frac{Q_d \pi D}{\frac{1}{4} \pi D^2} = \frac{4Q_d}{D}$$

- Q_d = Specific discharge through dam (per metre) ($m^3/d/m$)
- k = Permeability (=0.01 m/d for weak clay) (m/d)
- H_{max} = Maximum head difference (m)
- L = Flow length (m)
- H_{loss} = Head loss of reservoir due to seepage (m)
- D = Diameter of reservoir (m)

For the various scenarios with different head ranges and storage capacities, the discharge through the dam ranges from 350 m^3/d ($H_{max} = 40m$ and $E = 10GWh$) to 1400 m^3/d ($H_{max} = 60m$ and $E = 30GWh$). The resulting head loss due to water flowing in via the dam is only 0.03 – 0.12mm per day.

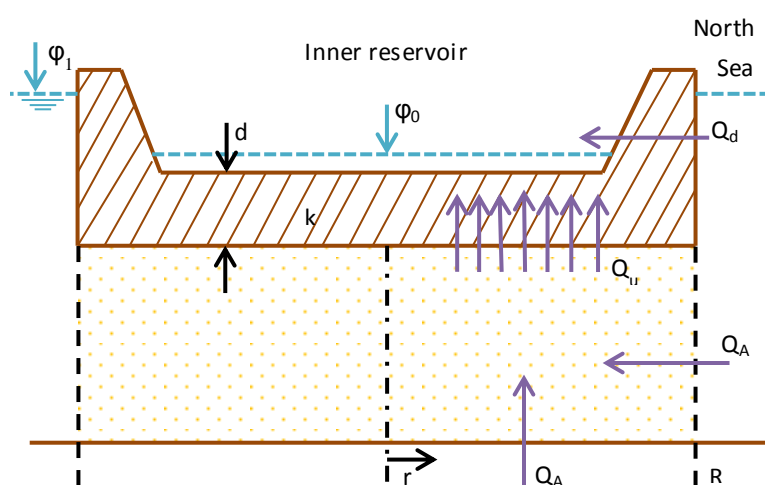


Figure 61: Seepage through the dam (Q_d) and the underlying clay layer (Q_u) when the recharge of the aquifer (Q_A) is equal to the discharge through the clay layer ($Q_A = Q_u$)

In the schematic drawing of Figure 61 one can see how the water flows into the reservoir via the dam and the aquifer (the sand layer) underneath. The situation as in Figure 61 withholds that the conveying aquifer is either in direct contact with the North Sea or the recharge of the aquifer is equal to the seepage into the inner reservoir. The beneficial case, when the aquifer is closed and barely recharges, is also worked out in Appendix G: Seepage and bursting mechanism

for a closed aquifer. The leakage through the bottom of the reservoir can be computed with the flow equations derived from Darcy's law. The results of the seepage through the dam and bottom of the reservoir are gathered in Table 17.

$$Q_u = \int_0^R 2\pi r \frac{\varphi - \varphi_0}{d} k dr = 2\pi R^2 \frac{(\varphi_1 - \varphi_0)}{d} k$$

- Q_u = Total leakage through bottom of reservoir (m³/d)
- R = Radius of reservoir (m)
- r = distance from the centre of the reservoir (m)
- φ = Piezometric level for a specific r ($\varphi = \varphi_1$ for $r = R$ and $\varphi = \varphi_0$ for $r = 0$) (m)
- k = Permeability of clay layer (=0.01m/d) (m/d)
- d = Thickness of clay layer (=35m or 25m depending on depth of the reservoir) (m)

Scenario	Unit	1	2	3	4	5	6	7	8
Maximum head	m	40	40	40	40	40	60	60	60
Radius reservoir	m	964	2,309	2,259	3,083	3,715	1,684	2,234	2,655
Storage capacity	GWh	1.22	10.51	10	20	30	10	20	30
Seepage dam	mm/d	0.12	0.05	0.05	0.04	0.03	0.10	0.08	0.06
Seepage bottom	mm/d	10.29	10.29	10.29	10.29	10.29	21.60	21.60	21.60
Total discharge	10 ⁵ m ³ /d	0.3	1.72	1.65	3.07	4.46	1.93	3.39	4.78
Total head loss	mm/d	10.4	10.3	10.3	10.3	10.3	21.7	21.7	21.7

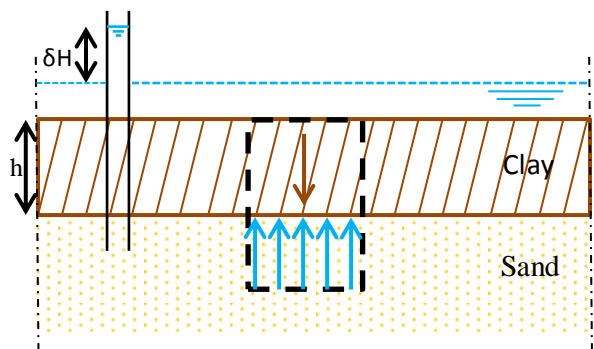
Table 17: The loss of head due to leakage. Note that the seepage through the dam and bottom are converted into a head loss per day. The water level in the inner reservoir is its average operational level

Even with the conservatively chosen permeability of 0.01m/d for the clay layer, the effect of seepage on the head loss in the reservoir is surprisingly small. Although the total discharges (in the order of 300,000m³/d) might seem like a lot, it is only around 0.2% of the total fluctuating water volume. The common permeability of clay is an order 100 to 10,000 times lower than the 0.01m/d that was used in the computations! Therefore the seepage can be later neglected in efficiency computations of the storage system.

4.4.5 Bursting of the clay layer

For determining the required thickness to prevent bursting of the bottom clay layer, it is firstly assumed that one of the water retaining measures is executed, as described in §4.3.3, and adequately ‘closes’ the top sand layer. Therefore only the bottom clay layer is checked here whether it meets the safety criteria regarding the bursting failure mechanism.

The possibility of the bursting (or ‘lifting-up’) of the clay layer has much to do with the computations performed previously to determine the seepage through the clay layer. The water pressure underneath the clay layer, resulting from the water level difference between the North Sea and the inner reservoir, drives both the seepage- as the bursting-mechanism (see Figure 61 for a schematisation of the acting water pressure). In principle the downward force from the self-weight of the soil has to outbalance the upward force by the water pressure, as shown in Figure 62⁸. This simplification leads to the following set of equations, based on the principles of Archimedes:



$$\begin{aligned}
 \text{Force upwards} &= \gamma_{w,d} \delta H \\
 \text{Force downwards} &= (\gamma_{s,d} - \gamma_{w,d}) h \\
 \text{Equilibrium when } h &= \frac{\gamma_{w,d}}{\gamma_{s,d} - \gamma_{w,d}} \delta H
 \end{aligned}$$

Figure 62: The difference in water pressure over an impermeable layer. To prevent bursting of the clay, the self-weight of the clay layer has to outbalance the difference in water pressure acting from underneath.

When we assume that the top of the sand layer starts at -85m relative to the sea level (see Figure 132 for the soil profile of the Dogger Bank) and the inner reservoir is completely empty; then δH becomes 85m minus h . After rewriting the above equation the minimally required soil overburden becomes 43.56m thick, which results in a maximum water level difference of 41.44m. Thus the 40m that has been used so far in the design is achievable. The tide and storm surges will not affect the water pressure in the aquifer underneath. Only sea level rise (3mm/year) will eventually alter the acting water force. To allow for construction tolerances and limited heterogeneity of the clay layer, a 40m head difference continues to be used in the design of a offshore pumped hydropower facility on the Dogger Bank.

⁸ In reality there is also the cohesion from the clay layer, which counterworks any movement of the clay. However, for a sufficiently large patch of clay the cohesive counterforces become negligible in comparison with its self-weight working downwards too.

4.4.6 Overtopping

Overtopping can cause crest and inner slope failure in two ways: either by direct erosion from the discharge or by firstly saturating the top layer, which makes it less resistant and secondly lose its stability. The crest level was set at +17m relative to still water level during the design of the outer protection in 4.3.1. An overtopping discharge of 10l/s/m was found acceptable, considering the erosion resistant characteristics of the inner slope. To limit the discharge to 10l/s/m the dam needs to have an elevation of +16 metres. By adding an extra metre to the crest height, the safety is enhanced following the guidelines (Bezuyen et al., 2012). Thirdly, settlement and creep of the dam body have to be accounted for. Therefore the constructed dam height will be higher. As a rule of thumb, ten percent of the volume should be added to counteract future settlement (Bezuyen et al., 2012).

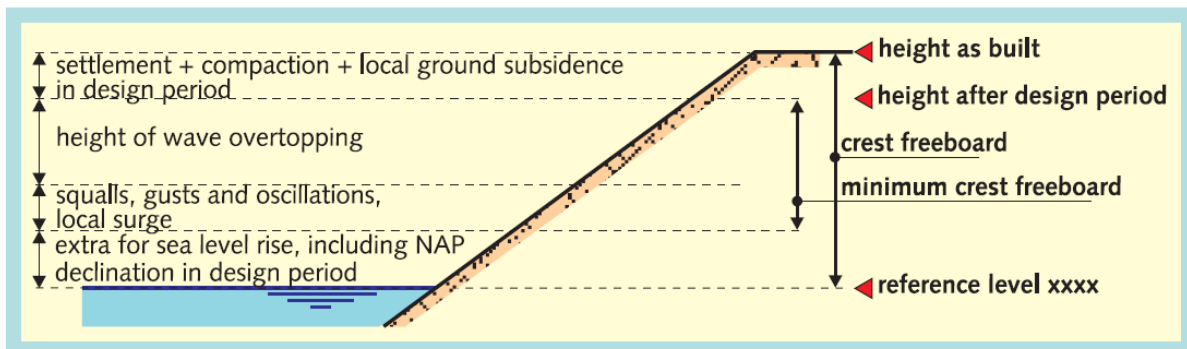


Figure 63: The level of the crest height, set to resist the various mechanisms of run-up, set-up, sea level rise and settlement (source: Van der Meer, 2012)

Consequently the real discharge will be lower, due to the added volume and height of the dam. Nevertheless the discharge of 10 litres per second per metre has to be taken into account. In order to allow such volumes, erosion preventive measures have to be taken on the inner slope. A well maintained grass cover should suffice (Van der Meer, 2012). According to the guidelines, there has to be a clay layer underneath the grass of at least 0.6m thick. These two directives are easily met in the design(s) considered. No further overtopping-mitigating measures are required.

4.5 Final design and concluding remarks

During the design of the dam it really became clear that the 'designing-phase' is not a linear process, but requires constant loops and iteration between design parameters and failure mechanisms. For now the dam design is as it is depicted in Figure 64 in which form it meets the safety standards of the discussed failure mechanisms. Due to the local geology and the bursting criteria, the maximum head difference would be 41.45m of which 40m has been chosen as a practical limit. As can be seen in Figure 64, a large inner berm had to be added in order to deal with the combination of inner slope stability and the uplift/bursting mechanism at the inner toe. This unfortunate mixture of forces led to an inner berm of 113m wide! From the seepage computations it appeared that, when choosing very conservative permeability characteristics, the leakage through the dam, retaining measure and underlying clay could all be neglected.

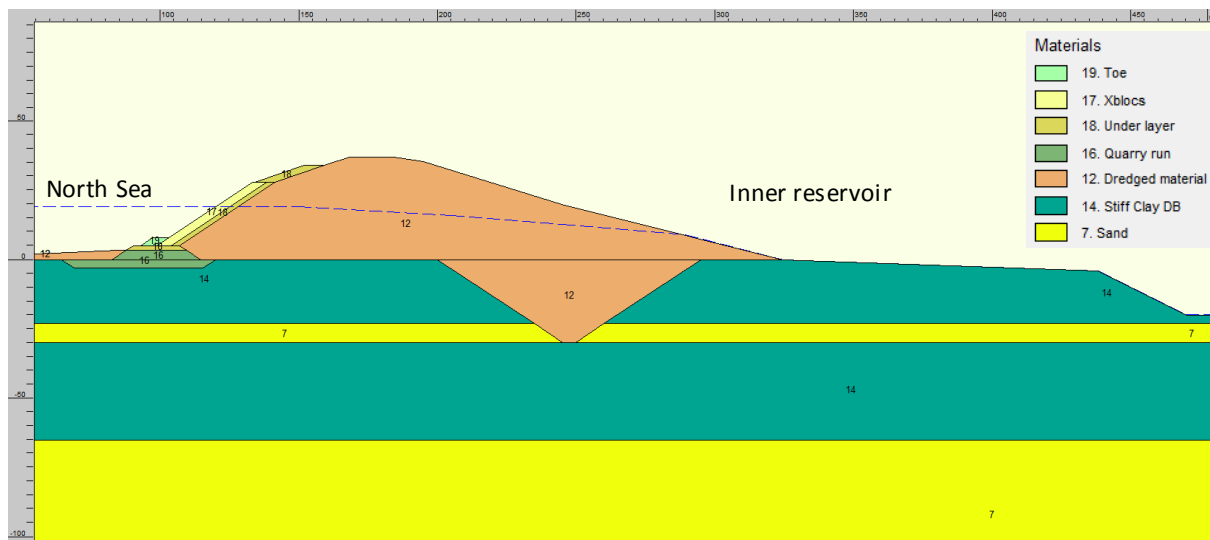


Figure 64: The dam design with the various materials that are used. The scales are in metres.

The costs for every individual layer and component are (as later explained in §8.1 Dam costs) for the discussed design 86.31 m€/km in total, with an investment of 310 m€ in dedicated dredging and transportation equipment. Why this specific dredging equipment is necessary and beneficial to use is later explained in the dredging chapter. This results in the dam costs versus storage capacity relation as shown in Figure 65.

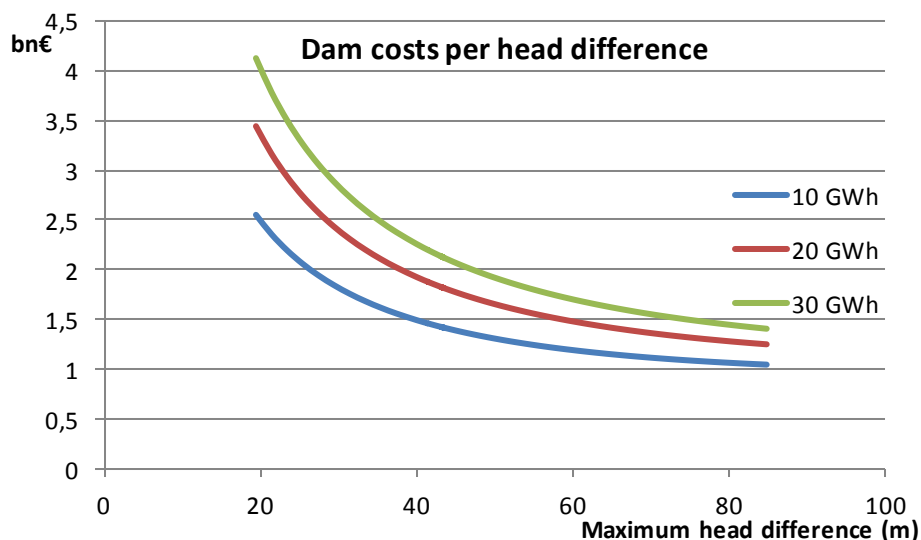


Figure 65: The total costs of the dam and dredging works per storage capacity, with the original seabed 20 metres below MSL. Note the rapid decline in capital costs once the head difference between the reservoirs increases.

The main trend that Figure 65 shows is that when the head difference between the North Sea and the storage reservoir increases, the total dam costs decline (not the dam costs per metre). This might appear counterintuitive, since the dam would have to enable a larger water level difference. However, the dam costs mainly originate from retaining the water column between MSL and the seabed (20m below MSL) plus the necessary crest height to restrict overtopping. When the head difference is then increased beyond 20 metres the dam size itself hardly changes and only the inner reservoir is deepened.⁹ Therefore the dam costs per metre only grow marginally when the water level difference surpasses 20 metres, due to higher dredging costs (a larger depth involves rising dredging costs).

The advantage of a higher head for the dam costs lays in the formulae (derived in §3.4) for storage capacity and dam length:

$$\text{Storage capacity: } E = \frac{1}{4} \pi D_w^2 \rho g \frac{(H_{max}^2 - H_{min}^2)}{2}$$

$$\text{Circumference: } L_D = \pi D$$

- E = Storage capacity (J)
- m = Mass of water (kg)
- g = Gravitational acceleration (m/s²)
- ρ = Density of water (=1025) (kg/m³)
- H_{max} = Maximum head difference (m)
- H_{min} = Minimum head difference (m)
- D_w = Average diameter of water surface (m)
- L_D = Total length of dam (m)
- D = Centre-to-centre diameter of the dam (m)

The first equation states that when the storage capacity (E) is kept constant the diameter of the storage reservoir (D_w) decreases when the head difference is increased. The second equation states that the total dam costs reduce as the diameter shrinks. Subsequently a larger head difference leads to a shorter dam length and thus to lower costs to store an equal amount of energy.

The combination of a marginal increase in dam costs per metre and large reduction in necessary dam length lead to the statement: as the head difference between the reservoirs is increased the overall dam costs decline.

The relation between dam costs and head difference is distinctive for an inverse offshore PHS facility. For other types of dams the costs usually rise according to the water level difference. In this case though, the dam costs are largely determined by the depth of the original bathymetry and the local wave conditions and not so much by the depth of the inner reservoir.

The acquired relation confirms the expectation that the maximum tolerable head difference is preferred. With the available geologic information from the Dogger Bank the practical maximum head difference is 40 metres.

⁹ Imagine when looking at the final design of Figure 64 that when the head difference over the dam would be enlarged, this would only require further excavation of the inner reservoir. Consequently it is solely the inner berm that would become larger, where the constructed dam itself remains mostly the same.

The computed dam costs from Figure 65 can be used to determine the necessary investment to obtain a certain storage capacity, with a known maximum head difference. To do so the acquired formula (from trend lines of Figure 65) in Table 18 can be used.

Storage capacity (GWh)	Reservoir costs formula (€)	Reliability number (R ²)
10	$10^9 * 12.867 * H_{max}^{-0.58}$	0.976
20	$10^9 * 22.853 * H_{max}^{-0.668}$	0.986
30	$10^9 * 31.658 * H_{max}^{-0.713}$	0.990

Table 18: Scaling formulae to determine the total dam costs for a given head difference, with the dam to be constructed in 20m deep water

For the chosen 40m water level difference between the North Sea and the inner reservoir, the storage capacity scales with the costs as presented in Figure 66.

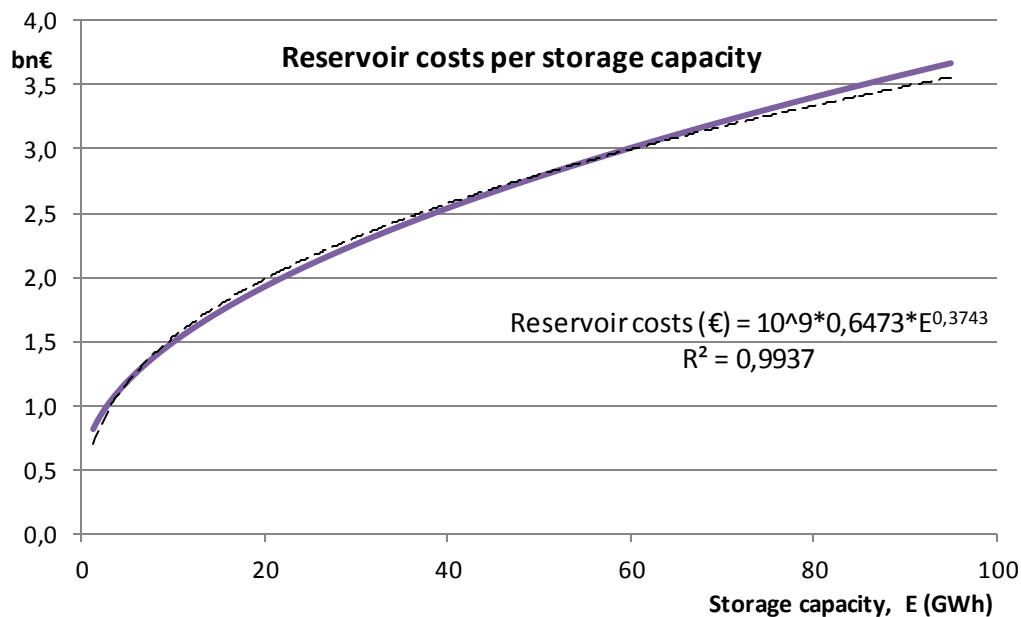


Figure 66: The relation between costs and storage capacity for a maximum head difference of 40m and dam costs of 86.31m€/km. The dashed line is the trend line of which the equation and reliability number (R²) is given to easily approximate the costs

The depicted relation between storage capacity and reservoir costs outline the main trend: A large storage reservoir is relatively cheaper than a smaller variant. The reason of this lays in the same formulae as stated on the previous page, where the storage capacity scales with the diameter squared and the dam costs linearly with the diameter.

Additionally it is advised to implement a storage capacity larger than 15GWh, since for smaller sizes the dam size is relatively large compared to the reservoir (the reason why the start of the graph in Figure 66 is steeper).

Furthermore one has to be aware that for the dredging costs the assumption was made that the material from the inner reservoir that is not needed for the dam construction, would be dredged and paid for by the creation of the 'Energy hub' and additional functions (the chosen scenario in §3.5 Volume balance). This is a reasonable presumption for small to medium sized reservoirs (10 – 25GWh). However, for larger reservoirs it will become problematic to allocate the redundant material for other purposes. Consequently these bigger schemes might have to carry higher dredging costs. Of course the size of the reservoir is also limited by suitable geologic conditions (presence of thick clay layers). These will be increasingly more difficult to find for larger areas.

From the dam design for an offshore pumped hydropower storage facility on the Dogger Bank three main conclusions can be drawn:

1. Constructing a dam that can cope with the discussed failure mechanisms is possible.
2. As the head difference between the reservoirs is increased the overall (not per metre) dam costs decline.
3. A large storage reservoir is more economical compared to a smaller one from a civil costs perspective.

Now a preliminary design for the dam is made and the maximum achievable head difference is known (40 metres), this provides the input for the necessary dredging works and the choice and housing of turbines.

5. Dredging works

The construction of the island to create the 'energy hub' and the circular dam for the storage facility itself require large amounts of building material. As explained in §3.5 Volume balance, this is a mutual beneficial situation. To create the desired storage capacity and head difference, the inner reservoir needs to be dredged. The material that becomes available can secondly be used for the dam and island construction (see Figure 67). Due to this scenario the average distance between the soil being dredged and deposited for the dam construction is only 400 metres.

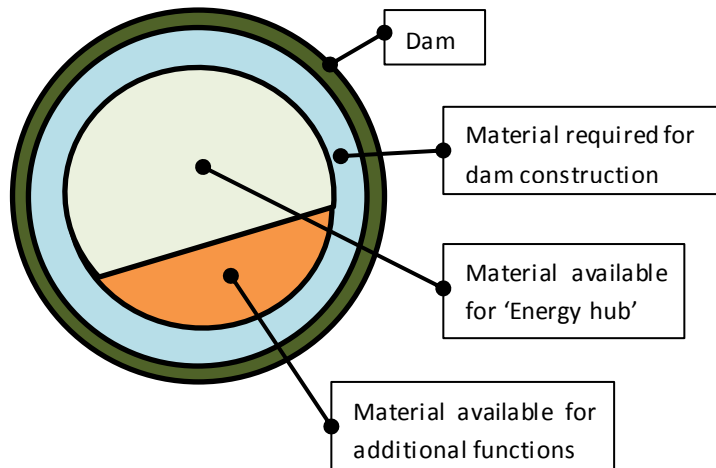


Figure 67: Schematic top view of the pumped hydropower reservoir. Note that the material, which is necessary for the dam construction can be dredged directly next to the future dam. The material in the centre is available for the island and additional functions.

5.1 Selection of dredger

There are two main types of dredging: hydraulic dredging and mechanical dredging. With suction dredging the soil is mixed with water by either: only suction, cutting or dragging/trailing of the suction mouth and then pumped into the vessel (see Figure 68). Mechanical dredging involves direct displacement of the soil by some sort of grab, without mixing the material with water (Figure 69).

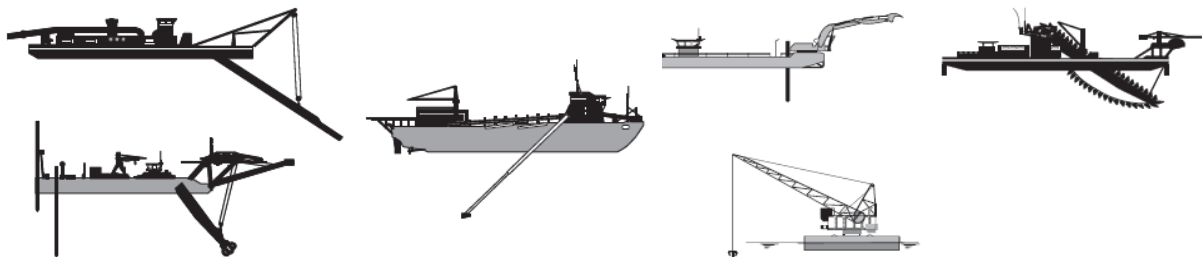


Figure 68: Suction dredgers: plain suction dredger (top left), cutter suction dredger (bottom left) and trailing suction hopper dredger (right) (source: Van 't Hoff & Van der Kolff, 2012) Figure 69: Mechanical dredgers: backhoe dredger (top left), grab dredger (bottom left) and bucket dredger (right) (source: Van 't Hoff & Van der Kolff, 2012)

Nearly all the material that has to be dredged will consist out of stiff clay. From the suction dredgers only the cutter suction dredger (CSD) is capable of efficiently removing such material. The trailing suction hopper dredger (TSHD) wastes too much power by trying to drag its 'arm' through the clay in order to remove it (S.A. Miedema, personal communication, August 3, 2017).

Although a CSD is able to dredge clay, it can only do so by first cutting it to small pieces before it can pump it up. During this process the clay already loses a lot of its strength features, due to the high water content (Van 't Hoff & Van der Kolff, 2012). Additionally, when hydraulically transporting the soil via a pipelines system, clay lumps can erode and turn into clay balls and a remaining slurry (see Figure 70). A (porous) clay ball structure will result in large settlements and poor permeability of the dam. To prevent clay ball formation the clay has to be cut into as small as possible pieces (Vandycke, 2002), excluding the clay for structural purposes.



Figure 70: The formation of clay balls by pipeline transport (source: Van 't Hoff & Van der Kolff, 2012)

All three mechanical dredging technologies are suitable to dredge clay. However, the backhoe- and bucket dredger are both limited to a maximum dredging depth of more or less 30m. A grab dredger (GD) on the contrary can excavate till extremely large depths (>500m), since it is only limited by the length of its wires.

The dredging depth of maximally 40 metres and the stiff clay that needs to be displaced (but remain intact!), make the grab dredger the preferred technology. Additionally it will not have any problems when it encounters large boulder that are left from the various glacial ages.



Electric hydraulic slewing system	
Hoisting load	690 ton
Working radius	31 m
Dredging depth	48m
Head above water	10m
Hoisting speed	In the air 0.758m/sec In the water 1.075m/sec
Lowering speed	0.905m/sec
Turning speed	0.6 times/min
Turning angle	±155°
Dredging depth	48m

Figure 71: The largest grab dredger in the World: Gosho (200m³) used for a terminal reclamation project in Singapore (2016). It uses a counterweight system to reduce the energy consumption and simplify the hoisting mechanism (source: http://www.kk-kojimagumi.co.jp/english/news/excepteur_sint_occaecat_cupidatat_non.html)

With a dedicated clamshell it will be possible to obtain a 100% filling ratio of the grab. A conventional grab will have problems dredging the stiff glacial clay, because the grab does not penetrate into the seabed deep enough and thus it will only ‘shave-off’ the top layer. Therefore the dedicated grabber should be designed to do exactly this: ‘shaving-off’ the top layer, but still in large quantities (in the order of 50m³ per grab). This can be done with a very wide grab, so it will have a large ‘footprint’/ ‘distance between cutting-teeth’ on the seabed when it is about to start grabbing (S.A. Miedema, personal communication, August 3, 2017).

5.2 Dredging operation

One of the conventional methods of using a grab dredger would be that the grabber would be installed on its own pontoon/vessel, like in Figure 71 and dump the dredged material directly in a barge. The barge would then sail to the area where the dam needs to be constructed and unload. Since the dumped material will be reshaped afterwards by a backhoe, it does not require precise dumping (Figure 72). Therefore a split hopper barge (SHB) will be the quickest and most efficient barge for this process (Van den Bos, 2017b).

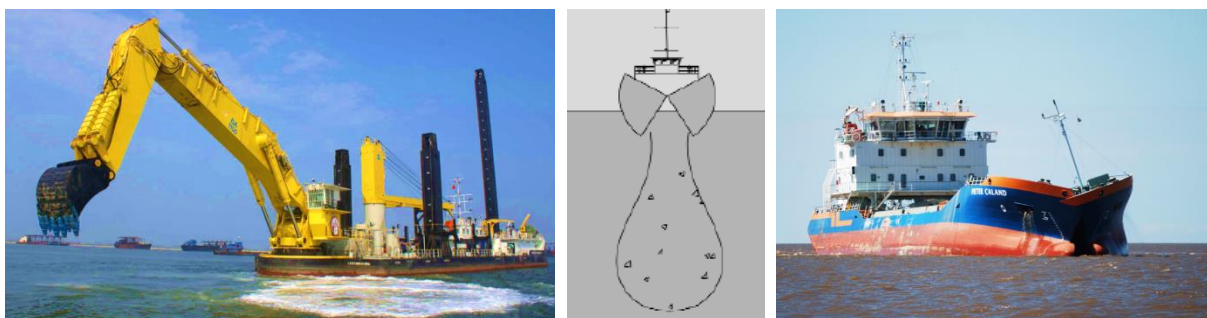


Figure 72: A backhoe with a maximum dredging depth of 32m (left) (source: <http://www.jandenul.com/en/equipment/fleet/backhoe-dredger>) and a split hopper barge (middle and right) (source: Van den Bos, 2017b; <https://www.vanoord.com/activities/hopper-barge-and-pushbuster>)

Although there is a lot of experience using the mentioned process and equipment of using a grab for dredging, split hopper barges for transport and a backhoe dredger for reshaping the dam. They all have in common that they cannot cope very well with offshore wave conditions. The three of them are limited to wave heights around 1.0 – 1.5 metres (Van den Bos, 2017b; Van 't Hoff & Van der Kolff, 2012). Partly this can be mitigated by upscaling the equipment (the larger the vessel, the larger its limiting wave height/length). However, aligning a split hopper barge for loading next to the grab dredger with larger waves will be a precarious enterprise. The mean wave heights from Table 20 ranging from 1.3m to 1.7m for the various directions will significantly reduce the workability of the conventional dredging process (obtained by Frölke (2017) from Argos data: 55°N 3°E measured over Jan 1992 – Dec 2016).

To ensure a quick and reliable construction period a solution has to be found to the vigorous waves on the North Sea. Both in the oil and gas as in the offshore wind industry, jack-up systems are often deployed to get rid of restricting wave conditions. By hauling the hull or pontoon out of the water the surface area that is in contact with the attacking waves is limited to its (four) spuds (see Figure 73). Consequently jack-up systems can deal with much stronger wave conditions.

Yet, when a grab dredger would be installed on a jack-up platform, the grab would dig away the soil on which its own spuds are standing! This makes a combination of dredging and a jack-up system impossible.



Figure 73: An offshore wind turbine installation vessel performing its jack-up tests (top) and a working platform (bottom) (source: <http://www.ziton.eu/wp-content/uploads/WIND-SERVER-jacked-03-low-res.jpg>; <http://www.thinkdefence.co.uk/ship-to-shore-logistics/increment-2-pier/>)

The problem of dealing with severe wave conditions and not being able to use a jack-up system has been previously encountered by the oil and gas industry. May it from different reasons (namely too deep water for a competitive jack-up platform), a solution has been found none the less. Instead of deploying spuds that need to be supported by the seabed, the spuds are connected to a submerged pontoon, depicted in Figure 74. By doing so the vessel is barely affected by the surrounding wave action, due to the limited interaction with the sea, just like for the jack-up equivalents.

The vessel is powered and can remain on its position by using a dynamic positioning system (DPS). Various sensors measure the displacement and acceleration of the vessel continuously. The influence of the wind, waves and current is then transformed into a signal to counter the movements, by powering several thrusters individually. This combination of a semi-submersible vessel and a DPS is frequently used in deep sea (>300m) oil and gas exploration and production (Yamamoto & Morooka, 2005). Therefore these technologies offer a trustworthy alternative to the conventional dredging processes. The semi-submersible vessel equipped with grab dredgers will remain stable and operational in much extremer wave conditions than traditional grab dredgers and barges.

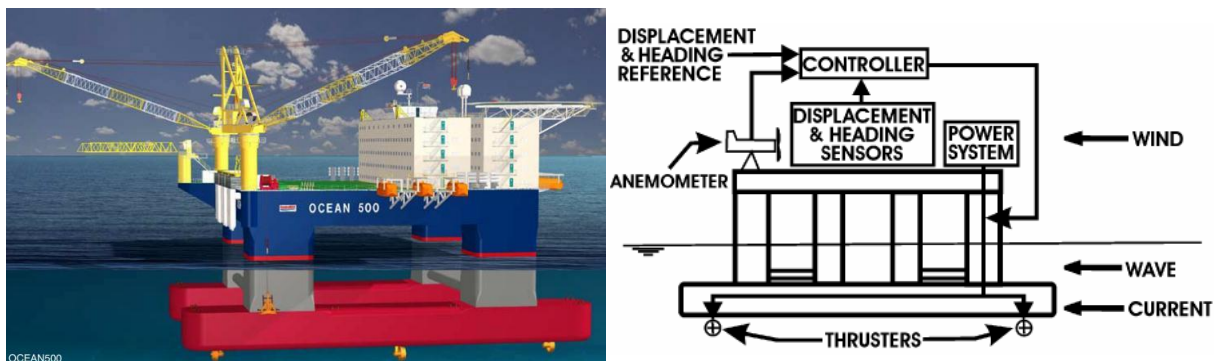


Figure 74: A semi-submersible accommodation vessel for harsh environments (left). It can host 750 people on board and is powered by a dynamic positioning system (right). Ordered for 200 million USD (source: <http://worldmaritimeneews.com/archives/89220/cosco-nantong-secures-accommodation-vessel-order/>; Yamamoto & Morooka, 2005)

Of course when someone desires to use a semi-sub vessel with a dynamic positioning system, one desires to know how large the maximum displacement will be in specific wave conditions. Yamamoto and Morooka studied exactly this (2005) for a semi-submersible platform connected via eight columns to two pontoons of 115m length, 15m wide and 8m high. Their results are presented in Table 19.

Wave spectrum	Wave height, H_s (m)	Wave period (s)	Maximum displacement (m)
Regular waves	3	10	3
Irregular waves	5.1	11	25
Irregular waves	6.3	12	38

Table 19: Maximum displacements of a semi-submersible platform powered by a DPS during various wave conditions. Results obtained by Yamamoto & Morooka (2005)

Based on the studied literature and improvements of dynamic positioning systems it is assumed that a maximum displacement of 10m in an irregular wave spectrum with a significant wave height of 4.5m is feasible. A particular problem of using a semi-submersible vessel for the dredging process is the possibility of grounding, due to its large draught. The studied semi-sub has a draught of 20m, which would require it to dredge its own trench in order to relocate. However, all semi-subs are custom made and the pontoons can simply be made a little wider to generate more lifting force. The design with wider pontoons should result in a more practical draught of around 17 metres.

As explained and depicted in Figure 67 earlier, the average distance between dredging and depositing the material for the dam construction is only 400m. The maximum distance is 420 metres. The weakest link between the dredging and transporting chain will govern the achievable productivity. The transportation link should therefore also be able to cope with fierce wave conditions (out ruling any sort of barge), when used in cooperation with grab dredgers mounted on a semi-submersible vessel.

The seabed between the grab dredger(s) and the dam will be stable: either at the level of the original bathymetry, at the desired reservoir depth (-40m to MSL) or on the level of the (partly) constructed dam (see Figure 75). For all of these three situations a jack-up pontoon could be used in order to safeguard a continuous production. The jack-up platform will thereby bridge the distance between the 'semi-sub' and the future dam.

To transport the dredged material from the dredger to the dam a conveyor belt system will be most efficient. The expanse in between the semi-sub and the jack-up will be covered by large rotatable cranes (to cover 10m of orthogonal displacement) that lift the extendable conveyor belts (to deal with 10m of parallel displacement). A similar crane and conveyor belt will be used at the other end of the jack-up platform, which can accurately deposit the dredged clay.

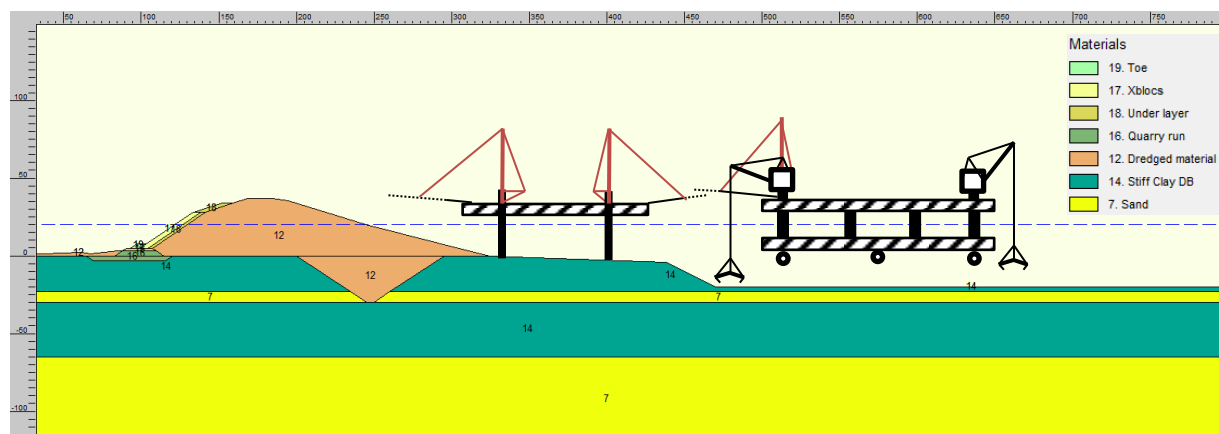


Figure 75: Schematisation of the dredging process using four grab dredgers, which are mounted on one semi-submersible vessel and a jack-up pontoon, both fitted with conveyor belts. The striped black lines indicate the extendable conveyor belts to adjust for movements of the semi-submersible platform and allow for flexibility

The rotating cranes that carry the conveyor belts permit (limited) sideways movement of either the semi-sub or the jack-up, while continuing transport of the dredged material. Therefore the jack-up can be repositioned, without halting the production capacity. There are a few options for relocating the jack-up pontoon:

- Multiple spuds allow for the lifting of one or two spuds who can reposition, while others temporarily carry their weight. Secondly the moved spuds take over the weight again and so the others can be lifted and positioned. This way of moving is common for (floating!) grab- and backhoe dredgers.
- The pontoon can be lowered till it is floating, lift up the spuds and be pushed or towed into position by a tugboat.
- The pontoon can be lowered till it is floating, lift up the spuds and propel itself.

The process of repositioning the jack-up is not further considered, but remains for future investigation

5.3 Specifications and costs

In this section the two mentioned dredging processes will be compared on their weekly production capacity and the corresponding costs. The costs are largely based on the guide to costs standards for dredging equipment (2009) by CIRIA. First of all the dredging capacity of the grab dredger will be presented when afterwards the conventional ‘grab & barge’ and the innovative ‘semi-sub & convey’ processes will be specified.

Grab production

Both the grab dredger as the semi-submersible platform will be equipped with the same grab. The production depends on the size of the grab (60m³) and the cycle time. The cycle time depends on the dredging depth, the hoisting and lowering speed, the turning time and the time it takes to open and close the grab. The used values and the dependence of the dredging depth are shown in Figure 76.

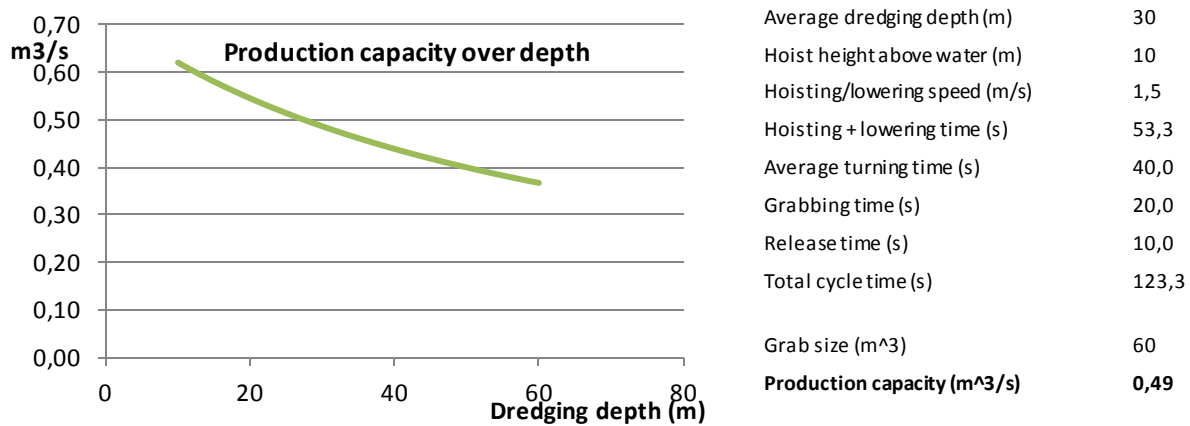


Figure 76: The dependence of the dredging capacity on the depth and the cycle time, with a 100% filling ratio of the bucket

For the Dogger Bank and the chosen water level difference of 40 metres between the North Sea and the inner reservoir, the average dredging depth is 30m (from 20 to 40m below MSL). The production capacity during operational hours will therefore be taken as 0.5m³/s per grabber.

Grab & barge process

The grab dredger will be specially constructed for 80 million euros, 30 million for the grabber and 50 million for the vessel and auxiliary equipment. Half the investment will be covered by the energy storage project and the other half under the creation of the ‘Energy Island’ and the additional functions. A grab dredger is typically 84 hours per week in operation (CIRIA, 2009), for such expensive equipment and in offshore conditions 168hr/wk is more likely. The weekly production then becomes 136,512 m³ as computed in Table 20. The time it takes for a split hopper barge to sail back and forward and unload the dredged material is given in the same table.

Week production (net) dedicated grab dredger		Split hopper barge cycle time	
Time in service	168 hr/wk	Sailing distance	396 m
Repairs	6 hr/wk	Total sailing time (3 knots)	8.5 min
Workability (operational waves)	60%	Positioning	10 min
Productivity (delay & spillage of clay)	80%	Offloading	5 min
Time operational	= 75.8 hr/wk		
Week production (44.5*3600*0.5)	136,512 m³/wk	Total cycle time	23.5min

Table 20: Grab dredger production and the cycle time for transport by a split hopper barge. Note the low workability, due to the exposed environment

According to Table 20 it takes the split hopper barge 23.5 min to complete its offloading cycle. To allow for some minor discrepancies 25 minutes is used. In the same timespan the grab dredger is capable of dredging 750m^3 ($=25*60*0.5$). However, the original bathymetry is only 20m deep, which results in the higher production capacity of 825m^3 (as explained by Figure 76). To get rid of waiting times between the grab dredger(s) and split hopper barge(s), two small SHBs can be combined with one grab dredger or two medium sized SHBs with two grab dredgers. For the latter option the barge needs to have a minimum capacity of 1650m^3 . Therefore split hopper barges of 2000m^3 (a little bigger to have some extra flexibility in the process) will be employed to take care of the transport of the dredged material. This is common equipment and can simply be hired.

Furthermore a backhoe dredger is required to reshape the dam below water and a normal land-based excavator to do the same above water level. As soon as the dam approaches the sea level, construction will have to continue from land. Barges will sail to the dam, where they will be unloaded and transport will continue via dump trucks. For a more detailed construction process of the dam, see §Appendix H: . The project costs of the most advantageous arrangement of operating four grab dredgers and four split hopper barges are given in Table 21.

Element	OPEX (€/wk)	CAPEX (€)
Grab dredger (60m^3) (dredging)	4*350,000	4*0.5*80,000,000
Split hopper barge (2000m^3) (transport)	4*100,000	-
Backhoe dredger (profiling)	250,000	-
Excavator (profiling)	10,000	-
Total	2,060,000	160,000,000

Table 21: Costs of 'grab & barge' process. The OPEX include depreciation, interest, maintenance, repairs, fuel, personnel and all other operating costs. The other half of the investments costs of the grab dredgers are carried by the 'energy hub' project.

The costs as in Table 21 are chosen on the conservative side. Especially for the grab dredger the costs may be lower than indicated, since a large part of the OPEX is the depreciation of the equipment. Thereby the depreciation is already discounted in the capital expenditure under the assumption that the complete costs of the grab dredger will be covered by the dam and island construction, instead of over its service life (CIRIA, 2009).

With the weekly production of a grab dredger and all corresponding costs known the unit price becomes as presented in Table 22.

Week production (net)	546,048 m^3/wk
Dam construction speed	103.6 m/wk
Operational costs	2,060,000 €/wk
Capital costs	160,000,000 €
Operational unit price	3.77 €/m ³
'Constructed' unit price (*1.5)	5.66 €/m ³
Unit price including capital costs (for 20GWh)	8.00 €/m ³

Table 22: Unit price for grab & barge process. The 'constructed' unit price includes all project related costs like site investigation, monitoring, design, profit, uncertainty and risk. This in combination with the capital costs can be used to determine the overall dredging costs. The bottom unit price is an example of where the CAPEX is already included for a 20GWh storage system with a 40m head difference

Semi-sub & convey process

The grabs that are mounted on the semi-submersible platform are the same as on the self-operating dredgers. However, the working platform can be in service all week round and it is not as much affected by the waves. Therefore the week production of a single grab significantly increases as reflected by Table 23.

Week production (net) dedicated grab on semi-sub vessel	
Time in service	168 hr/wk
Repairs	6 hr/wk
Workability (operational wave conditions)	95%
Productivity (delays & spillage of clay)	80%
Time operational	= 123.1 hr/wk
Week production (146.2*3600*0.5)	221,616 m³/wk

Table 23: Production capacity of a single grab installed on the semi-sub

Four grabs in total will be installed on the floating platform, in each of its corners. Just like for the grab & barge process, a backhoe dredger and an excavator on tracks are necessary to shape the dam. The main specifications of the equipment involved are shown in Table 24.

Element	Specification
Grab size	60 m ³
Grab reach	30 m
Grab production (average)	0.5 m ³ /s
Semi-submersible vessel (LOA * beam)	150m * 60m
Maximum length (extendable) conveyor belt	60 m
Crane capacity	1200 t at 30 metres
Jack-up pontoon (LOA * beam)	120m * 30m
Length spuds	50 m
Jack-up speed	0.5 m/min
Maximum length (extendable) conveyor belts	60 m
Crane capacities	1200 t at 30 metres
Conveyor belt velocity	2 m/s
Conveyor belt capacity	4 m ³ /s
Backhoe dredger (profiling)	250 m ² /hr
Excavator on tracks (profiling)	250 m ² /hr

Table 24: Characteristics of the main equipment involved in the semi-sub & convey process

The semi-submersible vessel and its four grabbers will have to be specifically made and so does the jack-up platform and the whole conveyor belt system. The costs of the semi-sub and grabbers can be shared with the Energy Island and additional functions, but the jack-up will be entirely paid for. For the initial island construction the semi-sub could potentially be equipped with a sort of mooring facility in order to let barges berth and load at the end of the conveyor belt system. The costs of the involved equipment is summarised in Table 25.

Element	OPEX (€/wk)	CAPEX (€)
Grab (60m ³)	4*175,000	4*0.5*30,000,000
Semi-sub vessel with DPS	500,000	0.5*300,000,000
Conveyor belt system semi-sub	100,000	Included in semi-sub
Jack-up pontoon	300,000	100,000,000
Conveyor belt system jack-up	150,000	Included in jack-up
Backhoe dredger (profiling)	250,000	-
Excavator (profiling)	10,000	-
Total	2,010,000	310,000,000

Table 25: Operational and capital costs concerning the semi-sub & convey process

Just like in the grab & barge process the costs are evenly chosen on the conservative side. It does become clear that for such expensive equipment it is really beneficial to be able to share the investment costs with another project (like the energy island in this case). Although the complete project seems rather expensive, one can see in Table 26 that due to the enormous production rate the unit price is very low!

Week production (net)	886,464 m ³ /wk
Dam construction speed	168.3 m/wk
Operational costs	2,010,000 €/wk
Capital costs	310,000,000 €
Operational unit price	2.27 €/m ³
'Constructed' unit price (*1.5)	3.40 €/m ³
Unit price including capital costs (for 20GWh)	7.17 €/m ³

Table 26: Unit price for semi-sub & convey process. The 'constructed' unit price includes all project related costs like site investigation, monitoring, design, profit, uncertainty and risk. This in combination with the capital costs can be used to determine the overall dredging costs. The bottom unit price is an example of where the CAPEX is already included for a 20GWh storage system with a 40m head difference

Comparison dredging processes

From the discussed two working methods it can be concluded that the achievable production rate is governing. By using a semi-submerged vessel for the dredging and a jack-up pontoon for the transport, the whole procedure becomes almost independent from the wave conditions. The advantage of using the semi-sub & convey process is confirmed by Table 27 and Figure 77.

Dredging process	Costs dedicated equipment (€)	Unit price (€/m ³)
Grab & barge	160,000,000	5.66
Semi-sub & convey	310,000,000	3.40

Table 27: The capital and operational costs of the two reviewed dredging processes

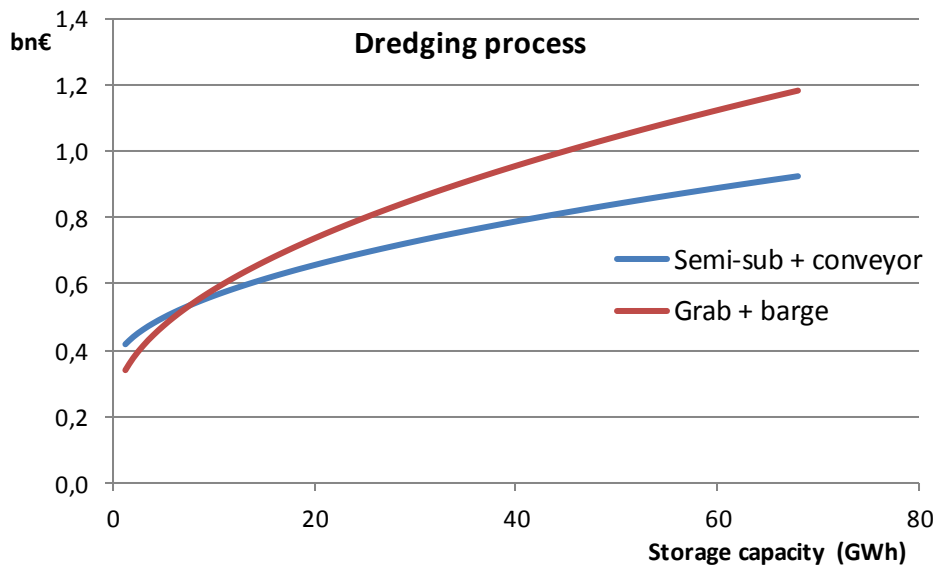


Figure 77: The total dredging costs for a storage reservoir with a 40m maximum head difference and 5545m³/m of dam to be dredged. The grab & barge process is more competitive till 7.7GWh, afterwards the semi-sub & convey process is preferred

Based on the large price difference the innovative semi-sub & convey construction process is the chosen alternative (the storage capacity is likely to exceed 7.7GWh). It is a convenient paradox that due to the harsh working conditions on the North Sea eventually a very efficient dredging process has been developed. The semi-submersible and jack-up platform optimally benefit from the unique occasion of having to transport such large volumes over a very short distance.

5.4 Environmental measures

Optionally measures can be taken to reduce the impact on the surrounding area. Silt screens can be used around the grab dredgers, who prevent fine particles that slip or are stirred-up from the clamshell mix with the surrounding water. In combination with the relatively 'clean' dredging process of the grabbing, the silt screens will restrict the spillage of the clay even further. By connecting the fixed silt screens directly to the dredging vessel (as in Figure 78) no complicated floating and easily movable system has to be devised.



Figure 78: Silt screens directly attached to the grab dredgers. Note the difference in turbidity in- and outside the silts screens (source: <https://nippon.zaidan.info/seikabutsu/2000/00736/images/174-1.jpg>)

The top of the clamshell can be designed with a closed cap, so when the grab is pulled-up the dredged material does not mix with the water, which results in less spillage. This measure reduces the turbidity of the water caused by the hoisting of the grab itself.

Within the scope of the project of creating the 'Energy Island' first, one might consider utilising the opportunities this

offers. Depending on the construction schedule it is imaginable that, when the dam for the energy storage reservoir needs to be built, the 'energy hub' and wind farms are already (partly) operational. By either connecting or transporting the renewable energy, it can be used on the jack-up pontoon for its conveyor belt system. Although this might seem farfetched, charged batteries could easily be transported in containers in a rotating manner (Figure 79). Furthermore, flywheels could be used to provide peak power for heavier duties. The possibilities regarding the use of RES for the dredging operations are recommended for future studies.

In case it is proven that renewable energy in the combination of storage techniques can manage to run dredging/transport operations then a way of 'carbon neutral dredging' is developed.

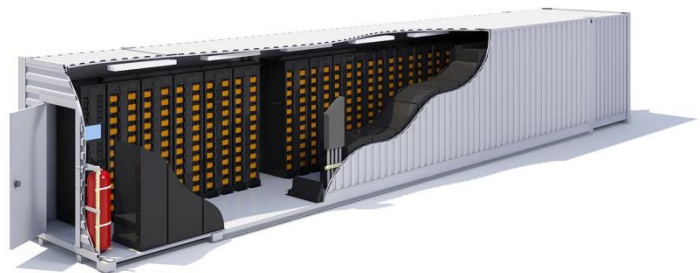


Figure 79: A one MWh battery storage container with 1.2MW of nominal power (source: <http://usiscored.com/?product=1-mwh-energy-storage-system&v=47e5dceea252>)

6. Power generation

In the previous chapters it has been demonstrated that the construction and operation of a stable dam and storage reservoir in the middle of the North Sea is feasible. Now it is time to complement the reservoir with actual power generation capabilities (see Figure 80 top). In terms of the design of the turbines, not too much attention will be given to the sizing of all the turbine parts itself. Instead, the main goal is to obtain the key dimensions in order to estimate the required depth of the turbines and its overall footprint. To do so first a type of turbine will be chosen, secondly the runner diameter will be determined and thirdly the measures that are required to prevent cavitation¹⁰. Afterwards the corresponding housing and the installation process of the turbines can be established.

6.1 Selection of turbine

For the energy storage reservoir water has to go two ways. The transport directions can be split, in case the water is pumped up and comes down to generate power in separate systems. They could also be combined, which results in one set of in- and outlets and one turbine that does both the pumping as the power generation. Since the latter option requires less civil works and space (Bricker, 2016), it is the preferred option.

For the water level difference of 40 metres there are two obvious pump-turbine alternatives: The Francis turbine and the Kaplan turbine (Figure 80). Both are pretty similar and are established technologies. Since the Francis type is able to achieve slightly higher efficiencies and they have been recommended by all the previous studies in similar conditions, it is the favoured choice (De Boer et al., 2007; Rijkswaterstaat et al., 1985).

To achieve the desired power output, one could either install a large amount of small turbines or a small amount of large turbines. Generally it is preferred to equip larger turbines, which often result in less civil works (Marence, 2016; Rijkswaterstaat et al., 1985).

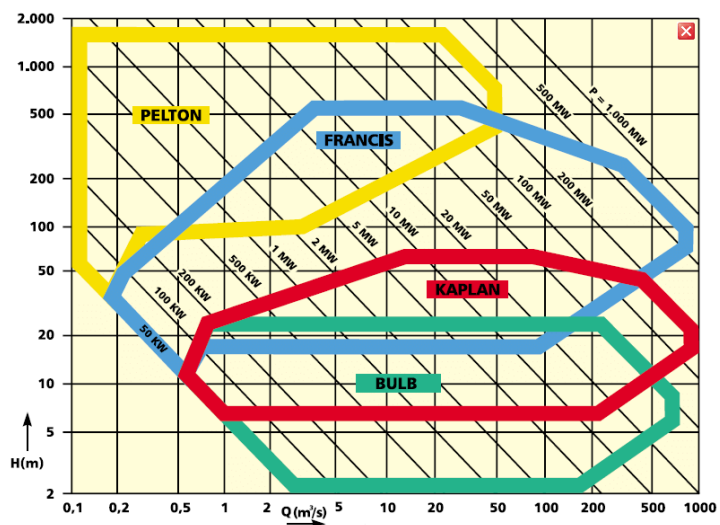
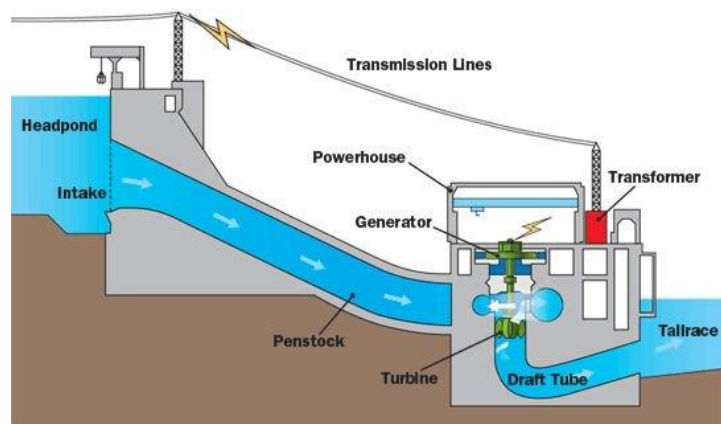


Figure 80: Schematisation of the powerhouse and in- and outlet works (top) and the application field of turbines (bottom) (source: i01.i.aliimg.com/img/pb/928/662/252/1275966164919_hz-fileserver3_2089574.jpg; Uamusse et al., 2017)

¹⁰ Cavitation is the formation of (vapour) bubbles in the water, due to low pressures (the boiling temperature of water decreases as the pressure drops below atmospheric pressure). Around the turbine low pressures can occur, which can result in 'bubbles'. When these bubbles pop they can severely damage the turbines and cause excessive deterioration.

A Francis turbine utilises both reaction- and impulse force, which it turns into rotational movement of the runner (see Figure 81). The reaction force is generated by water flowing over wing-shaped panels that cause a high and low pressure. The impulse is given to the runner when the water flows out (falls down) and hits the pitched panels at the bottom of the runner.

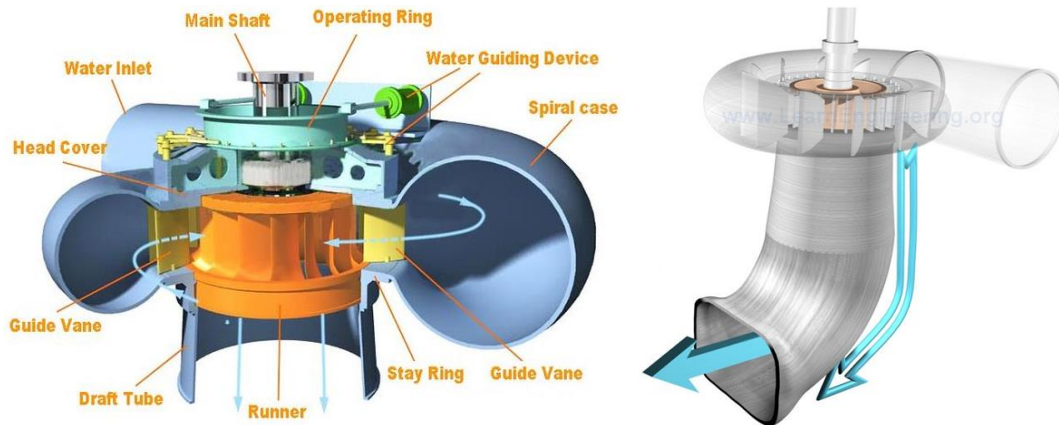


Figure 81: The parts that make a Francis turbine (left) and the general outlook (right) with the spiral case and draft tube (source: <https://i.pinimg.com/736x/ea/c0/13/eac0135d94321a5e6b480bd10df3af39--francis-turbine.jpg>; <http://www.learnengineering.org/2014/01/how-does-francis-turbi-ne-work.html>)

The design of the turbine is limited by the achievable sizes of each single element. Thereby the runner, generator and discharge are considered governing for the overall design. It is assumed that the largest hydro projects in the world, see Table 28, give a good indication of what is possible.

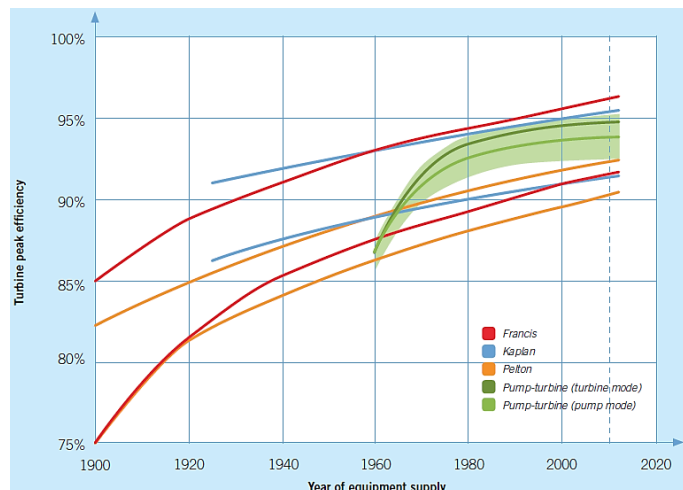
Element	Itaipu dam (Brazil/Paraguay)	Three gorges dam (China)
Discharge per turbine (m ³ /s)	700	600 – 950
Runner diameter (m)	9.7	10.4
Generator diameter (m)	20.0	21.4

Table 28: Characteristics of the two largest hydropower projects in the world (source: https://en.wikipedia.org/wiki/List_of_largest_hydroelectric_power_stations)

The system efficiency is dependent on many elements. There are the friction losses through the penstocks, hydraulic losses in and around the turbine itself and of course the losses that are inevitable when converting one type of energy to another. It has been concluded that basically “efficiency is bliss” and everything should be done to enhance the efficiencies as much as possible (De Boer et al., 2007; De Joode et al., 2014). The chosen efficiencies per part are given in Table 29.

Efficiencies	Turbine	Pump
Head loss (friction)	98.5%	98.5%
Turbine/pump	94%	92%
Motor/generator	98%	98%
Transformer	99.5%	99.5%
Total turbine/pump	90.3%	88.4%
Roundtrip efficiency	80%	

Table 29: Pump-turbine efficiencies (source: Hydro Equipment Association, 2013; Bricker, 2016)



6.2 Runner diameter

The runner is perhaps the most important element of a turbine, since it is the part that turns the kinetic energy of the water into a rotation. Most other elements that make up a complete turbine scale with the runner and its rotational speed. There is a whole set of equations (Marence, 2016), which lead to the eventual runner dimensions.

First of all the power delivered by a water turbine needs to be estimated, where the head difference and discharge are given as input:

$$P_T = \rho g Q H \eta_T$$

- P_T = Turbine power (W)
- ρ = Density of seawater (=1025) (kg/m^3)
- g = Gravitational acceleration (=9.81) (m/s^2)
- Q = Discharge (input) (m^3/s)
- H = Head difference (=40) (m)
- η_T = Turbine efficiency (=0.94) (-)

To begin the computations an initial specific rotational speed has to be estimated for the given head (see Figure 82). The head difference of 40m leads to a first approximation for the specific rotational speed of 100 rounds per minute (RPM).

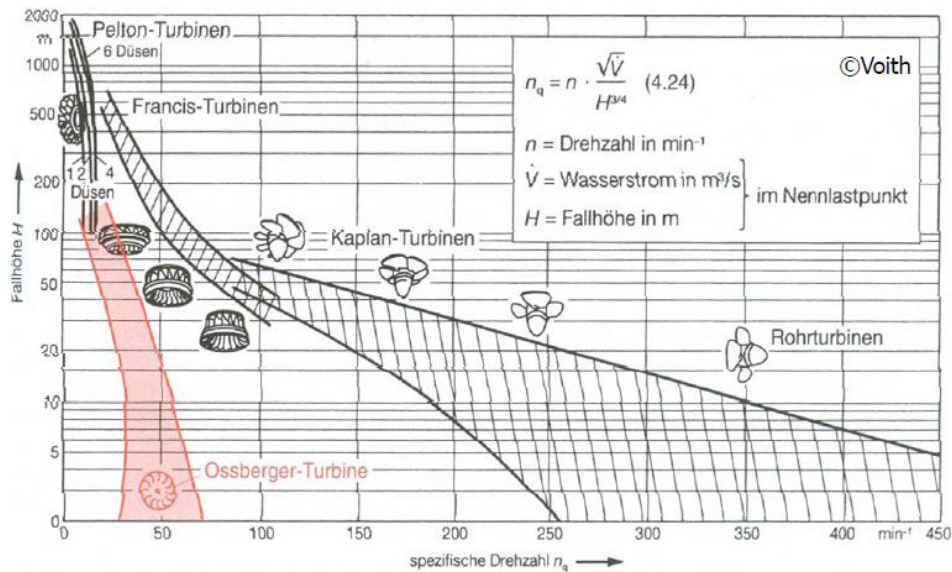


Figure 82: Diagram of specific rotational speed (n_q) per turbine type for a given head (source: Marence, 2016)

Secondly the rotational speed is calculated:

$$n = n_q \frac{H^{\frac{3}{4}}}{\sqrt{Q}}$$

- n = Rotational speed (RPM)
- n_q = Specific rotational speed (=100 from Figure 82) (RPM)

The obtained rotational speed has to be adjusted to the closest synchronous rotational speed. To do so the number of poles have to be computed, when afterwards the nearest number divisible by four

is chosen as true number of poles (Van Duivendijk, n.d.). The true number of poles is then used to attain the synchronous rotational speed. Consequently the newly gathered synchronous speed results in the final specific rotational speed:

$$n_{syn} = \frac{f \cdot 120}{p} \quad ; \quad n_q = n_{syn} \frac{\sqrt{Q}}{H^{\frac{3}{4}}}$$

- n_{syn} = Synchronous rotational speed (RPM)
- f = Net frequency (=50Hz for Europe) (Hz)
- p = number of poles (divisible by four) (-)

In case the resulting specific rotational speed still lies within the admissible range of Figure 82, the perimetral speed can be calculated. The speed coefficient that is necessary can be extracted from Figure 83. With all the inputs known the perimetral speed becomes:

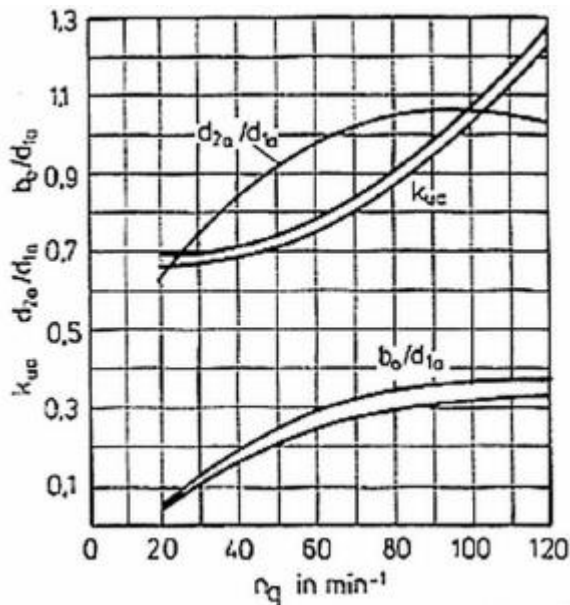


Figure 83. With all the inputs known the perimetral speed becomes:

$$u = k_{uc} \sqrt{2gH}$$

- u = Perimetral speed (m/s)
- k_{uc} = Speed coefficient (-)

At last all the parameters to compute the runner diameter itself have been established. The size of the runner is determined by:

$$d_{1a} = \frac{60u}{\pi \cdot n}$$

- d_{1a} = Runner diameter (m)
- n = Rotational speed (RPM)

Figure 83: Diagram for relative runner dimensions and speed coefficient (source: Marence, 2016)

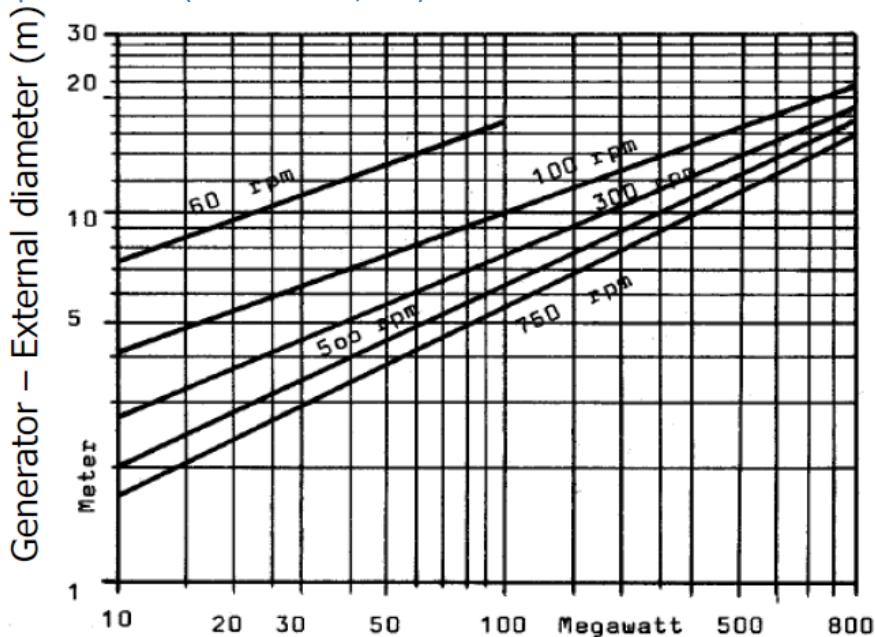


Figure 84: Diagram for generator size estimations (source: Marence, 2014)

With the runner diameter at the intake from the spiral case identified, the runner diameter at the bottom outlet (d_{2a}) follows from Figure 83.

The size of the generator can be estimated by using the diagram of König (Figure 84) and a 10% overload from the earlier computed turbine power (Marence, 2014).

According to the formulae stated above, a variety of discharges lead to the runner and generator dimensions as in Table 30:

Discharge (m ³ /s)	50	100	200	500	700
Turbine power (MW)	18.9	37.8	75.6	189.0	264.7
Specific rotational speed (RPM)	95.3	104.8	102.6	100.4	99.8
Runner diameter (d _{1a} /d _{2a}) (m)	2.52/2.7	3.53/3.7	5.00/5.3	7.97/8.5	9.43/10.0
Generator diameter (m)	4.5	6.5	8.9	17.5	21.9

Table 30: Runner and generator diameters for a 40m head difference and specified discharge

From the obtained results in Table 30 it cannot yet be determined what discharge and relative turbine dimensions are preferable. Obviously the largest possible machine (for 700m³/s) necessitates fewer turbines and connecting in- and outlets, but its dimensions challenge the constructability. The issue of constructability will be further emphasized in the next section.

In order to fully utilise the head difference between the upper and lower reservoir a draft tube needs to be added to the turbine outlet (see Figure 81). The draft tube gradually increases its cross section and thereby creates a smooth transition for the pressure and flow conditions. If there would not be a draft tube then part of the head difference will be lost and so will the kinetic energy that still remains in the water as it leaves the runner. Therefore the draft tube needs to be carefully designed. As shown in Figure 85, the draft tube scales with the runner diameter. Consequently a larger turbine will necessitate a greater construction depth.

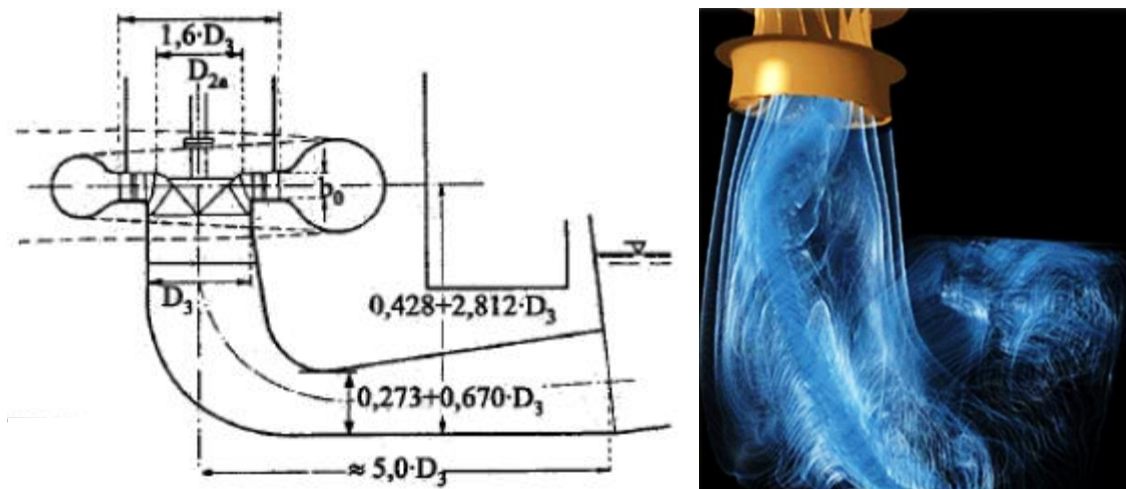


Figure 85: Design of the draft tube and tailrace of a Francis turbine (left) and an animation of water flowing through (right). Note that D_3 here is equal to the previously determined d_{2a} (source: Marenc, 2016; <https://www.slideshare.net/swargpatel283/draft-tube>)

6.3 Cavitation prevention

The impact of under pressures in and around turbines can be absolutely catastrophic (see Figure 86). The not-so-tantalisingly-sounding effect of simple vapour bubbles popping has caused many turbines to fail and need replacing. Therefore it is of utter importance that the occurrence of under pressures near the pump-turbines is avoided.

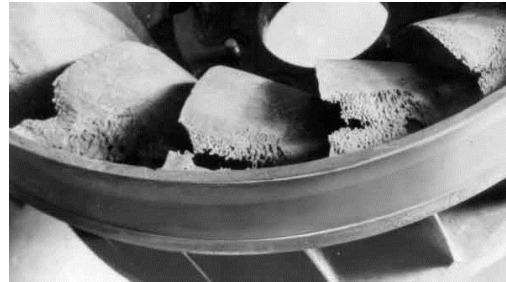
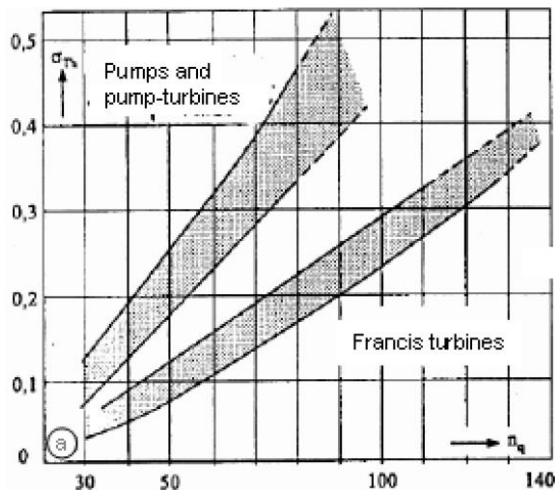


Figure 86: The effect of cavitation on runner blades (source: <http://authors.library.caltech.edu/25019/1/figs/fig604.jpg>)

It is possible to (almost completely) avoid cavitation by installing the turbines below the water level of the lower reservoir. The depth at which this should be done is computed by:

$$h_{S,adm} = h_{at} - h_v - \sigma_c \cdot h_f$$

- $h_{S,adm}$ = Admissible draft head (depth of top edge of runner blade) (m)
- h_{at} = Atmospheric pressure head (=10 at sea level) (m)
- h_v = Vapour pressure of water (=0.18 for 15°C) (m)
- σ_c = Thoma's cavitation coefficient (see Figure 87) (-)
- h_f = Head difference (=40) (m)



Temperature [°C]	Vapour pressure head h_v [m]
0	0.062
10	0.125
20	0.238
30	0.433
40	0.752

Figure 87: Diagram to determine (by extrapolation) Thoma's cavitation coefficient (left) and the vapour pressure head (right) (source: Marence, 2016)

6.4 Pump-turbine characteristics

The main dimensions of the turbines are formed by the runner and generator diameter, the depth to avoid cavitation and the draft tube. The measures for the turbine housing are given in Table 31. Since all working depths are problematic, it will first be explored if the largest turbine is constructible.

Discharge (m ³ /s)	50	100	200	500	700
Turbine power for 40m head (MW)	18.9	37.8	75.6	189.0	264.7
Specific rotational speed (RPM)	95.3	104.8	102.6	100.4	99.8
Runner diameter (d_{1a}/d_{2a}) (m)	2.52/2.7	3.53/3.7	5.00/5.3	7.97/8.5	9.43/10.0
Generator diameter (m)	4.5	6.5	8.9	17.5	21.9
Runner depth below low reservoir (m)	13.98	17.62	17.17	17.20	17.43
Draft tube depth below runner (m)	7.9	11.0	15.3	24.2	28.5
Draft tube depth below MSL (m)	61.9	68.6	72.5	81.4	86.0

Table 31: Dimensions of the main parts of the Francis pump-turbines to be used for the design of the turbine housing. All measures have been verified with the UNESCO-IHE HydroPower design tool and are equal to the centimetre.

7. Housing of turbines

In order to generate electrical energy there are more things necessary than the runner and generator alone. First of all the water has to be transferred from the upper reservoir (the North Sea) via a 'penstock' to the turbine. The water leaving the turbine exits the power plant via the draft tube and tailrace. Besides these civil works there is also the electrical equipment consisting out of: transformers, buswork, circuit breakers, disconnects and the switchyard. Some of the electrical gear can either be located outdoors or within the powerhouse itself (Figure 88). Furthermore a service area, control room and auxiliary equipment complement the hydropower plant (Marence, 2016).

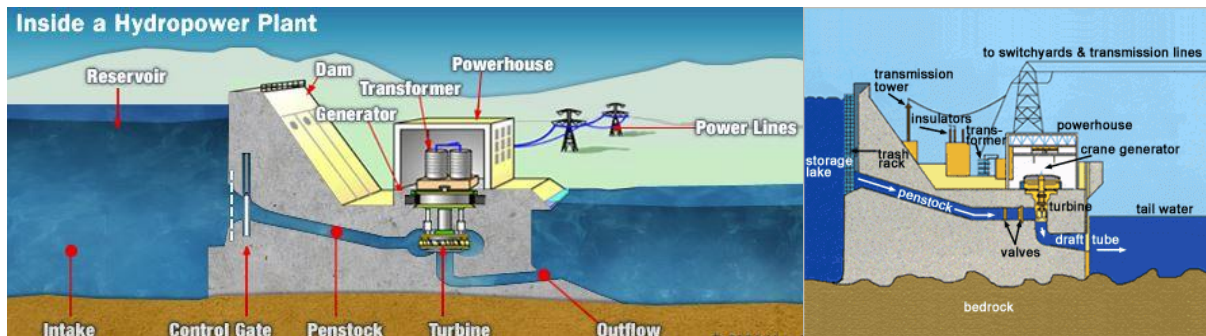


Figure 88: Exemplary hydropower layouts: indoor powerhouse (left) and semi-outdoor powerhouse (right) (source: <https://www.linkedin.com/pulse/power-plants-efficiency-capacity-utilization-factor-v-r-v/>; <http://www.jasonmunster.com/tag/hydroelectric/>)

The type of powerhouse, indoors or semi-outdoors can best be chosen when the general layout and construction method have been developed. For the initial Plan Lievense it was concluded that installing the powerhouse inside the dam itself is not beneficial for earth bodies higher than 10 metres (due to added loads on the housing). However, when the powerhouse would be installed behind the dam, the longer penstocks would reduce the roundtrip efficiency by an extra 2.7% (see Appendix I: Location of the powerhouse and penstock design)

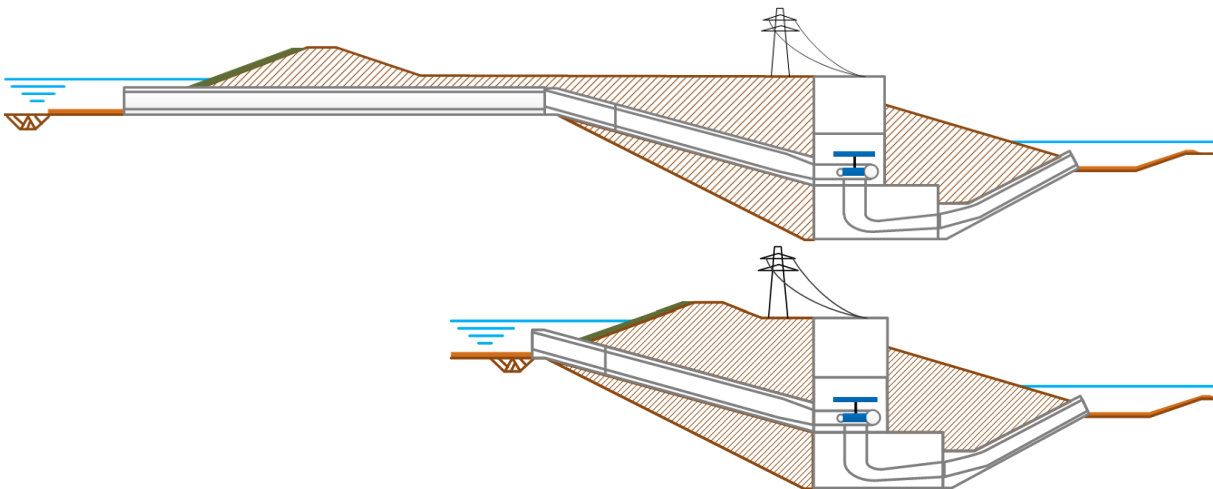


Figure 89: Alternatives for the location of the powerhouse: behind the dam (top) and inside the dam (bottom)

It is presumed that in previous studies into offshore PHS the requirements to avoid cavitation were seriously underestimated. In case the pump-turbines would not need to be installed as deep, it somehow could make sense to house them behind the dam (easier accessible and possibly a 'lighter' design). Yet, due to the deep position of the turbines a trench needs to be dredged to install them. When the powerhouse cannot be inside the dam, the trench has to be sufficiently far away from the dam (+inner berm). Hence the penstocks would have to be roughly 240m longer than required.

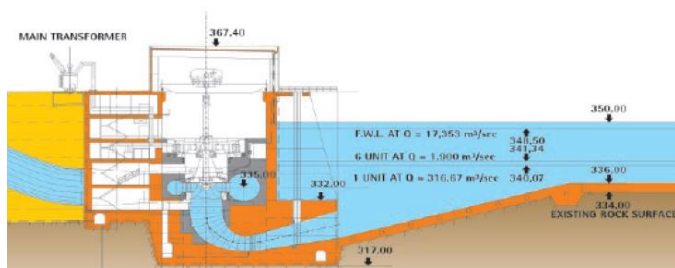


Figure 90: Powerhouse of a Francis turbine. The draft tube has a significantly wider footprint than the powerhouse itself (source: Marence, 2016)

excavated. However, the enormous depth of circa 86 metres below MSL poses an incredible challenge from a construction perspective. The building process will therefore significantly impact the design and has to be dealt with simultaneously.

To restrict the necessary excavation works the powerhouse and tail race will be designed as slim as possible. The powerhouse itself can be executed narrower than the draft tube, like is done in Figure 90. According to Figure 85 the footprint of the draft tube segment will be seven times the runner diameter by twice the generator size (70m x 40m). The powerhouse on top of the draft tube can have a square footprint of (40m x 40m).

7.1 Construction method

In this section it will be investigated if it is possible to install the largest applicable turbine of 265MW. If not, either a smaller or another type of turbine can be tested. The upside of placing the turbine housing at a depth of 86m below MSL is that it can be founded directly onto the deep sand layer, which starts at 85m below MSL (see Figure 132). Hence no sophisticated foundation needs to be developed and no excessive settlements are to be expected for the powerhouse itself. The downside is that it is too deep for a temporary building pit to utilise the thick clay layer as a bottom seal.

There are four main options considered to construct the power generation plant in deep water:

1. In-situ: pneumatic caisson
2. In-situ: open caisson
3. Prefab: modular box caissons
4. Hybrid: prefab bottom caisson + in-situ superstructure

The four alternatives are briefly introduced and qualitatively checked on whether they offer a feasible construction method that can install the powerhouse at a maximum depth of 90 metres. The bottom of the housing of a single turbine is first assumed to have a footprint of 70m by 40m (excluding the tailrace and penstock).

¹¹ The Itaipu dam operates under an equal discharge of $700\text{m}^3/\text{s}$ and has similar runner and generator sizes. Its penstocks have a diameter of 10.5 metres, its spiral casing a diameter of 9.6m and the draft tube goes from 8.7 to 17.7 metres in diameter. The heaviest indivisible piece is the runner, weighing 296 tonnes (source: <https://www.itaipu.gov.br/en/energy/generating-units>)

7.1.1 In-situ: pneumatic caisson

This technology was often used to construct bridge pier foundations in the past. Underneath the caisson there is a confined space that is under air pressure equal to the level of surrounding water pressure (Figure 92). Consequently the soil can be excavated in the dry and so the pneumatic caisson slowly 'sinks' its way down (see Figure 91). In order to sink the caisson the self-weight has to outweigh the bearing capacity of the soil, the 'buoyancy' of the working chamber and the friction around the periphery.

Due to the high pressure (fluctuations) in the working chamber many casualties have fallen in the past to compression sickness (also known as "the bends" or "caisson sickness"). The maximum overpressure is legally defined at 3.5atm, which corresponds to a working depth of 35 metres below MSL, at which only 2 hour shifts are allowed (Van Corven, 2015).

Alternatively a method has been developed, where the manual labour is replaced by a remote controlled excavator. With this technology a caisson of 25.2m x 15.6m was successfully brought till a depth of 29m in Shanghai to construct a tunnel shaft (Peng et al., 2010). However, the bottom of the powerhouse with dimensions of circa 70m x 30m needs to be sunk till 90m. Considering the required depth, friction around the large periphery and the possibility of tilting it is not expected that this will ever become a feasible alternative.

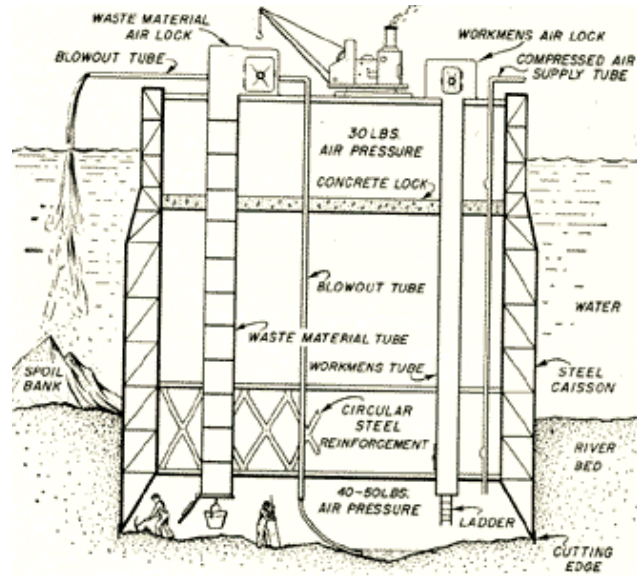


Figure 91: Schematization of a pneumatic caisson (source: <http://www.caroldenney.com/concerti.htm>)

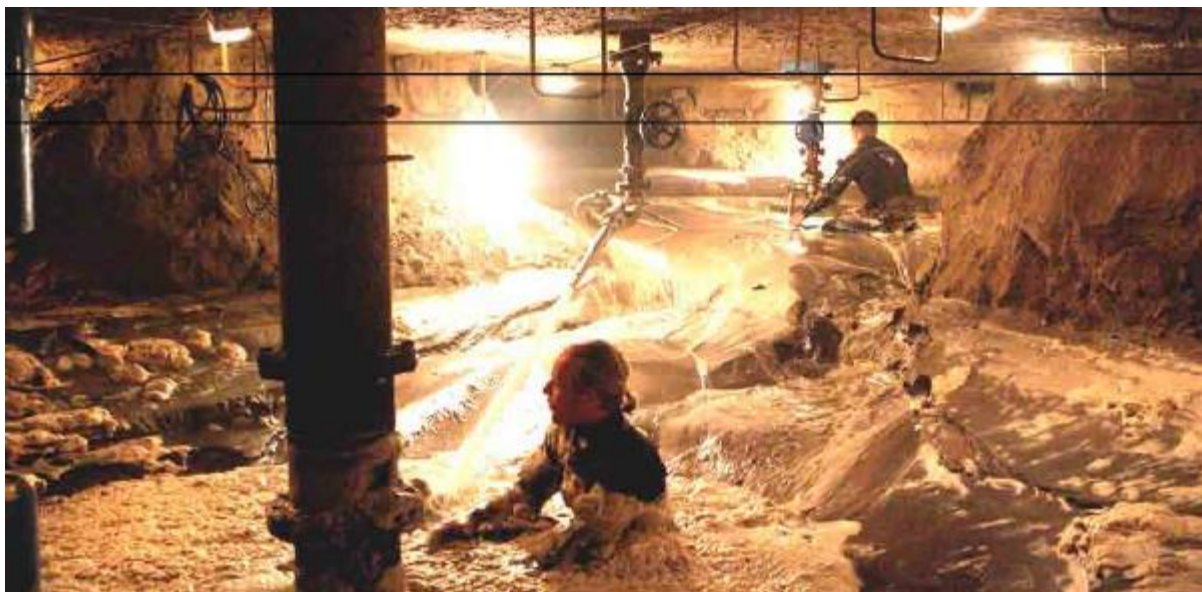


Figure 92: The working chamber from a caisson. This caisson was sunk till 25m below NAP directly in front of the Amsterdam Central Station to construct the Noord-Zuidlijn (source: Pepers, 2011)

7.1.2 In-situ: open caisson

An open caisson has much in common with a pneumatic caisson. By excavating the ground within the caisson, it slowly sinks into the soil by its own weight and potentially hydraulic jacking forces from above. Secondly an extension of the caisson is added to the top and the process of excavating and sinking repeats itself.

The main difference compared to the pneumatic caisson is that within the open caisson the soil is not excavated in dry but in wet conditions (see Figure 93). Although the open caisson does not require continuous labour under high compressive forces like the pneumatic caisson. It is almost inevitable that divers will be necessary when obstructions (like boulders left from the glacial times) are encountered underneath the cutting edge/shoe. Divers may even be required to excavate near the cutting edge to stimulate the soil failure that allows the sinking of the caisson.

Besides the challenges of overcoming the peripheral friction in the stiff clay and preventing tilting of the caisson during the sinking procedure, sealing the bottom of the caisson might prove most difficult. The seal has to be able to resist more than 900kN/m^2 of hydrostatic water pressure. Since the placing of the concrete seal (plus reinforcement) has to be executed under water it is an understatement to say it will be extremely difficult to obtain a reliable closure. All stated issues combined lead to the conclusion that an open caisson construction method does not provide a realistic solution.

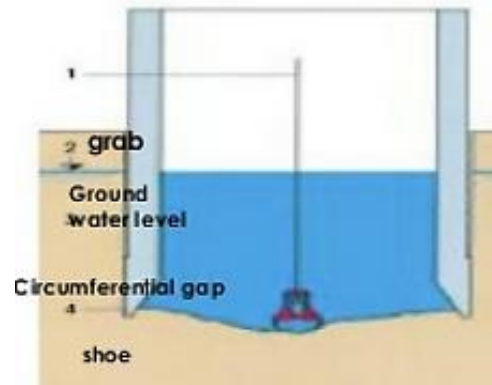
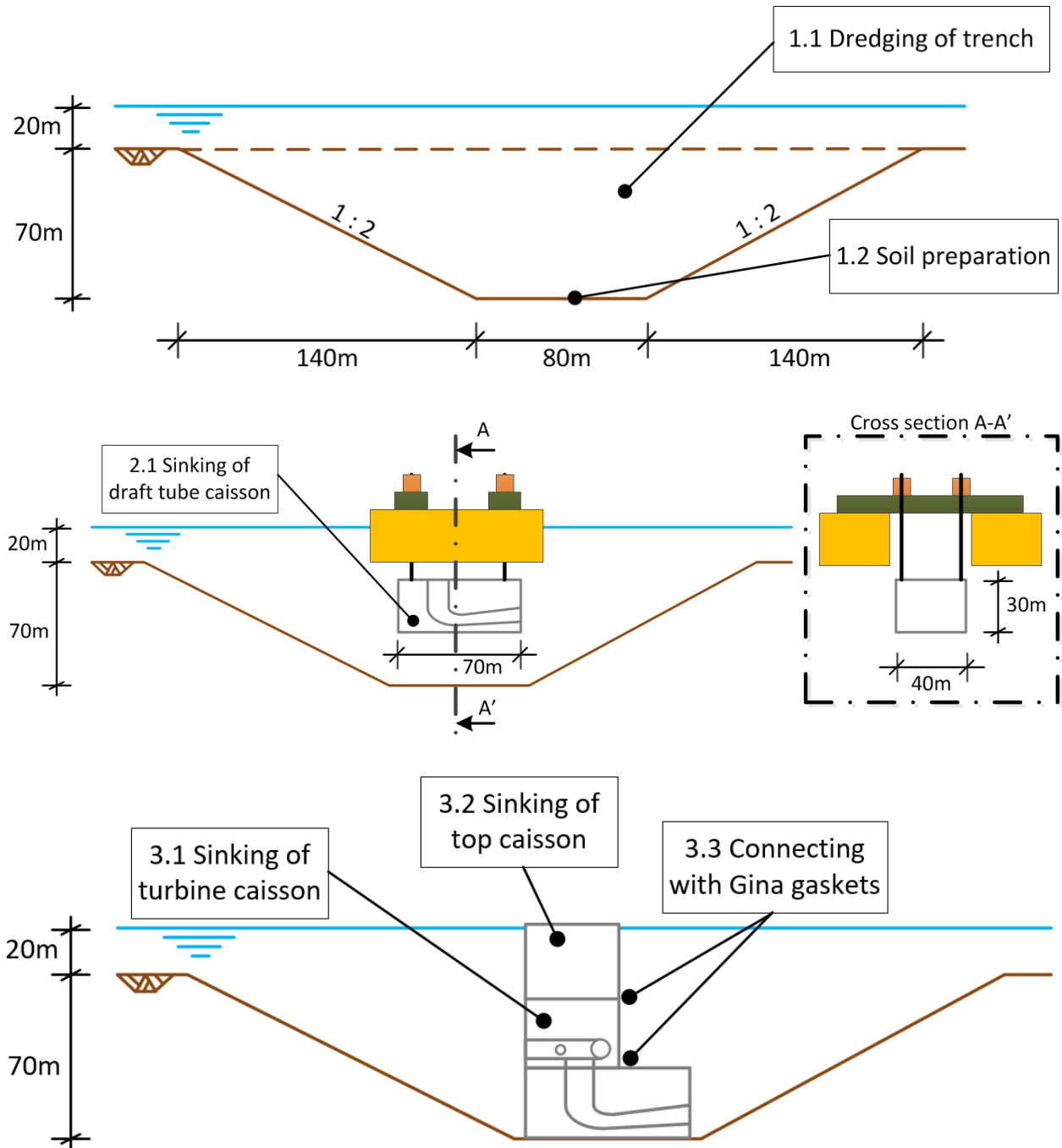


Figure 93: Schematization of an open caisson (source: https://www.slideshare.net/_Yasir_/underwater-construction-58501529)

7.1.3 Prefab: modular box caissons

In order to sink prefabricated box caissons a large excavation up to 90 metres below MSL is required. Although this requires a tremendous amount of dredging, most of it would be necessary anyway in order to connect the tailrace and the penstock with the turbine. Once the trench has been dug and the foundation layer prepared, the caissons can be sunk and positioned. The process of erecting a powerhouse with modular box caissons is best explained along a set of figures:



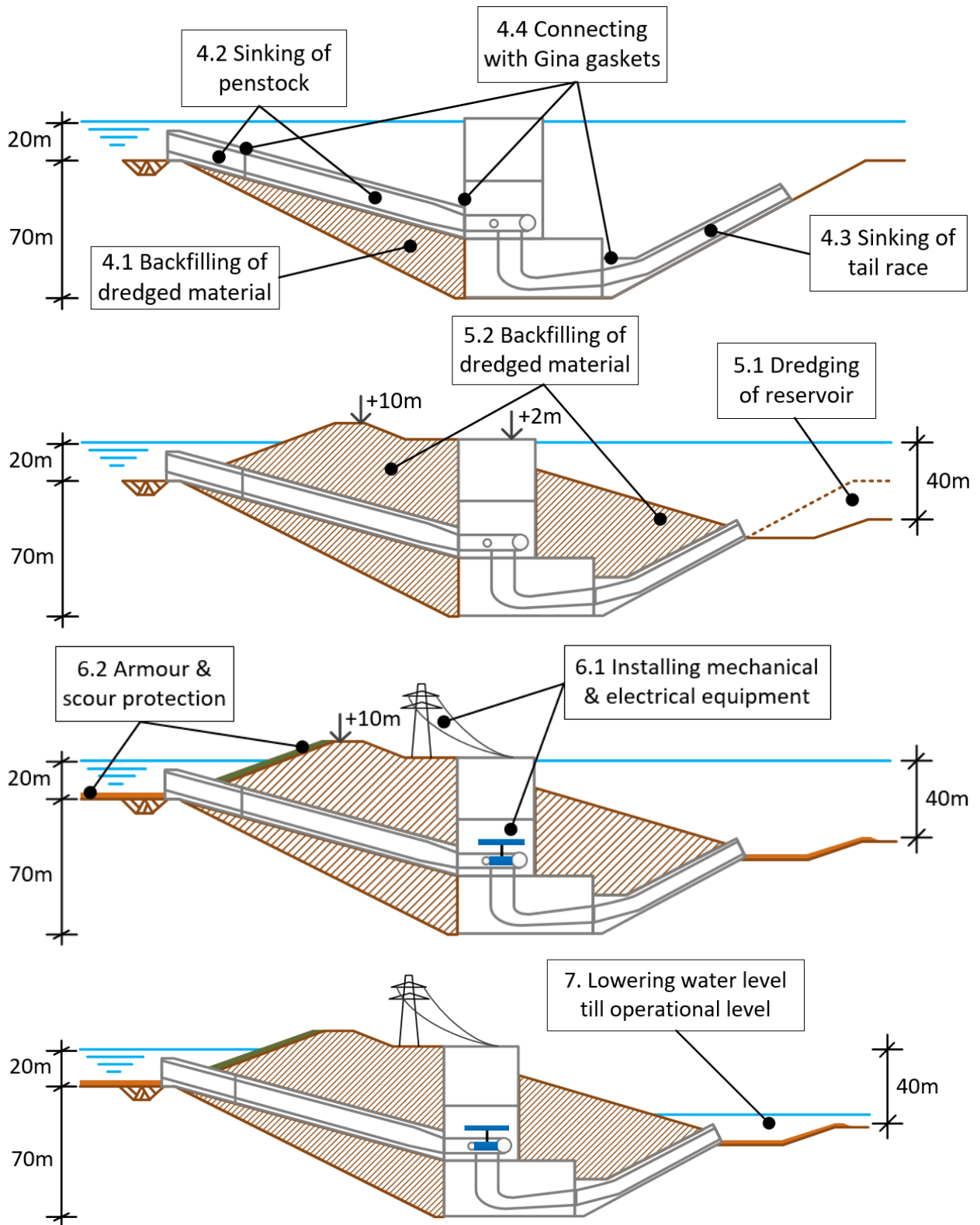


Figure 94: The indicative construction process of the turbine housing using modular prefab elements

In case the vertical connection between the caissons with Gina profiles as explained in ‘Appendix J: Connecting box caissons with Gina gaskets’ is undesirable, one could resort to an alternative construction method like elaborated in the next section.

7.1.4 Hybrid: prefab bottom caisson + in-situ superstructure

Alternatively to the pure prefab method where the caissons are stacked upon each other to eventually form the powerhouse, another process has been devised. To avoid vertical connections and limit the number of sinking operations a mixture between prefab and in-situ construction could be adopted.

Just like for the modular technique, the draft tube segment is prefabricated in a dock. Once it has been floated into position the remainder of the powerhouse will be constructed in-situ. Compared to the modular approach only the steps 2 and 3 differ, as shown in Figure 95.

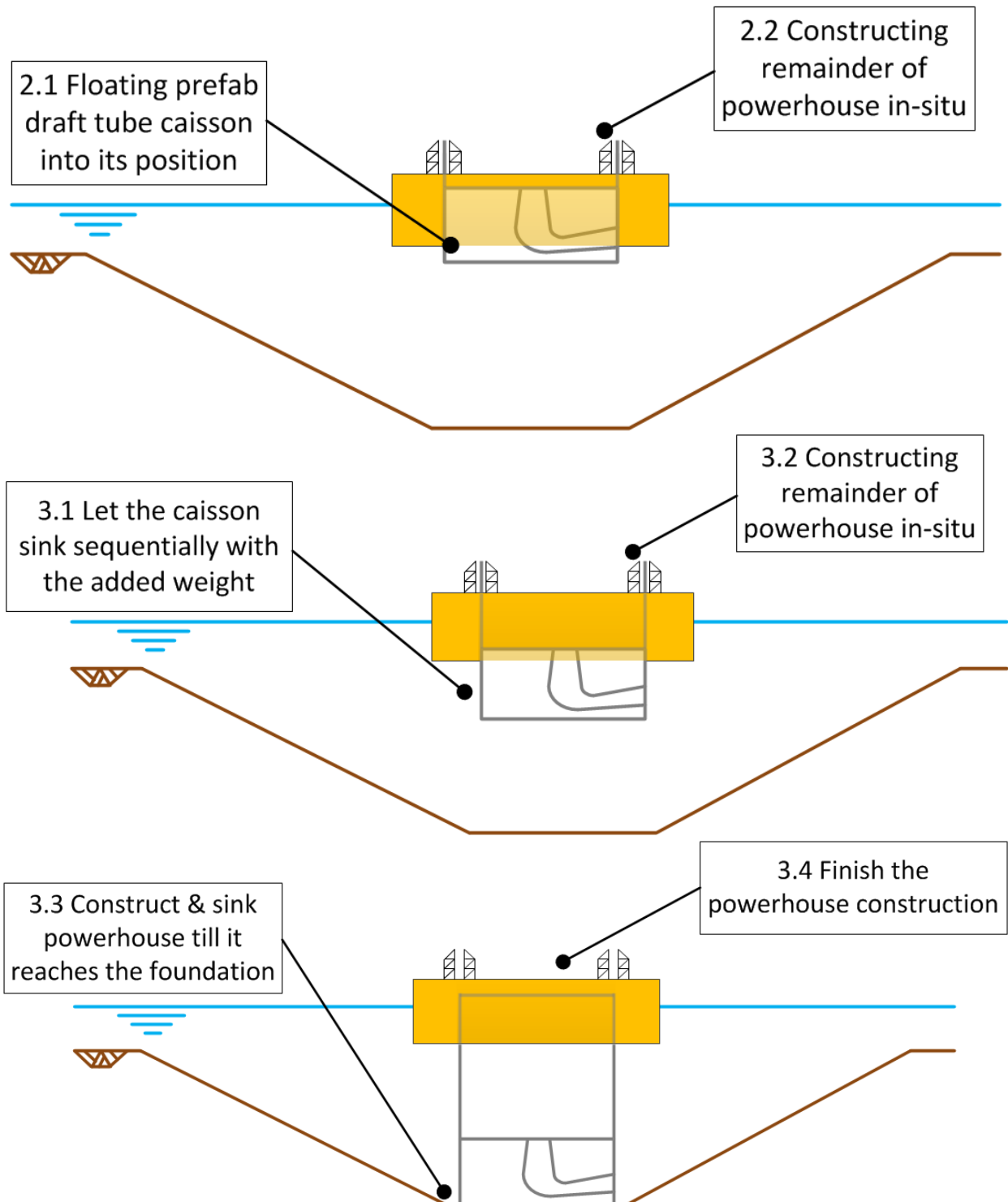


Figure 95: the hybrid construction process of the turbine housing. Step 1, 4, 5, 6 and 7 are the same as for the modular approach

7.1.5 Choice of method

From the discussed four options it has been concluded that:

- A pneumatic caisson cannot be used to install the powerhouse at 90m below MSL
- An open caisson construction would be extremely difficult to successfully sink and seal and should be avoided
- The modular box caisson method seems viable at first sight and is the preferred technique
- The hybrid scheme could theoretically work, but may be challenging to realise

The use of modular box caissons is chosen as best applicable. By dredging till the required depth the slopes that are necessary for the tailrace and penstocks are simultaneously created. For the in-situ options dredging would be needed to install the in- and outlets anyway.

The pure prefab method has the advantage over the hybrid method that everything can be built at one main construction site. Furthermore the balancing during construction of the floating powerhouse seems precarious. Most likely both alternatives need a (temporary) dam to shield the construction process from the surrounding wave climate. Even when the whole dam around the storage reservoir would already have been completed, the powerhouse installation would still need protection from locally induced wind waves (who can exceed 2 metres, see Figure 45).

Preferably the housing of the turbines would be placed in deep water. The necessary dredging works would be limited and the flow velocities at the in- and outtake lower. Hence the scour protection could be executed 'lighter'.

All things considered, an excavation with box caissons is the mostly likely option to be feasible. The technology has been widely applied in for example immersed tunnelling projects¹² and breakwaters. There are many things yet to investigate besides the actual design of the caissons like: best suitable location of the construction dock (conventional or floating), type of formwork and the number of elements to be produced per submerging and transport cycle.

To obtain insight in the main volumes and dimensions of the turbine housing some initial computations are performed in the next section. These could provide a little guidance to estimate the costs.

Finally it should be stated that this powerhouse construction differs from most PHS plants in the way that there is no lateral transport possible between the several pump-turbines. This is due to the caisson structure. Therefore all transport of people and equipment takes place vertically.

¹² World's deepest immersed tunnel segments have been installed in the Marmaray link that connects Europe and Asia via the Bosphorus. The segments are 150m long, sunk till a maximum depth of 60m and total a length of 1,387m. For the new Fehmarn connection between Germany and Denmark a 17.6km long immersed tunnel is planned that reaches till 40m below MSL (source: https://en.wikipedia.org/wiki/Fehmarn_Belt_Fixed_Link).

7.2 Main dimensions and volumes

Critical for the execution of the prefab methodology is the vertical stability of the caissons during transport, sinking and in their final position. As a rule of thumb: with the (floating) transportation the weight of the caisson should be no more than 99% of the maximum buoyancy force, including bulkheads and sinking equipment. In the final position the weight needs to be 107.5% of the uplift force caused by the displaced water (Bakker, 2014). Subsequently it will be necessary to increase the ballast of the caissons once they are positioned. This can be done by either adding more concrete or by locally sourced material. The latter is preferred since it is much cheaper. Hence the caissons should be designed in such a way that they can incorporate dredged material. By using the Archimedes principle of displaced water the necessary concrete and reinforcement (estimated at 1%) volumes can be computed:

$$V_{rc} = V_{caisson} \frac{\gamma_w}{\gamma_c} 0.99$$

$$V_{conc} = 0.99V_{rc}$$

$$V_{rein} = 0.01V_{rc}$$

$$V_{fill} = 0.085V_{caisson} \frac{\gamma_w}{\gamma_s}$$

- V_{rc} = Volume reinforced concrete (m³)
- $V_{caisson}$ = Volume caisson (m³)
- V_{conc} = Volume concrete (m³)
- V_{rein} = Volume reinforcement (m³)
- V_{fill} = Volume dredged backfill (m³)
- γ_w = Volumetric weight sea water (=1025) (kg/m³)
- γ_c = Volumetric weight reinforced concrete (=2400) (kg/m³)
- γ_s = Volumetric weight dredged material (=2000) (kg/m³)

Caisson	Dimensions (l*w*h) (m)	Volume concrete (m3)	Volume reinforcement (m3)	Volume dredged backfill (m3)
Draft tube	70*40*30	35,161	355	3,659
Turbine	40*40*30	20,092	203	2,091
Top	40*40*30	20,092	203	2,091

Table 32: Volume and material characteristics of modular box caissons

The volumes stated in Table 32 can be used for a first approximation of the powerhouse costs. The costs of the penstocks, tailrace, excavation, backfill and in- and outlet need to be added to obtain a full estimation of turbine housing costs.

The maximum height of the box caisson is practically limited by the bathymetry. As a rule of thumb a caisson would be able to float halfway out of the water (A.Q.C. van der Horst, personal communication, September 12, 2017). A 30 metre high caisson could therefore have a draught of only 15 metres. To allow for some movements and irregularities this should be acceptable for the Dogger Bank where the average depth is around 20m.

The excavation works will form an important factor in the scaling of the turbine housing costs. Since the dredged trench is three-dimensional, it will be attractive to install more turbines, because each added turbine requires relatively less material than the first one. This is illustrated in Figure 96.

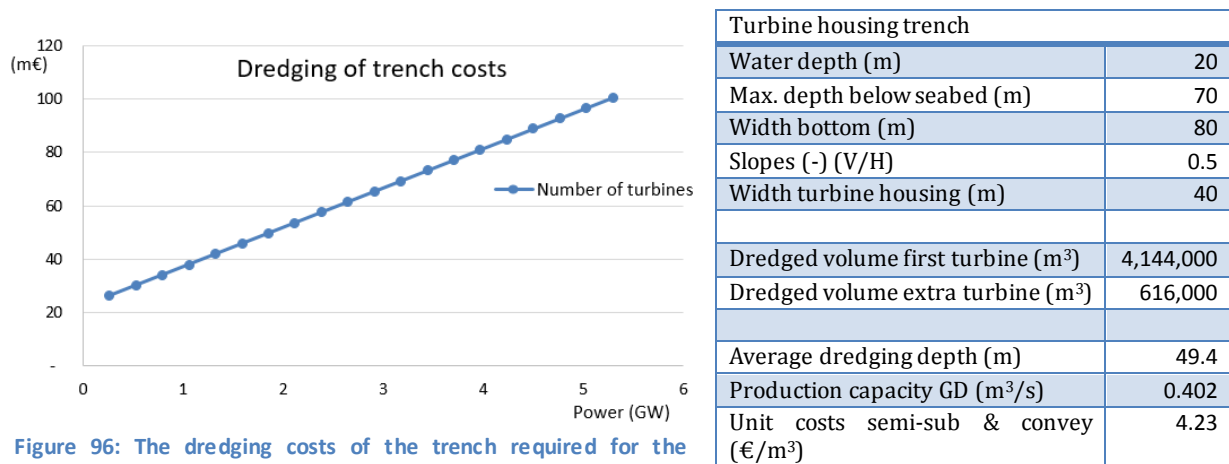


Figure 96: The dredging costs of the trench required for the installation of the turbines. The dots on the line indicate a turbine

For the dredging of the trench the identical semi-submersible vessel and jack-up pontoon will be used as for the dam construction. Due to the larger depth the unit costs are slightly higher. The dredging costs from Figure 96 are obtained by multiplying the volumes in the given table by 1.5. This is to account for dredging 50% of the material twice, once to excavate and construct the temporary dam and once to backfill. The other half of the initially dredged material can immediately be used for the large 'storage' dam.

In the dredging costs computed above, the several pump turbine caissons are placed directly next to each other. Besides the fact that this might be difficult from an execution point of view it also raises concern regarding seepage. The turbine housing will be placed directly onto the deep sand layer at 90m below MSL. Consequently there is a direct link between the water conveying sand and the inner reservoir. To avoid water flowing in backfill is placed on top of the tailrace and penstocks. However, the backfill does not help against water seeping in along the tailrace or in between the different turbines. As a result one might want to place the different turbine units a little apart from each other, so that an 'impermeable' clay layer can be dumped in between. The seepage along the tailrace requires more research, but is expected to be manageable (by for instance grouting).

8. Costs & benefits

The costs are largely made up out of four parts: the dam structure, the dredging process, the pump-turbines and the powerhouse and turbine related structures. First these costs will be treated separately when afterwards the potential benefits of the energy storage plant are estimated.

8.1 Dam costs

The dam costs are largely formed by the construction of the core from dredged material, its outer protection and the soil preparation and drainage costs. For the North side, where the incoming waves are most severe the dam costs are presented in Table 33. The direct costs include labour, plant and material. The construction costs are obtained by multiplying the direct costs with a factor of 1.75 that include: transportation of material, building site costs, execution costs, general costs, profit, risk and later to be determined building costs (25%). The costs are excluding engineering and planning costs.

Element	Weight / size	Volume (m ³ /m)	Construction method	Unit price	Costs (€/m)	
					Direct	Construction
Dredged material	18.3 – 21.6 kN/m ³	5545.5	Grabs mounted on a semi-sub platform and jack-up conveyor	€3.4/m ³	11,945	17,918
Geotextile		150m ² /m	Pontoon and anchor tube	€ 6/m ²	900	1,575
Drainage and soil prep.		226m ² /m	Vertical drainage	€ 40/m ²	5,166	9,040
Quarry run foundation	5 kg – 1 t	243.9	Side stone dumping vessel (SSDV)	€25/ton	10,976	19,207
Foundation layer	0.3 – 1 t	56.8	Crane on rig	€25/ton	2,556	4,473
Filter & scour protection	d _{n50} > 58mm	17.0	Side stone dumping vessel	€25/ton	765	1,339
Filter layer	1 – 3 t	61.9	SSDV and backhoe	€25/ton	2,786	4,875
Under layer	3 – 6 t	82.5	SSDV and backhoe	€25/ton	3,714	6,500
Toe	6 – 10 t	17.1	Crane on rig	€25/ton	770	1,347
Xbloc armour	48.0 t	156.65 (=3.24 Xblocs)	Wire rope crane	€2933/pcs	9,504	16,632
Upper slope protection	3 – 6 t	43.2	Dump truck (end tipping)	€25/ton	1,944	3,402
Total					51,025	86,307

Table 33: Dam costs. The dredged volume includes 10% extra to cope with future settlements (Bezuyen et al., 2012) and 5% spillage of clay during the dredging process. Dredging costs are for an average depth of 30 metres and without capital investments in dedicated equipment.

The total costs are shown in Figure 97 to get a better understanding of the most cost-important factors. Note that not even a quarter of the costs are made up of the dam core itself! Including the drainage and soil preparation works the dam structure is responsible for about the third of the overall costs. Thereby the costs of the dam are largely dependent on the wave conditions it has to provide armour protection for to obtain the desired safety level.

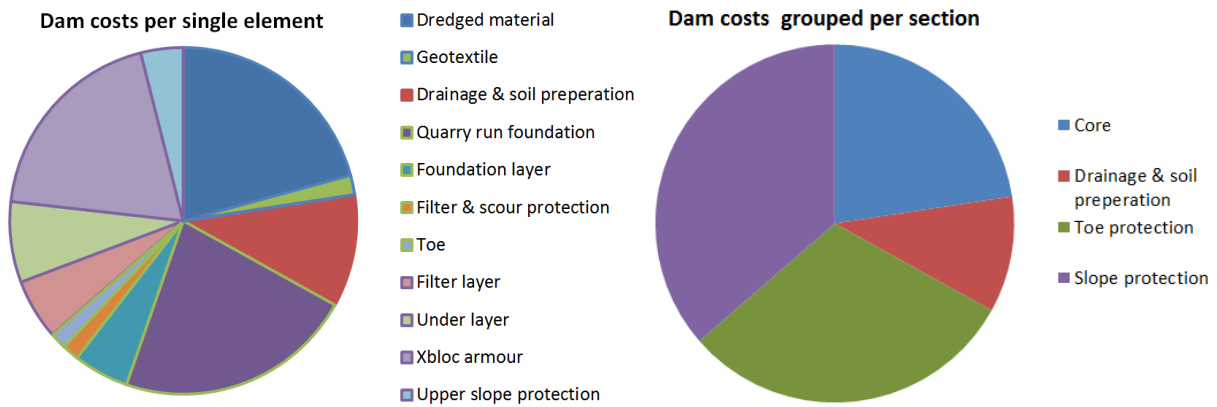


Figure 97: The dam costs per single element (left), where the items with the same colour outline are grouped together (right). The total costs of 86,307€/m are for a dam that is able to retain 40m of water level difference and handle 8m high waves.

8.1.1 Water retaining costs

In order to operate the storage reservoir, the top sand layer has to be sealed. From the various techniques that can do so, the simple dredging and replacing the sand with firm clay option is favoured (Figure 98). The sand layer that lays between -43m and -50m relative to MSL will be replaced for a costs of 11,825€/m.

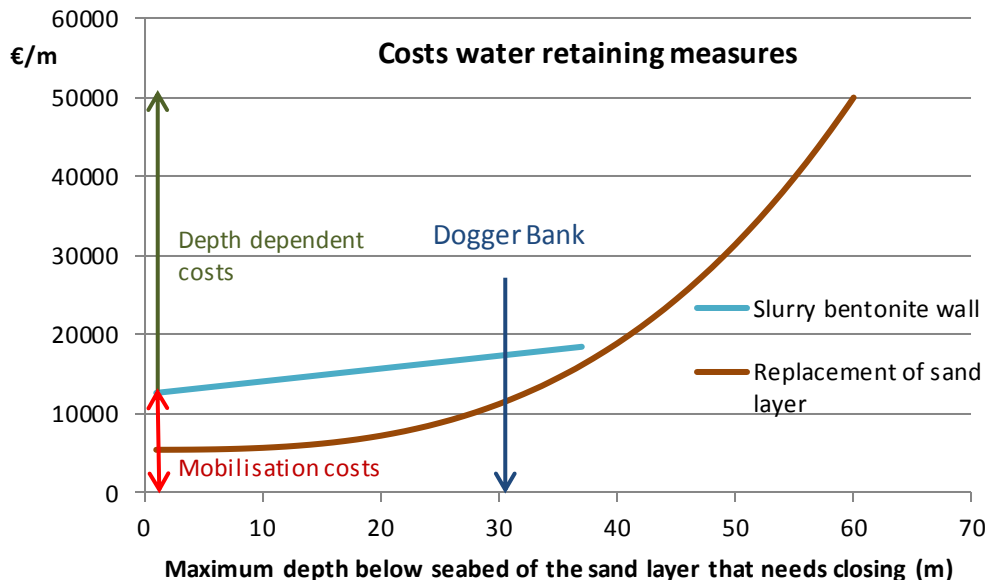


Figure 98: The costs of the retaining measures as they progress over depth. The mean sea level is 20m above the bed level. Based on the large costs difference and the flexibility the dredging alternative offers, this is the preferred technique

8.2 Dredging costs

The dredging costs have already been specified in (5.3 Specifications and costs) to provide insight in what dredging process can best be applied. It proved that the innovative 'semi-sub & convey' process is most competitive.

In order to dredge the stiff glacial clay dedicated grabbers need to be made. These specialised grabbers are mounted on a semi-submersible vessel that can operate in extreme wave conditions. The dredged material is then transported and placed via a conveyor belt system and over a specifically made jack-up pontoon. The investment costs of the grabbers (0.5 x 30m€) and the semi-sub (0.5 x 300m€) are shared with the creation of the Energy Island. The jack-up platform (100m€) is solely used for the dam construction and will be fully paid for. These are all conservative assumptions, since the dredging equipment will definitely still have a rest value.

The investment costs in equipment and operational unit price is given in Table 34. The dredging cost to create a certain storage capacity for the inner reservoir is shown in Figure 99.

Dredging process	Costs dedicated equipment (€)	Unit price (€/m ³)
Grab & barge	160,000,000	5.66
Semi-sub & convey	310,000,000	3.40

Table 34: The capital and operational costs of the two reviewed dredging processes

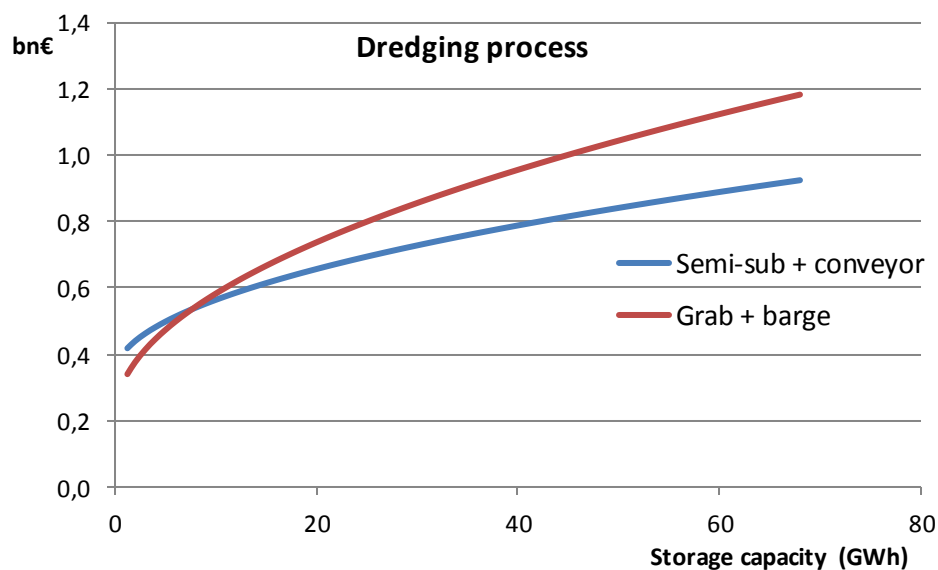


Figure 99: The total dredging costs for a storage reservoir with a 40m maximum head difference and 5545m³/m of dam to be dredged. The grab & barge process is more competitive till 7.7GWh, afterwards the semi-sub & convey process is preferred

8.3 Pump-turbine costs

The power generation modules for large hydropower plants are always custom made. The tailored pump-turbines therefore form an expensive piece of engineering. The advantage is that they will exactly suit the particular site conditions.

In order to deal with the corrosive saline environment measures have to be taken. Experiences from the Okinawa Yanbaru seawater PHS plant and various tidal energy plants proof that using a stainless steel runner and cathodic protection for other steel parts is ample to deal with the harsh surroundings (Fujihara et al., 1998; Rijkswaterstaat et al., 1985).

The costs of the turbines are estimated via other sources. General levelised costs of hydropower energy and maintenance and operational costs can be found in IRENA (2013). Alvarado Ancieta (2012) has collected data on costs of turbines from 150 different hydropower projects. According to his formula (in which P is turbine power) the costs scale with the turbine power in the following way:

$$\text{Turbine costs} \left(\frac{\text{m\$}}{\text{MW}} \right) = 1.0654P^{-0.277}$$

$$\text{Total electrical and mechanical costs (m\$)} = 1.0439P^{0.7823}$$

These two formulae are very convenient for usage. However, the costs are based on 150 projects where all kinds of turbines have been installed. To get a better insight on the costs of Francis pump-turbines themselves, Alvarado Ancieta his data has been analysed and the costs of the desired turbines were extracted. Based on twelve schemes the Francis pump-turbine scale like shown in Figure 100.

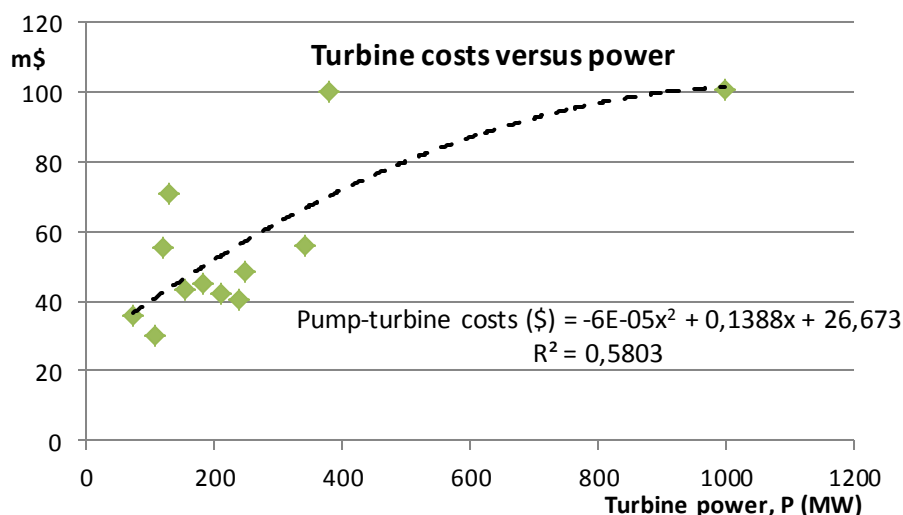


Figure 100: Turbine costs per installed power capacity. Data obtained from Alvarado Ancieta (2012). 1 USD from 2012 corresponds to 0.819 Euro anno 2017.

As can be seen in Figure 100, the gathered data does not provide a very convincing accuracy. When the turbine costs are plotted against the discharge the relation is slightly more reliable. Yet the considered discharge of 700m³/s lies far outside the dataset. Therefore this relation does not provide a conclusive estimate either.

8.4 Housing of turbine costs

There is no detailed design yet of the powerhouse, penstocks and other civil works. The scalar that was obtained in the literature study will be applied instead (see §2.6 Overview of energy storage islands). Although quite some information has already been gathered on concrete and reinforcement volumes and the overall dimensions of the penstocks and powerhouse are approximated (see §7.2 Main dimensions and volumes). It is not enough to make a reliable cost computation.

Until further costs are elaborated the housing of the turbines are scaled with: 602 m€/GW. Thereby the dredging costs originating from the excavation of the trench and the temporary dam will be added on top. Though the scalar of 602 million euros per Gigawatt already includes costs for a building pit, it is the notion of the author that the issue of cavitation has been severely underestimated in previous studies. The cavitation and draft tube combined necessitate a much larger construction depth than was previously accounted for.

Nevertheless the housing may be a little cheaper compared to the case studies. When assumed that the structure costs increase linearly over the depth and the housing is placed 60m below MSL in the case studies, the structure would be 1.5 times as expensive (90/60). However, the turbines are twice as large resulting in the need for only half of the number of 'powerhouses' (265MW compared to 125MW). Ten percent is added for the longer transportation costs towards the Dogger Bank. For one Gigawatt the housing costs then become: $1.5 \cdot 0.5 \cdot 1.1 \cdot 602$ (scalar) + 38 (dredging) = 535 m€/GW = 89% of the scalar. Of course the housing could be a little narrower for a smaller turbine. To account for this and the uncertainty in the actual caisson design the initial assumption of 602m€ + dredging costs is maintained (see Figure 103).

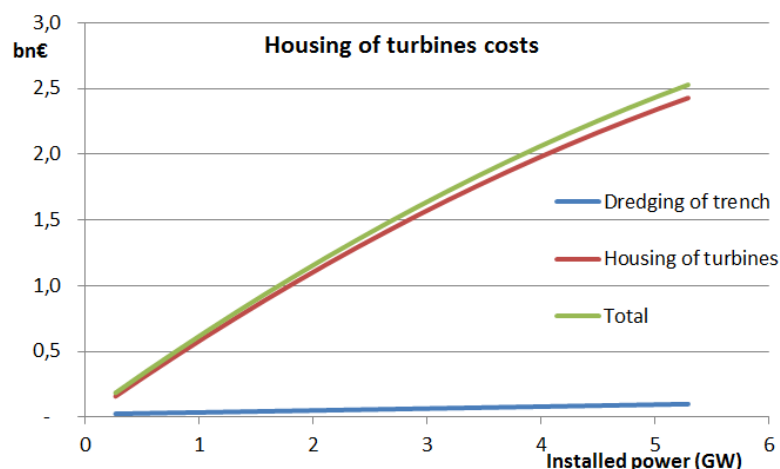


Figure 103: The scaling of the turbine housing per installed power capacity

A similar approach in terms of scaling as for the turbines has been adopted. The housing to accommodate the first turbine is rated at 100%, for the second turbine at 97.5%, third at 95% etcetera. The reduction in costs as the power increases accounts for the learning curve during the construction works, sharing of equipment and mobility costs, economies of scale and the relatively lower dredging costs¹³. It has to be stated that the presented costs graph for the turbine housing is indicative and needs much more investigation to attain a reliable estimation. The computed concrete and steel volumes could serve as a preliminary guidance.

¹³ For all pump-turbines a trench has to be dug from 20m below MSL till around 90m below MSL. The trench is 'three dimensional'. Therefore relatively less material needs to be dredged when there are many turbine units lined-up next to each other.

8.5 Operational and maintenance costs

Hydropower projects are marked by relatively large investment costs and low running costs. Typical costs are 1 – 4% of the initial investment. For large schemes 2.2% can be assumed (IRENA, 2013). Most of the maintenance works will go into the electrical and mechanical parts.

For the civil works and namely the outer protection it has to be noted that maintenance is a choice and not an unknown variable. The costs and time that are taken up by maintenance works are largely dependent on the initial design (Burcharth & Rietveld, 1987). The three factors that mostly influence

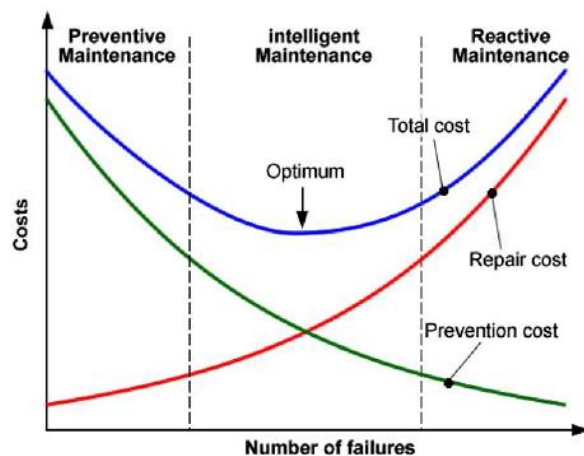


Figure 104: Maintenance strategies. Note the concaved shape of the optimal line (source: Burcharth & Rietveld, 1987)

the required time and costs are accessibility, the level of specialized equipment needed and the material used. Generally land based equipment is cheaper than their floating counterparts. Therefore it would be convenient if all the repair works on the dam can be executed from the land itself. Additionally it is recommended to use locally available materials as much as possible and have certain prefabricated parts for spare to reduce the repair time. Overall the goal is to minimise the costs over the whole life cycle, so that the capital costs are optimised together with the operation, maintenance and inspection costs as in Figure 104.

Due to 'valley-shaped' optimum level of the maintenance costs (see Figure 104) it is possible to increase the safety level at virtually no additional costs. This risk aversion strategy is pursued, because of the poor accessibility of the PHS plant in the middle of the North Sea.

For all involved civil works an operation and maintenance costs of 1% of the capital costs is used. Due to the corrosive environment 4% of the capital expenditure in electrical and mechanical parts is adopted.

8.6 Total costs

The costs that are presented in the previous sections can be divided into two groups: storage capacity and power capacity. The storage capacity is created by the dredging of the inner reservoir, the subsequent construction of the dam and the water retaining measure (replacing the sand layer). The Francis pump-turbines and its necessary housing and in- and outlet system compose the power capacity. Figure 105 and Figure 106 show both the capital costs that are required to establish an offshore pumped hydropower storage plant on the Dogger Bank.

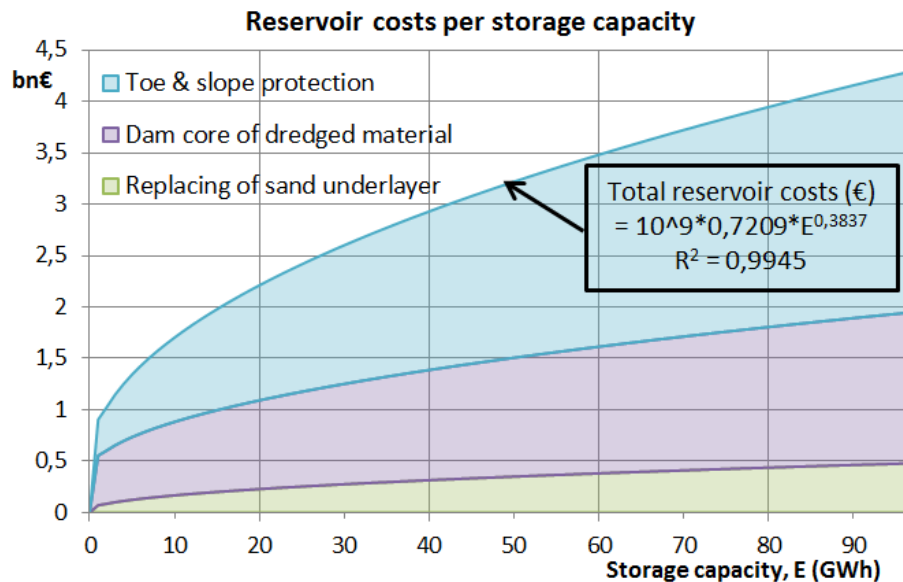


Figure 105: The relation between dam and dredging costs and storage capacity for a maximum head difference of 40m and dam costs of 98.13m€/km.

The relation between the dam circumference (responsible for the costs, scales with the diameter) and the quadratic reservoir surface area (and thus storage capacity, scales with diameter squared) can clearly be seen in Figure 105. A storage capacity of 20GWh costs 2.2bn€, whereas a 40GWh equivalent would only require 2.9bn€. Therefore it is beneficial from a civil costs perspective to deploy a large energy storage system.

Additionally a steep increase in costs can be observed at the lower tail of the graph (1 – 15GWh). This is the result of a relatively large dam compared to the storage area. The larger the reservoir becomes, the less the dam size influences the costs.

Furthermore one has to be aware that for the dredging costs the assumption was made that the material from the inner reservoir that is not needed for the dam construction, would be dredged and paid for by the creation of the 'Energy hub' and additional functions. This is a reasonable presumption for small to medium sized reservoirs (10 – 25GWh). However, for larger reservoirs it will become problematic to allocate the redundant material for other purposes. Consequently these bigger schemes might have to carry higher dredging costs. Of course the size of the reservoir is also limited by suitable geologic conditions (presence of thick clay layers). These will be increasingly more difficult to locate for larger areas. More explanation about the scaling and the impact of different cost components can be found in §4.5 Final design and concluding remarks.

The costs related to the power generation from Figure 106 are almost linear. For the pump-turbines there is only a scale advantage when more than one turbine is installed. All the others will continue having a price of 90% of this first unit.

The turbine housing has not yet been thoroughly investigated and computed. Instead the costs that were found in the case studies have been employed to inter- and extrapolate. A similar approach in terms of scaling as for the turbines has been adopted. The housing to accommodate the first turbine is rated at 100%, for the second turbine at 97.5%, third at 95% etcetera. The reduction in costs as the power increases accounts for the learning curve during the construction works, sharing of equipment and mobility costs, economies of scale and the relatively lower dredging costs. It has to be stated that the presented costs graph for the turbine housing is indicative and needs much more investigation to attain a reliable estimation. The computed concrete and steel volumes could serve as a preliminary guidance.

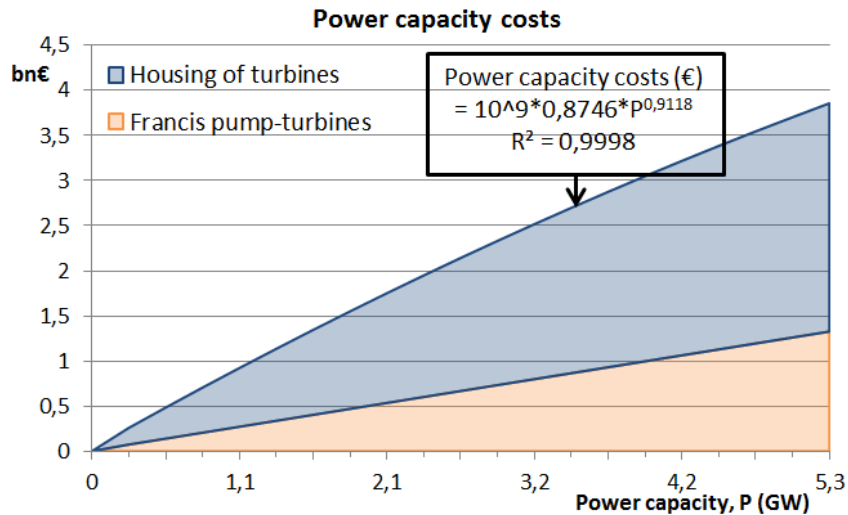


Figure 106: The costs of the Francis pump turbines and all related electrical, mechanical and civil works. Note that the horizontal axis is divided according to the number of turbines (265MW each)

All the involved cost components are quantified in Table 36. These costs can be used to estimate the expenditure to develop an offshore pumped hydropower storage facility in the North Sea on the Dogger Bank.

Element	Capital costs (€)	Operational and maintenance costs (€/yr)
Dedicated equipment	310,000,000	-
Storage reservoir (E=GWh)	$10^9 * 0.7209 * E^{0.389}$	$10^7 * 0.7209 * E^{0.389}$
Power generation (P=GW)	$10^9 * 0.8746 * P^{0.9118}$	$4 * 10^7 * 0.8746 * P^{0.9118}$

Table 36: Total costs related to the creation and operation of an offshore pumped hydropower storage plant in the North Sea

To acquire an impression in the order of magnitude of the costs: a 20GWh reservoir with 2GW of power costs 4.24 billion euros and has yearly operation and maintenance costs of 90.5 million euros, whereas a 40GWh equivalent with 4GW of turbine power costs 6.45bn€ and has 165m€ of running costs.

After all it appears that the volume balance and amount of dredged material that can be allocated to other functions limits the choice of storage capacity (for the storage business case itself). This restriction is the result of the initial choice to construct the storage reservoir in shallow water (20m). In case more than 25GWh needs to be stored it is advised to move to deeper water. Thereby the storage capacity costs will rise slightly. For the chosen shallow water scenario and when assumed that besides the 'energy hub' another 300 million cubes (size of the Tweede Maasvlakte) can be assigned to new uses, a moderate storage capacity of 25GWh is favoured. By installing 10 turbines, providing 2.65GW, the CAPEX becomes 4.65 billion euros and the OPEX 110 million euros per year.

8.7 Levelised cost of storage

To be able to compare different storage technologies the levelised cost of storage (LCOS) can be used, just like the levelised cost of energy (LCOE) is used for power plants. It must be clearly understood that the LCOS does not cover the true benefits of energy storage: energy security and allowing large shares of renewable energy sources to be integrated into the grid. These and other benefits will be discussed in the next section.

Although the LCOS suggests that all factors of influence on costs are covered, not all LCOS-analyses contain the same inputs. Thus one has to be cautious when using LCOS from different sources. In this analysis the same approach of the World Energy Council (WEC) from 2016 is adopted that was also used for the comparison between storage technologies earlier in §2.3.6 Comparison of energy storage technologies:

$$LCOS = \frac{I_0 + \sum_{t=1}^n \frac{A_t}{(1+i)^t}}{\sum_{t=1}^n \frac{M_{el}}{(1+i)^t}}$$

- LCOS = Levelised Cost Of energy Storage (€/MWh)
- I_0 = Investment costs (CAPEX) (€)
- A_t = Annual total costs in year t (OPEX) (€)
- M_{el} = Produced electricity in each year (MWh)
- n = Technical lifetime (years)
- t = Year of technical lifetime (1,2,...,n) (-)
- i = Interest rate (WACC¹⁴ = 6.43¹⁵) (%)

To get a better insight in how these parameters influence the LCOS and what would be a reasonable assumption ten scenarios are presented. First a basic situation when afterwards a single parameter is changed at the time.

- **Standard:** Power is produced on average for a morning peak of 3 hours and in the afternoon peak for another 3 hours. The preferred alternative of 25GWh and 2.65GW is operational for 95% of the time. The lifetime is 50 years, till the pump-turbines and electrical-mechanical equipment are deteriorated. The interest rate is 6.43% as was suggested by previous research (De Boer et al., 2007).
- **Long lifetime:** The operational life is elongated till 80 years, without refurbishment.
- **Refurbishment E&M:** The operational life is elongated till 80 years, with a full revision of the turbines and all other electrical and mechanical equipment at a cost of 667m€.
- **Low interest:** The interest rate is lowered to 5%.
- **High generation:** Besides the peak-shaving additional power is generated due to the charging of a surplus of wind energy and discharging at times of shortage. This almost continuous cycle of buying and selling leads to an electricity production of 10 hours a day.
- **Grid deferral:** By adding the energy storage facility to the 'Energy hub' on the North Sea, the amount of interconnector cable (IC) capacity can be restricted. The exact ratio

¹⁴ WACC = Weighted Average Cost of Capital

¹⁵ As was determined by the study for the Energy Island by KEMA and Lievense. This value includes taxes and was found acceptable for an investment made by a governmental body (De Boer et al., 2007).

between wind-IC-storage is unknown and dependent on a comprehensible cost-benefit analysis. A beneficial choice would be to extract the complete avoided IC cost from the CAPEX of the energy storage facility. It is unlikely though that the optimum interconnector plus energy storage capacity is equal to the wind power capacity. However, the interconnector cables are expected to have a much shorter lifetime than the pumped hydropower plant. Therefore the installed power of the PHS might actually defer twice the IC cable capacity. All in all it is found acceptable to completely extract the installed power capacity (2.65GW) in IC costs from the CAPEX. The average distance to shore is assumed at 350km. The deferred cost of subsea interconnector cables (obtained from 17 IC projects in the North Sea region by Gerrits (2017)) becomes:

$$Deferred\ costs_{subsea\ IC}(m\text{€}) = -596 + 0.952 \cdot P(MW) + 1.589 \cdot 350(km) = 2480m\text{€}$$

- **Large scale:** The storage and power capacity are doubled to 50GWh and 5.3GW.
- **Small scale:** The storage and power capacity are reduced to 10GWh and 1.06GW.
- **Utopia:** Combines all the benefits to indicate the lower boundary.
- **Realistic:** Combines all parameters into a feasible alternative:
 - an 80 year lifetime with full E&M refitting after 40 years
 - 2 hours of extra generating due to the combination with a giant wind farm
 - Deferred grid investments worth 2.48bn€, extracted from the CAPEX
 - An acceptable interest rate (WACC) of 6.43%

All stated scenarios are presented in Table 37. From the LCOS ranging between 106.8 to 16.9, the 'Realistic' scenario with 40.0€/MWh is most reasonable.

Parameter	Symbol	Unit	Standard	Long lifetime	Refurbished E&M	Low interest	High generation	Grid deferral	Large scale	Small scale	Utopia	Realistic
Storage capacity	E	GWh	25	25	25	25	25	25	50	10	50	25
Power capacity	P	GW	2.65	2.65	2.65	2.65	2.65	2.65	5.29	1.06	5.29	2.65
CAPEX	l_o	€	4.65E+09	4.65E+09	4.65E+09	4.65E+09	4.65E+09	2.17E+09	7.30E+09	2.69E+09	2.30E+09	2.17E+09
OPEX	A_t	€	1.10E+08	1.10E+08	1.10E+08	1.10E+08	1.10E+08	1.10E+08	1.93E+08	5.45E+07	1.93E+08	1.10E+08
Generating hours/day	h_{ge}	h	6	6	6	6	10	6	6	6	10	8
Produced energy/year	M_{el}	MWh	5.51E+06	5.51E+06	5.51E+06	5.51E+06	9.18E+06	5.51E+06	1.10E+07	2.20E+06	1.84E+07	7.34E+06
Technical lifetime	n	years	50	80	80	50	50	50	50	50	80	80
Interest rate (WACC)	i	%	6.43	6.43	6.43	5	6.43	6.43	6.43	6.43	5	6.43
Levelised costs of storage	LCOS	€/MWh	76.8	74.6	82.5	66.2	46.1	46.5	62.1	106.8	16.9	40.0

Table 37: LCOS for all scenarios (with a 40m head difference, 8m waves and constructed in 20m deep water). The 'Refurbished E&M' and the 'Realistic' scenario contain a refitting of E&M equipment after 40 years. The storage facility is assumed to be operational 95% of the time. Note the large impact of the WACC, energy production, grid deferral and scale of the facility.

8.7.1 Comparison with other energy storage technologies

Now the range of possible LCOS and a specific achievable alternative is known, it can be compared with the other existing storage technologies. Hence it will become clear whether it is actually a good idea to combine energy storage in the shape of an inverse offshore pumped hydropower storage (IOPHS) facility to the 'Energy hub' that is planned in the North Sea.

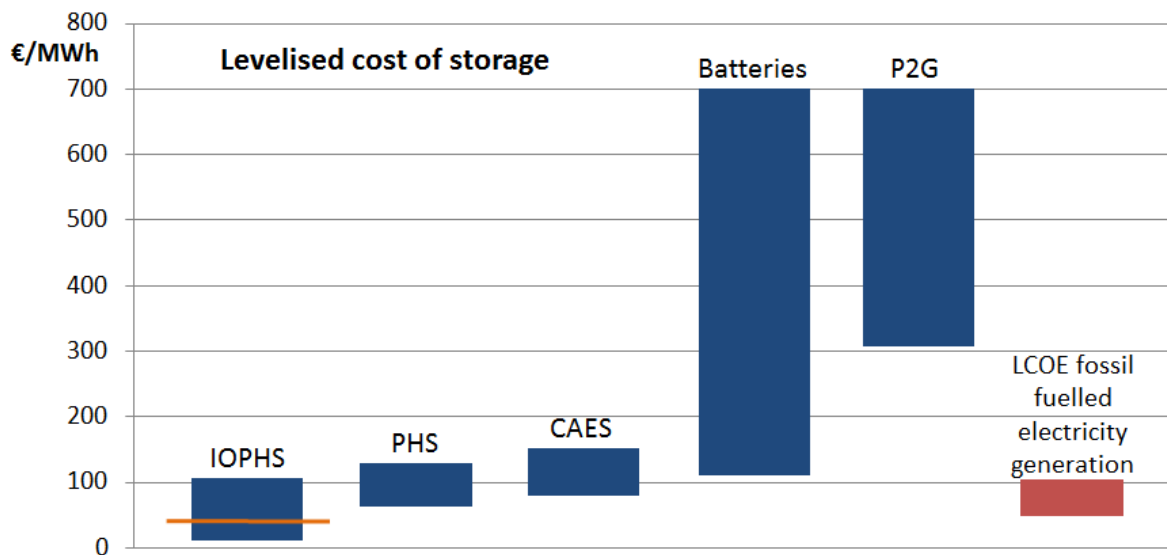


Figure 107: The LCOS for 2030 of the studied IOPHS compared to other storage techniques (WEC, 2016a) and relative to the LCOE of conventional fossil fuelled plants (50–106€/MWh) in OECD countries (<http://costing.irena.org/media/4110/fig-esi-3.png>). The orange line indicates the chosen alternative of 40€/MWh

In Figure 107 it can be seen that clearly the considered IOPHS alternative is the most competitive. Perhaps most surprisingly the offshore version is not even half the costs of its counterpart in the mountains (PHS mean LCOS = 85€/MWh). This seems hard to fathom, especially because in the energy formula there is the 'height squared' and the water level differences in a mountainous region can be much larger. The combination of not having to do expensive rock removal or tunnelling works, the large installed power of the IOPHS and corresponding electricity production and the combination with a large wind farm plus 'energy hub' make the difference.

Note that the desired IOPHS is 3 to 18 times less expensive than batteries or power to gas! Especially in recent times energy storage is getting more attention and plans are being developed, like power to gas on the Dogger Bank¹⁶ or the cooperation between Tesla Inc. and Vestas for storing wind energy with batteries¹⁷. Together with the late increase in PHS investments (Pérez-Díaz et al., 2014), one could not conclude otherwise than that the opportunities for offshore pumped hydro are gigantic.

Not unimportantly, the chosen IOPHS has a lower storage costs than the fossil fuel generating costs (40€/MWh versus 50 – 106€/MWh). What this indicates is that it is more beneficial to store energy and release it at a later time than letting the energy go to waste and just generate new fossil fuelled electricity instead. Consequently it should be more beneficial to employ energy storage instead of a Combined Cycle Gas Turbine (CCGT) in order to generate the daily variable load.

Ultimately it can be concluded that in case every technical design presented in this report is nonsense and the overall costs proof to be twice as high, the concept of IOPHS would still be viable!

¹⁶ <https://nos.nl/artikel/2192724-nederlandse-energiereuzen-gaan-wind-en-zonne-energie-opslaan.html>

¹⁷ <https://www.windpowermonthly.com/article/1443471/vestas-confirms-tesla-joint-project>

8.8 Benefits

The value of energy storage lies above all in providing energy security. Secondly it enables the integration of intermittent RES into the grid. Regardless how much wind or solar capacity would be installed, without energy storage conventional fossil fuelled plants would have to take over when the wind is not blowing and the sun not shining. Hence the desired reduction in carbon output of 80 – 95% could never be achieved.

Besides these social advantages of safeguarding the electricity supply and allowing the transition from a fossil fuel based economy to a sustainable market, there are of course also the economic benefits. Pumped hydro storage is typically profitable in the daily storage cycle, where electricity is generated for one till ten hours a day. Lately with the development of variable-speed pump-turbines it is possible to adjust the power output to the second for both the pumping and generating mode. This possibility opens up a whole new market for PHS in the short-term energy world. Together a modern PHS facility can thus cover almost all revenue creating applications (see Figure 16 for all services). Only seasonal storage is not beneficial, due to its low utility rate (Rauwerda, 2017).

To accurately compute the benefits of the energy storage system on the Dogger Bank would be extremely challenging, because of all the uncertainties in future energy prices, installed wind capacity and all the connected countries with their own policies and power generation units. As was concluded in the LCOS section, the business case for offshore PHS is as good as a storage technology has ever been. Based on this fact and the current trend of developing all kinds of lesser (in costs) storage alternatives, it could safely be assumed that the studied storage method will be profitable.

In order to get a little bit of an insight in the revenue streams and the payback period, a few future scenarios are presented in the next section.

Additionally other functions could be added to the energy storage reservoir itself (besides other uses that can contribute via the redundant material). Some of the possibilities that directly originate from the existence of the storage facility are:

- The inner slopes and berm (250m) could be covered in solar panels. Imagine a spatial coverage of 70% and a 25GWh system (6830m diameter), then the surface covered by photovoltaic (PV) panels becomes:

$$0.7 \cdot \frac{1}{4} (\pi \cdot D^2 - \pi \cdot (D - 250)^2) = 1.84 \text{ km}^2 \text{ with } 0.35 \frac{\text{GW}}{\text{km}} \rightarrow 0.65 \text{ GW of PV capacity}^{18}$$

With a 10% capacity factor the annually produced electricity from PV would be 569GWh. This is equivalent to 5% of the solar production of 2016 in the Netherlands.

- Aquaculture. The inner reservoir could be used to grow mussels, oysters and possibly fish. Since there is some redundancy in the reservoir depth (40m, where 41.5m is possible) it could be considered to locally dredge a little deeper to create a minimum water level.
- Biomass. The growing of seaweed to use as biomass for electricity generation offers a lot of potential¹⁹. Just as for the aquaculture it needs to be investigated if the proper (tidal) conditions are present.

¹⁸ 0.35GW/km obtained from <https://www.deingenieur.nl/artikel/heel-nederland-groen>

¹⁹ See <http://www.wur.nl/nl/show/Seaweed-as-a-source-of-biofuels-and-chemicals.htm> for a description of why exactly seaweed is so promising

8.8.1 Hypothetical revenues and payback period

In the original plan the benefits side of the North Sea ‘Energy hub’ would be studied simultaneously with this research. Currently it is expected that this research will become public in 2018. To be able to still get an impression of the scale of the benefits and the eventual Net Present Value (NPV) some indicative scenarios are worked out. With the NPV the difference between the revenues and costs are discounted back to the present. This discounting is performed because money is worth less in the future than it is now: a euro put in the bank will grow due to interest and a euro invested in a project will not. Future income will therefore have to be discounted back with the interest rate to the present value. Consequently the profitability of a project depends more on the revenues from the first years of operation than at the end of its lifetime. The Net Present Value is computed by:

$$Net\ Present\ Value = \sum_{t=1}^n \frac{C_t}{(1+r)^t} - C_0$$

- n = Technical lifetime (years)
- t = Year during lifetime (1, 2, ... n) (-)
- C_t = Cash flow in year t (=Revenue – OPEX costs) (€)
- r = Interest rate (WACC) (%)
- C₀ = CAPEX of the project discounted to t=0 (€)

For the preferred storage reservoir with 25GWh and 2.65GW the NPV is presented in Figure 108 for conditions with a different interest rate and profit from electricity trading as shown in Table 38.

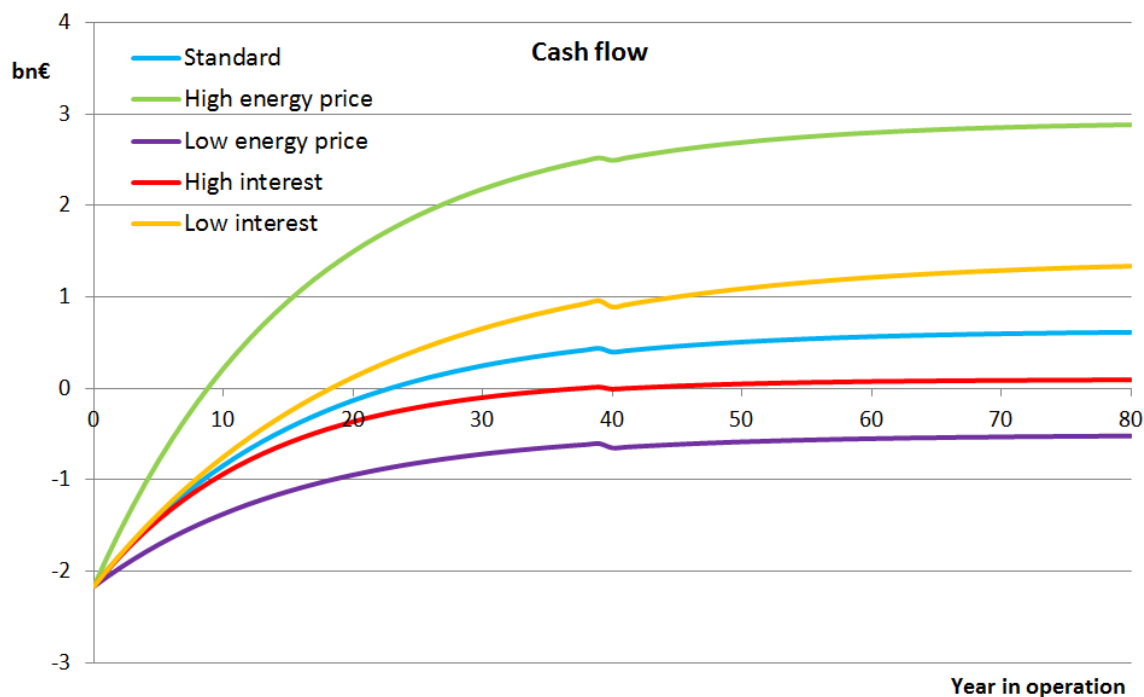


Figure 108: The cash flow for different electricity prices and interest rates. From these scenarios the 'Standard' one is found most appropriate, with a payback period of 23 years. Note the refitting of the turbine equipment after 40 years

Payback period	unit	Standard	High energy price	Low energy price	High interest	Low interest
Interest rate (WACC)	%	6.43	6.43	6.43	8	5
Profit from electricity production	€ / MWh	40	60	30	40	40
Net Present Value	bn€	0.61	2.88	-0.52	0.09	1.34

Table 38: Characteristics of the five considered economic models

Figure 108 confirms the theory that the energy prices in the distant future do not affect the NPV that much (compare the tail of the green and purple line). During the first operational years the profitability of the whole project is largely influenced by the energy prices, after 30 years the NPV gap between the high and low price scenario is already 3bn€, where after 80 years the difference has increased to only 3.4bn€. The interest rate has a relatively larger impact in the second half of its lifetime, where the difference between low and high interest still increases with 0.8bn€ between 30 and 80 years.

From the cash flow and NPV analysis two main things can be concluded:

1. The profitability of the project is sensitive to the energy prices and the interest rate.
2. The economic value is largely determined by the electricity prices during the first 30 years of operation.

Consequently it is important that the project is commissioned when the electricity prices or the daily/hourly fluctuations are high. The fluctuations in energy supply are expected to increase considerably in the future, due to the large shares of intermittent RES (see Figure 109).

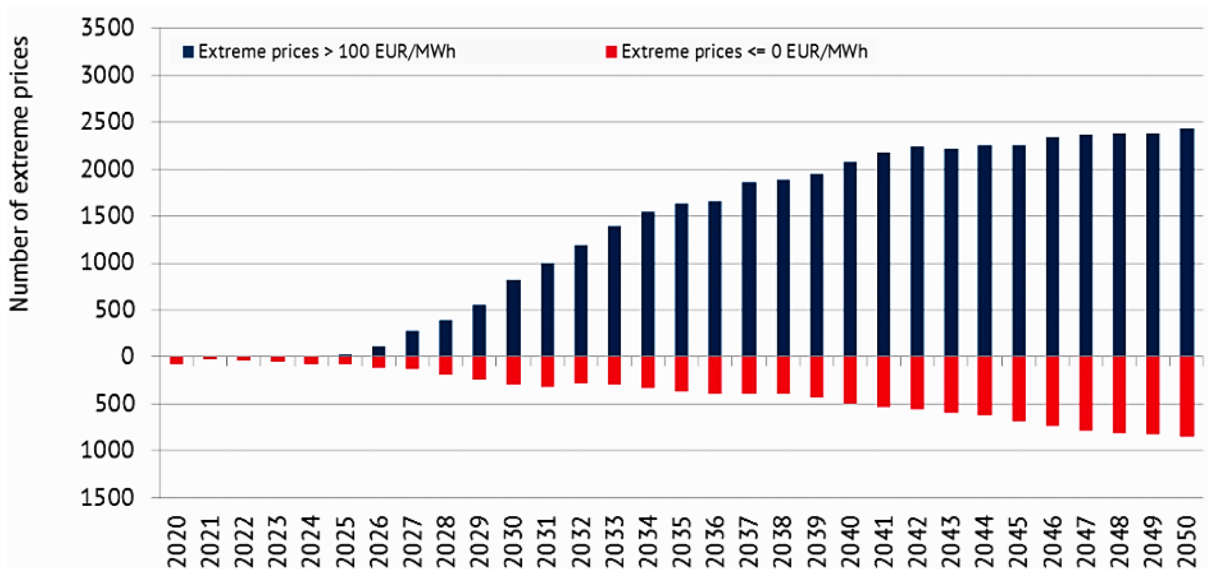


Figure 109: The increase in extreme electricity prices in the future for the EU-28 plus Norway and Switzerland (source: <https://energybrainpool.com/en/trends-in-the-development-of-electricity-prices-eu-energy-outlook-2050/>)

From the discussed alternatives of varying interest rates and profit from electricity vending, the standard option is found most reasonable. The average profit of 40€/MWh leads to an annual revenue of 294 million euros and a NPV of 610m€. Compared to the 242m€ in a study by ECN for a 1.5GW storage island in 2023 for the Netherlands, the 40€/MWh seem to be quite a lower boundary (De Joode et al., 2014). When extrapolating the revenues over the installed power the annual income would become $2.65/1.5 \cdot 242 = 428\text{m€}$. This would correspond to a net profit of 58€/MWh, which approximates the 'High energy price' scenario that leads to a NPV of 2.9bn€. Remarkably this would still be a conservative scenario, since the storage facility would not just be connected to the Dutch market, but also to the other North Sea countries.

All in all it can be concluded that billions of euros are to be eamed for a well-connected offshore pumped hydropower facility in the North Sea.

8.8.2 Contribution of energy storage to the 'Energy hub' in the North Sea

During the design and the costs calculations it already became clear that the combination of a storage reservoir and the energy island is mutually beneficial. The dredged material that becomes available from the inner reservoir can directly be used for the construction of the island. Additionally the installed power of the storage plant can be extracted from the necessary interconnector cables (IC) running to the mainland. The pumped hydro plant itself benefits from the prime location directly next to the giant wind farm and the linkage with the multiple North Sea power markets.

One of the research questions within the group of students enlightening different aspects of the energy hub was: "What is the optimal location for the Hub and Spoke concept in the North Sea?" The scope contained an offshore wind farm (OWF) of 30GW to be connected via an artificial island to all the North Sea countries. One of the envisioned locations is the Dogger Bank (at 55.48N; 3.73E). For this location it is checked how energy storage can affect the overall business case. For determining the required size of the storage and power capacity the earlier 20 to 40% rule is adopted (see §2.2.3 Required energy storage capacity). Considering the very well-connected grid the lower limit of 20% of intermittent RES capacity is applied. The storage facility then consists out of 60GWh and 6GW of installed power.²⁰ The results are depicted in Figure 110.

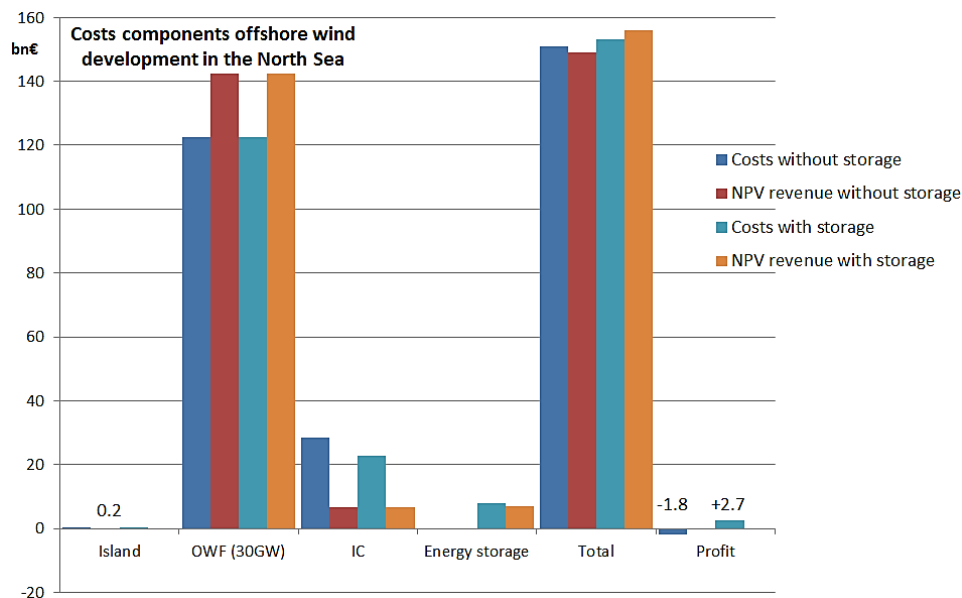


Figure 110: The business case of creating a giant offshore wind farm in the North Sea with or without energy storage. Note the negligible costs of the island itself and the reduction in interconnector cable costs in the storage alternative. The island, OWF and IC costs are discounted and obtained from Gerrits (2017)

From the figure above it could be deduced that energy storage is the key to turn the whole project from being unrewarding into a profitable case. Although this may be the case, it should be approached with great care. Large uncertainties lay in both the OWF costs and the OWF revenue, which are the largest and governing factors of influence.

The difference in profitability of 4.5 billion euros is only of secondary importance. The main benefit lies in the fact that when energy storage is included the whole energy supply becomes both sustainable and reliable. Without storage the energy supply will remain variable and will thus have to be supplemented by fossil fuelled generating units, which diminishes the overall sustainability.

²⁰ Such a large scheme will have to be placed in slightly deeper water (>20m) to avoid obtaining an excessive amount of redundant dredged material. Therefore the CAPEX will be a bit higher (max. 10%). In this indicative computation this added costs is neglected.

9. Discussion

The obtained results are evaluated in this chapter on their reliability and general applicability. The costs components are all defined by using deterministic values. Most of the values however are uncertain and could either improve or worsen the business case for offshore pumped hydropower. Due to the limited amount of time and vast complexity a full probabilistic approach could not be performed. Instead the current design is critically reviewed to see which components might turn out to be more costly than expected and where there lies potential for savings.

First the elements that determine the storage and power capacity expenditure are reviewed and afterwards the levelised cost of storage. Ultimately it is discussed how these values can be applied in the future and what the impact of inverse offshore pumped hydropower storage could be.

9.1 Storage capacity

To assess how the construction costs may alter from the earlier presented formula, the components are reviewed individually. By analysing the designs and the used data it can then be estimated how these costs may change. When all upper and lower limits are combined they can form a reasonable upper and lower boundary.

Be aware that only the governing engineering parameters are mentioned. There are many other factors of influence (technical and financial) that could affect the cost range.

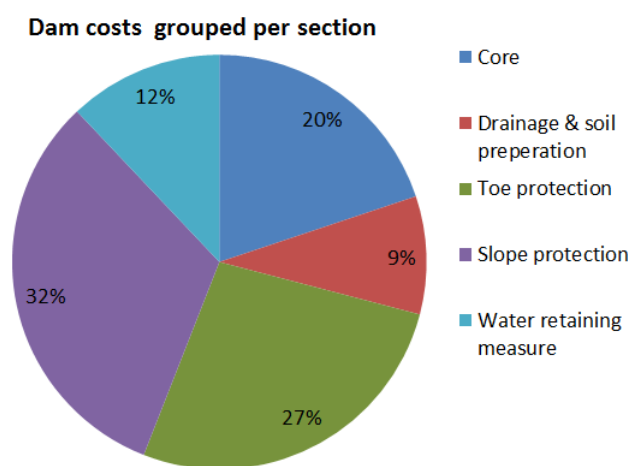


Figure 111: The components that constitute the dam construction. Note that the core and water retaining measure originate from the dredging process

The relative factors of each part can be multiplied with each other to arrive at a new 'cost factor'. The 'scaling factor', the power in the cost formula does not change, since the circumference and storage capacity ratios stay the same. The potential higher costs or savings are explained in Table 39.

Element	Potential extra costs or savings	Upper limit ²¹	Lower limit
Core & water retaining measure	Both rely on the dredging process and costs of equipment. In case it proves to be impossible to obtain a 100% filling ratio of the grab and only 50% can be achieved, the costs double. A 20% change in dedicated equipment costs results in +-9.5%	2.18 (1.50)	0.905
Drainage & soil preparation	40€/m ² was assumed over a perhaps more feasible 30€/m ² . However, when the consolidation process and draining of excessive poor water pressures runs into problems, the whole construction process will be delayed. To mitigate this, large investments might be made in order to speed up the soil preparation. Therefore a cost of 100€/m ² might be required	2.5 (2.0)	0.75
Toe protection	From physical modelling it might proof that the dimensions	1.1	0.182

²¹ The values between brackets indicate a more likely scenario when the large risks of the filling ratio of the grab dredger and laborious soil preparation are adequately mitigated

	<p>obtained from the guidelines are not sufficient or excessive. Therefore a 10% ratio is assumed for the toe design.</p> <p>In the current design the complete periphery is armoured to resist 8m waves. Waves from the south or east are only 4 to 5m high for a similar return period. This leads to the assumption that approximately half of the circumference can be executed at half the protection costs (25% reduction).</p> <p>All possible measures were taken in terms of macro stability. After a comprehensible soil investigation it might prove that the expensive toe foundation of quarry run can be avoided. This would save 73% on the toe design.</p>		
Slope protection	Just like the toe, the slope protection is evenly designed according to the guidelines. Physical modelling may influence the design with 10%. The savings in armouring around the periphery also apply to the slope (approximately 25%).	1.1	0.675
Weighted total	All upper- and lower limits are multiplied with each other after their relative share in the overall costs has been accounted for (see Figure 111)	1.57 (1.31)	0.62

Table 39: The upper and lower boundary of the costs to create a certain storage capacity. Note that differences in construction or material costs are not incorporated and neither is the planning

The largest risks of higher costs lie in the dredging process and soil preparation. Therefore extensive research will be necessary to ensure an efficient dredging method and drainage. Both these things can partially be avoided by thorough testing and try-outs. Consequently it is assumed safe in a worst case scenario to obtain a 75% filling ratio of the grab and perform the drainage and soil preparation for 80€/m². The resulting upper limits are stated in Table 39 between brackets. It shows that an early inventory of the potential risks and appropriate mitigation could lead to a maximum cost reduction of 26% (see Figure 112).

Table 39 states that there lies great potential in improvements of the slope and especially the toe design. Currently a lot of quarry run material is present in the design to safeguard the macro stability. Appendix F: Influence of toe material on slope stability shows that when normal clay conditions are present the use of quarry run could be avoided. This requires soil investigations and geo-modelling.

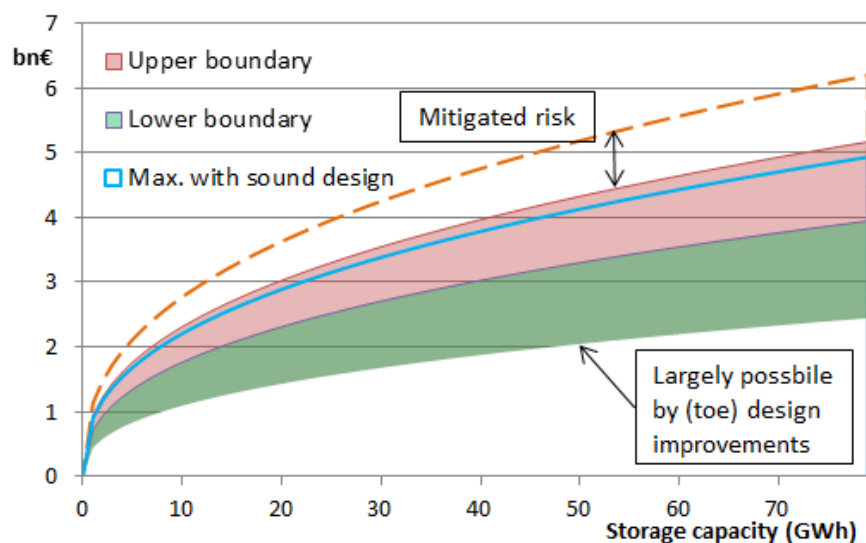


Figure 112: The upper and lower limits of the reservoir construction costs. The blue line indicates the maximum costs for an optimised design (=upper boundary x improved design)

The upper and lower boundary together with the actual costs forms the graph shown in Figure 112. Since the lower boundary can mostly be achieved by a better design, the maximum costs are actually quite close to the one that has been used ($0.96 \times 1.31 = 1.25$ =blue line).

9.2 Power capacity

For the assessment of the reliability of the Francis pump-turbine and housing costs the same methodology is applied. Only now there are only two elements distinguished: the turbines and the civil works. The civil works have to deal with the same uncertainty and risks from the dredging process for the excavation of the trench. However, it was proven that compared to the turbine housing costs the dredging of the pit is minimal (Figure 103).

For 2.65GW of power the housing and the turbines are responsible for 69% and 31% respectively. Since the costs of the turbine housing has not been properly calculated (interpolated from literature data), the largest uncertainty lies there. Consequently it could be imaginable that the costs may be 50% higher or perhaps 30% lower. This large range would not apply in the real world, since the construction of the prefab elements would actually take place in the most controlled environment. Until a rightful cost calculation has been made the unfavourable range of +50% to -30% will be maintained.

A similar situation exists for the pump-turbines. All Francis units would be custom made and the corresponding costs could be accurately estimated by the manufacturer. Only during the transportation and the installation of the electrical and mechanical equipment minor setbacks could be encountered (~5%). However, the reviewed literature does not provide enough confidence to adopt an evenly small uncertainty range. Twelve projects with Francis pump-turbines and a manual has been analysed from the Norwegian Water Resources and Energy Directorate (SWECO Norge AS., 2012). Yet not a very convincing relation between power and costs was found which leads to the assumption of an uncertainty range of 20%.

Together the cost ranges sum up to an upper boundary of 141% and a lower boundary of 73% as depicted in Figure 113. Note that these are not physical boundaries, but only present due to a lack of information. In reality it is more likely for the expenditure to vary between 110% and 90%.

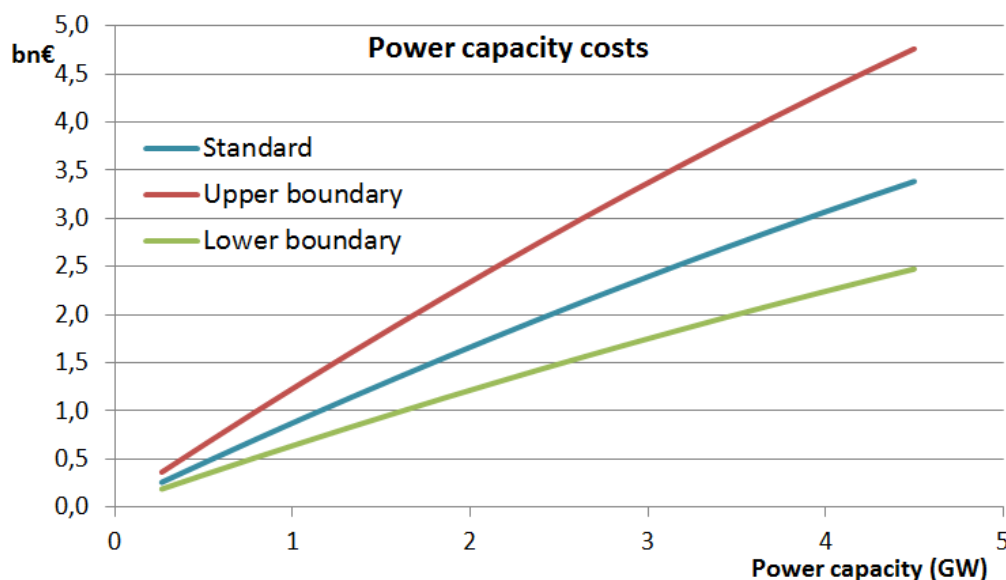


Figure 113: The range in CAPEX for the power capacity. Note that the large range is the result of a lack of information, not from technical risks!

9.3 Levelised cost of storage

All percentages and factors named are extremely rough estimations and mostly without proper scientific background. They are based on experiences and insights gained during this research. Although the cost ranges may be hard to justify, they can offer a potential worst and best case scenario.

To get a good understanding of how competitive an offshore pumped storage plant could become, the discussed CAPEX ranges for the storage and power capacity are turned into LCOS values. Additionally the annual operation and maintenance (O&M) cost range needs to be determined. Initially 1% for the civil costs and 4% for the electrical and mechanical equipment were implemented. As an upper boundary double the O&M costs are used and half for the lower boundary. Combined with the CAPEX scenarios this leads to a maximum and minimum LCOS. The results along with the standard case are presented in Table 40.

	Standard	Maximum	Minimum
CAPEX (bn€)	2.17	3.67	0.634
OPEX (bn€)	0.110	0.220	0.055
LCOS (€/MWh)	40.0	68.2	19.0

Table 40: The uncertainty in various aspects of the construction and maintenance works lead to a most costly and most beneficial case realistically conceivable. All three scenarios are based on the chosen variant of 25GWh and 2.65GW from §8.7 Levelised cost of storage in which the amount of installed power defers an equal quantity in grid investments that is extracted from the CAPEX. The 'Maximum' cost is based on the upper boundary cost with an optimised design (blue line Figure 112).

The outcomes of the extreme maximum and minimum situations indicate two things:

1. In the worst case scenario the offshore pumped hydropower variant is just as lucrative as a competitive conventional PHS plant (LCOS ranging from 60 – 130)
2. In the best case the storage facility in the North Sea would truly enter territory unknown to historical energy storage plants.

Based on the findings in this report it can comfortably be concluded that the business case for inverse pumped hydro is very strong. Even when the project faces enormous setbacks like: half the production rate of the dredging equipment, twice as much spending on soil treatment, double the maintenance costs and a 50% more expensive turbine housing, the enterprise would still be viable.

9.4 Comparison with previous literature

Even though the offshore pumped hydropower storage idea has been around for decades, limited research has been performed to understand the mechanisms and complexities regarding the realisation of such a project.

In the four case studies which have been investigated that similarly construct one reservoir themselves and employ the sea as the other reservoir were reviewed. Plan Lievense and the Slufter rely on an inner reservoir with a water table that is above the sea level and the Energy Island and TIESI have their reservoir below the sea, just like in this thesis.

To compare the scalars from the literature and the ones produced in this report, the thoroughly analysed 25GWh with 2.65GW variant will represent the obtained results (see Figure 114).

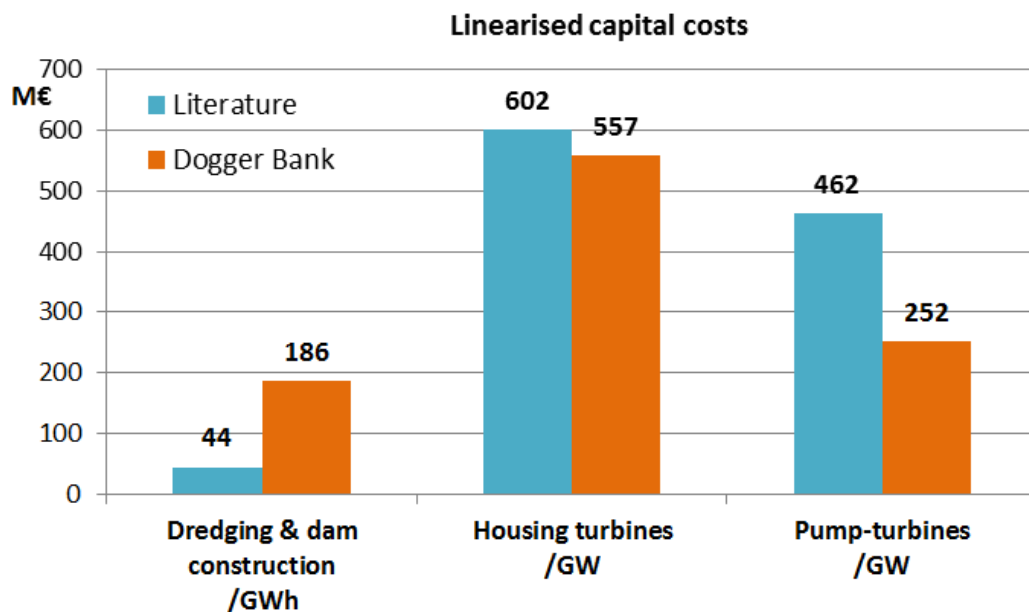


Figure 114: The linearised scalars that were obtained from the case studies ('Literature') and the performed research ('Dogger Bank'). Note that the scalars for the Dogger Bank change for different storage and power capacities.

As can be observed no trend can be distinguished between the results from the literature and the newly gained insights. This is caused by the many different parameters that determine the overall costs, which can cancel out against one another. However, large deviations and technical choices were encountered:

The dam costs for the pumped storage facility on the Dogger Bank are four times as high as was accounted for in the literature. For the 'Energy Island' that would be placed in front of the Dutch coast, the dam and dredging costs would be 27,000 €/m compared to 98,000 €/m for the Dogger Bank. Even in the most optimistic scenario the dam costs will not go below 60,000€/m (lower boundary from Table 39). Although the wave conditions in the middle of the North Sea exceed the environment in front of the coastline, it can be concluded that the necessary armouring has been seriously underestimated.

In the previous studies most dams were constructed out of sand, therefore a slurry bentonite (SB) wall had to be included in order to create an 'impermeable' system. For the considered clay dam though, no additional water retaining measures are required. Solely a potential sand layer near the

reservoir bottom would need sealing. This can best be executed by dredging and replacing the conveying material with selected clay.

The turbine housing component is nearly equal, since the costs were estimated by this scalar obtained from the case studies. The small difference is caused by the assumption that the CAPEX decline for the housing with 2.5% per installed turbine. The reduction in costs as the power increases accounts for the learning curve during the construction works, sharing of equipment and mobility costs, economies of scale and the relatively lower dredging costs. Until a more detailed construction method and cost computation is made it cannot be said whether the literature over- or underestimated the costs. It is likely that the housing costs will be lower, because the employed turbines are twice the size, necessitating only half the number of 'powerhouses', penstocks and tailraces.

The pump-turbines are clearly less costly than previously thought. This is the result of using a turbine twice as large, 265MW instead of 125MW. Thereby it is proven that it was a misconception that the costs of a turbine do not relatively decline as the power is increased.

9.5 Remarkable findings

In general another few remarkable characteristics were discovered that were either not identified or ignored in previous research:

A very large inner berm has to be added to overcome the combination of macro slope stability and uplift at the inner toe.

The optimum depth of the reservoir does not lie between 30 and 40 metres, but much deeper. Effectively only the water level between the MSL and the seabed needs to be retained by the dam (which does need to be high enough to restrict the overtopping). In case the inner reservoir is excavated below the original seabed, the water level that the dam has to resist remains the difference between MSL and the seabed. The water level difference between the bottom of the inner reservoir and the seabed is simply retained by the existing soil (underneath the constructed dam).

The use of a grab dredger takes away the limitation of the practical maximum dredging depth of a suction dredger. Since the storage capacity is a function of the head difference squared, a deeper reservoir is preferred, because it will shorten the necessary dam length. For an inverse offshore pumped hydro storage reservoir the optimal depth will rather approach 60 metres.

The need for shallow water to enable the implementation of an offshore storage system is not as correct as would be first assumed. Naturally the dam costs will increase when it is located in deeper water. However, the dam costs only form about a third of the total capital expenditure. In case a storage system larger than 25GWh is desired the facility should gradually move to deeper waters. If not, it is likely that the amount of material that becomes available (>500 million cubic metres) cannot be allocated to other purposes (the 'energy hub' requires about 200 million cubic metres). The depositing and transporting of left over material is unwanted and it would be favourable to move to deeper water instead.

A larger reservoir (>25GWh) does benefit from its scale compared to smaller alternatives. This scaling advantage counters the added dam costs induced by the larger water depth. Consequently the relation exists: "the larger the reservoir, the deeper the water depth should be". Therefore the

inverse storage plant is not limited to depths of maximally 20 metres, but more likely to 40 metres (afterwards the dam and armouring costs will counter all scale benefits). Ultimately the concept of inverse pumped hydropower storage has a much wider application range than was until recently believed.

The influence of cavitation on the design for the turbine housing is immense. To avoid this catastrophic phenomenon the turbines need to be installed at depths far below the bottom of the storage reservoir (14– 18 metres). Additionally a draft tube that enables the maximum use of the head difference between the reservoirs is necessary. This draft tube reaches a depth of roughly three times the runner diameter. For a 40m head difference the maximum depth of the powerhouse extends till 90 metres below mean sea level.

The challenges regarding the turbine housing were not clearly identified and pose a critical obstacle in the realisation of the whole energy storage scheme. The proposed construction method with modular box caissons is deemed appropriate to deal with the circumstances and consequently enable the implementation of an inverse offshore pumped hydropower storage facility.

It should be noted that the results are certainly not limited to a single case on the Dogger Bank, rather they are universally applicable. The stated design choices and relative costs components may act as guidance from which the given formulae and factors could easily be transposed to any other case. By doing so it can quickly be assessed if an inverse PHS system is possible and whether it provides a profitable business case.

10. Conclusion

Billions of euros lay for the taking in the newly emerged storage market. Therefore the offshore pumped hydropower storage plant does not only offer environmental benefits (integrating large shares of RES to combat climate change) or societal benefits (employing thousands of people) it is also extremely lucrative from an economic perspective.

In this chapter the main conclusions of the performed research are first briefly stated when afterwards the choice and the scaling of the four building blocks of the storage facility (dam, dredging, turbines and housing) are elaborated. Thereby the research question: “How do the costs of an offshore pumped hydropower storage facility on the Dogger Bank scale with the power and storage capacity, using existing construction technologies?” will be answered and reflected upon.

Regarding the technical characteristics and scaling it was found that:

- Constructing an inverse offshore pumped hydropower storage facility in the middle of the North Sea that can cope with the discussed failure mechanisms is possible.
- As the head difference between the reservoirs is increased the overall (not per metre) dam costs decline. This is characteristic for inverse offshore pumped hydropower.
- The optimum depth of the reservoir does not lie between 30 and 40 metres, but will rather approach 60 metres (enabled by the use of a grab dredger).
- A large storage reservoir is more economical compared to a smaller one from a civil costs perspective. Storage systems smaller than 10GWh should be avoided.
- In case the pumped hydro system is built in 20 metre deep water a storage capacity of 25GWh is preferred for the wind development plans in the North Sea. In case a storage system larger than 25GWh is desired the facility should gradually move to deeper waters to limit the amount of material that becomes available.
- The inverse storage plant is not limited to depths of maximally 20 metres, but more likely to 40 metres for reservoirs larger than 40GWh (afterwards the dam and armouring costs will counter all scale benefits).

Concerning the costs and benefits an alternative with a 25GWh reservoir and 2.65GW of installed power has been researched, which showed:

- The levelised cost of storage for various (economic) conditions is estimated to vary between 16.9 and 106.8€/MWh of which 40€/MWh appears most reasonable for an energy storage system connected to the North Sea countries and a large wind farm (~10GW).
- Due to technical uncertainties in the present soil conditions, equipment and design the LCOS of 40€/MWh may range from 68.2€/MWh to 19.0€/MWh in the relative worst and best case scenario.
- In the worst case scenario the offshore pumped hydropower variant is just as lucrative as a competitive conventional PHS plant (LCOS ranging from 60 – 130)
- In the best case the storage facility in the North Sea would truly enter territory unknown to any historical energy storage plant.
- The 40€/MWh would make offshore PHS 3 to 18 times less expensive than batteries or power to gas (both are currently under consideration to incorporate the large shares of wind energy from the North Sea).

- It is more beneficial to store energy and release it at a later time than letting the energy go to waste and just generate new fossil fuelled electricity instead. This is caused by the fact that the chosen facility has a lower storage costs than fossil fuel generating costs (40€/MWh versus 50 – 106€/MWh).
- The considered reservoir is expected to have a Net Present Value of 610 million euros, which could reasonably become 2.9 billion euros.
- The profitability of the project is sensitive to the energy prices and the interest rate.
- The economic value is largely determined by the electricity prices during the first 30 years of operation.

The whole research into energy storage was instigated by the plans for the development of a massive wind farm (>30GW) on the Dogger Bank via an artificially created island. The cost of the island, offshore wind farm and the interconnector cables were acquired simultaneously by Gerrits (2017). Therefore a scenario with and without storage could be developed. Although large uncertainties lay in especially the wind farm costs and revenues, it did show promising results: For a 30GW wind farm and all related costs the NPV ended up at minus 1.8 billion euros. By adding an adequate storage system (6GW of installed power) the value turned into a plus of 2.7 billion euros.

All signs and gathered results point in the same direction: the opportunities for offshore pumped hydropower storage are immense. There are first-mover advantages while largely relying on late-mover technology. In other words: operating such a large scale storage facility, without comparable competition (monopoly), could lead to large profits. While the research and development costs, which are usually exceptionally high for pioneering concepts, stay limited since almost all technology used has been long proven.

Though it is certainly helpful, the profitability of adding storage to a renewable energy powered economy is only of secondary importance. The main benefit lies in the fact that when energy storage is included the whole energy supply can become both sustainable and reliable. Without storage the energy supply will remain variable and will thus have to be supplemented by fossil fuelled generating units, which diminishes the overall sustainability.

This research presents the first viable offshore pumped hydropower storage facility that is undoubtedly lucrative, without relying on potential revenues or investments from other functions. Thereby it may offer a valuable link in the transition towards a green economy and within the development of large scale offshore wind energy in the North Sea.

In the following sections the general conclusions from the technical design of the four building blocks are stated. It should be noted that the scalars are certainly not limited to a single case on the Dogger Bank, rather they are universally applicable. With the stated design choices and relative costs components, combined with some engineering judgement, the given formulae and factors could easily be transposed to any other case.

10.1 Dam design

The design of the dam roughly consists out of three aspects: The outer protection against waves, the inner slope and the water retaining measure that is used to seal the underlying water conveying sand layer.

An Xbloc design was made for the sea defence, because of its ability to deal with extreme wave conditions, large dependence on locally sourced core material and a less-brittle failure mode than a caisson structure. It proved that for the whole dam the costs are for two-thirds shaped by the armouring against the severe wave environment. Therefore massive savings can be accomplished when the pumped storage plant would be located in calmer waters.

Due to the local geology and the bursting criteria, the maximum head difference would be 41.45m of which 40 metres was chosen as a practical limit. A large inner berm was added in order to deal with the combination of inner slope stability and the uplift/bursting mechanism at the inner toe. This mixture of forces led to an inner berm of 113m wide!

In order to operate the storage reservoir, the top sand layer has to be sealed. From the various techniques that can do so, the simple dredging and replacing the sand with firm clay option is favoured. The sand layer that lays between -43m and -50m relative to MSL will be replaced with the 'work with work' method for a costs of 11,825€/m.

From the seepage computations it appeared that, when choosing very conservative permeability characteristics, the leakage through the dam, retaining measure and underlying clay could all be neglected. The final design passed all the safety criteria that were considered. The dam costs including the sealing measure are estimated at 98,130€/m. This clay dam is able to resist a water level difference of 40m and waves of 8m.

10.2 Dredging process

In order to reuse the dredged clay directly in the core of the dam it was found that the clay has to be dredged mechanically. Hydraulic dredging would destroy the good qualities of clay and turn it into an impractical slurry. From the discussed two working methods it can be concluded that the achievable production rate is governing. The conventional grab dredgers and barges can only operate in calm waters, which would be an exception for the North Sea. By using a semi-submerged vessel for the dredging and a jack-up pontoon for the transport, the whole procedure becomes almost independent from the wave conditions.

In order to dredge the stiff glacial clay dedicated grabbers need to be made. These specialised grabbers are mounted on a semi-submersible vessel that is powered by a dynamic positioning system to maintain its location. The dredged material is then transported and placed via a conveyor belt system and over a specifically made jack-up pontoon. The investment costs of the grabbers (0.5 x 30m€) and the semi-sub (0.5 x 300m€) are shared with the creation of the Energy Island. The jack-up

platform (100m€) is solely used for the dam construction and will be fully paid for. These are all conservative assumptions, since the dredging equipment will definitely still have a rest value.

Based on the large price difference the innovative 'semi-sub & convey' construction process is the chosen alternative. It is a convenient paradox that due to the harsh working conditions on the North Sea eventually a very efficient dredging process was developed. The semi-submersible and jack-up platform optimally benefit from the unique occasion of having to transport such large volumes over a very short distance. In total 310 million euros are required to invest in dedicated dredging equipment to construct the dam. For a storage reservoir on the Dogger Bank with a 40m head difference the dredging unit price is 3.4€/m³.

10.3 Power generation

To limit the need for civil works a turbine was chosen that can both generate power and pump water back up. Since the Francis type is able to achieve slightly higher efficiencies than the Kaplan equivalent and the Francis one was recommended by all the previous studies in similar conditions, it is the preferred choice.

It was discovered that it is much more economical to install a few large turbines, instead of many small turbines. Hence, the largest pump-turbine (which is feasible today) and capable of converting a 700m³/s discharge into 265MW is the favoured choice at an estimated cost of 73.3 million euros per unit (excluding the additional costs for a stainless steel runner and cathodic protection). The discharges and dimensions are comparable to the two largest hydropower projects in the world: The Three Gorges Dam in China and the Itaipu Dam on the border of Brazil and Paraguay.

The effect of cavitation managed to have a drastic impact on the turbine design. To prevent disastrous under pressures in and around the turbines, the units need to be placed sufficiently far below the lower reservoir level. Since the installation depths for all turbine sizes were problematic, the largest turbine was chosen anyway. Although the civil works are more costly per turbine the number of required penstocks and tailraces decrease, leading to an overall saving.

In order to deal with the corrosive saline environment measures had to be taken. Experience from the Okinawa Yanbaru seawater PHS plant and various tidal energy plants proof that using a stainless steel runner, and cathodic protection for other steel parts is ample to deal with the harsh surroundings (Fujihara et al., 1998; Rijkswaterstaat et al., 1985).

10.4 Housing of turbines

The pump-turbines should be placed inside the future dam itself. When the powerhouse would be installed behind the dam, the longer penstocks would reduce the roundtrip efficiency by an extra 2.7%.

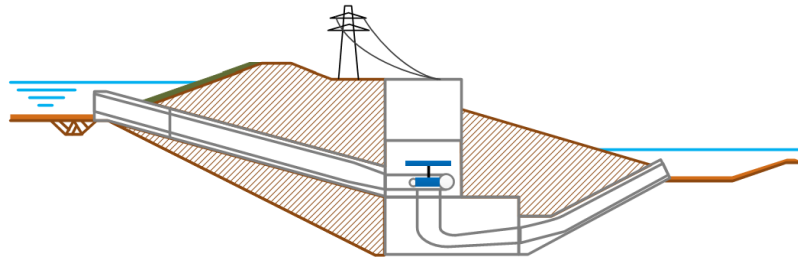


Figure 115: Design of the turbine housing constructed with modular caissons

Per turbine a single reinforced concrete penstock with a diameter of 13 metres was chosen, based on its minor losses and reasonable construction costs.

From the available construction methods, an excavation with modular box caissons is the mostly likely option to be able to construct the powerhouse till 90 metres below MSL. Three prefabricated box caissons are sequentially sunk and stacked upon each other. Afterwards the penstock and tailrace are connected and the dam can be built on top.

Connecting such large structures horizontally with Gina gaskets is common practise in immersed tunnelling projects. Vertically however a detail was developed to ensure sufficient compression of the rubber to seal the linkage. To prevent sliding or movement between the caissons a horizontal shear key will be necessary.

Although the individual caisson elements have not been designed up to great detail yet, the construction method together with the studied connections provide enough confidence to assume the turbine housing can indeed be realised.

Thereby the final link in the energy storage system has been analysed. With all four 'building blocks' feasible it can be concluded that installing and operating an inverse pumped hydropower plant in the North Sea is possible.

10.5 Scaling of an offshore pumped hydropower storage facility

In this section the main research question of how an offshore energy storage plant scales with its storage and power capacity is answered. The costs of the discussed energy storage plant are largely determined by:

- Armouring of the dam to cope with the wave conditions
- Sealing of the underlying sand layer
- Combination of inner slope stability and uplift of the inner toe
- Operational waves for dredging the stiff clay
- Preventive measures against cavitation for the turbine runners
- Construction method of the powerhouse
- High maintenance costs of the electrical and mechanical parts

The costs that are stated above were divided into two groups: storage capacity and power capacity. The storage capacity is created by the dredging of the inner reservoir, the subsequent construction of the dam and the water retaining measure (replacing the sand layer). The Francis pump-turbines and its necessary housing and in- and outlet system compose the power capacity.

For all involved civil works an operation and maintenance costs of 1% of the capital costs was used. Due to the corrosive environment 4% of the capital expenditure in electrical and mechanical parts was adopted.

When all costs are combined (except for planning and design costs) the expenditure scales as in Table 57.

Element	Capital costs (m€)	Operational and maintenance costs (m€/yr)
Dedicated equipment	310	-
Storage reservoir (E=GWh)	$10^3 * 0.7209 * E^{0.389}$	$10 * 0.7209 * E^{0.389}$ (= 1% of CAPEX)
Power generation (P=GW)	$10^3 * 0.8746 * P^{0.9118}$	$4 * 10 * 0.8746 * P^{0.9118}$ (= 4% of CAPEX)

Table 41: Total costs related to the creation and operation of an offshore pumped hydropower storage plant in the North Sea with a maximum head difference of 40 metres

From the obtained results it can be concluded that it is beneficial from a civil costs perspective to deploy a large energy storage system. Moreover it is advised to implement a storage capacity larger than 15GWh, since for smaller sizes the dam size is relatively large compared to the reservoir.

Furthermore one has to be aware that for the dredging costs the assumption was made that the material from the inner reservoir that is not needed for the dam construction, would be dredged and paid for by the creation of the 'Energy hub' and additional functions. This is a reasonable presumption for small to medium sized reservoirs (10 – 25GWh). However, for larger reservoirs it will become problematic to allocate the redundant material for other purposes. Consequently these bigger schemes might have to carry higher dredging costs or be located in deeper water.

Contrary to the storage capacity, the power generation scales almost perfectly linear. Therefore hardly any scale advantages are realisable, especially not when concerning the costs of capital.

To decide how large the storage and power capacity should be per case, extensive modelling is required. The profitability is largely determined by the (fluctuating) electricity prices. This research is expected to become available in 2018 through Witteveen+Bos.

11. Recommendations

The idea of Luc Lievense about artificially creating an energy storage reservoir has been laying on the shelf for nearly four decades. At the time wind energy did not develop as quickly as initially expected and the project lost interest. Nowadays offshore wind is being installed and planned on an unprecedented scale, making the business case for energy storage more lucrative than it has ever been before. Therefore the time to initiate the realisation of inverse pumped hydropower storage is now.

The performed research proves that energy storage can be a valuable contribution to the planned North Sea 'energy hub'. Although at first the location was planned at the Dogger Bank, Gerrits (2017) found that it may be more advantageous to commence the whole wind project further into Danish waters. Thereby the sensitive natural area of the Dogger Bank would be avoided. The obtained results show that the storage system is versatile and could even be constructed in deeper water (up to 40 metres). The sole restriction is the presence of an appropriate clay layer.

In order to attain more profound knowledge of the optimal dam design, best time of investment and required storage and power capacities, some recommendations are made. They are stated in the same order of: dam, dredging, turbines, housing and benefits.

Dam & reservoir

Most important to realise the offshore pumped hydropower storage facility is a detailed soil investigation. The presence and condition of the clay can determine whether the project is practically feasible. Slight differences in soil properties between the assumed and actual values can already result in large savings or additional expenses for the dam design.

Other failure modes like settlement (partially dealt with for the outer protection), collision by ships or drifting ice should be investigated. The drifting ice loads both from the North Sea as from the inner reservoir need to be quantified. The Dogger Bank sea water temperature varies from 5°C to 15°C (Eisma, 2006). Therefore only drifting ice may pose a threat.

From guidelines it was concluded that micro stability for embankments with a clay core does not pose a threat. However rapid drawdown of the water table in the inner reservoir should still be regarded.

The effect of infiltration on the phreatic line in the dam has to be analysed. A raised water table leads to lower effective soil stresses and thereby shear resistance.

The inner slope protection of the dam for during the construction phase is yet to be optimised. See §Slope protection during construction.

Possibly a crown wall against run-up may be advantageous. Adding a crown wall to limit the run-up and corresponding discharge over the crest might be more economical than a high dam (plus its larger inner berm required for the stability).

The dam closure operation needs special attention. No serious problems are expected since the tidal differences and flow velocities are relatively limited (compared to for example the Deltawerken in the Netherlands).

The unknown achievable depth together with an unconvincing history led to the fact that jet-grouting was set aside. After further research and a comprehensive reliability study, jet-grouting might become a potential candidate to seal an underlying sand layer.

Effects of an offshore energy storage facility and the in- and outflow on surrounding morphology. Similarly the occurrence of sedimentation or erosion of the inner reservoir needs studying. The sequential in- and outflow may cause the formation of gullies and channels in the reservoir bottom. In an extreme case this might affect the stability of the clay layer, which would result in a restriction of maintaining a minimum water level to reduce local flow velocities. Therefore it could lead to a reduction in effective storage capacity.

How the water quality in the inner reservoir is affected by (temporary) stagnation of the water table.

Dredging

The possibilities regarding the use of RES for dredging operations are recommended for future studies (using the neighbouring energy hub for the construction of the dam).

The influence the conveying transportation method and the dropping of clay above the water level have on the clay properties.

Turbines

It can be interesting to research the possibility of using a Kaplan pump-turbine. In case it can be positioned higher than the Francis alternative or the draft tube would not need to be as deep then it might be more competitive, since it requires less excavation and civil works. Alternatively the use of horizontally placed axis Francis turbines or inverted Francis turbine could reduce the necessary runner and draft tube depth. The extra costs that come with these options, due to smaller turbine sizes, can then be weighed against the reduced housing costs per turbine.

Housing of turbines

Better insight in turbine housing costs and the proposed construction method. A question that remains is whether it is possible to apply the same construction process for a deeper reservoir (~60m). In case there proofs to be a (practical) limit the statement of: “the largest achievable head difference is recommended” might have to be adjusted.

In order to achieve the desired lifetime of the pumped hydropower plant, the presence of sulphates and other chemicals in the clay or soil that can harm concrete should be investigated.

Benefits

The benefits of energy storage on both a societal and financial level need further understanding. Compared to electricity generating plants, storage provides other advantages like energy security or the integration of large shares of RES. Those assets are hard to quantify and monetise.

Energy price modelling is required to estimate the revenues and best time of commissioning. Thereby the expected peak in prices around 2025 – 2035 needs to be weighed against the larger fluctuations and spot prices around 2050 and afterwards.

Ultimately the contribution of other functions to the storage facility need studying like solar panels on the inner slope and berm, aquaculture and biomass inside the reservoir, natural areas, port and marina facilities, recreation and housing.

Bibliography

Abadal, A. M., Dornhelm, E., Elakel, M., Feys, C., & Naderi, N. (2017). *Energy hub in the North Sea*. TU Delft.

Alvarado-Ancieta, C. A. (2012). Kostenschätzung 2012 für die elektrische und mechanische Ausrüstung des Krafthauses in Wasserkraft- und Pumpspeicher-Projekten. *Wasserkraft & Energie*, 22-35.

Anastasopoulos, I., Gerolymos, N., Drosos, V., Kourkoulis, R., Georgarakos, T., & Gazetas, G. (2007). Nonlinear Response of Deep Immersed Tunnel to Strong Seismic Shaking. *Journal of Geotechnical and Geoenvironmental Engineering*, 133(9), 1067-1090. doi:10.1061/(asce)1090-0241(2007)133:9(1067)

Bakker, K. J. (2014, September). *Immersed tunnels* [PDF].

Barends, F. B.J., & Uffink, G. J.M. (2006). *Groundwater mechanics, flow and transport*.

Beurskens, J., De Haan, S., Bauer, P., & Dieleman, R. (2014). *Taiwan integrated energy storage island*. Alliander.

Bezuyen, K. G., Stive, M. J.F., Vaes, G. J.C., Vrijling, J. K., & Zitman, T. J. (2012). *Inleiding waterbouwkunde*. Delft, The Netherlands: TU Delft.

Börger, T., Hattam, C., Burdon, D., Atkins, J. P., & Austen, M. C. (2014). Valuing conservation benefits of an offshore marine protected area. *Ecological Economics*, 108, 229-241. doi:10.1016/j.ecolecon.2014.10.006

Boscardin, M., Patterson, C., Landis, M., Younan, J. C., & Aghjayan, D. (2006). Evaluation of permeability of containment slurry walls. In *GeoCongress 2006: Geotechnical Engineering in the Information Technology Age*. Atlanta, GA: American Society of Civil Engineers.

Bricker, J. (2016, June 1). *Pumped storage power* [PDF].

Burcharth, H. F., & Rietveld, C. F. W. (1987). Construction, Maintenance and Repair as Elements in Rubble Mound Breakwater Design. Paper presented at The 2nd international Conference on Coastal and Port Engineering In Developing Countries, Beijing, China.

CIRIA, CUR, CETMEF (2007). *The Rock Manual. The use of rock in hydraulic engineering* (2nd edition). C683, CIRIA, London

CIRIA. (2009). A guide to costs standards for dredging equipment. London, UK: Author.

Clerens, P. (2016). *An overview on energy storage - what are the prerequisites for its European integration?* EASE

Van Corven, T. A. W. (2015). *Construction of the new lock in Terneuzen using pneumatic caissons: A construction alternative to conventional construction methods* (Master's thesis, TU Delft, Delft, The Netherlands). Retrieved from <https://repository.tudelft.nl/islandora/object/uuid:5f203b83-fe87-4221-8912-1c9a1aa095ae/datastream/OBJ>

De Boer, W. W., Verheij, F. J., Moldovan, N., Van der Veen, W., Groeman, F., Schrijner, M., ... Zwemmer, D. (2007). *Energie-eiland, de haalbaarheid van drie verschillende opties van energieopslag voor Nederland*. KEMA Consulting/Lievense.

De Ingenieur. (2015). Lievense, de man van het opslagbekken. *De Ingenieur*. Retrieved from <https://www.deingenieur.nl/artikel/lievense-de-man-van-het-opslagbekken>

De Ingenieur. (2016, June 13). [Schematisation of North Sea (wind) infrastructure]. Retrieved from <https://www.deingenieur.nl/artikel/gigantisch-stopcontact-op-eiland-doggersbank>

De Joode, J., Özdemir, Ö., & Van Hout, M. (2014). *The market value of large scale electricity storage options* (ECN-E--14-042). ECN.

Delta Marine Consultants. (2014). *Guidelines for Xbloc concept designs*. Retrieved from <http://www.xbloc.com/downloads/brochures-and-drawings-and-videos/xbloc-design-guidelines/item556>

Delte Marine Consultants. (n.d.). Calculator | Armour Layer Design Tool for Xbloc® Breakwater Units. Retrieved from <http://www.xbloc.com/technical-information/calculator/item697>

Deutsche Energie-Agentur. (2017). *Power to gas*. Retrieved from <http://www.powertogas.info/power-to-gas/>

DNV GL. (2015). *Energy storage roadmap NL 2030*. KEMA

Dickson, G. (2017, June). European wind power. *Opening&keynotes*. Symposium conducted at WindDays, Amsterdam.

EASE. (2017). *Energy storage technologies*. Retrieved from <http://ease-storage.eu/energy-storage/technologies/>

Eisma, D. (2006). *Dredging in coastal waters*. London, UK: Taylor & Francis.

Energy Storage Association. (2017). *Compressed Air Energy Storage (CAES)*. Retrieved from <http://energystorage.org/compressed-air-energy-storage-caes>

EMU Ltd, SKM Enviros, RPS Energy, BTO, Anatec Ltd, Brown & May Marine Ltd, & Cork Ecology. (2011). *Dogger Bank zonal characterisation* (11/J/1/06/1761/1218). Forewind.

eStorage. (2015). *Overview of potential locations for new pumped storage plants in EU 15, Switzerland and Norway* (D4.2 Final Report).

European Commission. (2012). *Energy roadmap 2050*

European Commission. Directorate-General for Energy. (2016). *EU energy in figures: Statistical pocketbook*

European Power to Gas Platform. (2017). *Power to gas*. Retrieved from <http://www.europeanpowertogas.com/index>

Forewind. (2015). *The geology of Dogger Bank: Geological factsheet*.

Frölke, G. (2017). *Nature enhancing opportunities for coastal defences: Opportunity study for the Dogger Bank* (Master's thesis, TU Delft, Delft, The Netherlands).

Fujihara, T., Imano, H., & Oshima, K. (1998). *Development of pump turbine for seawater pumped-storage power plant* (5). Hitachi Review

Garg, A., Lay, C., & Füllmann, R. (2012). *Stored energy in sea: The feasibility of an underwater pumped hydro storage system [Powerpoint slides]*. Retrieved from <http://docplayer.net/8559477-Stensea-stored-energy-in-sea-the-feasibility-of-an-underwater-pumped-hydro-storage-system-dr-andreas-garg-christoph-lay-robert-fullmann.html>

Gerrits, S. B. J. (2017). *Feasibility study of the hub and spoke concept in the North Sea: Developing a site selection model to determine the optimal location* (Master's thesis, TU Delft, Delft, The Netherlands).

Gimeno-Gutiérrez, M., & Lacal-Aránz, R. (2013). *Assessment of the European potential for pumped hydropower energy storage: A GIS-based assessment of pumped hydropower storage potential*. Luxembourg: Publications Office of the European Union.

Heinberg, R., & Fridley, D. (2016). *Our renewable future: Laying the path for 100% clean energy*.

Himelic, J., & Novachek, F. (2011). *Sodium sulfur battery energy storage and its potential to enable further integration of wind (wind-to-battery project)* (Final Report). Retrieved from Xcel website: <https://www.xcelenergy.com/staticfiles/xcel-responsive/Energy%20Portfolio/Renewable%20Energy/Renewable%20Development%20Fund/rdf-completed-wind-projects-milestone-final-report.pdf>

Hydro Equipment Association. (2013). *Hydro equipment technology roadmap*. Retrieved from <http://www.thehea.org/roadmap>

Imre, E., Nagy, L., Lőrincz, J., Rahemi, N., Schanz, T., Singh, V., & Fityus, S. (2015). Some comments on the entropy-based criteria for piping. *Entropy*, 17(4), 2281-2303. doi:10.3390/e17042281

Intergovernmental Panel on Climate Change. (2013). *IPCC Fifth Assessment Report (AR5)*. Geneva: WMO, IPCC Secretariat.

International Energy Agency (IEA). (2014). *Technology roadmap: Energy storage*

International Energy Agency (IEA). (2016). *World Energy Outlook 2016*

International Partnership for Hydrogen and Fuel Cells in the Economy (IPHE). (2011). *Utsira wind power and hydrogen plant*. Retrieved from <http://www.statoil.com/en/NewsAndMedia/Multimedia/features/Pages/HydrogenSociety.aspx>

IRENA. (2017). *REthinking Energy: Accelerating the global energy transformation*. Abu Dhabi: International Renewable Energy Agency.

IRENA. (2013). *Renewable power generation costs in 2012: An overview*.

Kempener, R., & De Vivo, G. (2015). *Renewables and electricity storage. A technology roadmap for REmap 2030*. IRENA.

Kempton, W., & Tomić, J. (2005). Vehicle-to-grid power fundamentals: Calculating capacity and net revenue. *Power Sources*, 144, 268-279.

Kibrit, B. (2013). *Pumped hydropower storage in the Netherlands* (Master's thesis, TU Delft, Delft, The Netherlands). Retrieved from <http://repository.tudelft.nl/islandora/object/uuid%3A6f98d3d5-6454-4e20-af5e-5b8615dcaba0?collection=education>

Kvale, E. P. (2006). The origin of neap–spring tidal cycles. *Marine Geology*, 235(1-4), 5-18. doi:10.1016/j.margeo.2006.10.001

Lazard. (2015). *Lazard's levelized cost of storage analysis* (Version 1.0). Retrieved from <https://www.lazard.com/media/2391/lazards-levelized-cost-of-storage-analysis-10.pdf>

Letcher, T. M. (2016). Pumped hydroelectric storage. In *Storing energy: with special reference to renewable energy sources* (pp. 25-38).

Makhijani, A., Mills, C., & Ramana, M. V. (2012). *Renewable Minnesota: A technical and economic analysis of a 100% renewable energy-based electricity system for Minnesota*. Institute for Energy and Environmental Research.

Marence, M. (2016, May). *Powerhouse and M&E equipment* [PDF].

Marence, M. (2014). *Storage and hydropower: Exercise - turbine design* [PowerPoint slides].

Miller, J. (2013, January 29). *Typical U.S. power supply and demand load curves* [Graph]. Retrieved from http://www.theenergycollective.com/jemiller_ep/178096/expanded-wind-and-solar-power-increase-need-natural-gas

Ministerie van Economische Zaken. (2016). *Energieagenda: Naar een CO2-arme energievoorziening*.

Ministerie van Verkeer en Waterstaat. (2007). *Voorschrift Toetsen op Veiligheid Primaire Waterkeringen*. Den Haag: Author.

Nederlands Normalisatie-instituut. (2016). *NEN 9997-1 Geotechnisch ontwerp van constructies - Deel 1: Algemene regels*.

NIOZ, Deltares, IMARES, & Rijkswaterstaat. (2015). *De staat van de Noordzee*. Noordzeedagen.

Peeters, P. (2012). Integratie toetsing, inspectie en monitoring [Powerpoint slides]. Retrieved from <https://www.slideshare.net/Waterbouwkundiglaboratorium/eerste-stappen>

Peng, F., Wang, H., Tan, Y., Xu, Z., & Li, Y. (2011). Field Measurements and Finite-Element Method Simulation of a Tunnel Shaft Constructed by Pneumatic Caisson Method in Shanghai Soft Ground. *Journal of Geotechnical and Geoenvironmental Engineering*, 137(5), 516-524. doi:10.1061/(asce)gt.1943-5606.0000460

Pepers, R. (2011, October). Pneumatische caissons Noord-Zuidlijn Amsterdam. *KOersief*, 85, 16.

Pérez-Díaz, J.I., Cavazzini, G., Blázquez, F., Platero, C., Fraile-Ardanuy, J., Sánchez, J.A. and Chazarra, M. (2014). *Technological developments for pumped-hydro energy storage*, Technical Report, Mechanical Storage Subprogramme, Joint Programme on Energy Storage, European Energy Research Alliance

Posthumus, A., & Van der Vegte, H. (2017, June). WindStock: Haalbaarheid windmolens, energieopslag en zonnepanelen. *Windenergie en energieopslag: Een veel belovende kans*. Symposium conducted at WindDays, Amsterdam.

Rauwerda, A. (2017, June). A sustainable energy future will be hybridized. *R&D projects and required technical developments*. Symposium conducted at WindDays, Amsterdam.

Rahman, F., Rehman, S., & Abdul-Majeed, M. A. (2012). Overview of energy storage systems for storing electricity from renewable energy sources in Saudi Arabia. *Renewable and Sustainable Energy Reviews*, 16(1), 274-283. doi:10.1016/j.rser.2011.07.153

Rijkswaterstaat, Hollandsche Beton Groep NV, Ballast Nedam Groep NV, & Raadg. Ing. Bur. Lieveense. (1985). *Pomp accumulatie centrale Noordzeekust* (Hoofdrapportage fase 1).

Rudelle, G. (2016). *eStorage project update [Powerpoint slides]*. Retrieved from <http://www.estorage-project.eu/wp-content/uploads/2013/06/3-eStorage-WS4-2016-GE-Project-presentation.pdf>

San Martín, J. I., Zamora, I., San Martín, J. J., Aperribay, V., & Eguía, P. (2011). Energy storage technologies for electric applications. In *International conference on renewable energies and power quality (ICREPQ'11)*. Las Palmas de Gran Canaria, Spain: Author.

Schiereck, G. J. (2004). *Introduction to bed, bank and shore protection, Engineering the interface of soil and water*. Delft, The Netherlands: VSSD.

Simbolotti, G., & Kempener, R. (2012). *Electricity storage technology brief (E18)*. Retrieved from IRENA website: <http://www.irena.org/Publications>

Sündermann, J., & Pohlmann, T. (2011). A brief analysis of North Sea physics. *Oceanologia*, 53(3), 663-689. doi:10.5697/oc.53-3.663

Sumer, B. M., & Fredsøe, J. (2005). *The mechanics of scour in the marine environment*. Singapore: World Scientific.

SWECO Norge AS. (2012). *Cost base for hydropower plants*. Retrieved from Norwegian Water Resources and Energy Directorate website: <http://www.nve.no>

Timmer, H., & Van Zuijlen, E. (2017, June). Opening & Keynotes. Symposium conducted at WindDays, Amsterdam.

Trelleborg Ridderkerk BV. (n.d.). *Gina Gasket*. Retrieved from www.trelleborg.com/infrastructure

Uamusse, M. M., Aljaradin, M., & Persson, K. M. (2017). Micro-hydropower plant - Energy solution used in rural areas, Mozambique. *Sustainable Resources Management*, 1(1). doi:10.5281/zenodo.255257

- Ugarte, S., Larkin, J., Van der Ree, B., Swinkels, V., Voogt, M., Friedrichsen, N., ... Michaelis, J. (2015a). *Energy storage: Which market designs and regulatory incentives are needed?* Retrieved from European Parliament website: <http://www.europarl.europa.eu/studies>
- Ugarte, S., Larkin, J., Van der Ree, B., Swinkels, V., Voogt, M., Friedrichsen, N., ... Michaelis, J. (2015b). *At a glance. Energy storage: Which market designs and regulatory incentives are needed?* Retrieved from European Parliament website: <http://www.europarl.europa.eu/studies>
- Van den Bos, J. P. (2017a, March 10). *Breakwaters and closure dams: Breakwaters cross-sectional design* [PDF].
- Van den Bos, J. P. (2017b, March 17). *Breakwaters and closure dams: Constructability and project execution* [PDF].
- Van der Hage, R. (2017, June). Offshore grid roll out. *Trends in the offshore wind system*. Symposium conducted at WindDays, Amsterdam.
- Van der Meer, J. W. (2002). *Technical report wave run-up and wave overtopping at dikes*. Technical Advisory Committee on Flood Defence, The Netherlands.
- Van Duivendijk, J. (n.d.). *Water power engineering: Principles and characteristics* [PDF].
- Van 't Hoff, J., & Van der Kolff, A. N. (2012). *Hydraulic fill manual: For dredging and reclamation works* (1st edition). Boca Raton, FL: CRC Press/Balkema Taylor & Francis Group.
- Vandycke, S. (2002). Dredging stiff to very stiff clay in the Wielingen using the DRACULA system on a hopper dredger. *Terra et Aqua*, 89.
- Verhagen, H. J., D'Angremond, K., & Van Roode, F. (2012). *Breakwaters and closure dams* (Second edition). Delft, The Netherlands: VSSD.
- Waterpowermagazine. (2000, August 14). *Japanese pumped storage embraces the ocean waves*. Retrieved from <http://www.waterpowermagazine.com/features/featurejapanese-pumped-storage-embraces-the-ocean-waves/>
- World Energy Council (WEC). (2016a). *E-storage: Shifting from cost to value wind and solar applications*. Retrieved from <http://www.europeanpowertogas.com/documents>
- World Energy Council (WEC). (2016b). *Variable renewable energy sources integration in electricity systems: How to get it right*. Retrieved from www.worldenergy.org
- World Energy Council (WEC). (2016c). *World energy scenarios: The grand transition*. Retrieved from www.worldenergy.org
- Yamamoto, M., & Morooka, C. K. (2005). Dynamic positioning system of semi-submersible platform using fuzzy control. *Journal of the Brazilian Society of Mechanical Sciences and Engineering*, 27(4), 449-455. doi:10.1590/s1678-58782005000400014

List of figures

Figure 1: World primary energy consumption per fuel type from 1850 to 2014, based on data from BP, Statistical Review of World Energy (source: Heinberg & Fridley, 2016)	12
Figure 2: European Union 2020 objectives for renewable energy source (RES) shares in the energy mix (source: European Commission, 2016)	13
Figure 3: The renewable power capacity worldwide and its growth rate over the last years (source: Irena, 2017)	13
Figure 4: Typical power curve in the United States (source: Miller, 2013)	14
Figure 5: The hourly supply and demand of energy for Minnesota, USA, in a hypothetical 100% RES scenario during a week (Wed – Tue) in July, 2007. Note how energy storage and withdrawal levels the difference between the intermittent supply and the energy demand (source: Makhijani et al., 2012)	14
Figure 6: The loss of revenue according to network operators in Germany (Timmer & Van Zuijlen, 2017), mostly due to insufficient energy storage and grid capacity between the (enlarged) wind power generation in the north and the energy demand in the south (source: Dickson, 2017)	15
Figure 7: Flexibility options that can help absolving the differences in electric energy supply and demand (source: Posthumus & Van der Vegte, 2017)	15
Figure 8: The hypothetical location on the Dogger Bank of the energy hub with its interconnector cables indicated with the dashed lines (top) and an impression of the envisioned island by TenneT (bottom). The figure was modified from Van der Hage (2017) and Börger et al. (2014)	16
Figure 9: The existing storage technologies and their global share in energy storage (source: IRENA, 2017)	17
Figure 10: An artist impression of an inverse offshore pumped hydropower storage plant (source: De Boer et al., 2007)	18
Figure 11: Value of storage in the whole energy chain (source: Ugarte et al., 2015a)	22
Figure 12: Focus on energy storage per level	23
Figure 13: Decrease in gross annual energy consumption in million toe (source: European Commission, 2012)	24
Figure 14: Range of fuel shares in primary energy consumption (%) (source: European Commission, 2012)	25
Figure 15: Share of variable renewable energy generated (source: IEA, 2014)	25
Figure 16: Energy storage applications categorised by their power output, time of discharge and their location in the energy chain (source: IEA, 2014)	27
Figure 17: Schematisation of a PHS system (left) and the development of PHS in the EU (right) (source: Letcher, 2016 and Pérez-Díaz et al., 2014)	28
Figure 18: Pumped hydro storage facility Hohenwarte 2, Germany (source: Deutsche Energie-Agentur).....	28
Figure 19: The Okinawa Yanbaru seawater PHS plant in Japan (source: Fujihara et al., 1998)	30
Figure 20: Schematization of a CAES system (source: San Martín et al., 2011)	31
Figure 21: The McIntosh CAES plant in Alabama, USA (source: https://www.wired.com/2010/03/compressed-air-plants/)	32
Figure 22: Schematization of a classic battery (left) and a flow battery (right) (source: http://hyperphysics.phy-astr.gsu.edu/hbase/Chemical/electrochem.html)	33
Figure 23: The sodium-sulfur battery connected to the wind farm (source: Himelic & Novacheck, 2011)	34

Figure 24: V2G schematisation within a smart-grid (source: http://www.seminarreports.in/2013/05/vehide-to-grid.html)	35
Figure 25: Power to gas technology and possible applications (source: Deutsche Energie-Agentur) ..	36
Figure 26: Power to gas to power schematization (source: http://energy.sia-partners.com/enabling-integration-renewables-europes-energy-system).....	36
Figure 27: The wind power and hydrogen plant in Utsira, Norway (source: IPHE, 2011)	37
Figure 28: Maturity level of energy storage technologies (source: IEA, 2014)	38
Figure 29: Range of levelised cost of storage for various technologies (source: WEC, 2016a)	39
Figure 30: Levelised cost of storage for various technologies in combination with a wind farm (source: WEC, 2016a).....	40
Figure 31: Realisable potential per country (source: eStorage, 2015)	43
Figure 32: Relation between storage capacity and costs (left) and between power and costs (right) .	45
Figure 33: Costs breakdown (left) and linearized 'scaling' components (right) further explained in Appendix B.....	45
Figure 34: The stepwise design approach of the inverse offshore pumped hydropower facility	46
Figure 39: Failure tree of operation based on the functional requirements.....	48
Figure 40: Failure tree of the dam.....	49
Figure 41: Reservoir design with the parameters that are necessary as input. The numbers used for the parameters are given in Table 10. The maximum and minimum head depend on till what depth the reservoir is excavated.....	50
Figure 42: The relation between the storage capacity, average head difference and reservoir diameter	52
Figure 43: The volume balance depends on the relation between the initial water depth, the required dam size and the volume that needs to be excavated from the inner reservoir to attain the desired head difference	53
Figure 44: Design process of the dam.....	54
Figure 45: Cross section of outer dam protection. All measures are in metres. This is a preliminary design, a few adjustments where necessary to meet the macro stability criterion as explained in §4.3.4.1 Macro stability.....	55
Figure 46: Layout of a toe on a sandy seabed (source: Delta Marine Consultants, 2014).....	56
Figure 47: The inner side of the dam with the various slopes that are considered during the design phase	59
Figure 48: Probability density function of the wind speed at the Dogger Bank and near- and onshore for reference (source: Gerrits, 2017)	59
Figure 49: Nomogram valid for shallow and intermediate waters (source: Bezuyen et al., 2012)	60
Figure 50: Inner slope protection. All measures are in metres and relative to the reservoir bottom. .	62
Figure 51: Phreatic line through the dam according to the Dupuit method. Note that no infiltration from precipitation is taken into account. Due to the hard surface on the crest and the nature of the material used for the dam, infiltration is neglected.....	63
Figure 52: Possible measures that can be taken to 'close' the sand layer: 1) Slurry bentonite wall. 2) Sheet piles. 3) Jet grouting. 4) Replacement of sand layer.	64
Figure 53: The construction sequence of a jet-grouted wall (source: http://udc.com.vn/en).....	65
Figure 54: Slope stability of the trench to replace the sand layer. The critical sliding mechanism through the stiff clay and the sand has a safety factor of 1.08	66

Figure 55: The costs of the retaining measures as they progress over depth. The mean sea level is 20m above the bed level. The slurry bentonite wall is assumed to be installed from 3m above the sea level and have a maximum length of 60m. Therefore the maximum reachable depth of the SB wall is 37m.	67
Figure 56: Most occurring failure mechanisms for dikes (source: Peeters, 2012)	68
Figure 57: Schematisation of a slope stability analysis. The slices are in vertical force equilibrium. The resulting moments (M_1+M_2) and shear force along the circular failure plain are in moment equilibrium (source: Bezuyen et al., 2012).	70
Figure 58: The uplift mechanism that is caused by a water overpressure under the clay layer (source: Van 't Hoff & Van der Kolff, 2012)	70
Figure 59: Critical sliding plane for the outer slope. Under uniform top load of 100kN/m^2 and a maximally developed scour hole in front of the toe	71
Figure 60: The critical sliding mechanism for the inner slope. The continuous phreatic line at +20m (=MSL) is the water pressure in the bottom sand layer, which tries to uplift the thick clay layer. Without the large inner berm the slope would only have a safety factor of close to 1.0	72
Figure 61: The influence of the inner berm on the shear resistance. When there is no surcharge on the reservoir bottom there is almost no effective soil stress, the difference between the green and blue pressures (right). Hence the inner berm is added to create sufficient shear stress in the thick clay layer to prevent sliding failure (left).	72
Figure 62: The dam design that is checked safe from a macro stability perspective. Note that the inner berm solely consists out of material that remains untouched (it has not been dredged and deposited there like the rest of the dam). The continuous phreatic line at +20m (=MSL) is the water pressure in the bottom sand layer, which tries to uplift the thick clay layer. The other phreatic line reflects the water table for the other layers.	73
Figure 63: The type of micro-instability depends on the type of dike: a homogeneous clay dike poses no threat (1), a sand dike is susceptible to the washing out of material (2), a sand core with clay cover can cause excessive pressure on the (impermeable) clay layer and 'push' it off (3). (source: Ministerie van Verkeer en Waterstaat, 2007)	74
Figure 64: The development of piping for a river dike: Water level rises (a) ; Seepage initiates (b) ; Sand boil appears (c) ; Backward erosion (d-e) ; Failure (f) (source: Imre et al., 2015).....	75
Figure 65: Seepage through the dam (Q_d) and the underlying clay layer (Q_u) when the recharge of the aquifer (Q_A) is equal to the discharge through the clay layer ($Q_A = Q_u$).....	76
Figure 66: The difference in water pressure over an impermeable layer. To prevent bursting of the clay, the self-weight of the clay layer has to outbalance the difference in water pressure acting from underneath.	78
Figure 67: The level of the crest height, set to resist the various mechanisms of run-up, set-up, sea level rise and settlement (source: Van der Meer, 2012)	79
Figure 68: The dam design with the various materials that are used. The scales are in metres.....	80
Figure 69: The total costs of the dam and dredging works per storage capacity, with the original seabed 20 metres below MSL. Note the rapid decline in capital costs once the head difference between the reservoirs increases.....	80
Figure 70: The relation between costs and storage capacity for a maximum head difference of 40m and dam costs of $86.31\text{m}\text{€}/\text{km}$. The dashed line is the trend line of which the equation and reliability number (R^2) is given to easily approximate the costs.....	82

Figure 71: Schematic top view of the pumped hydropower reservoir. Note that the material, which is necessary for the dam construction can be dredged directly next to the future dam. The material in the centre is available for the island and additional functions..... 84

Figure 72: Suction dredgers: plain suction dredger (top left), cutter suction dredger (bottom left) and trailing suction hopper dredger (right) (source: Van 't Hoff & Van der Kolff, 2012) 84

Figure 73: Mechanical dredgers: backhoe dredger (top left), grab dredger (bottom left) and bucket dredger (right) (source: Van 't Hoff & Van der Kolff, 2012) 84

Figure 74: The formation of clay balls by pipeline transport (source: Van 't Hoff & Van der Kolff, 2012) 84

Figure 75: The largest grab dredger in the World: Goshu (200m³) used for a terminal reclamation project in Singapore (2016). It uses a counterweight system to reduce the energy consumption and simplify the hoisting mechanism (source: http://www.kk-kojimagumi.co.jp/english/news/excepteur_sint_occaecat_cupidatat_non.html)..... 85

Figure 76: A backhoe with a maximum dredging depth of 32m (left) (source: <http://www.jandenul.com/en/equipment/fleet/backhoe-dredger>) and a split hopper barge (middle and right) (source: Van den Bos, 2017b; <https://www.vanoord.com/activities/hopper-barge-and-pushbuster>)..... 85

Figure 77: An offshore wind turbine installation vessel performing its jack-up tests (top) and a working platform (bottom) (source: <http://www.ziton.eu/wp-content/uploads/WIND-SERVER-jacked-03-low-res.jpg>; <http://www.thinkdefence.co.uk/ship-to-shore-logistics/increment-2-pier/>)..... 86

Figure 78: A semi-submersible accommodation vessel for harsh environments (left). It can host 750 people on board and is powered by a dynamic positioning system (right). Ordered for 200 million USD (source: <http://worldmaritimeneews.com/archives/89220/cosco-nantong-secures-accommodation-vessel-order/>; Yamamoto & Morooka, 2005)..... 87

Figure 79: Schematisation of the dredging process using four grab dredgers, which are mounted on one semi-submersible vessel and a jack-up pontoon, both fitted with conveyor belts. The striped black lines indicate the extendable conveyor belts to adjust for movements of the semi-submersible platform and allow for flexibility 88

Figure 76: The dependence of the dredging capacity on the depth and the cycle time, with a 100% filling ratio of the bucket..... 89

Figure 81: The total dredging costs for a storage reservoir with a 40m maximum head difference and 5545m³/m of dam to be dredged. The grab & barge process is more competitive till 7.7GWh, afterwards the semi-sub & convey process is preferred 93

Figure 82: Silt screens directly attached to the grab dredgers. Note the difference in turbidity in- and outside the silts screens (source: <https://nippon.zaidan.info/seikabutsu/2000/00736/images/174-1.jpg>) 94

Figure 83: A one MWh battery storage container with 1.2MW of nominal power (source: <http://usiscored.com/?product=1-mwh-energy-storage-system&v=47e5dceea252>)..... 94

Figure 84: Schematisation of the powerhouse and in- and outlet works (top) and the application field of turbines (bottom) (source: i01.i.aliimg.com/img/pb/928/662/252/1275966164919_hz-fileserver3_2089574.jpg; Uamusse et al., 2017) 95

Figure 85: The parts that make a Francis turbine (left) and the general outlook (right) with the spiral case and draft tube (source: <https://i.piniimg.com/736x/ea/c0/13/eac0135d94321a5e6b480bd10df3af39--francis-turbine.jpg>; <http://www.learnengineering.org/2014/01/how-does-francis-turbine-work.html>)..... 96

Figure 86: Diagram of specific rotational speed (n_q) per turbine type for a given head (source: Marence, 2016)	97
Figure 87: Diagram for relative runner dimensions and speed coefficient (source: Marence, 2016) ..	98
Figure 88: Diagram for generator size estimations (source: Marence, 2014)	98
Figure 89: Design of the draft tube and tailrace of a Francis turbine (left) and an animation of water flowing through (right). Note that D_3 here is equal to the previously determined d_{2a} (source: Marence, 2016; https://www.slideshare.net/swargpatel283/draft-tube).....	99
Figure 90: The effect of cavitation on runner blades (source: http://authors.library.caltech.edu/25019/1/figs/fig604.jpg)	100
Figure 91: Diagram to determine (by extrapolation) Thoma's cavitation coefficient (left) and the vapour pressure head (right) (source: Marence, 2016)	100
Figure 92: Exemplary hydropower layouts: indoor powerhouse (left) and semi-outdoor powerhouse (right) (source: https://www.linkedin.com/pulse/power-plants-efficiency-capacity-utilization-factor-v-r-v ; http://www.jasonmunster.com/tag/hydroelectric/).....	102
Figure 93: Alternatives for the location of the powerhouse: behind the dam (top) and inside the dam (bottom)	102
Figure 94: Powerhouse of a Francis turbine. The draft tube has a significantly wider footprint than the powerhouse itself (source: Marence, 2016)	103
Figure 95: Schematization of a pneumatic caisson (source: http://www.caroldenney.com/concerti.htm)	104
Figure 96: The working chamber from a caisson. This caisson was sunk till 25m below NAP directly in front of the Amsterdam Central Station to construct the Noord-Zuidlijn (source: Pepers, 2011)	104
Figure 97: Schematization of an open caisson (source: https://www.slideshare.net/_Yasir_/underwater-construction-58501529)	105
Figure 98: The indicative construction process of the turbine housing using modular prefab elements	107
Figure 99: the hybrid construction process of the turbine housing. Step 1, 4, 5, 6 and 7 are the same as for the modular approach	108
Figure 100: The dredging costs of the trench required for the installation of the turbines. The dots on the line indicate a turbine.....	111
Figure 101: The dam costs per single element (left), where the items with the same colour outline are grouped together (right). The total costs of 86,307€/m are for a dam that is able to retain 40m of water level difference and handle 8m high waves.....	113
Figure 102: The costs of the retaining measures as they progress over depth. The mean sea level is 20m above the bed level. Based on the large costs difference and the flexibility the dredging alternative offers, this is the preferred technique	113
Figure 103: The total dredging costs for a storage reservoir with a 40m maximum head difference and 5545m ³ /m of dam to be dredged. The grab & barge process is more competitive till 7.7GWh, afterwards the semi-sub & convey process is preferred	114
Figure 104: Turbine costs per installed power capacity. Data obtained from Alvarado Ancieta (2012). 1 USD from 2012 corresponds to 0.819 Euro anno 2017.	115
Figure 105: Francis pump-turbine runner costs (source: Sweco et al., 2012). Price levels are from January 1 st 2010. Therefore 0.133 NOK from the diagram is equal to 1 Euro anno 2017.	116
Figure 106: Total electrical and mechanical costs per turbine size	116
Figure 107: The scaling of the turbine housing per installed power capacity.....	117

Figure 108: Maintenance strategies. Note the concaved shape of the optimal line (source: Burcharth & Rietveld, 1987)	118
Figure 109: The relation between dam and dredging costs and storage capacity for a maximum head difference of 40m and dam costs of 98.13m€/km.	119
Figure 110: The costs of the Francis pump turbines and all related electrical, mechanical and civil works. Note that the horizontal axis is divided according to the number of turbines (265MW each)	120
Figure 111: The LCOS for 2030 of the studied IOPHS compared to other storage techniques (WEC, 2016a) and relative to the LCOE of conventional fossil fuelled plants (50–106€/MWh) in OECD countries (http://costing.irena.org/media/4110/fig-esi-3.png). The orange line indicates the chosen alternative of 40€/MWh.....	123
Figure 112: The cash flow for different electricity prices and interest rates. From these scenarios the 'Standard' one is found most appropriate, with a payback period of 23 years. Note the refitting of the turbine equipment after 40 years	125
Figure 113: The increase in extreme electricity prices in the future for the EU-28 plus Norway and Switzerland (source: https://energybrainpool.com/en/trends-in-the-development-of-electricity-prices-eu-energy-outlook-2050/)	126
Figure 114: The business case of creating a giant offshore wind farm in the North Sea with or without energy storage. Note the negligible costs of the island itself and the reduction in interconnector cable costs in the storage alternative. The island, OWF and IC costs are discounted and obtained from Gerrits (2017)	127
Figure 115: The components that constitute the dam construction. Note that the core and water retaining measure originate from the dredging process	128
Figure 116: The upper and lower limits of the reservoir construction costs. The blue line indicates the maximum costs for an optimised design (=upper boundary x improved design).....	129
Figure 117: The range in CAPEX for the power capacity. Note that the large range is the result of a lack of information, not from technical risks!.....	130
Figure 118: The linearised scalars that were obtained from the case studies ('Literature') and the performed research ('Dogger Bank'). Note that the scalars for the Dogger Bank change for different storage and power capacities.	132
Figure 119: Design of the turbine housing constructed with modular caissons.....	139
Figure 120: Most favourable design for the Haringvliet location, using "wet" dikes (source: Rijkswaterstaat, 1985).....	162
Figure 121: Artist impression of the Energy island and its multifunctional purposes (source: De Boer et al., 2007)	164
Figure 122: Impression of the design of the waterpower plant (source: De Boer et al., 2007)	164
Figure 123: The old silt-depot: the Slufter (source: portofrotterdam.com).....	167
Figure 124: Cross-section of dam design for the Slufter.....	167
Figure 121: Artist impression of the multifunctional island by Reinout Prins (Source: Beurskens et al., 2014)	169
Figure 126: Impression of the various components belonging to an underground PHS facility (source: http://www.sogecom.nl/energy.html)	172
Figure 127: Concept of Stored Energy in Sea (source: http://forschung-energiespeicher.info/en/projektschau/gesamtliste/projekt-einzelansicht/95/Kugelpumpspeicher_unter_Wasser/)	174

Figure 128: Cross-section of concrete sphere (source: http://forschung-energiespeicher.info/en/projektschau/gesamtlste/projekt-einzelansicht/95/Kugelpumpspeicher_unter_Wasser/)	175
Figure 129: The 1:10 pilot being installed (source: https://www.energiesystemtechnik.iwes.fraunhofer.de/en/projekte/search/laufende/stensea.html)	175
Figure 130: Shares of total costs per component	176
Figure 131: Scalars of linearised costs per component of a PHS facility.....	177
Figure 132: Sea level rise in the North Sea (mm/year). Local differences can be explained by storm surges, sensitivity to water set-up and subsidence of the land. From this figure a sea level rise of 3mm/year is assumed for the Dogger Bank (source: NIOZ et al., 2015).	179
Figure 133: Storm surge levels in the North Sea (cm) obtained via a schematic storm with a constant northerly wind of 23.2m/s and real bathymetry (Sündemann & Pohlmann, 2011). For the Dogger Bank a storm surge of 1.2 – 1.4m will be taken into account.....	179
Figure 134: Illustration of the amphidromic points in the North Sea. The Co-range lines indicate lines of equal tidal range (high water level is thus in the order of half the range!). The outline of the Dogger Bank is depicted in red and the Dutch part of the bank has a blue perimeter. The figure was modified from Börger et al. (2014) and Kvale (2006).	179
Figure 135: Extreme value analysis on the wave return period (source: Frölke, 2017)	180
Figure 38: Soil profile taken from Dutch part of the Dogger Bank. Leem = mud/loam, Klei = clay, Zand fijne categorie = fine sand category, Zand grove categorie = coarse sand category. Coordinates: 530958, 6172188 (source: https://www.dinoloket.nl/ondergrondgegevens).....	181
Figure 136: The outer slope stability with a quarry run toe foundation. The safety factor is 1.18. Note that the length of the critical slip surface through the quarry run is minimal since it causes a lot of friction.....	183
Figure 137: The outer slope stability with a stiff clay toe foundation. The safety factor is 1.11.	183
Figure 138: The outer slope protection with a weak muck layer underneath the toe structure. The resulting safety factor is 0.78.....	184
Figure 139: The outer slope protection with the existing seabed replaced with dredged material. The safety factor is 1.09.....	184
Figure 140: Seepage through the dam (Q_d) and the underlying day layer (Q_u) in case the aquifer is barely recharged through the surrounding environment ($Q_A < Q_u$).....	185
Figure 141: Potential head in a semi-confined aquifer. Note the influence that the leakage factor λ has on how quick the head decreases towards the centre of the reservoir (source: Barends & Uffink, 2006).	187
Figure 142: The process of how the soil parameters eventually affect the (savings on) dam length. See Figure 143 for the quantitative relation between the leakage factor and savings.	188
Figure 143: The green line indicates the relation between the leakage factor and achievable depth of the reservoir, which ultimately determines the potential savings in the dam circumference (in comparison with scenario 4, with 40m water pressure under the whole reservoir , 20GWh storage capacity and dam costs of 136.88m€/km). The black striped line shows the trend of the relation between the soil characteristics and savings on the dam length. The R^2 value shows the level of reliability of the given ‘Savings’ approximation (the maximum R^2 is 1, therefore the given formula is very accurate).....	189

Figure 144: The stability of the clay layer against bursting for an infinitely long strip. Note that this is a conservative assumption, since the cohesive forces will also act along the ‘ δx ’ sides..... 190

Figure 145: The vertical stability of the clay layer. The x-axis depicts the distance from where the inner dam slope intersects with the reservoir bottom ($x=0$) till 300m towards the centre of the basin. The equilibrium of forces is computed for an infinitely long strip and a conservative leakage length of 5000m. The blue line reflects the maximum achievable depth. The red line portrays the chosen excavation depth..... 190

Figure 146: Construction sequence of a breakwater. The process for the dam construction will be mostly similar, except for the core construction and lack of a crown element and heavy inner protection (source: Van den Bos, 2017b) 191

Figure 147: The serial construction process of the dam in the longitudinal direction. First the core has to be placed, when after the under layers and final armour layer can be positioned (source: Van den Bos, 2017b) 192

Figure 148: Alternatives for the location of the powerhouse: behind the dam (top) and inside the dam (bottom)..... 193

Figure 149: Head loss through penstocks for different scenarios..... 194

Figure 150: Head loss for a short and long single penstock with a 700m³/s discharge 196

Figure 151: The procedure of connecting two immersed tunnel units explained above and a detail of the connection below (source: Trelleborg Ridderkerk BV, n.d. ; https://www.researchgate.net/figure/234044892_fig5_Fig-5-Aseismic-design-of-the-immersed-section-of-the-proposed-railway-link)..... 197

Figure 152: Geometric and deformation characteristics of existing Gina gaskets (Type-A) and projected profiles (Type-B). Both have been tested and verified on half-scale tests (source: Anastasopoulos et al., 2007) 198

Figure 153: The vertical connection between the box caissons. Instead of the whole top structure weighing down on the Gina gaskets, a small recess in the top caisson ensures a watertight seal while the downward forces are simply transmitted via the concrete structure 199

List of tables

Table 1: Total costs of an offshore pumped hydropower storage plant in the North Sea with a maximum head difference of 40 metres. The operational cost of the dredging equipment is included in the storage capacity	VI
Table 2: PHS characteristics	29
Table 3: CAES characteristics	32
Table 4: Characteristics for classic and flow batteries combined	33
Table 5: Characteristics of a power to gas energy storage system	37
Table 6: Generalised characteristics of energy storage technologies	38
Table 7: Selection criteria used by the GIS-model to recognise potential PHS sites.....	42
Table 8: Results obtained by the eStorage study	42
Table 9: Soil stratification and characteristics per layer according to NEN 9997	47
Table 10: Parametric values used for the dam dimensions and storage capacity computations.....	51
Table 11: Dimensions and storage capacities for the various scenarios.....	52
Table 12: The characteristics of the three volume balance scenarios. Note that the numbers relate to a storage reservoir with a maximum head difference of 40m and 20GWh storage capacity (Scenario 4). The dam and dredging volumes are indicative and may change slightly according to the choice of slopes and crest width.....	53
Table 13: Governing situations per failure mechanism. The high and low water levels on the North Sea are respectively $\pm 1.5\text{m}$ from still water level (Kvale et al., 2006). A full inner reservoir corresponds to H_{\min} level of Table 11	69
Table 14: Safety factors of soil parameters for overall stability by NEN9997	69
Table 15: Material properties (design values) of the elements which are used.....	69
Table 16: The influence of the material from the toe/dam foundation layer on the slope stability....	71
Table 17: The loss of head due to leakage. Note that the seepage through the dam and bottom are converted into a head loss per day. The water level in the inner reservoir is its average operational level.....	77
Table 18: Scaling formulae to determine the total dam costs for a given head difference, with the dam to be constructed in 20m deep water	82
Table 19: Maximum displacements of a semi-submersible platform powered by a DPS during various wave conditions. Results obtained by Yamamoto & Morooka (2005)	87
Table 20: Grab dredger production and the cycle time for transport by a split hopper barge. Note the low workability, due to the exposed environment	89
Table 21: Costs of 'grab & barge' process. The OPEX include depreciation, interest, maintenance, repairs, fuel, personnel and all other operating costs. The other half of the investments costs of the grab dredgers are carried by the 'energy hub' project.	90
Table 22: Unit price for grab & barge process. The 'constructed' unit price includes all project related costs like site investigation, monitoring, design, profit, uncertainty and risk. This in combination with the capital costs can be used to determine the overall dredging costs. The bottom unit price is an example of where the CAPEX is already included for a 20GWh storage system with a 40m head difference.....	90
Table 23: Production capacity of a single grab installed on the semi-sub.....	91
Table 24: Characteristics of the main equipment involved in the semi-sub & convey process	91
Table 25: Operational and capital costs concerning the semi-sub & convey process.....	92

Table 26: Unit price for semi-sub & convey process. The 'constructed' unit price includes all project related costs like site investigation, monitoring, design, profit, uncertainty and risk. This in combination with the capital costs can be used to determine the overall dredging costs. The bottom unit price is an example of where the CAPEX is already included for a 20GWh storage system with a 40m head difference.....	92
Table 27: The capital and operational costs of the two reviewed dredging processes.....	93
Table 28: Characteristics of the two largest hydropower projects in the world (source: https://en.wikipedia.org/wiki/List_of_largest_hydroelectric_power_stations)	96
Table 29: Pump-turbine efficiencies (source: Hydro Equipment Association, 2013; Bricker, 2016)	96
Table 30: Runner and generator diameters for a 40m head difference and specified discharge	99
Table 31: Dimensions of the main parts of the Francis pump-turbines to be used for the design of the turbine housing. All measures have been verified with the UNESCO-IHE HydroPower design tool and are equal to the centimetre.....	100
Table 32: Volume and material characteristics of modular box caissons	110
Table 33: Dam costs. The dredged volume includes 10% extra to cope with future settlements (Bezuyen et al., 2012) and 5% spillage of clay during the dredging process. Dredging costs are for an average depth of 30 metres and without capital investments in dedicated equipment.	112
Table 34: The capital and operational costs of the two reviewed dredging processes.....	114
Table 35: Total electrical and mechanical costs for two turbine sizes	116
Table 36: Total costs related to the creation and operation of an offshore pumped hydropower storage plant in the North Sea.....	120
Table 37: LCOS for all scenarios (with a 40m head difference, 8m waves and constructed in 20m deep water). The 'Refurbished E&M' and the 'Realistic' scenario contain a refitting of E&M equipment after 40 years. The storage facility is assumed to be operational 95% of the time. Note the large impact of the WACC, energy production, grid deferral and scale of the facility.	122
Table 38: Characteristics of the five considered economic models	125
Table 39: The upper and lower boundary of the costs to create a certain storage capacity. Note that differences in construction or material costs are not incorporated and neither is the planning.....	129
Table 40: The uncertainty in various aspects of the construction and maintenance works lead to a most costly and most beneficial case realistically conceivable. All three scenarios are based on the chosen variant of 25GWh and 2.65GW from §8.7 Levelised cost of storage in which the amount of installed power defers an equal quantity in grid investments that is extracted from the CAPEX. The 'Maximum' cost is based on the upper boundary cost with an optimised design (blue line Figure 116).	131
Table 41: Total costs related to the creation and operation of an offshore pumped hydropower storage plant in the North Sea with a maximum head difference of 40 metres	140
Table 42: Characteristics of Haringvliet design	163
Table 43: Costs of Haringvliet pumped accumulation plant.....	163
Table 44: Characteristics energy islands	165
Table 45: Costs and benefits of both energy storage islands	165
Table 46: Benefits for the various storage options after 40 years (source: adapted from De Boer et al., 2007)	166
Table 47: Characteristics of energy storage system the Slufter.....	168
Table 48: Costs and benefits of the Slufter.....	168
Table 49: TIESI reservoir characteristics.....	170

Table 50: TIESI costs and benefits	170
Table 51: Characteristics of an underground pumped hydro storage facility	173
Table 52: Characteristics of a single sphere placed at a depth of 700m.....	174
Table 53: Target costs of STENSEA	175
Table 54: Energy storage island properties and costs. Note that all costs are discounted to 2015 values with http://www.iisg.nl/hpw/calculate-nl.php	176
Table 55: Dogger Bank conditions and properties (source: EMU Ltd et al., 2011). Directional mean wave heights, to be used as operational waves, are obtained from Frölke (2017) and tidal elevations from Abadal et al. (2017)	178
Table 56: Risk levels for a pumped hydropower plant in the Netherlands (source: Rijkswaterstaat et al., 1985)	182
Table 57: The influence of the material from the toe foundation layer on the slope stability	184
Table 58: The loss of head due to leakage. Note that the seepage through the dam and bottom are converted into a head loss per day. The potential head at the centre is basically the ‘pressure’ that remains from the water level difference.....	186
Table 59: The impact of the soil characteristics on the achievable depth of the reservoir and respective savings on the necessary dam circumference. Note that the ranges of soil parameters are all fully possible (only the clay is assumed to be homogeneously 35m thick). The potential head is the additional water pressure acting upon the clay layer at the inner toe (most critical point), resulting from a water level difference of 40m. The values between brackets indicate the potential head when the reservoir would be excavated till the maximum depth. The maximum reservoir depth is equal to the achievable water level difference between the North Sea and the inner reservoir (with a safety factor for bursting of 1). The savings on dam length refer to the dam costs of scenario 4, with 40m water pressure under the whole reservoir, 20GWh storage capacity and dam costs of 136.88m€/km.	188
Table 60: Head loss through the 400.4m long double penstock with 350m ³ /s per penstock.....	195
Table 61: Head loss through the 400.4m long single penstock with 700m ³ /s per penstock.....	195
Table 62: Head loss through the 160.4m long double penstock with 350m ³ /s per penstock.....	195
Table 63: Head loss through the 160.4m long single penstock with 700m ³ /s per penstock.....	195

Appendices

Appendix A: Options to help integrating intermittent renewables

Appendix B: Alternative pumped hydropower storage systems

Appendix C: Scalars of energy storage islands

Appendix D: Dogger Bank conditions

Appendix E: Risks associated to inverse offshore pumped hydro storage

Appendix F: Influence of toe material on slope stability

Appendix G: Seepage and bursting mechanism for a closed aquifer

Appendix H: Construction method of the dam

Appendix I: Location of the powerhouse and penstock design

Appendix J: Connecting box caissons with Gina gaskets

Appendix A: Options to help integrating intermittent renewables

An overview of the five possible options to deal with the intermittency of variable RES:

Flexibility options	Purpose	Example	Strength	Limitation	Costs, CAPEX (€)
1. Flexible power	Generate power exactly according to the demand	Start a gas, hydro or coal fired power plant when demand outweighs supply	+ Some infrastructure is already in place, since this is the conventional method	- Relies mostly on fossil fuel power plants - The surplus of RES is wasted	For a CCGT ²² : 500€/kW
2. Demand side management	Adjust the energy demand to the supply	Charging of electric vehicles in times of an energy abundance	+ Reduces the need for flexible power, energy storage and grid expansion	- Effect still unproven - Limited potential in mobility and industry sectors	Unknown
3. Energy storage	Store energy when supply exceeds demand and release when required	Stock energy when it is windy/sunny and release when there is no wind/sun	+ Energy reliability and security + Allows high RES shares in the grid + Deferral of grid extension	- High capital investment - Largely unknown revenue streams	600 – 1400 €/kW
4. Supergrids/ interconnector	Connect regions/countries with different energy demands and supplies	Link 'sunny' Southern Europe with 'windy' Northwest Europe	+ Avoid energy wastage + Reduces peak energy prices	- Does not work when 'neighbours' rely on the same RES - Requires double energy generation capacity	For 700 MW: 2,000,000 €/km
5. Do nothing	Accept irreversible climate change	Do not fully commit to RES and stick with fossil fuel	+ Most infrastructure is in place	- Global tensions - Giant curtailment of RES	Curtailment Germany ²³ in 2016: 1.0 bn€ Possible curtailment EU-27 in 2050 ²⁴ : 20 bn€/yr

²² The Combined Cycle Gas Turbine (CCGT) is a conventional peak power plant, which can be quickly ramped up and -down. The lifetime however is only 20-30 years. Furthermore, a CCGT plant carries high operational costs (fuel consumption) and emits 670 kton more CO₂ annually than a 20 GWh offshore pumped hydro storage facility (De Boer et al., 2007).

²³ According to German network operators (Dickson, 2017).

²⁴ Projections from the European Commission for when extensive Pan-European grid investments are not placed in coherence with the growing RES share (e-Highway2050, 2013).

Appendix B: Alternative pumped hydropower storage systems

Unfortunately not all economic regions are located near a mountainous area, which allows for PHS facilities that can ensure a reliable energy supply. In this section PHS alternatives are explored that utilise man-made or underground reservoirs to 'artificially' create the required hydraulic head difference that enables power generation. At first, four case studies that construct one reservoir themselves and employ the sea as the other reservoir are reviewed. Secondly, an alternative using underground cavities is discussed. Ultimately, an option that stores energy below the sea surface is presented.

B.1 Plan Lievense

All information on this case study is gathered from: Rijkswaterstaat, Hollandsche Beton Groep NV, Ballast Nedam Groep NV, & Raadg. Ing. Bur. Lievense. (1985). *Pomp accumulatie centrale Noordzeekust* (Hoofdrapportage fase 1).

Motivation

Multiple designs for various locations have been made by the founding father of the pumped accumulation reservoir Luc Lievense and his engineering company. Lievense launched his idea of a pumped accumulation plant for the Netherlands in 1979. In a response to the prior oil boycott from the Middle-East and resistance against nuclear energy, the energy storage system would reduce the dependency on foreign policies and help integrating renewable energy into the grid.

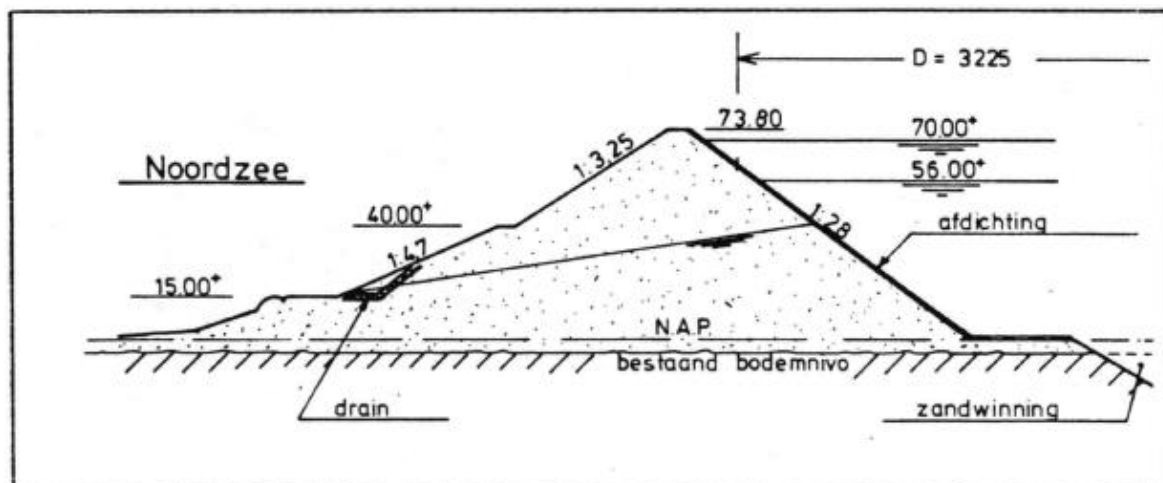


Figure 116: Most favourable design for the Haringvliet location, using "wet" dikes (source: Rijkswaterstaat, 1985)

Design

The original idea was made up of a 100km long and 14m high ring-dike in the Markermeer. The dike would host four to five hundred wind turbines and contain four waterpower stations (De Ingenieur, 2015). Due to opposition regarding the large investment, environmental impact and potential flood risk other locations were sought for. In the Hoofdrapportage fase 1 three sites are reviewed; Haaksgronden (near Texel), Haringvliet and Brouwersdam, all with a storage capacity of 20 GWh and for different levels of high and low water (100 - 78.9, 70 - 56 and 40 - 35 respectively) and either "wet" or "dry" dikes. Although the '70 - 56' alternative for the Haringvliet and the '70 - 56' or '40 - 35' variants for the Brouwersdam differ slightly in capital costs, only the '70 - 56' option at the Haringvliet (see Figure 116) is worked out here, since it represents the lowest investment.

The reservoir has a circular shape, since this has the most optimal capacity versus circumference ratio. A variation of 1.25 between high and low water is maintained to enable optimal performance from the Francis turbines. From the optimal failure probabilities; economic $3 \cdot 10^{-3}/\text{yr.}$, personal $10^{-4}/\text{yr.}$ and societal $10^{-3}/\text{yr.}$, the normative personal acceptable risk level was used for the design. The in-outlet works for a discharge of 3000 – 7000 m³/s would need to be 500m wide and 10m deep. For all scenario's the turbine clusters would be placed outside the dike, 'sheltered' from the dominant storm direction and disembogue in a deep (old) flow channel. Sixty percent of the sand necessary to construct the dikes could be sourced from within the reservoir. The ring-dike itself would have an impermeable layer on the inner-slope that continues for only a bit on the reservoir bottom, resulting in a high phreatic line in the dike. Under normal operation 20cm of water would be lost daily, due to seepage.

	Unit	Quantity
Storage capacity	GWh	20
Power output	GW	2.0 (2.9 pumping power)
Surface area reservoir	km ²	11.95
Head range	m	70 – 56
Turbines (Francis)	MW	15 * 134
Roundtrip efficiency	%	80

Table 42: Characteristics of Haringvliet design

Costs & benefits

Costs are given in the original Dutch guilders and discounted to their 2015 value in euros (by the Internationaal instituut voor sociale geschiedenis, <http://www.iisg.nl/hpw/calculate-nl.php>). No data on the operation and maintenance were reported, nor were the benefits. The costs for the Haringvliet project are given in Table 43.

	Costs (mfl. / m€)
Dredging & dam construction	1473 / 1,160
Housing of pumps etc.	1,202 / 946
Pumps, generators etc.	1,401 / 1,103
HV cable + grid connection	200 / 157
Total capital costs	4,276 / 3,367

Table 43: Costs of Haringvliet pumped accumulation plant

Why is it not constructed?

During the years that the feasibility of an artificial PHS facility for the Netherlands was analysed, the wind energy technology did not develop as quickly as initially expected. Additionally, the electric infrastructure could handle a far greater share of wind energy than was first thought (20%), reducing the need for storage. Ultimately the discussion moved towards nuclear energy and interest in PHS was lost.

B.2 Energy Island

The information presented in this case study is retrieved from: De Boer, W. W., Verheij, F. J., Moldovan, N., Van der Veen, W., Groeman, F., Schrijner, M., ... Zwemmer, D. (2007). *Energie-eiland, de haalbaarheid van drie verschillende opties van energieopslag voor Nederland*. KEMA Consulting/Lievensse.

Motivation

In this comprehensive study three alternatives of providing storage are reviewed; an energy island with interior reservoir that acts as a reversed pumped hydro storage plant (Figure 117), a compressed air energy storage option and a second interconnector cable between the Netherlands and Norway. The study was performed to find the measure that could best be implemented to deal with the



Figure 117: Artist impression of the Energy island and its multifunctional purposes (source: De Boer et al., 2007)

increasing amount of fluctuating power supply generated by wind farms. The 'Energy Island' was found particularly interesting, because the benefits are not confined to the energy sector, but could also support other functions.

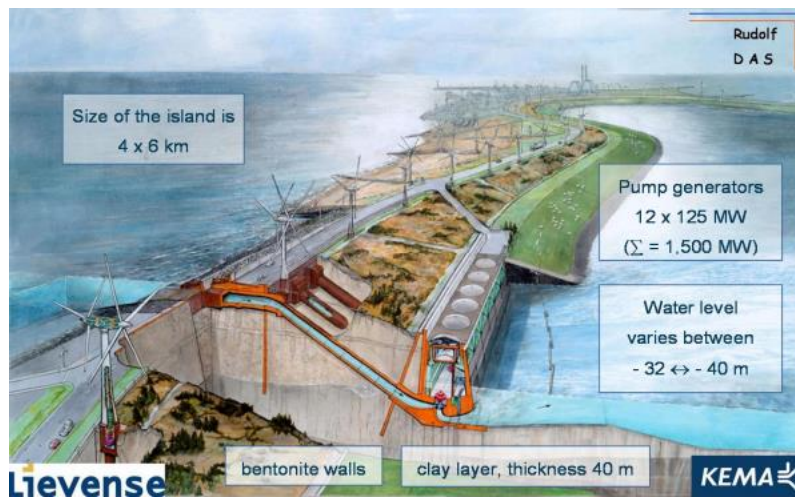


Figure 118: Impression of the design of the waterpower plant (source: De Boer et al., 2007)

Design

For the island two alternatives are worked out, of which one has 50% more capacity. The larger variant proves to be more ideal from a constructability perspective, where the smaller one is preferred based on its economic value. Since this is expected to offer an interesting insight in the cost/benefit relation, both alternatives are analysed.

No detailed technical design was made. To limit seepage into the inner reservoir the island should be constructed on top of a thick clay layer. Together with bentonite walls in the surrounding dam that reach into the clay layer, a near impermeable ‘tub’ will be created. The technical characteristics of the two island variants are given in Table 44.

	Unit	Energy Island 1	Energy Island 2
Storage capacity	GWh	20	30
Power output	GW	1.5	2.25
Surface area reservoir	km ²	40	60
Head range (below sea level)	m	32 – 40	32 - 40
Turbines (Francis)	MW	12 * 125	18 * 125
Roundtrip efficiency	%	80	80

Table 44: Characteristics energy islands

Costs & benefits

The benefits are dependent on either a high or a low fossil fuel price scenario, where a higher fossil fuel price will result in higher benefits for energy storage. For computing the benefits, the existence of 6 GW offshore (scenario G20) and 3 GW onshore are taken into account (a higher wind penetration will lead to larger fluctuating energy prices and thus to higher benefits for energy storage solutions). The costs and benefits are shown in Table 45.

	Costs Island 1 (m€)	Benefits Island 1 (m€/yr.)	Costs Island 2 (m€)	Benefits Island 2 (m€/yr.)
Dredging	650		800	
Building pit and bentonite walls	150		200	
Housing of pumps etc.	900		1300	
Pumps, generators etc.	500		850	
HV cable + grid connection	250		250	
Total capital costs	2,450		3,400	
Total annual benefits (by a LCC-analysis)		77 – 130		74 - 126

Table 45: Costs and benefits of both energy storage islands

Construction time for both islands would be around six years. The lifetime of the island is in the order of 80 years, in the computations however a lifetime of 40 years is used, so the comparison with the other storage alternatives can be made.

Benefit of storage system compared to conventional peak power (CCGT) plant (discounted over 40yr.)	Low fossil fuel price scenario, including dredging costs (m€)	High fossil fuel price scenario, excluding dredging costs (m€)
CAES	+1,300	+1,300
Energy Island 1 (20GWh)	+0.0	+800
Energy Island 2 (30GWh)	-400	+300
NorNed 2 nd interconnector	+900	+1300

Table 46: Benefits for the various storage options after 40 years (source: adapted from De Boer et al., 2007)

In Table 46 the ‘benefits’ are compared to a conventional peak-power plant. Note the large impact a higher gas-coal price would have on the indicative benefits for the pumped hydro storage systems. In case the dredging costs would be paid by adding other functions to the island, the **payback period would be 17 years** in the high fossil fuel price scenario for the smaller variant. When no other revenue creating assets contribute to the island and with the low fossil fuel price scenario, the **payback period would be 40 years**.

Why is it not constructed?

Even though there did not seem to be a technical or environmental showstopper, no actions have been taken to realise the project. The lack of commitment can most likely be subscribed to the absence of an urgent need for energy storage capacity.

B.3 Slufter

All information for this case study is obtained from: Kibrit, B. (2013). *Pumped hydropower storage in the Netherlands* (Master's thesis, TU Delft, Delft, The Netherlands). Retrieved from <http://repository.tudelft.nl/islandora/object/uuid%3A6f98d3d5-6454-4e20-af5e-5b8615dcaba0?collection=education>

Motivation

With Europe moving towards a sustainable energy supply, relying on renewable energy sources, the issues regarding intermittency are only increasing. Currently peak-power is delivered by fossil-fuelled gas turbines. These two practises, together with the available Slufter (a silt-depot that lost its purpose, see Figure 119), offered a chance to investigate if the old depot could be repurposed as a



Figure 119: The old silt-depot: the Slufter (source: portofrotterdam.com)

PHS facility.

Design

The present dams of +23m NAP are raised, by using the subsided (contaminated) silt from the depot, to a level of +40m NAP. By placing filters at both sides of the low-permeable silty-core during construction, polluted particles are prevented from flowing into the sea. The sand necessary for the remaining part of the dam is dredged from neighbouring areas. The PHS plant could satisfy all peak-balancing needs of Zuid-Holland, Zeeland and a major share of North-Holland.

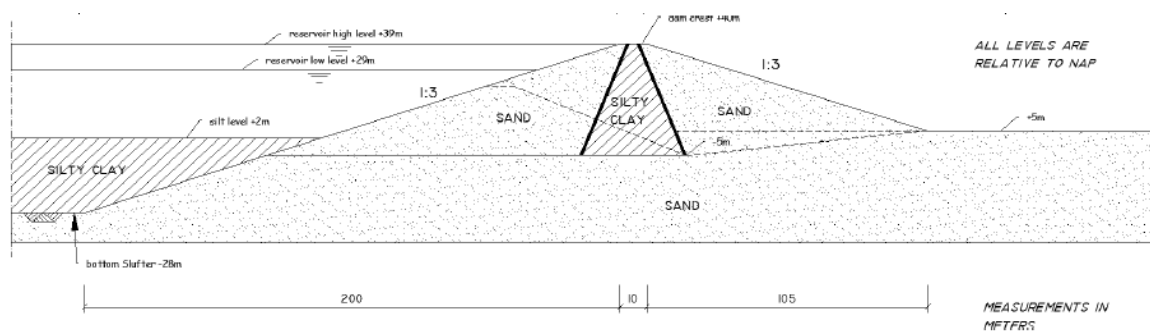


Figure 120: Cross-section of dam design for the Slufter

The dimensions and performance numbers are shown in Table 47. Expansion possibilities are given; either raising the capacity from 2.16 GWh to 4.32 GWh or even larger when there is a higher demand for storage in the future.

	Unit	Quantity
Storage capacity	GWh	2.16
Power output	GW	0.47
Surface area reservoir	km ²	3.14
Head range	m	39 - 29
Turbines (Francis)	MW	4 * 125
Roundtrip efficiency	%	78

Table 47: Characteristics of energy storage system the Slufter

Costs & benefits

Since the storage facility utilizes an already existing reservoir, the dredging and dam construction costs are much lower than for other alternatives. The benefits are generated by buying cheap power at night and selling it during peak-hours (arbitrage) and by deferred fuel costs that would have been made when a conventional peak-power plant was employed, see Table 48.

	Costs (m€)	Benefits (m€/yr.)
Dredging	64	
Dam construction	26	
Housing of pumps etc.	115	
Pumps, generators etc.	280	
Labour, risk & gen. expenses	95	
Total capital costs	580	
Annual O&M cost (page 133)	0.5 (pot. error, should be 46.9)	
Arbitrage		20
Saved fuel costs		10
Total annual benefits		20 (+10 of saved fuel)

Table 48: Costs and benefits of the Slufter

With a time-preference (discounting) rate of 1.1% the **payback period is 30 years**. Note the potential flaw in the annual operation costs. Costs are excluding the connection and the possible investments in transmission infrastructure.

Why is it not constructed?

The study was performed as a Master thesis and the commercial drivers to actually realise the project were most likely not as significant as they would be when executed by a governmental or private body.

B.4 Taiwan Integrated Energy and Service Island

All information obtained from this case study comes from the source: Beurskens, J., De Haan, S., Bauer, P., & Dieleman, R. (2014). *Taiwan integrated energy storage island*. Alliander.

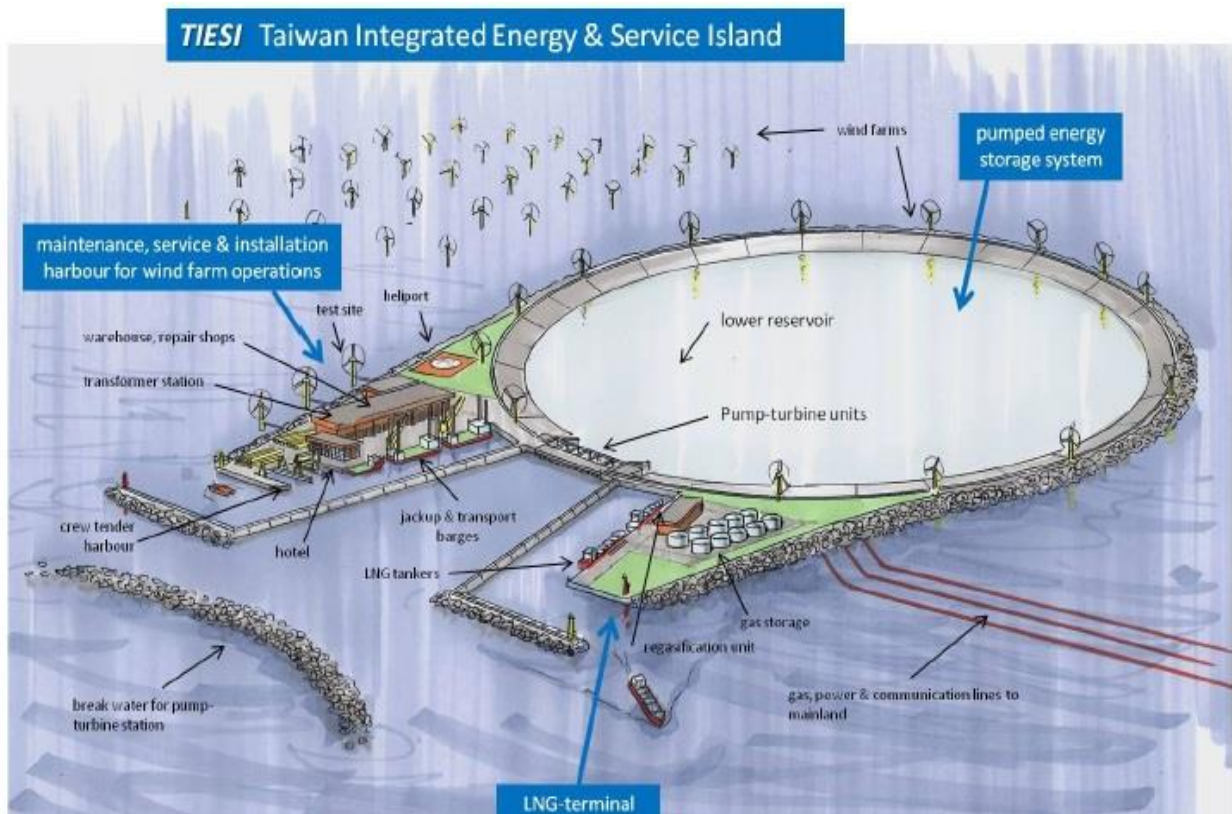


Figure 121: Artist impression of the multifunctional island by Reinout Prins (Source: Beurskens et al., 2014)

Motivation

Compared to well (inter) connected networks like in Northwest Europe, investments in large scale energy storage are more urgent in isolated or island grids like for Taiwan. Other flexibility options like international exchange of electric energy, load management and smaller storage solutions are relatively expensive. Currently Taiwan is almost fully reliant on the import of fossil fuels, which it desires to change by increasing the local power generation share with namely (offshore) wind and solar energy to 7.3 GW in 2030. The demand for large scale energy storage and the possibility of integrating the future offshore wind farms led to the 'pre-feasibility' study on a multipurpose energy storage island.

Design

The storage capacity and power output was chosen equal to the design made by KEMA and Lievense (2008), since it corresponds well with the power output of the wind farms and the capacity to store the energy when the wind park is at full power for nearly 7 hours. Furthermore, the head over the dam also ranges between 40m to 32m below sea level. The basin characteristics are shown in Table 49.

	Unit	Quantity
Storage capacity	GWh	20
Power output	GW	1.5
Surface area reservoir	km ²	32.6
Head range (below sea level)	m	32 - 40
Turbines (Francis)	MW	12 * 125

Table 49: TIESI reservoir characteristics

The turbine facility consists out of 4 modules of 3 pumps each. The modules are then separately connected to shore via a substation. This ‘modular’ approach provides flexibility by being able to expand according to the need and is more robust in securing operation in case one segment is down.

Costs & benefits

The reservoir costs, made up almost fully by the dredging works, are about a third of the total costs. The works required for the turbines and their subsequent connection to the grid make up the rest of the capital investment.

Since no such system has ever been built, there is no experience with the respective operation and maintenance costs. As a rule of thumb, 1% of the initial civil engineering costs are used and 10% of the initial investment in the turbine and electrical equipment.

The benefits are estimated by using a study from Energy Valley on the potential income of an energy storage island in the North Sea. In the study the same storage and power capacities were applied for three different services: arbitrage, balancing power and services to avoid congestion. Note that additional benefits from other functions of the island like a port terminal, wind farm hub, aquaculture or recreational assets were not taken into account. All costs and benefits are summarised in the following table.

	Costs (m€)	Benefits (m€/yr.)
Dredging	775	
Building pit	210	
Housing of pumps etc.	1,100	
Pumps, generators etc.	615	
HV cable + grid connection	300	
Total capital costs	3,000	
Annual O&M cost civil works	24/yr.	
Annual O&M cost mech. works	61/yr.	
Arbitrage		160
Balancing power		20
Avoiding congestion		20
Total annual benefits		200

Table 50: TIESI costs and benefits

Considering the numbers from Table 50, the energy island would have roughly a **payback period of 26 years**. The technical lifetime is expected to be more than 30 years and therefore the island would have a slightly positive business case (without other services on the island). It appeared that placing a casino on the island would make the project in Taiwan economically attractive (J. Beurskens, personal communication, February 15, 2017).

Potential environmental impact

Several potential impacts are mentioned, mostly regarding the effects of the change in morphology, salinity, hydrodynamics and land use on fish (larvae), benthos, birds and marine mammals like dolphins and seals.

Attention need to be paid to what extend the water in the reservoir is mixed, resulting from the filling and emptying of the waterbody. If insufficient, stratification of the stagnant water will occur and the lower water layer will be depleted from oxygen, due to the rotting of organic material on the bottom. Consequently the water would be unsuitable for marine life. On the contrary, a 'healthy' water reservoir offers opportunities for commercial fish, shellfish or bio-mass purposes.

The (hard) protection on the exterior side of the reservoir could offer a substrate for benthic species, which in their turn attract fish and so increase biodiversity. The in- and outlet system has to be designed in such a way that fish will not be harmed by the turbines. During the feasibility study there did not seem to be any environmental constraints and the island could even form a base for nature development.

Why is it not constructed?

Eventually the decision makers did not see the sheer need for energy storage on the short-term. Perhaps the project could be realised in the future (in circa twenty years), but then there should be a reference project to proof the concept (J. Beurskens, personal communication, February 15, 2017).

B.5 Underground pumped hydro storage

The information on this topic and the feasibility study for South Limburg has been obtained from: Van Duivendijk, J. (n.d.). *Water power engineering: Principles and characteristics* [PDF].

Motivation

The idea of using pumped hydro technology for underground storage originates like 'Plan Lievense' from the high fossil fuel prices in the 80's. To obtain a more reliable and efficient energy system an underground reservoir needs to be built or connected with shafts to the upper reservoir on the surface. In times of energy abundance, water is pumped from the cavities through the shaft to the upper reservoir. When peak power is required, the water flows back to the underground reservoir.

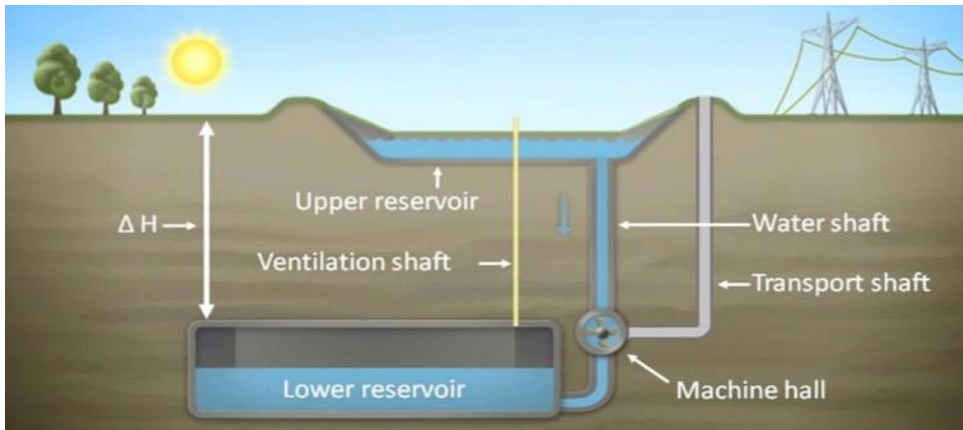


Figure 122: Impression of the various components belonging to an underground PHS facility (source: <http://www.sogecom.nl/energy.html>)

Design

Several feasibility studies have been performed on reusing old mine shafts in South Limburg, where suitable geologic conditions are found. The preferred location would contain: an impermeable layer at a large depth (up to 1400m), a thick homogeneous layer with no lateral soil variations, no (or minimal) groundwater flow, no seismic action, a nearby river, canal or estuary for rock transport and replenishment of the upper reservoir.

In South Limburg an appropriate limestone formation is present at a depth of 1200 – 1400 m. The underground reservoir could be either made up out of a few caverns or tunnel network. The 'leftover' rock could secondly be used for the construction of the upper reservoir or sold for other purposes. The lower reservoir has to be connected with shafts for the water conveyance, cables, ventilation and equipment and personal transport. Both the caverns or tunnels and the water transporting shaft will most likely need (concrete) lining to prevent the breaking loose of material. See Table 51 for details on the studied project.

	Unit	Quantity
Storage capacity	GWh	8
Power output	GW	1.4
Surface area upper reservoir	km ²	0.5
Head (below sea level)	m	1400
Turbines (Pelton)	MW	7 * 200
Roundtrip efficiency	%	77

Table 51: Characteristics of an underground pumped hydro storage facility

One of the advantages of Underground Pumped Hydro Storage (UPHS) over the ‘Energy Islands’ is an almost constant head, which leads to a stable power output. Additionally, there is minimal visual pollution due to the limited size of the upper reservoir. Note that besides the Pelton turbines, which generate the electric power, other ‘turbines’ that pump the water back up need to be installed too. The construction time is estimated to take 10 years and the storage system would operate for 50 years.

Costs & benefits

Back in 1985 the costs of an 8 GWh UPHS plant were projected at 2.5 billion Dutch guilders, which is equal to 2.0 billion euros anno 2017 (by the Internationaal instituut voor sociale geschiedenis, <http://www.iisg.nl/hpw/calculate-nl.php>). No detailed information is published on the various cost components or on the benefits. However, estimations suggest that the construction of the lower reservoir itself is responsible for 45% of the total costs and that the complete underground works and equipment accounts for 80% of the costs.

Why is it not constructed?

Most uncertainty within this concept lies in the underground construction works and the stability of the rock layers. Since the lower reservoir accounts for the largest cost component, the risk is significant. Moreover, the need for energy storage turned out less pertinent than initially thought in the 80’s.

B.6 Stored Energy in Sea

Most information from this concept in progress is obtained from: Garg, A., Lay, C., & Füllmann, R. (2012). *Stored energy in sea: The feasibility of an underwater pumped hydro storage system [Powerpoint slides]*. Retrieved from <http://docplayer.net/8559477-Stensea-stored-energy-in-sea-the-feasibility-of-an-underwater-pumped-hydro-storage-system-dr-andreas-garg-christoph-lay-robert-fullmann.html>

Motivation

With the rise of intermittent energy supply and development of floating wind turbines, an ‘opportunity’ for energy storage in deep water conditions arises. The desire for a storage technology with minor environmental impact, high efficiency and one that could be realised close to wind parks, led to the design of hollow spheres that could be placed between 600 m and 800 m below sea level (Figure 123).

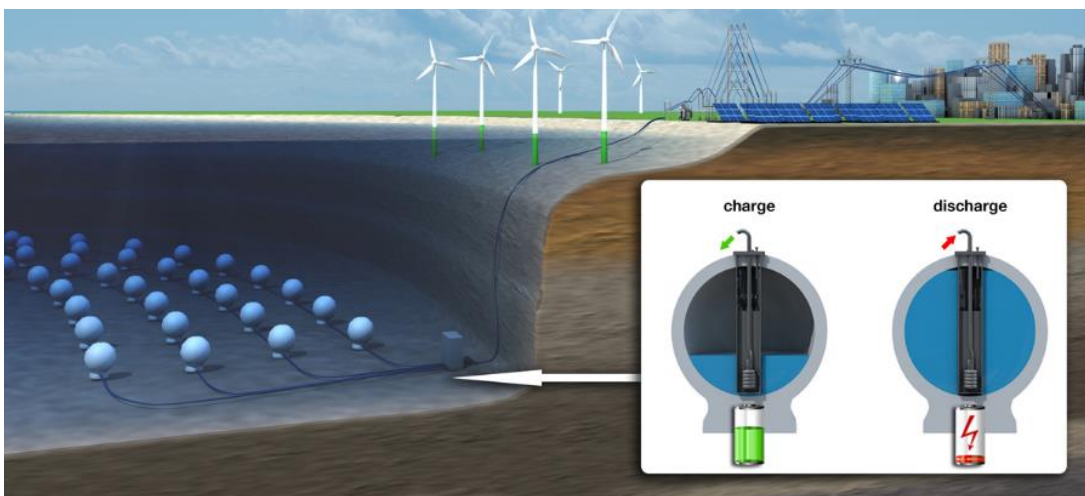


Figure 123: Concept of Stored Energy in Sea (source: http://forschung-energiespeicher.info/en/projektschau/gesamtliste/projekt-einzelansicht/95/Kugelpumpspeicher_unter_Wasser/)

Design

The concept is based upon the long proven pumped hydro storage principles. In times of energy abundance water is pumped out of the sphere and is allowed to flow back in when there is a demand for power. From a technical perspective the ideal diameter is 30 m, equivalent to 20 MWh when placed at a depth of 700 m. The concrete shell has a thickness of 2.7 metres, which due to its shape is only under compression. All electro- mechanical equipment is placed in the interior of the sphere and can be retrieved separately. Spheres can easily be added to form ‘storage parks’ to obtain a more competitive storage capacity of circa 400 MW. Technical details are shown in Table 52 and the various components belonging to the storage sphere are pointed out in the cross-section of Figure 124.

	Unit	Quantity
Storage capacity	GWh	0.020
Power output	GW	0.005
Head	m	700
Turbines	MW	5
Roundtrip efficiency	%	80 - 85

Table 52: Characteristics of a single sphere placed at a depth of 700m

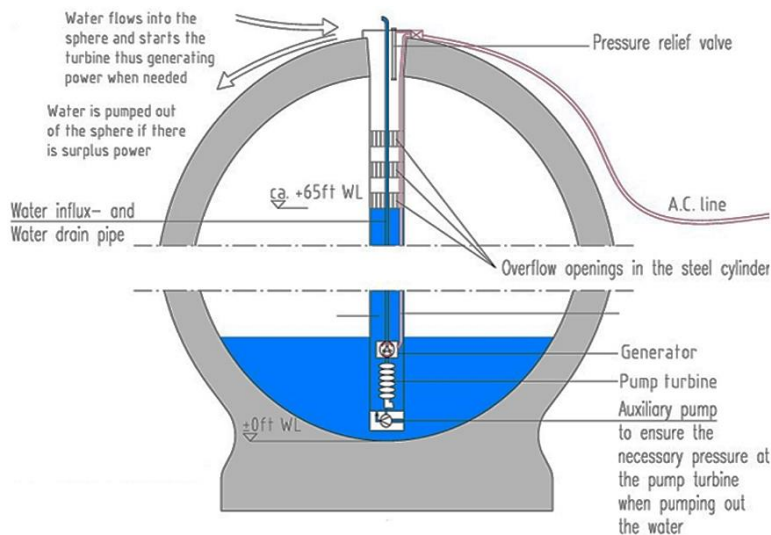


Figure 124: Cross-section of concrete sphere (source: http://forschung-energiespeicher.info/en/projektschau/gesamtliste/projekt-einzelansicht/95/Kugelpumpspeicher_unter_Wasser/)

Costs & benefits

The costs are estimated to be comparable to PHS and CAES, with 1,200 - 1,300 €/kW for the total construction costs. The costs for storage itself are circa 2 - 4 ct/kWh. Those figures combined make the STENSEA concept economically viable. The costs components per sphere and kW are shown in Table 53.

	Costs per sphere (m€)	Costs per kW (€)
Concrete sphere	2.065	413
Installation	1.500	300
Pump-turbine etc.	2.625	525
Total capital costs	6.190	1,238

Table 53: Target costs of STENSEA

Why is it not constructed?

At the moment, the STENSEA concept is still in development. A 1:10 pilot (see Figure 125) has just completed its test phase and successfully demonstrated its use (OffshoreWIND.biz, 2017). The next step is to deploy a full-scale 30-metre diameter demonstration project.



Figure 125: The 1:10 pilot being installed (source: <https://www.energiesystemtechnik.iwes.fraunhofer.de/en/projekte/se-arch/laufende/stensea.html>)

Appendix C: Scalars of energy storage islands

In Appendix B: Alternative pumped hydropower storage systems costs have been gathered on five previous studies into energy storage islands. Since they all have a lot in common with the prospected energy storage plant on the Dogger Bank, it is expected that their costs estimates can serve as a handhold to check upon the performed cost computations. Furthermore the costs can give an insight in what are the governing parts of a storage facility.

The considered case studies were chosen on the basis that they all had a detailed cost breakdown. This division between costs components enables the separation of for example civil and electrical and mechanical costs. The characteristics of the various projects and their relative costs are given in Table 54.

Reservoir characteristics	Unit	Plan Lievense	Energy Island 1	Energy Island 2	TIESI	Slufter
Year of study	-	1985	2007	2007	2014	2013
Storage capacity	GWh	20	20	30	20	2,16
Power output	GW	2	1,5	2,25	1,5	0,47
Surface area reservoir	km ²	11,95	40	60	32,6	3,14
Head range	m	70 – 60.3	32 - 40	32 - 40	32 - 40	39 - 29
Turbines (Francis)	MW	15 * 134	12 * 125	18 * 125	12 * 125	4 * 125
Roundtrip efficiency	%	80	80	80	80	78
Distance to grid	km	4	50	50	30	-
Costs components						
Dredging & dam construction	M€	1160	800	1000	985	90
Housing of turbines	M€	946	900	1300	1100	115
Pump-turbines	M€	1103	500	850	615	280
HV cable + grid connection	M€	157	250	250	300	0
Other	M€	0	0	0	0	95
Total capital costs	M€	3367	2450	3400	3000	580
Costs per turbine	m€	73,5	41,7	47,2	51,3	70

Table 54: Energy storage island properties and costs. Note that all costs are discounted to 2015 values with <http://www.iisg.nl/hpw/calculate-nl.php>

When the costs components are equally accounted for (by dividing the component with the total capital costs), the average share of the 5 groups becomes as in Figure 126:

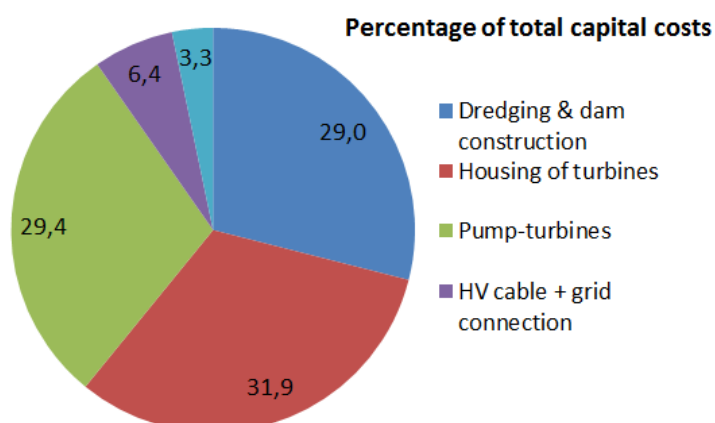


Figure 126: Shares of total costs per component

From the previous table and figure it is still hard to get an idea of the impact of a larger reservoir or higher installed power capacity. Therefore certain scalars have been developed that either depend on the storage capacity (reservoir size) or on the power capacity (number and size of turbines):

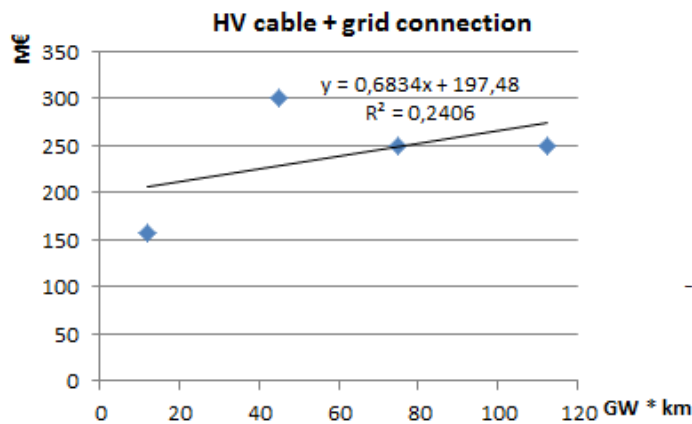
- Dredging and dam construction → scales with the reservoir dimensions/capacity
- Housing of turbines → scales with the required power output
- Pump-turbines and electrical- mechanical equipment → scales with the power output
- HV cable + grid connection → scales with the required power output and distance
- Other

Consequently the linear scalars become:

$$\text{Dredging \& dam construction} \left(\frac{\text{m€}}{\text{GWh}} \right) = \frac{\text{Sum of dredging \& dam construction costs (m€)}}{\text{sum of storage capacities (GWh)}}$$

$$\text{Housing of turbines} \left(\frac{\text{m€}}{\text{GW}} \right) = \frac{\text{Sum of housing of turbines costs (m€)}}{\text{sum of power capacities (GW)}}$$

$$\text{Pump - turbines} \left(\frac{\text{m€}}{\text{GW}} \right) = \frac{\text{Sum of pump - turbines costs (m€)}}{\text{sum of power capacities (GW)}}$$



The formulae above eventually result in the linearised capital costs of Figure 127. These costs can be used to obtain an insight in similarities and differences between previous research and work performed in this thesis.

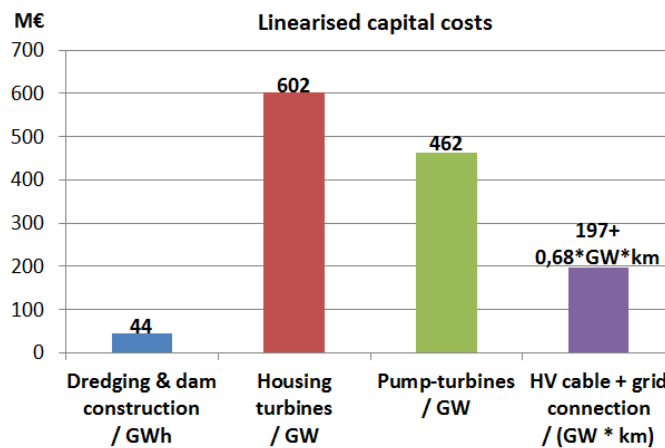


Figure 127: Scalars of linearised costs per component of a PHS facility

Appendix D: Dogger Bank conditions

In this section the present conditions on the Dogger Bank that have been collected are presented. All combined they lead to the boundary conditions.

Wind, waves and tides

What		Location	Unit	Value
Bathymetry		Dogger Bank	m	-40 to -15
Wave height		Dogger Bank		
Annual mean	H_s	-	m	1.7 to 2.0
One-year max	H_{max}	-	m	6.0
Northern mean	$H_{mean,N}$	-	m	1.56
Eastern mean	$H_{mean,E}$	-	m	1.32
Southern mean	$H_{mean,S}$	-	m	1.41
Western mean	$H_{mean,W}$	-	m	1.66
Sea level rise		Global (1993-2003)	mm/yr	2.4 - 3.8
		North Shields (1901-1996)	mm/yr	1.86
Tidal currents velocity		East side-Dogger Bank	m/s	0.4
		West side-Dogger Bank	m/s	0.2 - 0.6
Extreme tidal velocities		Dogger Bank		
Return period	1	-	m/s	0.88
	10	-	m/s	0.98
	100	-	m/s	1.11
Water level		Buoy D15 (yellow star Figure 130)		
Highest Astronomical Tide (HAT)		-	m	1.19
Mean High Water (MHW)		-	m	0.42
Mean Sea Level (MSL)		-	m	0.00
Mean Low Water (MLW)		-	m	-0.40
Lowest Astronomical Tide (LAT)		-	m	-1.04

Table 55: Dogger Bank conditions and properties (source: EMU Ltd et al., 2011). Directional mean wave heights, to be used as operational waves, are obtained from Frölke (2017) and tidal elevations from Abadal et al. (2017)

Figure 128 shows that for most parts of the North Sea the sea level rise (SLR) ranges from 2 to 4mm/year. The SLR for the Dogger Bank itself can be estimated at 3mm/year.

The tidal and storm surge (SS) elevations can be sourced from Figure 130 and Figure 129 respectively.

All combined, the future maximum water level could approach 0.3m (SLR) + 0.8m (tide) + 1.4m (SS) = 2.5m as of the year 2115.

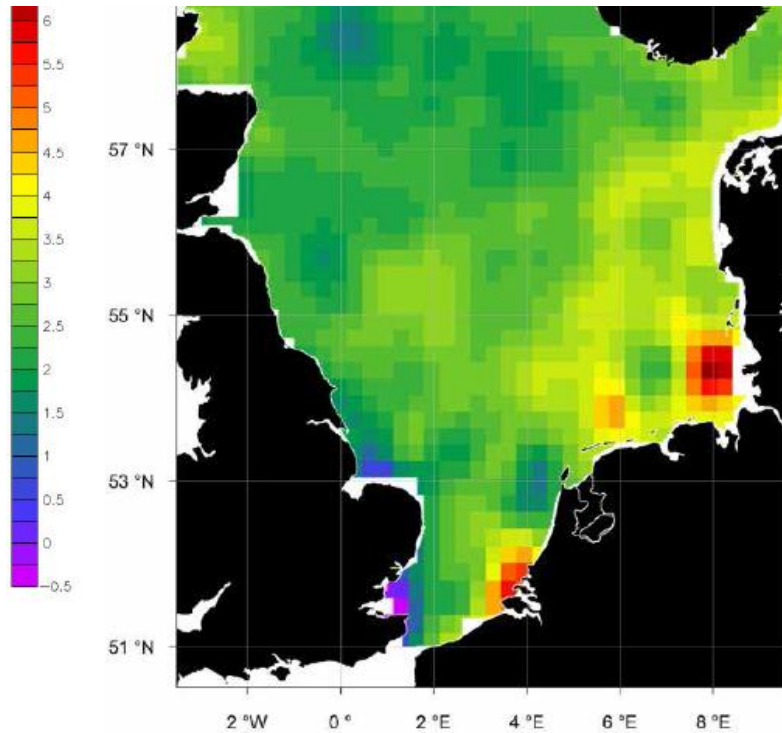


Figure 128: Sea level rise in the North Sea (mm/year). Local differences can be explained by storm surges, sensitivity to water set-up and subsidence of the land. From this figure a sea level rise of 3mm/year is assumed for the Dogger Bank (source: NIOZ et al., 2015).

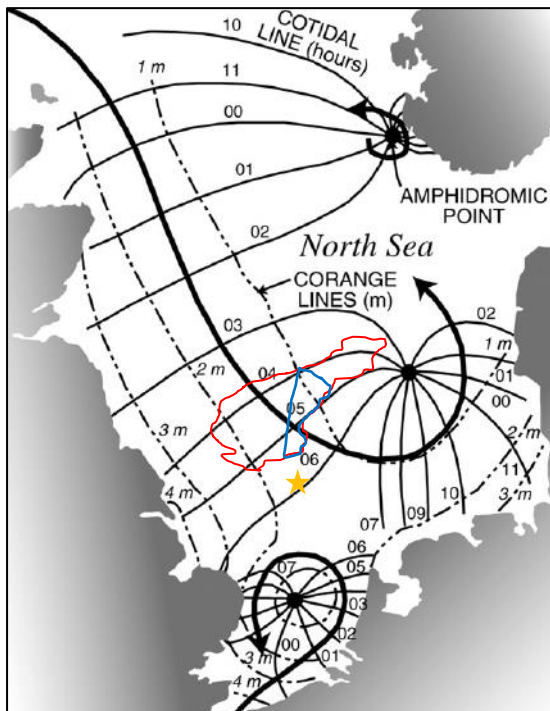


Figure 130: Illustration of the amphidromic points in the North Sea. The Co-range lines indicate lines of equal tidal range (high water level is thus in the order of half the range!). The outline of the Dogger Bank is depicted in red and the Dutch part of the bank has a blue perimeter. The figure was modified from Börger et al. (2014) and Kvale (2006).

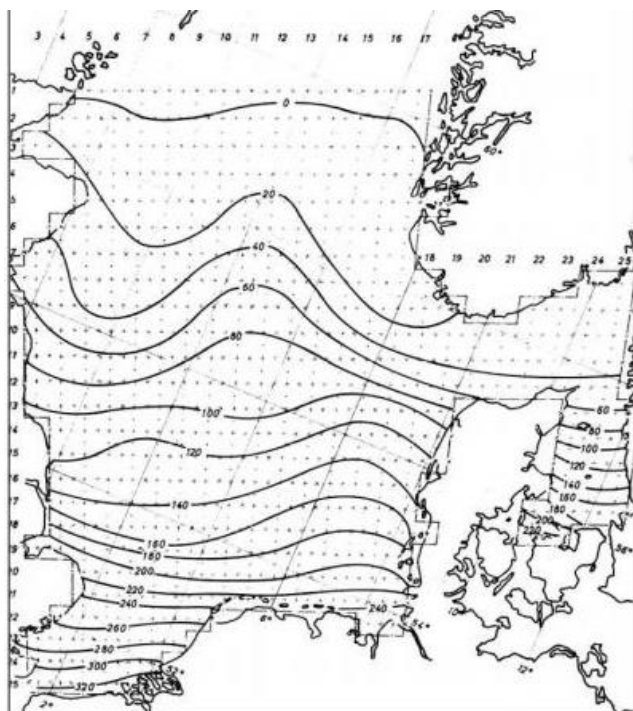


Figure 129: Storm surge levels in the North Sea (cm) obtained via a schematic storm with a constant northerly wind of 23.2m/s and real bathymetry (Sündermann & Pohlmann, 2011). For the Dogger Bank a storm surge of 1.2 – 1.4m will be taken into account.

An extensive extreme value analysis was performed by the parallel research of Frölke (2017). Both these embarked at the same time. At first it seemed that an 8 metre return period would correspond to a return period around 300 to 500 years, as was recommended by the PI an Lievense for an economically optimal design. Therefore the 8m significant wave height was used for the design of the armour protection. Only briefly before handing in this thesis it became clear that an 8m wave corresponds to a return period of circa 40 years instead (see the figure below). Consequently it would be advised to adopt a larger wave height for future design.

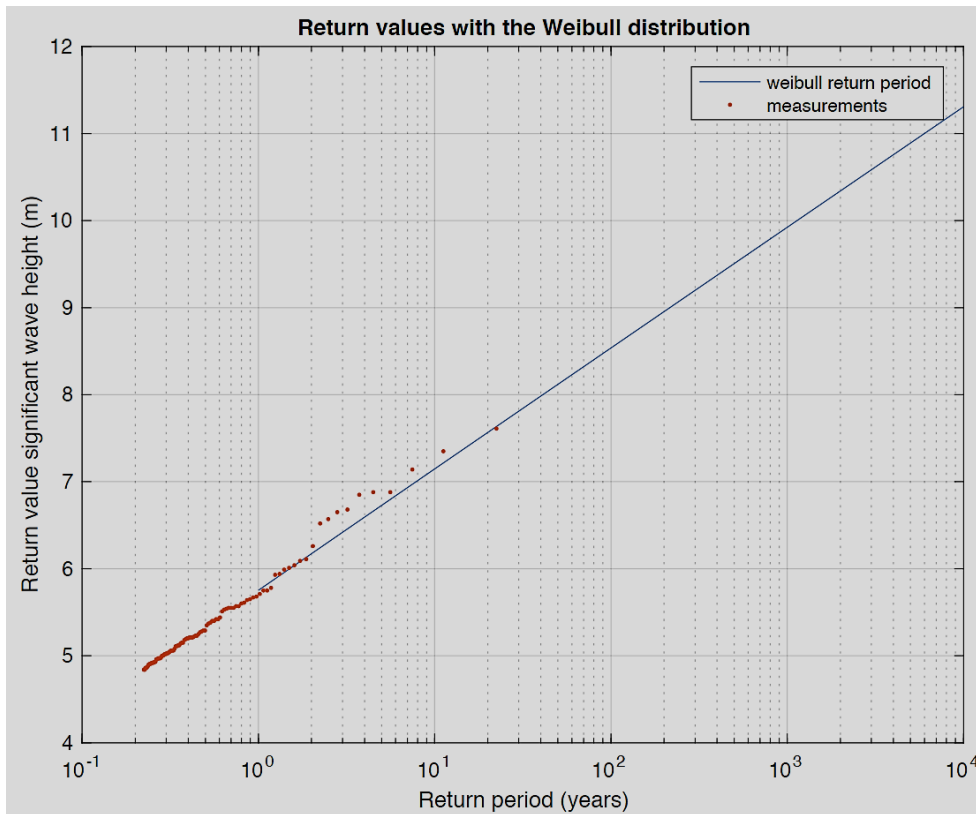


Figure 131: Extreme value analysis on the wave return period (source: Frölke, 2017)

Although the design wave height has been underestimated for the dimensioning of the Xbloc armour and corresponding layers, it does not affect the overall design and obtained results.

For the cost computations of the dam, the whole periphery was assumed to be protected against 8m waves. However, the wave heights from the other directions are far lower than the governing north-north-west waves. Hence only part of the dam requires a more robust armouring, where the remainder of the dam can be executed much lighter. Consequently the underestimated wave height and the sub-optimal design cancel out against one another.

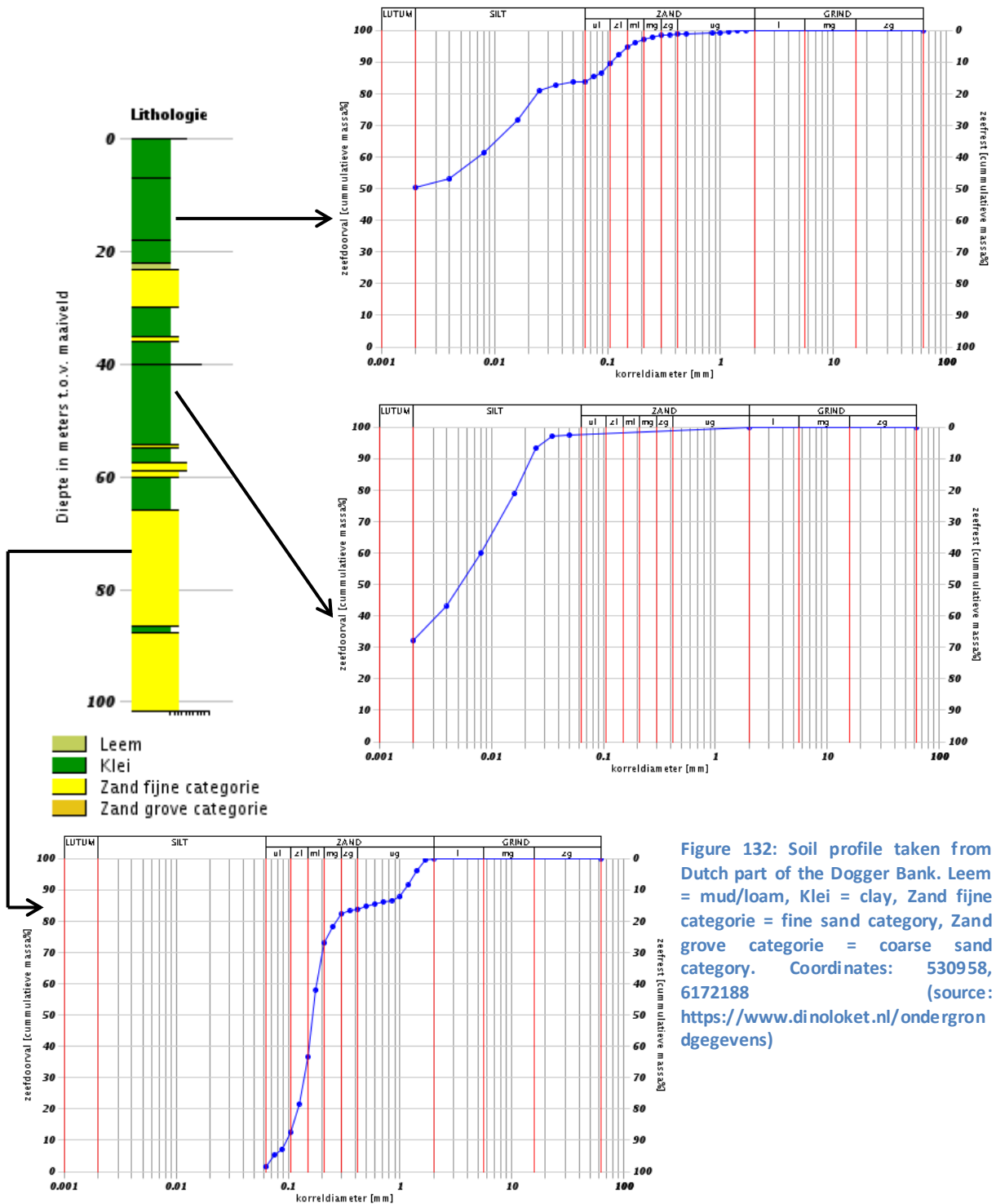


Figure 132: Soil profile taken from Dutch part of the Dogger Bank. Leem = mud/loam, Klei = clay, Zand fijne categorie = fine sand category, Zand grove categorie = coarse sand category. Coordinates: 530958, 6172188 (source: <https://www.dinoloket.nl/ondergrondgegevens>)

The Dogger Bank has a turbulent history of geological changes, especially due to ‘ice ages’. During these glacial times the soil has been heavily compressed. Thereby the Dogger Bank Formation has been formed that consists of “Glacimarine to glacialacustrine: Stiff to very stiff clay, and laminated gravelly sandy clay” (EMU Ltd. et al., 2011).

Appendix E: Risks associated to inverse offshore pumped hydro storage

One of the key advantages of an inverse offshore hydropower storage plant is that there is no potential flood risk posed by the storage facility. In fact: when the dam would break through the inner reservoir would be filled, instead of the reservoir flooding the surrounding area. The only threat is then the economic loss of damage to the dam and filling-up of the inner reservoir.

Since for the energy storage function no human activities are necessary within the storage reservoir, there is no risk for loss of life(s). This significantly reduces the demanded safety factor for the system. It is even possible to imagine that when a storm is forecasted of unprecedented magnitude, which could potentially breach the dam, the inner reservoir is filled-up to prevent a destructive flood wave coming in. This risk and damage mitigation measure is an interesting asset of the offshore energy storage system. In case other functions are added to the island the acceptable risk might change, which results in stricter requirements for the dam structure. Hence, the value and benefit of potential extra functions has to be weighed against the influence on the needed safety level (and thus added costs).

For the Plan Lievense in front of the Dutch coast a detailed risk analysis was performed that resulted in the risk levels as presented in Table 56.

Perspective acceptable risk	Optimal failure probability per year
Economic (minimal costs over the lifetime)	$3 \cdot 10^{-3}$
Personal (loss of lives)	10^{-4}

Table 56: Risk levels for a pumped hydropower plant in the Netherlands (source: Rijkswaterstaat et al., 1985)

Since the Plan Lievense contained an inner reservoir higher than the lower reservoir (the North Sea) a dam break through would cause a flood wave endangering the loss of lives. Therefore the 'personal' risk level from Table 56 was governing, with a failure probability of 1/10,000 years.

As the inverse offshore PHS has its reservoir below the North Sea, it does not imperil the surrounding area. Consequently the more competitive failure probability of 1/333 years can be applied. This economic risk level should result in the lowest costs of the storage facility over its lifetime (CAPEX + OPEX). Due to the similar structures and investments compared to the Plan Lievense it is expected that the economic acceptable risk is evenly alike for the inverse offshore PHS plant on the Dogger Bank. Consequently a design that meets the optimal failure probability of 1/333 years is recommended.

The design has not been executed in a probabilistic approach. This would be vastly more complicated, due to all the correlations between the failure mechanisms. Furthermore it would be overly detailed compared to the desired insight in the scaling of an energy storage facility. The economic risk level has only been used to choose design wave heights and safety factors.

The technical failure mechanisms are depicted in Figure 35 and Figure 36. The shown failure modes are purely technical. There are also financial and societal risks. Financial risks can encompass fluctuations in energy prices and the cost of capital. Societal risks contain mostly changes in policy and support by the government(s), the public or non-governmental organisations. The focus of this report lies within the technical part and no further attention is given to the financial and societal risks.

Appendix F: Influence of toe material on slope stability

During the safety checks for the macro stability it proved that the material at the toe of the outer slope has a large impact on the whole slope stability. So far it has been assumed that the seabed at the Dogger Bank (DB) consists out of homogeneous stiff clay. Besides the fact that present day layer is probably not perfectly consistent, it is likely that the top layer is of lesser structural quality, due to organic material or fishing activities. To illustrate the impact of the 'toe foundation' a 50 metre wide and 3 metre high strip²⁵ has been tested with different materials: quarry run, stiff clay, dredged material and muck.

The results are presented in the following four figures and table:

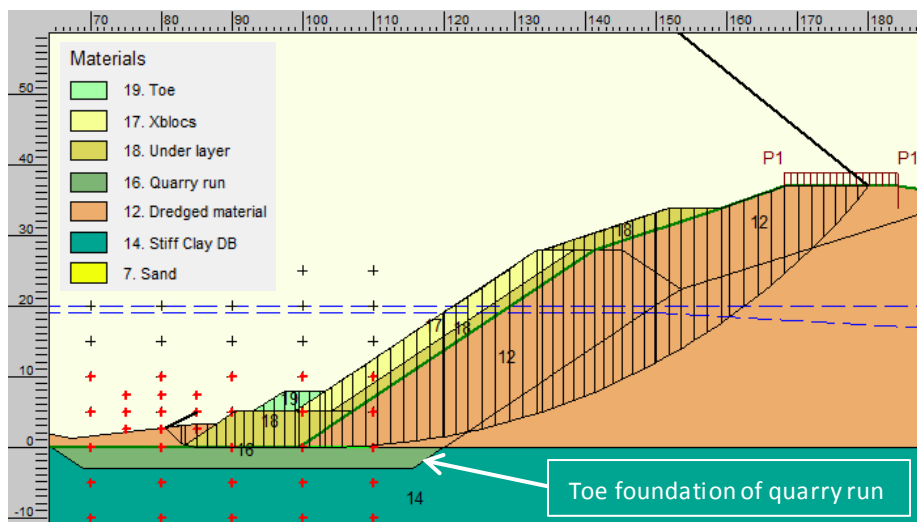


Figure 133: The outer slope stability with a quarry run toe foundation. The safety factor is 1.18. Note that the length of the critical slip surface through the quarry run is minimal since it causes a lot of friction

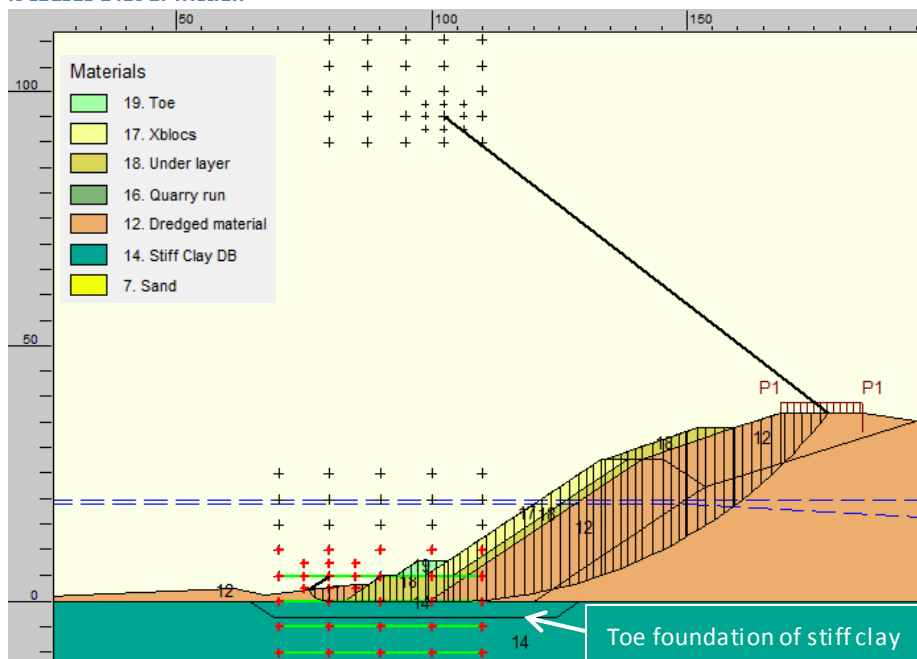


Figure 134: The outer slope stability with a stiff clay toe foundation. The safety factor is 1.11.

²⁵ Larger dimensions of the toe foundation hardly affect the slope stability of the critical slip circle. The slip plane would have to be that much larger to go 'around' or minimise crossing the replaced foundation layer that the additional length of the circle eventually leads to a much higher sum of shear resistance.

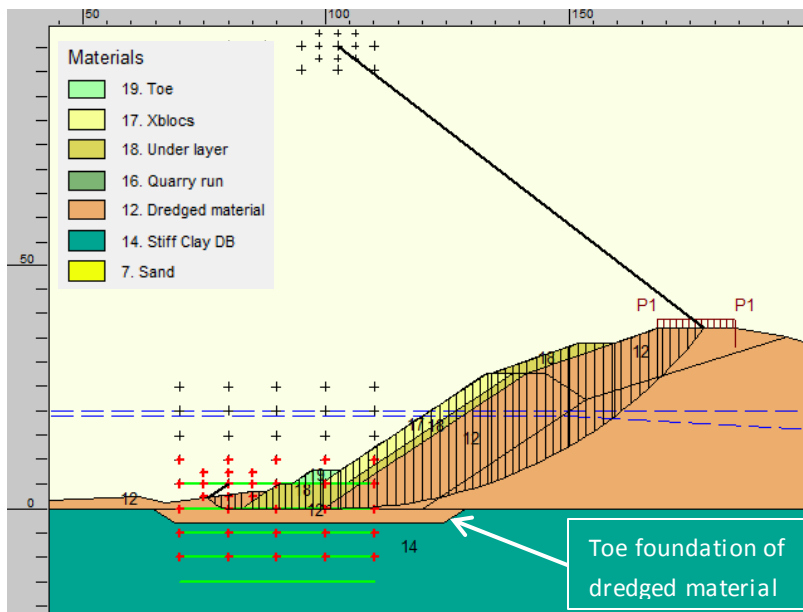


Figure 136: The outer slope protection with the existing seabed replaced with dredged material. The safety factor is 1.09.

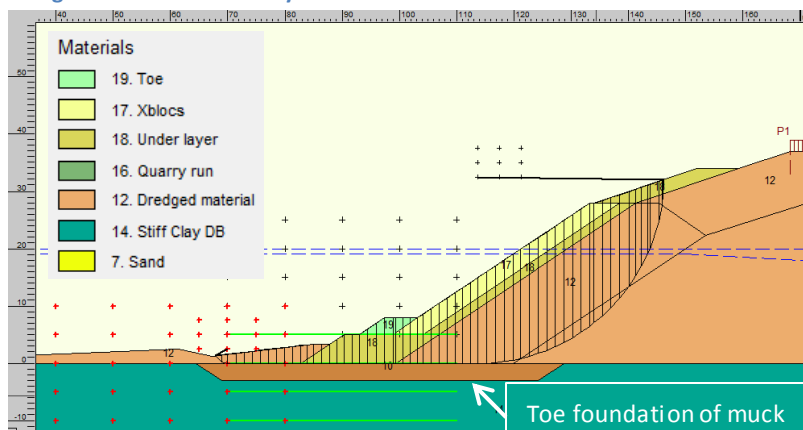


Figure 135: The outer slope protection with a weak muck layer underneath the toe structure. The resulting safety factor is 0.78

Soil parameters	Quarry run	Stiff clay DB	Dredged material ²⁶	Muck
Dry unit weight (kN/m ³)	23	19	17	11
Submerged unit weight (kN/m ³)	26.5	20	18	11
Cohesion (kN/m ²)	0	11.54	10.4	0
Friction angle (°)	39.81	21.24	19.04	0
Safety factor	1.18	1.11	1.09	0.78

Table 57: The influence of the material from the toe foundation layer on the slope stability

The table above confirms that as the shear resistance from the toe foundation decreases the overall slope stability quickly diminishes. Even though it is the most costly, the quarry run is chosen because it offers the highest level of safety. When more information about the exact soil characteristics is available it might prove that for certain parts dredged material or sand (if available) can be used.

²⁶ The dredged material consists out of stiff clay from the Dogger Bank. By dredging the clay mechanically the soil properties are minimally affected. In contrast to hydraulic dredging the clay does not need to be cut into fine pieces or mixed with water for transportation. Therefore the dredged material characteristics are 'only' reduced by 10% compared to the original clay parameters.

Appendix G: Seepage and bursting mechanism for a closed aquifer

In case the water conveying aquifer underneath the impermeable clay layer is not in direct contact with the sea and the discharge into the aquifer is lower than the discharge from the aquifer into the inner reservoir, eventually the water pressure under the clay layer will decrease. However, when the water level is first lowered, the pressure in the aquifer will still be equal to the original North Sea level. To end up with the decreased water pressure as in Figure 137, the original hydrostatic level will have to be pumped out of the aquifer too!

G.1 Seepage

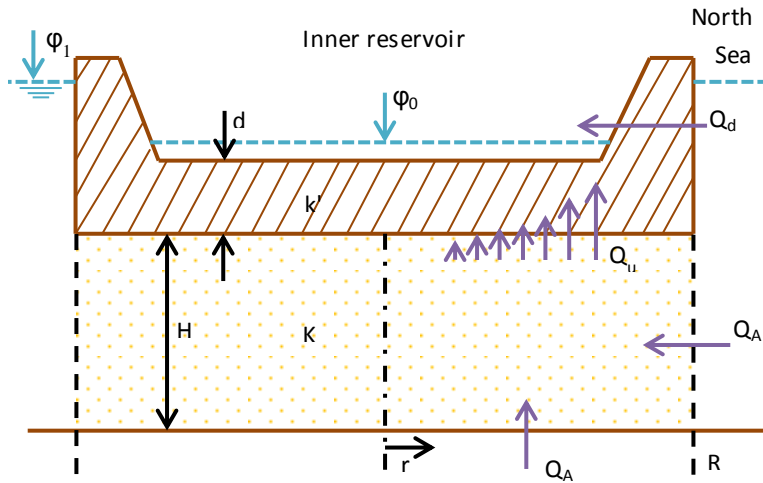


Figure 137: Seepage through the dam (Q_d) and the underlying clay layer (Q_u) in case the aquifer is barely recharged through the surrounding environment ($Q_A < Q_u$)

In the schematic drawing of Figure 61 one can see how the water flows into the reservoir via the dam and the aquifer (the sand layer) underneath. The piezometric head in the aquifer decreases exponentially, which is indicated with the dedining arrows of Q_u . After more or less two kilometres (three times the length of the leakage factor) towards the centre of the reservoir there is only two percent of the flow continuing and thus no seepage either (Barends & Uffink, 2006). The

leakage through the bottom of the reservoir can be computed with the flow equations derived from Darcy's law and the Bessel function. The results of the seepage through the dam and bottom of the reservoir are gathered in Table 17.

$$Q_u = \int_0^R 2\pi r \frac{\varphi - \varphi_0}{d} k' dr = \frac{2\pi(\varphi_1 - \varphi_0)}{d I_0\left(\frac{R}{\lambda}\right)} k' R \lambda I_1\left(\frac{R}{\lambda}\right) \quad ; \quad \lambda = \sqrt{\frac{KHd}{k'}}$$

$$I_n(x) = \frac{e^x}{\sqrt{2\pi x}} \left[1 - \frac{4n^2 - 1^2}{1(8x)} \left(1 - \frac{4n^2 - 3^2}{2(8x)} \left(1 - \frac{4n^2 - 5^2}{3(8x)} (1 - \dots) \right) \right) \right] \quad ; \quad x = \frac{R}{\lambda}$$

- Q_u = Total leakage through bottom of reservoir (m³/d)
- R = Radius of reservoir (m)
- r = distance from the centre of the reservoir (m)
- φ = Piezometric level for a specific r ($\varphi = \varphi_1$ for $r = R$ and $\varphi = \varphi_0$ for $r = 0$) (m)
- k' = Permeability of clay layer (=0.01m/d) (m/d)
- d = Thickness of clay layer (= 35m or 25m depending on depth of the reservoir) (m)
- λ = Leakage factor (m)
- K = Permeability of sand layer (=1m/d) (m/d)

- H = Thickness of sand layer²⁷ (= 135m) (m)
- I_n = Asymptotic approximation of modified Bessel function (for I₀ n = 0 and for I₁ n = 1)
- x = Leakage penetration factor (-)

Scenario	Unit	1	2	3	4	5	6	7	8
Maximum head	m	40	40	40	40	40	60	60	60
Pot. head centre	m	26.88	7.29	7.16	2.57	1.14	10.20	4.69	2.50
Storage capacity	GWh	0.77	9.84	10	20	30	10	20	30
Seepage dam	mm/d	0.83	0.28	0.28	0.21	0.17	1.06	0.79	0.66
Seepage bottom	mm/d	5.78	5.98	5.95	4.59	3.89	13.92	11.12	9.58
Total discharge	10 ⁴ m ³ /d	1.13	9.20	9.28	13.57	16.84	11.82	17.04	21.00
Total head loss	mm/d	6.6	6.3	6.2	4.8	4.1	15.0	11.9	10.2

Table 58: The loss of head due to leakage. Note that the seepage through the dam and bottom are converted into a head loss per day. The potential head at the centre is basically the 'pressure' that remains from the water level difference

Even with the conservatively chosen permeability of 0.01m/d for the clay layer, the effect of seepage on the head loss in the reservoir is surprisingly small. Furthermore, the values presented in Table 17 form the upper boundary, since they are computed with a continuously empty inner reservoir. Although the total discharges (in the order of 150,000m³/d) might seem like a lot, it is only around 0.1% of the total fluctuating water volume!

²⁷ The sand layer thickness is estimated at 135m based on the soil profile (which indicates that the sand layer starts at -65m relative to the seabed) and the geological conditions presented by the Forewind consortium who state that the Yarmouth Roads formation ("Marine and non-marine sands and plant debris with intertidal sand and mud rhythmites") extends till roughly -200m below the seabed (Emu Ltd. et al., 2011)

G.2 Bursting

In case the aquifer underneath the clay layer is dosed and the aquifer is (partly) pumped empty, the water table in the aquifer will gradually decrease towards the centre of the reservoir. This concept is explained in Figure 138.

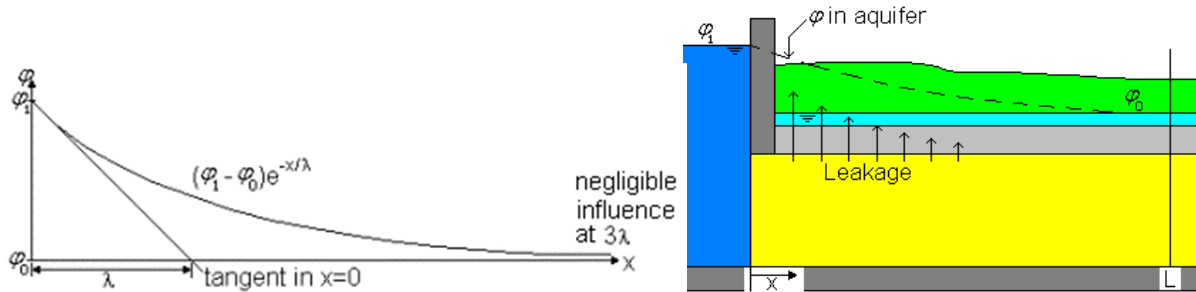


Figure 138: Potential head in a semi-confined aquifer. Note the influence that the leakage factor λ has on how quick the head decreases towards the centre of the reservoir (source: Barends & Uffink, 2006).

$$h = \frac{\gamma_{w,d}(\varphi_x - \varphi_0)}{\gamma_{s,d} - \gamma_{w,d}} \quad ; \quad \varphi_x = \varphi_0 + (\varphi_1 - \varphi_0)e^{-\frac{x}{\lambda}} \quad ; \quad \lambda = \sqrt{\frac{KHd}{k'}}$$

- h = Minimal required thickness of soil on top of the sand layer (m)
- γ = Volumetric weight design value ($\gamma_{w,d}$ for water; $\gamma_{s,d}$ for submerged soil) (kN/m^3)
- φ = Potential head ($\varphi = \varphi_1$ for $x = 0$; $\varphi = \varphi_x$ for $x > 0$; φ_0 = head inner reservoir) (m)
- x = Distance from the dam towards the centre of the inner reservoir (m)
- λ = Leakage factor (m)
- K = Permeability of bottom sand layer (m/d)
- H = Thickness of bottom sand layer (m)
- d = Thickness of bottom clay layer (= 35m) (m)
- k' = Permeability of bottom clay layer (m/d)

Figure 138 clearly shows the sensitivity of the leakage factor in order to estimate the required overburden on the conveying sand layer. Basically this leakage parameter determines how quick the pore water pressure dissipates towards the centre of the reservoir underneath the clay layer. When for example the clay layer would be highly impermeable or the underlying sand layer extends till large depths, the water pressure under the clay layer will tend to remain equal to the maximum water level difference between the reservoirs.

The effect that the choice for the parametric input has on the ‘perseverance’ of the water pressure underneath the clay layer, which ultimately either limits or enables the excavation of the inner reservoir to a larger depth (thereby determines namely the necessary circumference, number of turbines, in- and outlet work), is explained in Figure 139 and shown in Table 59.

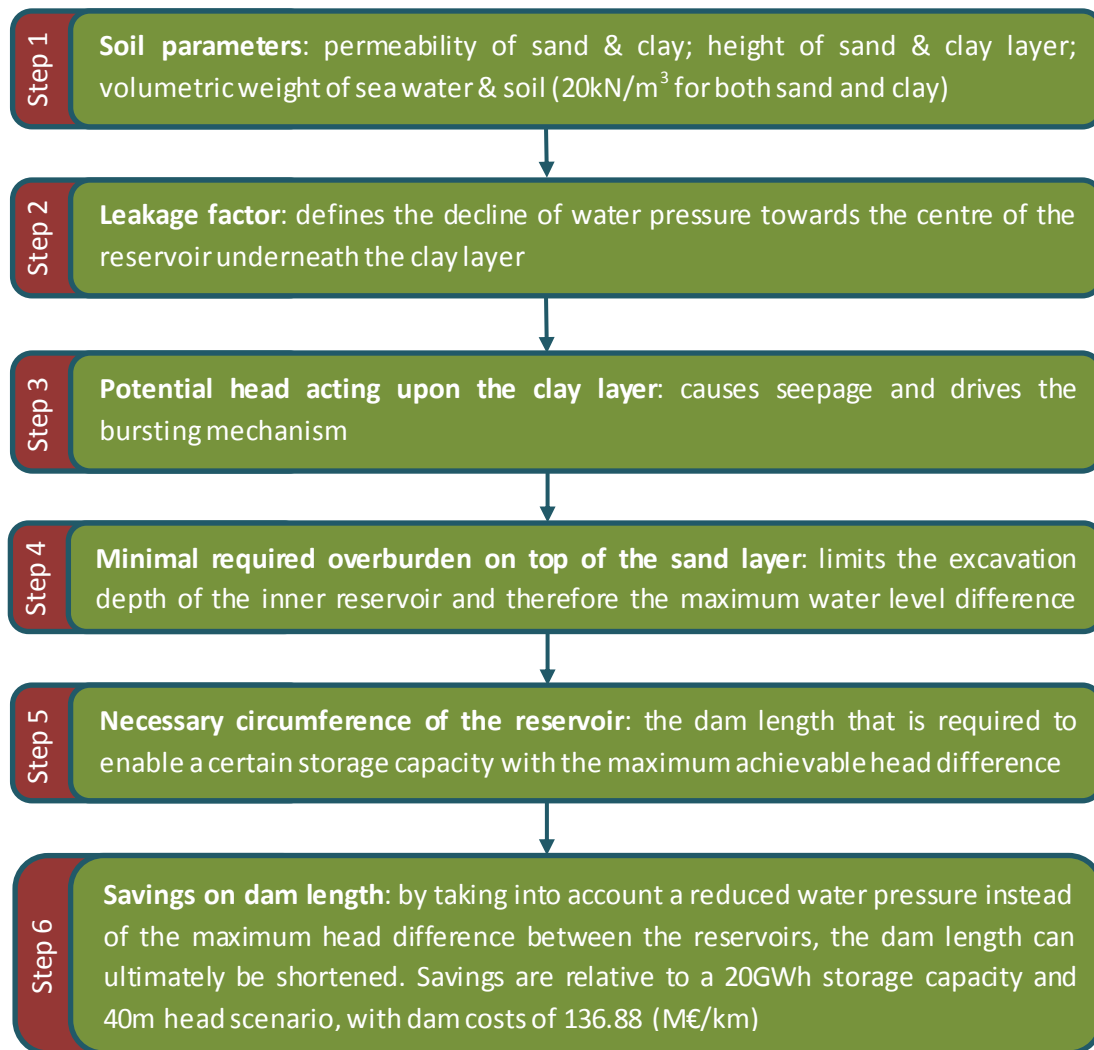


Figure 139: The process of how the soil parameters eventually affect the (savings on) dam length. See Figure 142 for the quantitative relation between the leakage factor and savings.

Plausible soil parameters			Potential head (m)	Maximum reservoir depth (m)	Savings on dam length (m€)
Permeability sand (m/d)	Permeability clay (m/d)	Thickness sand (m)			
1	0.01	135	25.1 (32.1)	51.2	495.3
10	0.01	135	34.5 (38.4)	44.5	231.0
1	0.0001	135	38.2 (40.5)	42.4	129.7
1	0.01	200	27.3 (33.8)	49.5	435.5

Table 59: The impact of the soil characteristics on the achievable depth of the reservoir and respective savings on the necessary dam circumference. Note that the ranges of soil parameters are all fully possible (only the clay is assumed to be homogeneously 35m thick). The potential head is the additional water pressure acting upon the clay layer at the inner toe (most critical point), resulting from a water level difference of 40m. The values between brackets indicate the potential head when the reservoir would be excavated till the maximum depth. The maximum reservoir depth is equal to the achievable water level difference between the North Sea and the inner reservoir (with a safety factor for bursting of 1). The savings on dam length refer to the dam costs of scenario 4, with 40m water pressure under the whole reservoir, 20GWh storage capacity and dam costs of 136.88m€/km.

From Table 59 it can be concluded that only a small deviation in soil characteristics could lead to a large difference in costs. Although the entire ranges of sand- and clay permeability are completely plausible, the available literature (boring from dinoloket.nl and Forewind Dogger Bank Characterisation) suggests that the leakage factor could vary from roughly 300m to 10,000m. Figure 140 shows that this range is exactly covering the exponential part of the potential savings on dam length, which could lead to a difference of at least 700 million euros! Note that this amount of savings is only originating from a reduction in diameter of the reservoir, due to a ‘milder’ water pressure driving the bursting mechanism. The potentially larger head difference would also have a large impact on the amount of turbines and the requisite discharge for the in- and outlet works. All combined, the leakage factor present on the Dogger Bank could be responsible for a difference in costs in the order of 1 billion euros!

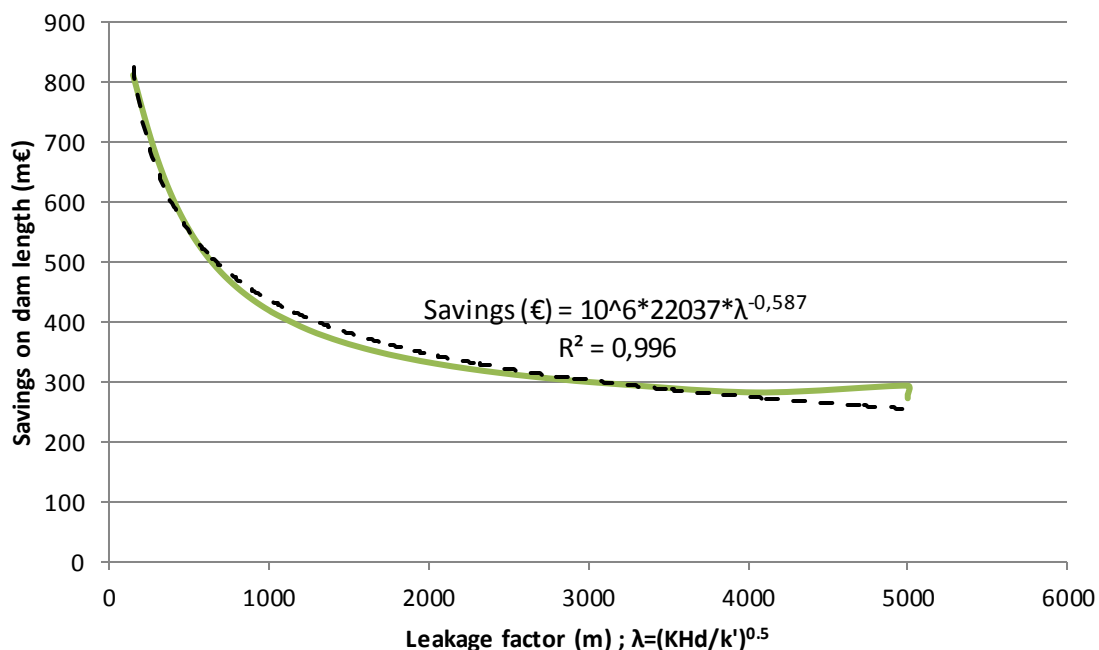


Figure 140: The green line indicates the relation between the leakage factor and achievable depth of the reservoir, which ultimately determines the potential savings in the dam circumference (in comparison with scenario 4, with 40m water pressure under the whole reservoir , 20GWh storage capacity and dam costs of 136.88m€/km). The black striped line shows the trend of the relation between the soil characteristics and savings on the dam length. The R^2 value shows the level of reliability of the given ‘Savings’ approximation (the maximum R^2 is 1, therefore the given formula is very accurate)

From Figure 140 it seems like a small leakage factor is preferable, implying that a location must be sought for that contains:

- A ‘conveying’ under layer with low permeability (K)
- A ‘conveying’ under layer with a small thickness (H)
- An impermeable layer with a **small** thickness (d)
- An impermeable layer with **high** permeability (k’)

Obviously the last two claims are completely counterintuitive, since they would lead to high seepage discharges and respective loss of efficiency/revenue. Hence an optimisation could be performed between the gains from a low bursting criterion and the losses caused by seepage. The resulting curve could be used to determine the number and level of research in the existent soil characteristics in order to lead to an optimal design.

Without the knowledge of the actual soil characteristics that determine the leakage length on the Dogger Bank, there is no scientific ground on which a more favourable choice for parameters can be based. From Figure 140 it can be derived that the minimum achievable reservoir depth and corresponding maximum head is 41.5m (for $\lambda \rightarrow \infty$). When realising that 43 metres below sea level the first sand layer starts, which would be preferable as a base of the reservoir, it makes it worth to recap on the initial assumptions. Additionally it has become clear that only a slightly larger water level difference could quickly results in millions of savings on the dam length.

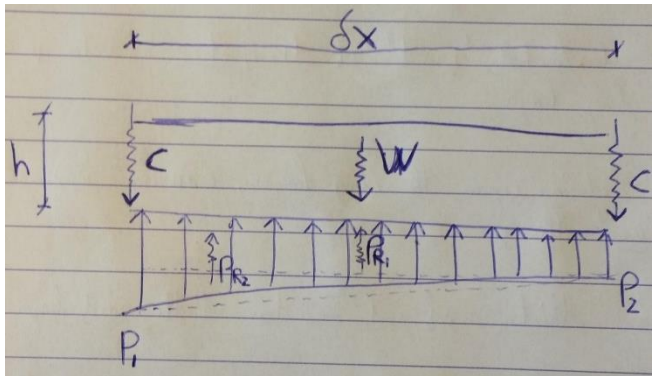


Figure 141: The stability of the clay layer against bursting for an infinitely long strip. Note that this is a conservative assumption, since the cohesive forces will also act along the 'δx'sides.

So far the cohesion of the clay layer has been neglected, under the assumption that if the area of clay would be large the cohesive forces would be negligible compared to the weight of the soil. However, the cohesive forces may just make the difference in allowing a maximum reservoir depth of 43m instead of 41.5m. To verify this, the schematisation as in Figure 141 has been tested.

The schematisation results in the fact that at a certain point the (declining) water pressure maximally outbalances the cohesive forces. Yet, as the distance towards the centre increases the acting water pressure declines exponentially. These two phenomena result in the occurrence of a specific width that is most susceptible to bursting. This most unfavourable width can be identified in **Fout! Verwijzingsbron niet gevonden.** as the distance where the sum of vertical forces is minimal (=37m for the red line and 154m for the blue one).

It turns out that for the parameters used the maximum water level difference is 43.5m. To incorporate some redundancy in the design, an excavation depth of 43m is chosen. This allows for inaccuracies in the dredging works and scour holes. Note that this scenario is solely for a clay layer on top of a closed aquifer that has been (partially) pumped empty.

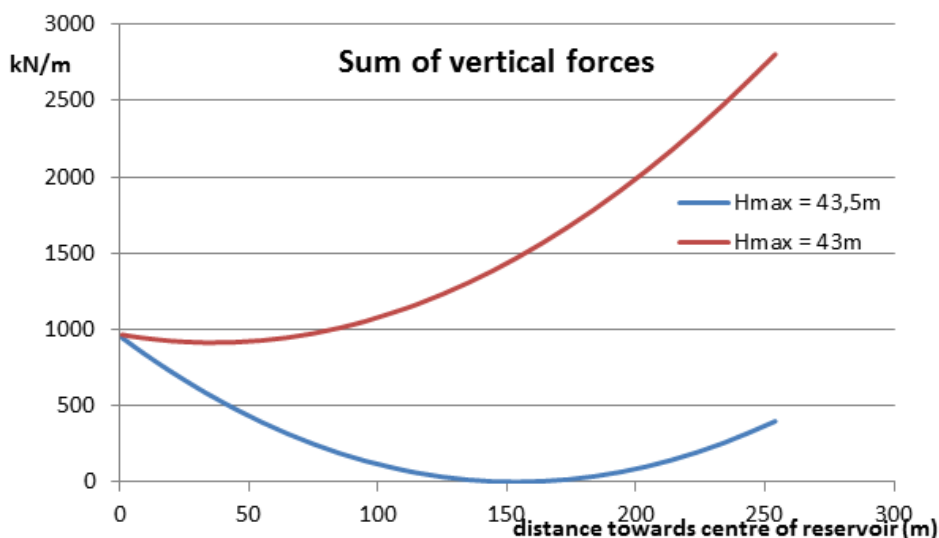


Figure 142: The vertical stability of the clay layer. The x-axis depicts the distance from where the inner dam slope intersects with the reservoir bottom ($x=0$) till 300m towards the centre of the basin. The equilibrium of forces is computed for an infinitely long strip and a conservative leakage length of 5000m. The blue line reflects the maximum achievable depth. The red line portrays the chosen excavation depth.

Appendix H: Construction method of the dam

The construction sequence of the dam is similar to breakwater construction works. The main differences compared to the method depicted in Figure 143 are the use of the dredging and depositing process as explained in §5. Dredging works and the lack of a crown element.

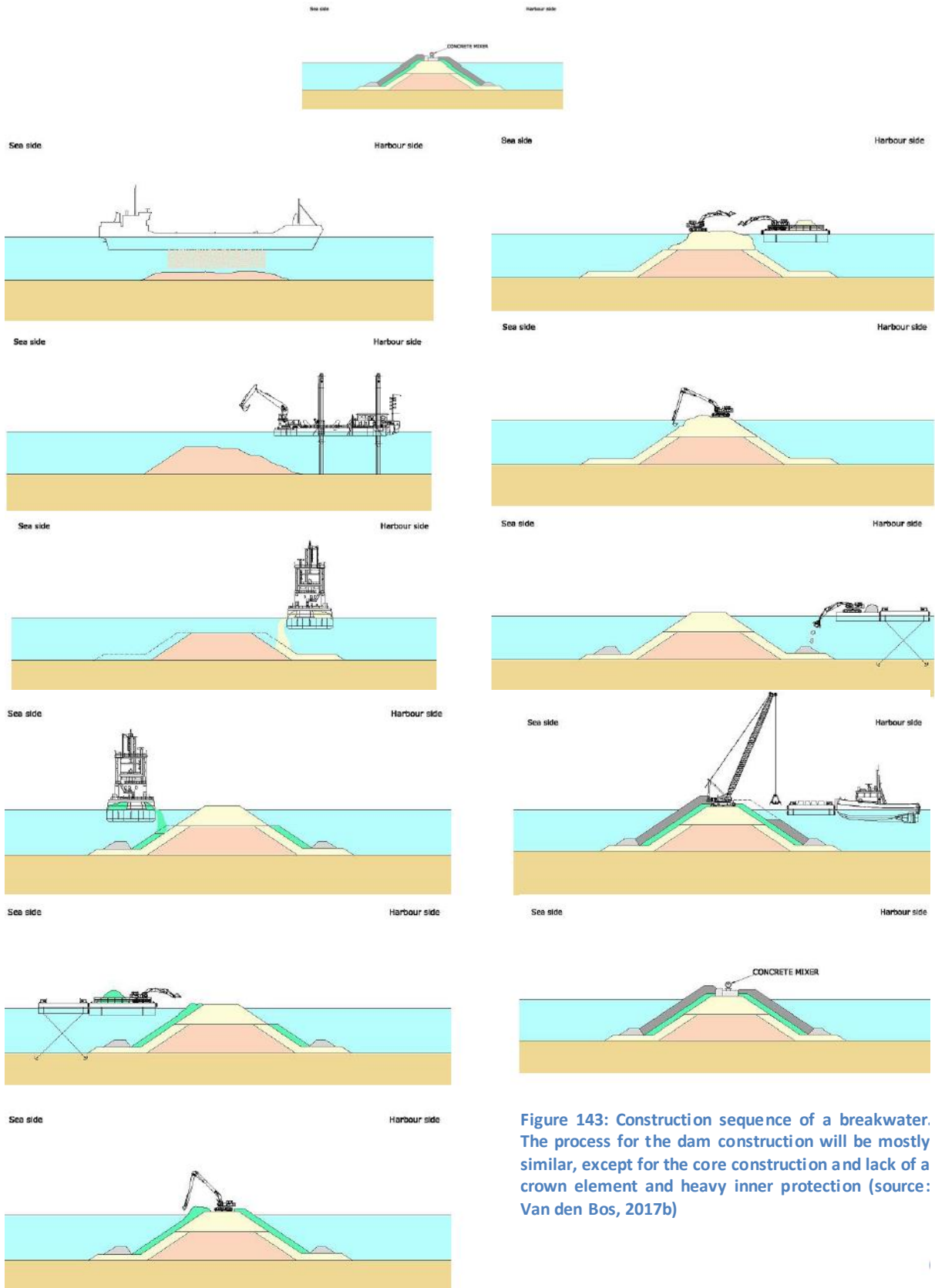


Figure 143: Construction sequence of a breakwater. The process for the dam construction will be mostly similar, except for the core construction and lack of a crown element and heavy inner protection (source: Van den Bos, 2017b)

Contrary to what Figure 143 suggests, the dam will not be built as a whole in the depicted order. The construction of the clay core and its armour will have to be executed consecutively. If not, the clay core will remain exposed to the wave action, which over a longer period of time will make the efforts undone. Therefore the dam also has to be sequentially installed not only in the cross-sectional plane, but also in the longitudinal direction (see Figure 144).

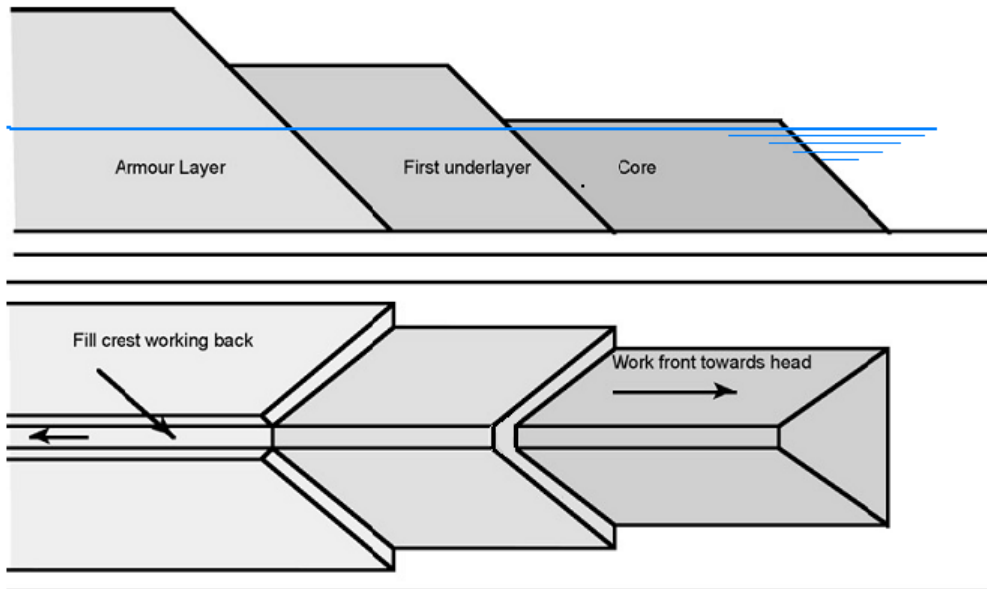


Figure 144: The serial construction process of the dam in the longitudinal direction. First the core has to be placed, when after the under layers and final armour layer can be positioned (source: Van den Bos, 2017b)

Appendix I: Location of the powerhouse and penstock design

To decide whether the powerhouse can best be placed inside the dam or behind (as in Figure 145), a brief analysis is made. The main things that are considered in order to make a choice are:

- Length of penstocks and corresponding efficiency losses
- Dam volume
- Loads on powerhouse and structural capability
- Influence on risk of failure of operation

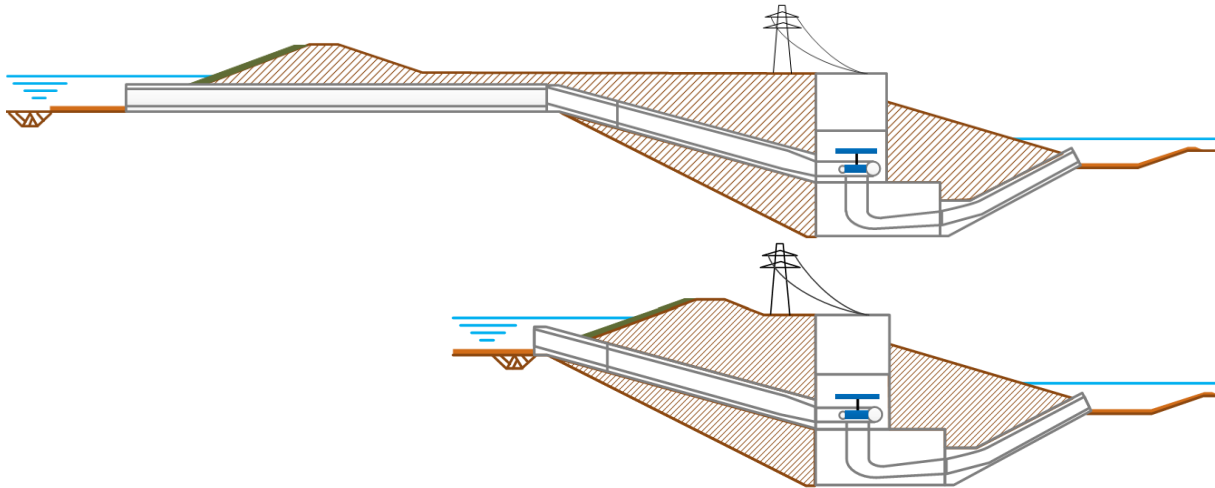


Figure 145: Alternatives for the location of the powerhouse: behind the dam (top) and inside the dam (bottom)

First of all the penstocks are reviewed for the large Francis pump-turbine (265MW). Only the diameter is determined and not the foundation or support structures. The diameter is the governing parameter to influence the head loss for the penstock due to wall friction at a maximum discharge of $700\text{m}^3/\text{s}$. It is the expectation that this enormous discharge will require an equally large diameter to reduce the flow velocity and the associated wall friction.

It might be more attractive from a construction point of view to install two separate penstocks that converge just before the turbine. Consequently the discharge per penstock will only be half and the corresponding friction loss a quarter (per penstock). When combined the double penstock alternative will then have half the head loss compared to a single penstock. Additionally the bifurcation will lead to some extra losses that have to be accounted for in this double penstock per turbine scenario.

The wall friction and head losses are determined by the subsequent formulae:

$$\text{Flow velocity in penstock: } U = \frac{Q}{nA} = \frac{Q}{n \frac{1}{4} \pi D^2}$$

$$\text{Coolbrook – White wall friction equation: } f = \left(\frac{1}{-2 \log \left[\frac{e}{3.7D} + \frac{2.51}{Re \sqrt{f}} \right]} \right)^2 ; \quad Re = \frac{U \cdot D}{\nu}$$

$$\text{Darcy – Weisbach head loss equation: } H_{loss} = n \cdot f \cdot \frac{L}{D} \cdot \frac{U^2}{2g} (\text{friction}) + \alpha \cdot \frac{U^2}{2g} (\text{bifurcation})$$

- U = Flow velocity in penstock (m/s)
- Q = Discharge through penstock (=700) (m³/s)
- n = Number of penstocks per turbine (=1 or 2) (-)
- A = Surface area of penstock (m²)
- D = Inner diameter of penstock (m)
- f = Friction coefficient (-)
- e = Colebrook-White roughness coefficient (=0.015mm) (mm)
- R_e = Reynolds number (-)
- ν = Viscosity (=10⁻⁶) (m²/s)
- H_{loss} = Total head loss due to wall friction and a possible bifurcation (m)
- L = Penstock length (=160.4 or 400.4 depending on place of powerhouse) (m)
- g = Gravitational acceleration (m/s²)
- α = Head loss coefficient (=0.04 for a 45° angle and two equal penstocks) (-)

Note that the Coolbrook-White friction equation is an iterative calculation. For the head losses only the penstocks itself are considered and no in-outlet or bend losses, since they are expected to be the same for both powerhouse locations. The head loss due to the transition between penstock and spiral case is evenly out of scope.

For the penstocks four scenarios are reviewed:

- Long double penstock (In case the powerhouse is installed behind the dam; maximum discharge of 350m³/s per penstock)
- Long single penstock (In case the powerhouse is installed behind the dam; maximum discharge of 700m³/s for the penstock)
- Short double penstock (In case the powerhouse is installed inside the dam; maximum discharge of 350m³/s per penstock)
- Short single penstock (In case the powerhouse is installed inside the dam; maximum discharge of 700m³/s for the penstock)

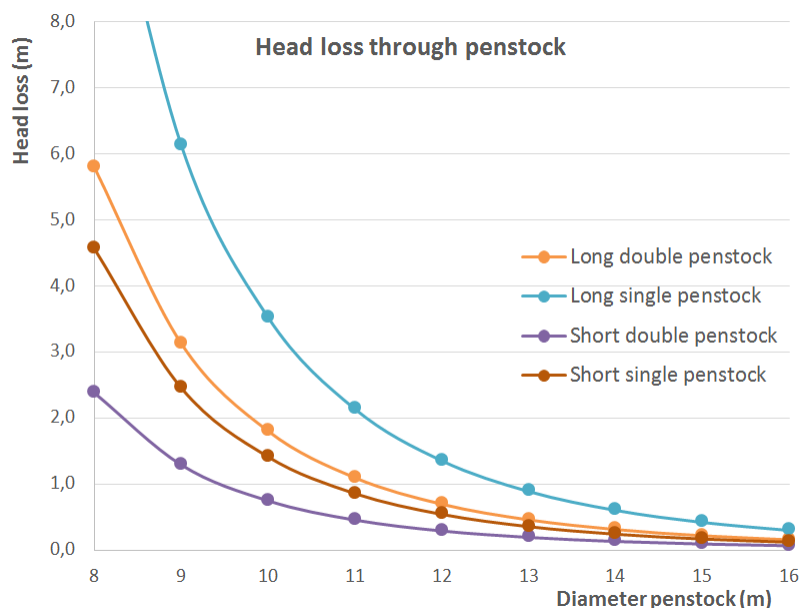


Figure 146: Head loss through penstocks for different scenarios

Diameter (m)	Flow speed (m/s)	Reynolds number (-)	Friction factor (-)	Head loss (m)	Head loss splitter (m)	Total head loss (m)
8	6,96	5,57E+07	0,0230	2,8	0,10	5,8
9	5,50	4,95E+07	0,0223	1,5	0,06	3,1
10	4,46	4,46E+07	0,0217	0,9	0,04	1,8
11	3,68	4,05E+07	0,0212	0,5	0,03	1,1
12	3,09	3,71E+07	0,0208	0,3	0,02	0,7
13	2,64	3,43E+07	0,0203	0,2	0,01	0,5
14	2,27	3,18E+07	0,0200	0,2	0,01	0,3
15	1,98	2,97E+07	0,0196	0,1	0,01	0,2
16	1,74	2,79E+07	0,0193	0,1	0,01	0,2

Table 60: Head loss through the 400.4m long double penstock with 350m³/s per penstock

Diameter (m)	Flow speed (m/s)	Reynolds number (-)	Friction factor (-)	Head loss (m)
8	13,93	1,11E+08	0,0230	11,4
9	11,00	9,90E+07	0,0223	6,1
10	8,91	8,91E+07	0,0217	3,5
11	7,37	8,10E+07	0,0212	2,1
12	6,19	7,43E+07	0,0208	1,4
13	5,27	6,86E+07	0,0203	0,9
14	4,55	6,37E+07	0,0200	0,6
15	3,96	5,94E+07	0,0196	0,4
16	3,48	5,57E+07	0,0193	0,3

Table 61: Head loss through the 400.4m long single penstock with 700m³/s per penstock

Diameter (m)	Flow speed (m/s)	Reynolds number (-)	Friction factor (-)	Head loss (m)	Head loss splitter (m)	Total head loss (m)
8	6,96	5,57E+07	0,0230	1,1	0,10	2,4
9	5,50	4,95E+07	0,0223	0,6	0,06	1,3
10	4,46	4,46E+07	0,0217	0,4	0,04	0,7
11	3,68	4,05E+07	0,0212	0,21	0,03	0,5
12	3,09	3,71E+07	0,0208	0,14	0,02	0,3
13	2,64	3,43E+07	0,0203	0,09	0,01	0,2
14	2,27	3,18E+07	0,0200	0,06	0,01	0,1
15	1,98	2,97E+07	0,0196	0,0	0,01	0,1
16	1,74	2,79E+07	0,0193	0,0	0,01	0,1

Table 62: Head loss through the 160.4m long double penstock with 350m³/s per penstock

Diameter (m)	Flow speed (m/s)	Reynolds number (-)	Friction factor (-)	Head loss (m)
8	13,93	1,11E+08	0,0230	4,6
9	11,00	9,90E+07	0,0223	2,5
10	8,91	8,91E+07	0,0217	1,4
11	7,37	8,10E+07	0,0212	0,9
12	6,19	7,43E+07	0,0208	0,5
13	5,27	6,86E+07	0,0203	0,4
14	4,55	6,37E+07	0,0200	0,2
15	3,96	5,94E+07	0,0196	0,2
16	3,48	5,57E+07	0,0193	0,1

Table 63: Head loss through the 160.4m long single penstock with 700m³/s per penstock

From Figure 146 it can quickly be concluded that the diameter should be larger than the runner diameter (9.4 – 10.0m) to avoid unacceptable losses. Furthermore it appears surprising that the effect of a double penstock is that small. For example: a short double penstock with diameters of 11m has a loss of 0.46m, where a short single penstock with a 13m diameter results in a loss of 0.36m. Even though the double 11m penstocks will have a much higher construction costs, they still lead to larger energy losses.

From all considered options the 13m single penstock is chosen, based on its minor losses and reasonable construction costs. The long and short version relate as shown in Figure 147.

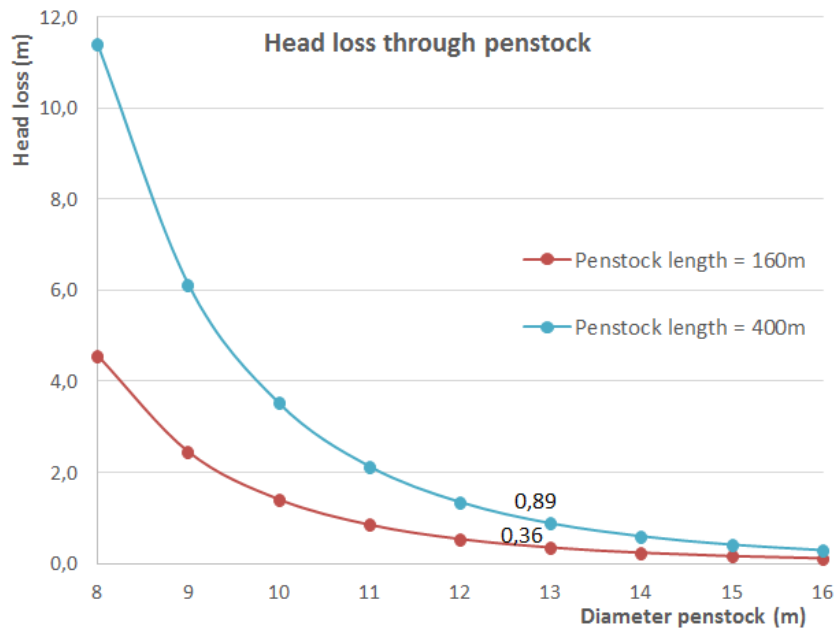


Figure 147: Head loss for a short and long single penstock with a 700m³/s discharge

It shows that the difference in head loss is almost perfectly linear with the penstock length, as could have been deduced from the Darcy-Weisbach equation. The difference in head loss can roughly be assumed double when considering roundtrip efficiency. The difference in roundtrip efficiency between a long and a short penstock then becomes:

$$\text{Difference in roundtrip efficiency} \approx \frac{(0.89 - 0.36) * 2}{40} * 100\% = 2.65\%$$

The large difference in efficiency leads to the preference for a powerhouse installed inside the dam itself. The other factors like savings on dam volume or different loads on the housing itself are all of inferior compared to the efficiency effect. From a risk perspective it may be favourable to place the powerhouse behind the dam, so in case the structure collapses it would not lead to a dam break through. Since the powerhouse already needs a lot of weight (concrete) to counter the uplift forces, it might as well be constructed in a very robust way. Therefore it is presumed that the difference in risk does not play a major role in deciding the position of the powerhouse.

All considered it appears best to install the powerhouse inside the dam and be connected to the North Sea via a single penstock with a 13m diameter. The maximum flow velocity is then 5.3m/s, which allows for either a reinforced concrete or steel penstock (Van Duivendijk, n.d.). A structural analysis and cost comparison is recommended to decide which is best. Due to the limited time a reinforced concrete penstock is assumed for now.

Appendix J: Connecting box caissons with Gina gaskets

In order to complete the powerhouse for the Francis pump-turbines, several caissons need to be connected. The linking of submerged tunnel (caissons) is a well-established and reliable technology that is explained in Figure 148. The Gina profile acts as a primary seal and the Omega profile as a secondary seal. Both have a lifetime of 100 years and are commonly used in saline environments (Trelleborg Ridderkerk BV, n.d.).

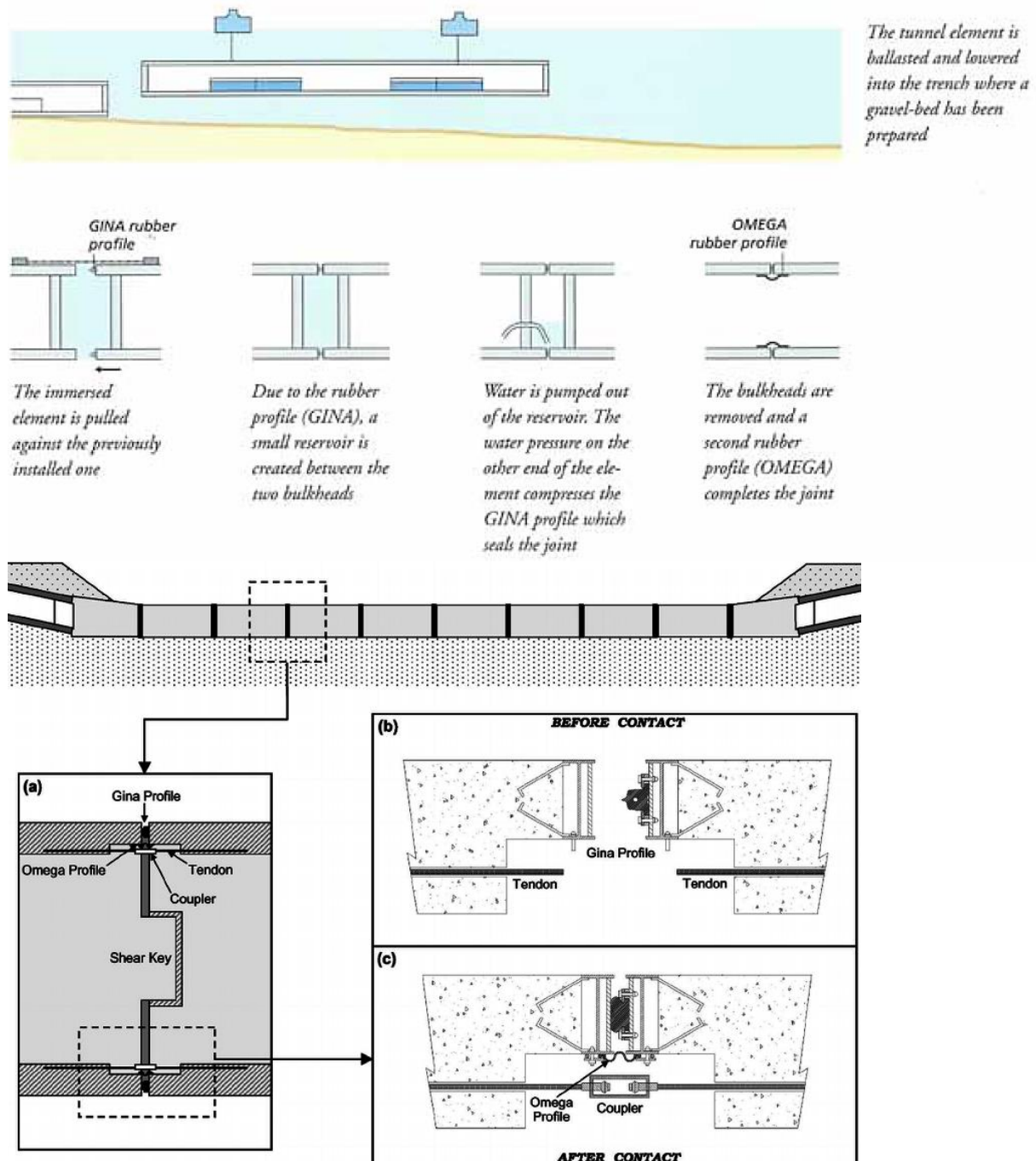


Figure 148: The procedure of connecting two immersed tunnel units explained above and a detail of the connection below (source: Trelleborg Ridderkerk BV, n.d. ; https://www.researchgate.net/figure/234044892_fig5_Fig-5-Aseismic-design-of-the-immersed-section-of-the-proposed-railway-link)

In case one wishes to connect caissons vertically, the closing mechanism works differently. For the horizontal link the hydrostatic pressure causes the Gina profile to be compressed. Vertically it is not the hydrostatic pressure but the weight of the top structure that compresses the Gina profile. The top structure has to be heavy enough to compress the Gina gasket in order to create an effective seal, but not too heavy to crush the profile. Especially the latter is thought to be a potential problem that needs further research.

There are many immersed tunnels constructed and planned in seismic active regions and in increasing depth. This lead to some research in allowable forces and occurring displacements like presented in Figure 149.

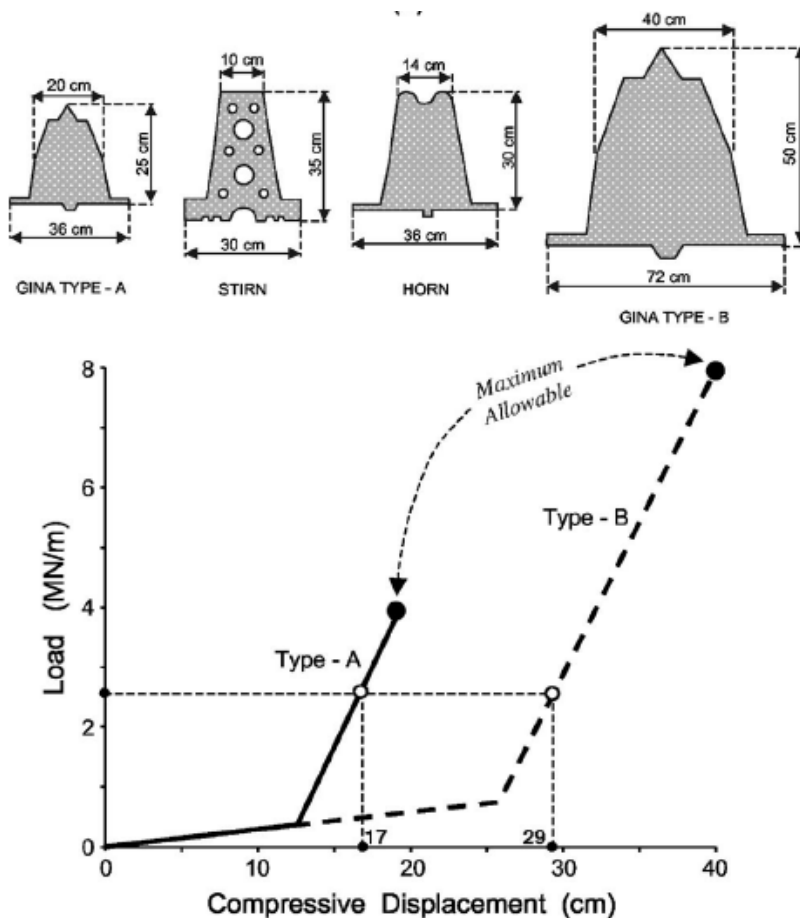


Figure 149: Geometric and deformation characteristics of existing Gina gaskets (Type-A) and projected profiles (Type-B). Both have been tested and verified on half-scale tests (source: Anastasopoulos et al., 2007)

The Marmaray tunnel that connects Europe with Asia via a 60 metre deep immersed tunnel in a seismically active region proves that the hypothetical Type-B profile is already instigated (with a force of roughly 3MN/m + earthquake forces on the Gina gasket).

The load weighing down from the top structure onto the bottom draft tube caisson can be computed along the same lines as was performed in §7.1.3 Prefab: modular box caissons, where the caisson outbalances the buoyant force by 7.5%.

The force pressing down on the Gina gasket (when placed all along the circumference) becomes:

$$\text{Force on Gina gasket: } F = \frac{2 \cdot \text{Caisson weight}}{\text{Caisson periphery}} = \frac{2 \cdot 0.075 \cdot V_{\text{caisson}} \cdot \rho_w \cdot g}{4 \cdot 40} = 0.45 \text{ MN/m}$$

One could tell from Figure 149 that the 0.45MN/m is actually on the lower end of the scale. Generally a Gina gasket needs to be compressed half its length in order to function properly (K.J. Reinders, personal communication, October 5, 2017). Furthermore, active earth pressures from the backfill and dam might create a kind of rotating moment, which could decrease the force on the inner Gina profile. Additionally the compressible connection between caissons could allow for minor continuous displacements caused by the vibrations of the turbine. This potential risk and the minimum required load result in the desire to develop an alternative connection method.

The Gina profile is only required to ensure a watertight connection between the elements and not for a fixed linkage of the elements itself. To enable the sealing of the connection the Gina profile only needs to be compressed a bit (in the order of 12cm). This feature is used for the design of the vertical connection between the caissons, which resulted in the detail as depicted in Figure 150.

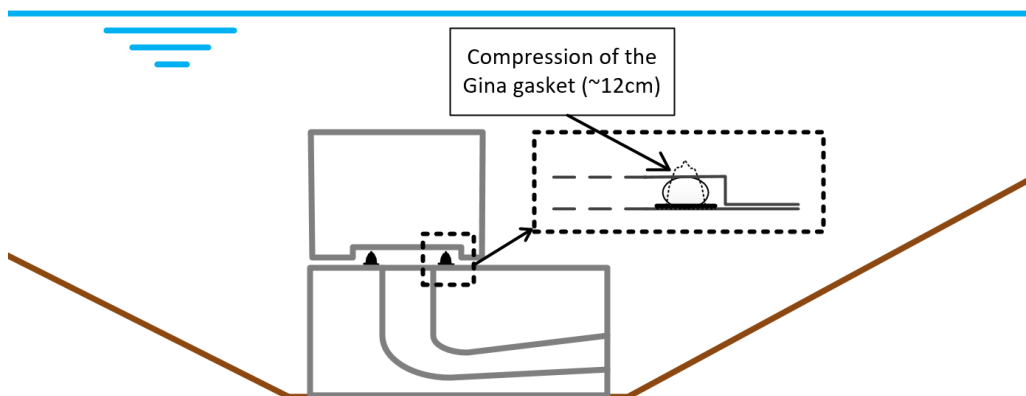


Figure 150: The vertical connection between the box caissons. Instead of the whole top structure weighing down on the Gina gaskets, a small recess in the top caisson ensures a watertight seal while the downward forces are simply transmitted via the concrete structure

Once the caissons are connected and the water in between has been pumped out, the bulkheads can be removed and the Omega profile can be attached to create a secondary seal. Besides a more stable link between the caissons this method can also do with a shorter Gina profile length. Consequently the compressive force per metre will be higher as was required:

$$\text{Force on Gina gasket: } F = \frac{2 \cdot \text{Caisson weight}}{\text{Gap periphery}} = \frac{2 \cdot 0.075 \cdot V_{\text{caisson}} \cdot \rho_w \cdot g}{4 \cdot 15} = 1.2 \text{ MN/m}$$

The resulting force on the Gina profile is exactly in the preferred range for the conventional Gina gaskets (see Type-A in Figure 150). The connection between the top and turbine caisson though is only compressed by the weight of 1 caisson (0.6MN/m). Therefore some additional ballast weight should be added to enhance the sealing. Note that the recess in the bottom of the to-be-connected caisson has to be sufficiently wide that during the positioning the caisson does not hit or scratch the gasket. To prevent sliding or movement between the caissons a horizontal shear key will be necessary (Figure 148 bottom).

The vertical connection system with Gina profiles that fall into a recess of the above caisson is found best applicable. Although a similar scheme is unknown to the author²⁸ it is expected that the described technology can offer a viable and secure solution for linking the caissons. This presumption results in the choice for the construction method that deploys modular box caissons to install the powerhouse.

²⁸ Many more linking alternatives exist and can potentially offer a viable or even better connection.

